4-2016

Investigating the role of the basic helix-loop-helix transcription factor MIST1 in pancreatic diseases

Anju Karki
Purdue University

Graduate School Form
30 Updated 12/26/2015

PURDUE UNIVERSITY
GRADUATE SCHOOL
Thesis/Dissertation Acceptance

This is to certify that the thesis/dissertation prepared

By Anju Karki

Entitled

Investigating the role of the Basic Helix-Loop-Helix Transcription Factor MIST1 in Pancreatic Disease

For the degree of Doctor of Philosophy

Is approved by the final examining committee:

Daniel Suter
Chair

Weiguo A. Tao

Ignacio Camarillo

Stephen F. Konieczny

To the best of my knowledge and as understood by the student in the Thesis/Dissertation Agreement, Publication Delay, and Certification Disclaimer (Graduate School Form 32), this thesis/dissertation adheres to the provisions of Purdue University's "Policy of Integrity in Research" and the use of copyright material.

Approved by Major Professor(s): Stephen F. Konieczny

Approved by: Jeffrey Lucas 4/20/2016

Head of the Departmental Graduate Program Date

INVESTIGATING THE ROLE OF THE BASIC HELIX-LOOP-HELIX TRANSCRIPTION FACTOR MIST1 IN PANCREATIC DISEASES

A Dissertation

Submitted to the Faculty

of

Purdue University

by

Anju Karki

In Partial Fulfillment of the

Requirements for the Degree

of

Doctor of Philosophy

May 2016

Purdue University

West Lafayette, Indiana

Dedicated to my late brother

RAJAN KARKI

ACKNOWLEDGEMENTS

I would like to express my deepest appreciation to my advisor Dr. Stephen Konieczny. Steve, you are the best mentor and scientist that a student could ask for. Your constant encouragement and valuable ideas instilled in me a desire to be a better scientist every single day. Without your untiring guidance this dissertation would not have been possible.

I would like to thank my committee members, Dr. Daniel Suter, Dr. Andy Tao and Dr. Ignacio Camarillo for insightful comments and questions during my meetings. Thank you Dr. Elizabeth Taparowsky for your constructive suggestions and support throughout my graduate career.

To all the present and past members of the Konieczny and Taparowsky labs, thank you! Dan, Dave, Chunjing, Sevim, Patrick, Brad, Rosie, Yi, Becky and Erin for being awesome and supportive throughout my graduate career. Thank you Dr. Sean Humphrey for helping me generate some mouse lines. Barbara, you deserve a special thank you for being a wonderful “lab goddess.”

Special gratitude goes to the past and present members of the NEPSAP community for the homey support. Dr. Swathi Devireddy, you are a great friend to have in one's life. The Gambill family deserves immense gratitude for being an important support system in my life.

Thank you, Nirajan, for your enormous support throughout this journey. I wouldn't have accomplished this task without you.

Finally, thank you to my parents (Indra Karki, Meena Karki and Yeshoda Karki; Surendra Karki and Laxmi Karki) and my siblings (Bindu Karki, late Rajan Karki, Pradip Karki, Prabin Karki, Sarthak Jung Karki and Dikshya Karki) for your unconditional love, encouragement, patience and support throughout my graduate career!!

TABLE OF CONTENTS

Page

Page

LIST OF TABLES

LIST OF FIGURES

Figure Page

Figure Page

Figure Page

LIST OF ABBREVIATIONS

RNA	Ribonucleic acid
BrdU	Bromodeoxyuridine
IHC	Immunohistochemistry
DAB	3,3’-Diaminobenzidine
BCA	Bicinchoninic acid assay
SDS-PAGE	Sodium dodecyl sulfate
HRP	Horseradish peroxidase
PVDF	Polyvinylidene fluoride
ECL	Enhanced chemiluminescence
PCR	Polymerase Chain Reaction
H&E	Hematoxylin and eosin
bHLH	Basic helix-loop-helix
DNA	Deoxyribonucleic acid
EMSA	Electrophoretic mobility shift assay
HLH	helix-loop-helix
TAD	Transactivation domain
MS/MS	Tandem mass spectrometry

DAPI	4’,6-diamidino-2-phenylindole
CO-IP	Co-immunoprecipitation
WT	Wildtype
ADM	Acinar-ductal-metaplaisa
PanIN	Pancreatic intraepithelial neoplasia
PDAC	Pancreatic ductal adenocarcinoma
K19	Keratin-19
PP	Pancreatic polypeptides
RIPA	Radioimmunoprecipitation assay
cKO	Conditional knockout
AP	Acute pancreatitis
qRT- PCR	Quantitative Real Time - Polymerase Chain Reaction
KO	Knockout
CAC	Centroacinar cells
ER	Endoplasmic reticulum
DP	Dorsal pancreatic bud
VP	Ventral pancreatic bud

ABSTRACT

Karki, Anju Ph.D., Purdue University, May 2016. Investigating the Role of the Basic Helix-Loop-Helix Transcription Factor MIST1 in Pancreatic Diseases Major Professor: Stephen F. Konieczny

Acinar cells of the exocrine pancreas are dedicated to synthesize, package and secrete immense quantities of pro-digestive enzymes to maintain proper metabolic homeostasis for the organism. Dysregulation of enzyme secretion in acinar cells can give rise to exocrine diseases including acute pancreatitis (AP), a disease that targets acinar cells, leading to acinar-ductal metaplasia (ADM), inflammation and fibrosis - events that can transition into the earliest stages of pancreatic ductal adenocarcinoma (PDAC). The focus of this thesis is to interrogate transcriptional regulatory networks that are susceptible to AP and the role that these networks play in acinar cell and exocrine pancreas responses. The overall goal is to determine the importance of the acinar-specific maturation transcription factor MIST1 to AP damage and organ recovery and its role in AP induced PDAC upon oncogenic transformation. Analysis of wild-type and *Mist1* conditional null mice revealed that *Mist1* gene transcription and protein accumulation are dramatically reduced as acinar cells undergo ADM alterations during AP episodes.

To test if loss of MIST1 function is primarily responsible for the damaged status of the organ, mice harboring a Cre-inducible *Mist1* transgene (*iMist1*) were utilized to determine if sustained MIST1 activity could alleviate AP damage responses. Surprisingly, constitutive *iMist1* expression during AP produced a dramatic increase in organ damage followed by acinar cell death. This result suggests that the transient silencing of *Mist1* expression is critical for acinar cells to survive an AP episode, providing cells an opportunity to suppress their secretory function and regenerate damaged cells. In order to further define the role of MIST1 in pancreatic neoplasia lesion formation (a precursor of PDAC), *Mist1* conditional null mice were generated that contained a mutated oncogenic $Kras^{G12D}$ allele. Direct comparison between embryonic *Mist1* null mice with conditional *Mist1* null mice in the context of $KRAS^{G12D}$ activity demonstrated that embryonic *Mist1* null mice are more susceptible to PanIN formation. The importance of MIST1 to these events suggests that modulating key pancreas transcription networks could ease clinical symptoms in patients diagnosed with pancreatitis and pancreatic cancer.

CHAPTER 1. INTRODUCTION

1.1 Cell Types in the Pancreas

The pancreas is a complex organ located behind the stomach and consisting of endocrine and exocrine components that are essential to maintain pancreas homeostasis **(Figure 1-1)**. The endocrine portion comprises about 2% of the organ mass and encompasses the islets of Langerhans which synthesize and secrete hormones into the bloodstream to regulate metabolism. The islets consist of five cell types dedicated to secreting a specific hormone: β-cells, α-cells, δ-cells, ε-cells and γ-cells secrete insulin, glucagon, somatostatin, ghrelin and pancreatic polypeptide, respectively (Slack 1995; Stefan et al. 1982; Murtaugh & Melton 2003). In mice, the central region of the islet consists of β-cells (60-80%) while the other cell types such as α-cells (15-20%), reside around β-cells (Murtaugh & Melton 2003). The primary hormones insulin and glucagon are essential for maintaining normal blood glucose levels. Glucagon produced by alpha cells converts glycogen into glucose in the liver and increases the glucose production in the blood. In contrast, insulin assists cells in absorbing and utilizing the glucose as a metabolite, leading to decreased blood sugar levels. Improper regulation of blood sugar balance gives rise to diseases such as diabetes mellitus (Ahmed 2002).

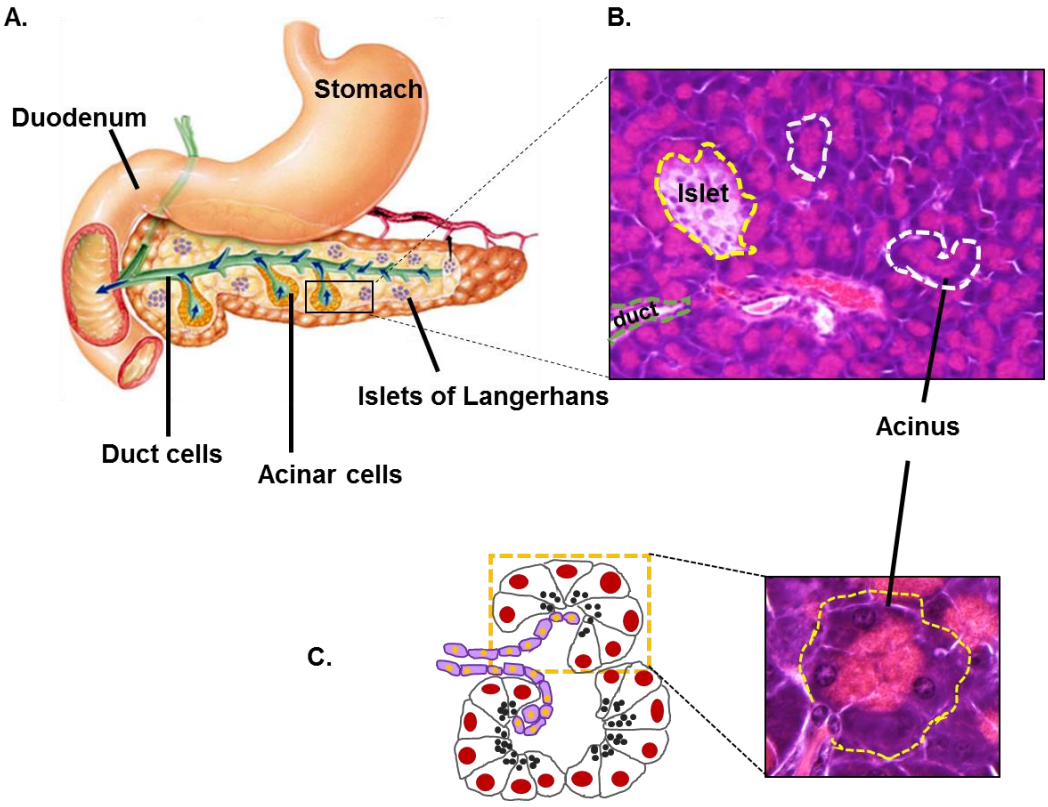

Figure 1-1.**Anatomy of the pancreas**. **(A)** The mature pancreas is located below the duodenum and stomach. The exocrine system consists of acinar cells and duct cells. The digestive enzymes are produced and secreted by acinar cells and ducts transport them to the intestine. The endocrine system consists of the Islet of Langerhans: β-cells (insulin), α-cells (glucagon), δ-cells (somatostatin), ε-cells (ghrelin) and γ-cells (pancreatic polypeptide) and is involved in hormone secretion. **(B)** H&E staining of a mouse pancreas illustrating the three cell types. Basal blue color signifies the presence of nuclei and the apical lumens are denoted in pink color where the digestive enzymes reside. **(C)** An acinus with apical-basal polarity consists of acinar cell nuclei at the base and the zymogens at the apical region. Also shown is a schematic of the exocrine pancreas with acinar clusters. Adapted from (Bardeesy & DePinho 2002).

The exocrine portion of the organ occupies nearly 95% of the total pancreatic mass and is comprised of acinar cells, duct cells and centroacinar cells. Individual acinar cells are grouped into a spherical structure known as an acinus as illustrated in **Figure 1-1** (Pandol 2010). Each acinus consists of 30-60 pyramidal epithelial cells that exhibit a defined apical-basal polarity. The basal aspect of the cell contains nuclei and an elaborate highly developed endoplasmic reticulum (ER) network that is necessary to produce massive amounts of digestive enzymes. Indeed, acinar cells are the largest protein producing factory in the body. Also located in the basal region of acinar cells are cholecystokinin (CCK) receptors that respond to hormones (CCK) and neurotransmitters as a part of the regulatory cascade to control proper secretion (exocytosis) of digestive enzymes (Slack 1995; Motta et al. 1997; Pandol 2010; Williams 2001; Pandol et al. 2011). In contrast, the apical portion of an acinar cell stores a host of pro-hydrolases as inactive enzymes in secretory vesicles known as zymogen granules. Acinar cells are professional secretory cells and are tasked with producing, modifying, packaging and secreting vast quantities of pro-digestive enzymes (zymogens) that breakdown carbohydrates (amylase), proteins (trypsin), lipids (lipase) and nucleic acids (DNAse and RNAse) (Stanger & Hebrok 2013; Puri & Hebrok 2010; MacDonald et al. 2010; Gittes 2009). Importantly, the enzymes produced by acinar cells remain as inactive zymogens located at the apex of the cell until secreted into the digestive tract to maintain metabolic homeostasis (Rukstalis et al. 2003; McNiven & Marlowe 1999).

Each acinar cell within an acinus maintains cell-cell communication by the presence of tight junctions and gap junctions. Actin tight junctions located at the apical region of the cells are utilized to insure that digestive enzymes are only secreted into ductal lumens and not to the outside of cells (Fallon et al. 1995; Pandol 2010). In contrast, intercellular gap junctions allow the movement of small molecules (i.e., Ca^{2+}) between neighboring acinar cells. This helps to insure that Ca^{2+}- regulated secretion affects all of the cells within an acinus simultaneously so that all cells in a unit secrete their products in a coordinated fashion. (Yule et al. 1996).

The duct cells of the exocrine pancreas play a vital role in transporting the enzymes secreted by the acinar cells. Duct cells are both pyramidal and cuboidal in shape and form a ductal network which consists of the Duct of Wirsung (the main pancreatic duct), numerous interlobular and intralobular ducts, and the smaller intercalated ducts which are directly associated with each acinus. Upon pancreatic enzyme secretion in to the lumen, this intricate ductal network functions as a carrier to release the acinar enzymes into the duodenum (Kern 1993; Reichert & Rustgi 2011). The duct cells secrete a high concentration of bicarbonate to neutralize acidity in the stomach and also maintain a neutral pH for the enzymes to work efficiently after consuming a meal (Steward et al. 2005). In addition to critical cell biology functions associated with acinar and duct cells, the exocrine pancreas is also subject to a number of disease states, including pancreatic ductal adenocarcinoma (PDAC) and pancreatitis. Thus, characterizing the molecular pathways associated with these cells is important to understand the biology behind

devastating exocrine diseases (Yadav & Lowenfels 2013; Bockman et al. 2003; Rooman & Real 2012; Kopp et al. 2012).

The region where the apical portion of acinar cells and duct cells converge, consists of paired centro-acinar (CAC) cells which are often referred to as terminal end duct cells (Means & Leach 2001). These cells mimic duct cells. CACs gene expression patterns appear only in the later part of the pancreas development and post birth (Pour 1994). Like duct cells, these cells also produce bicarbonate to neutralize the acidity in the stomach (Steward et al. 2005). Accumulating research evidence from mouse experiments implicate CACs as the reservoir for multipotent progenitor cells (Rovira et al. 2010; Seymour et al. 2007; Hayashi et al. 1999). For instance, experiments performed in rats revealed that CACs proliferate post pancreatectomy (Hayashi et al. 1999). These results have opened multiple venues of research in investigating potential stem cell markers of the pancreas biology.

1.2 Pancreas Development and Transcription Factors

In mice, pancreas development occurs in two distinct transition phases: primary and secondary. During the primary transition stage, the formation of pancreatic buds on the dorsal and ventral sides of the foregut endoderm takes place at embryonic day (e) 8.5 (Slack 1995) followed by the organogenesis of the pancreas at e9.0. Ultimately, by e12.5, the two buds unite to form a single organ

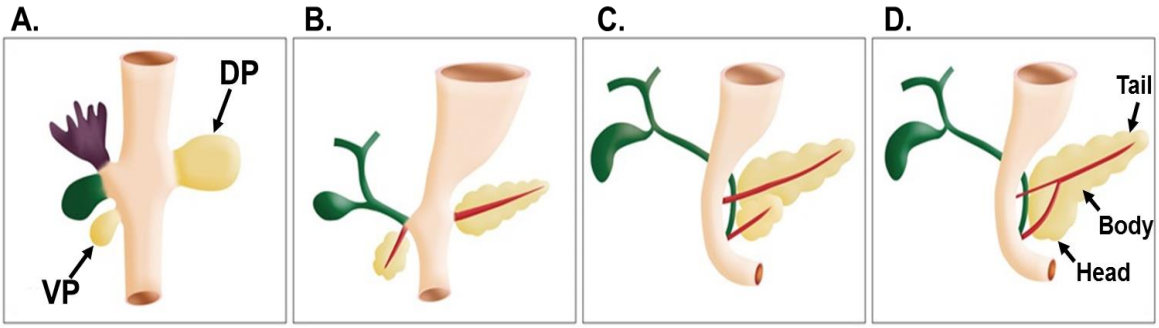

Figure 1-2. **Development of the pancreas from dorsal and ventral buds**. **(A)** The formation of the ventral pancreatic bud (VP) and the dorsal pancreatic bud (DP) marks the organogenesis of the pancreas. **(B-D)** As the pancreas matures, the two buds fuse to form the head, body and tail of the pancreas. Adapted from (Türkvatan et al. 2013)

(**Figure 1-2**). The pancreas develops the differentiated islet cells, acinar cells and duct cells during the secondary transition stage (Pictet et al. 1972; Gittes 2009).

Organogenesis and development of the pancreas is tightly dependent on multiple transcription factors. Key transcription factors for pancreas organogenesis and maturation include pancreatic and duodenal homeobox 1 (PDX1, also known as Ipf1), pancreas transcription factor 1 (PTF1a), Nr5a2/ liver receptor homologue 1 (LRH-1), MIST1 (also known as bHLHa15), SOX9, HNF6 and HNF1β. PDX1 is required for early pancreas development as early as e8.0 when the dorsal and ventral pancreatic buds start to form (Guz et al. 1995). The endocrine, exocrine and duct compartments all originate from PDX-1 expressing precursor cells (Guz et al. 1995; Gu et al. 2002). Accordingly, *Pdx1*$^{-/-}$ mice fail to form a pancreas (Ahlgren et al. 1996). In the adult pancreas, PDX1 is primarily dedicated to endocrine specification and PDX1 expression persists in insulin producing β-cells (MacFarlane et al. 1994) and is expressed at lower levels in acinar cells (Gannon et al. 2001; Gannon et al. 2008). Additionally, PDX1 directly regulates expression of a number of islet specific genes including *insulin*, *somatostatin*, *glucose transporter* (*glut*2) and *glucokinase* (Wilson et al. 2003). Thus, PDX1 is a critical transcription factor for both early and late stages of pancreas development.

Another protein that plays an essential role in pancreas development is the bHLH transcription factor, PTF1a (also known as p48) (Krapp et al. 1996). PTF1a plays two unique roles during pancreas development. First, PTF1a is essential for the formation of the early pancreas epithelium. PTF1a, along with PDX1, is expressed during the primary transition phase to determine a pancreatic fate for

the developing endoderm gut tube (Afelik et al. 2006). *Ptf1a* null mice fail to develop a ventral pancreatic bud and as a result formation of acinar cells and duct cells are perturbed, suggesting that proper temporal and spatial expression of PTF1a is essential for proper pancreas formation and development. Second, PTF1a is a key regulator of acinar cell differentiation, regulating genes which participate in the synthesis and secretion of digestive enzymes (Rose et al. 2001; Krapp et al. 1996; Masui et al. 2010). During the early phases of pancreas development, PTF1a partners with RBPJ (the vertebrate Suppressor of hairless) and E-proteins (DNA binding protein) to form a trimeric complex called PTF1-J. This complex is needed to form a pancreas. The PTF1-J complex consequently leads to activation of the RBPJ paralogue known as RBPJL which is essential for acinar cell differentiation. Additionally, in mature acinar cells, RBPJL swaps with RBPJ forming a PTF1-L complex. The PTF1-L complex is critical for acinar cell differentiation. This complex leads to transcriptional regulation of acinar genes producing digestive enzymes such as *Amylase*, *Carboxypeptidase* and *Elastase* (Masui et al. 2007; Masui et al. 2010; Beres et al. 2006). In the adult pancreas, PTF1a expression occurs exclusively in acinar cells and is inactivated in duct and islet cells (Masui et al. 2007). Thus, PTF1a transcription dictates the proper formation and development of the pancreas and more specifically regulates exocrine differentiation.

Another key transcription factor that contribute to establishing and maintaining a healthy pancreas state is the orphan nuclear hormone receptor LRH1/Nr5a2. In the initial stages of pancreas development, Nr5a2 expression is

prevalent in the inner cell mass in mouse embryos and plays a key role in the genesis of multipotent progenitor cells (Hale et al. 2014; Holmstrom et al. 2011). Hale et al., using *Nr5a2* null mice, revealed that islet cells, acinar cells and duct cells are affected resulting in impaired organ formation (2014). In the adult pancreas, Nr5a2 coordinates with the PTF1-L complex to transcriptionally regulate acinar cell secretory genes such as *Carboxypeptidase* and *Elastase*. These findings were verified using a mouse model where *Nr5a2* was conditionally deleted. Indeed, expression of the secretory genes in the acinar cells were lowered when *Nr5a2* is absent (Holmstrom et al. 2011). Additionally, through mouse studies it was also confirmed that the absence of *Nr5a2* sensitizes acinar cells to de-differentiate to cells resembling ducts (von Figura et al. 2014). Taken together, we can conclude that Nr5a2 is a key transcription factor in mediating and maintaining acinar cell differentiation during pancreas development.

MIST1 is a basic helix-loop-helix (bHLH) transcription factor expressed in pancreatic acinar cells of the adult pancreas. MIST1 is first expressed at e.10.5 in mice (Pin et al. 2001; Zhu et al. 2004). Although MIST1 is not essential for embryonic acinar development, it plays a key role in the maturation of acinar cells. MIST1 transcriptionally regulates genes essential for apical-basal cell polarity, the assembly and clustering of secretory granules, proper Ca^{2+} signaling, the expansion of the endoplasmic reticulum (ER), unfolded protein response (UPR) pathway homeostasis, cell cycle progression and regulated exocytosis (Direnzo et al. 2012; Garside et al. 2010; Hess et al. 2011; Jia et al. 2008; Luo et al. 2005; Pin et al. 2001; Rukstalis et al. 2003; Zhu et al. 2004). Thus, MIST1 plays an essential

role in the overall upregulation of the protein synthesis, processing and secretory machinery, often acting as a scaling factor to insure highly efficient regulated secretion for each cell type (Mills & Taghert 2012; Hess et al. 2011; Huh et al. 2010).

While PDX1, PTF1a, Nr5a2 and MIST1 are required for islet and acinar cell formation and maturation, SOX9, HNF6 and HNF1β transcription factors are dedicated in ductal specification and maturation. SOX9 is a member of the High Mobility Group box (HMG-box) family of transcription factors being expressed starting at e.9.5 in both the dorsal and ventral buds of the pancreas during organogenesis in mice (Lioubinski et al. 2003; Seymour et al. 2007). During the primary transition phase, SOX9 is a well-established marker for progenitor cells during pancreas development and this progenitor population gives rise to both endocrine and exocrine epithelial cells (Lioubinski et al. 2003; Seymour et al. 2007; Akiyama et al. 2005). As pancreas development reaches the second transition, SOX9 exclusively expressed in centro-acinar cells and duct cells in the pancreas (Kopp et al. 2011; Akiyama et al. 2005). Indeed, mouse studies using conditional *Sox9* knockouts in the pancreas revealed that due to the reduction in progenitor cells the pancreas is underdeveloped (Seymour et al. 2007; Seymour 2014).

Hepatocyte nuclear factors (HNFs) are a family of transcription factors that also regulate pancreas embryogenesis and pancreas maturation. Some of the key factors are HNF6 and HNF1β. HNF6 and HNF1β are expressed in the pancreatic endoderm and are required for the dorsal and ventral bud development during the primary transition of pancreas organogenesis (Rausa et al. 1997; Haumaitre et al.

2005; Jacquemin et al. 2003). *Hnf1β* knockout mice fail to develop ventral buds at e9.5 and are prone to undergo pancreas agenesis by e13.5 (Haumaitre et al. 2005). HNF6 and HNF1β transcription factors act upstream of PDX1 and PTF1a respectively, which have been previously discussed as key transcription factors required for endocrine and exocrine development (Poll et al. 2006). In the later part of pancreas development HNF6 is localized to ductal cells (Pierreux et al. 2006). Mouse studies revealed that HNF1β gives rise to epithelial ductal cells, but interestingly this factor is also found in endocrine cells. However, following birth, HNF1β expression becomes restricted to duct cells (Solar et al. 2009). Taken together, we can conclude that HNF6 and HNF1β play a universal role in determining proper pancreas specification and maintaining ductal differentiation.

A summary of the transcription factors involved in pancreas organogenesis and maturation described in this section is illustrated in **Figure 1-3**.

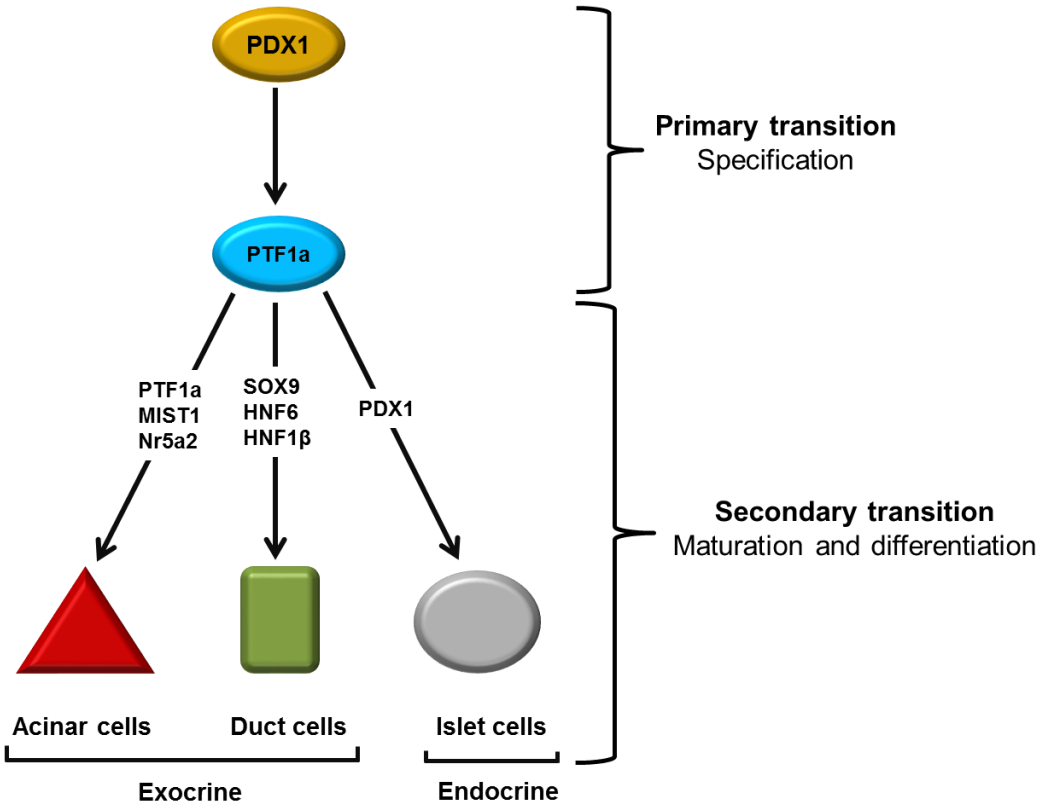

Figure 1-3. Summary of described transcription factors involved in pancreas organogenesis and maturation: The primary transition is a phase of pancreas specification. All pancreas cell types arise from PDX1^{+}, progenitor cells. The secondary phase marks the differentiation and maturation of the exocrine and endocrine cells. PTF1a is a key regulator of acinar cell fate and PTF1a, MIST1 and Nr5a2 help in acinar cell differentiation. SOX9, HNF6 and HNF1β are the markers of ductal cells. PDX1 exclusively marks mature islet cells in the adult organ.

1.3 Pancreas Diseases

1.3.1 Diabetes (Endocrine-specific Disease)

The endocrine compartment of the pancreas has a critical role in producing hormones (insulin and glucagon) to maintain blood glucose homeostasis. Under normal conditions, β-cells synthesize insulin which gets stored in secretory vacuoles. Upon increased blood glucose levels, insulin gets released from the β-cells into the blood circulation network where it regulates glucose uptake in cell types such as fat cells, liver cells and muscle cells (Lin & Sun 2010). Improper regulation of insulin and glucagon hormones leads to diseases such as diabetes mellitus (Type 1 and Type 2). According to the National Diabetes Statistics Report, it is estimated that 9.3% of the U.S population are victims of this metabolic disease (2014).

Type 1 diabetes (insulin-dependent or juvenile diabetes) is an autoimmune disease which is caused by selective β-cell damage in the islet of Langerhans. Since the body's immune system is involved in destroying the insulin secreting cells, insulin hormone level production is inhibited. As a consequence of no insulin production to regulate glucose in the blood, patients develop hyperglycemia (van Belle et al. 2011; Moore et al. 2001; Van Belle et al. 2009). The human leukocytes antigen (HLA) class III gene, also known as *IDDM1*, is estimated to cause 40 - 50% risk of inheriting type 1 diabetes (Hirschhorn 2003). Various human studies and mouse models have been used to unravel the mechanisms, signaling pathways and genetics behind Type 1 diabetes (Van Belle et al. 2009). The best mode of treatment for Type 1 diabetes patient is to take a lifelong supply of insulin.

Type 2 diabetes (non-insulin dependent or adult-onset) is associated with insulin resistance whereby cells have impaired response to insulin and dysfunction in β-cell insulin secretion. Hyperglycemia is a common consequence of dysregulated glucose uptake into cells (Lin & Sun 2010). If chronic hyperglycemia and insulin resistance occurs then the β-cells will often begin to die via apoptosis resulting in decreased β-cell mass (Butler et al. 2003).

As discussed earlier, the transcription factor PDX1 is essential for pancreas formation and for β-cell function. Heterozygous *Pdx1* mice are prone to developing glucose intolerance followed by late-onset Type 2 diabetes (Dutta et al. 1998). Similarly, patients with mutation in the *Pdx1* gene exhibit a very high incidence of developing late-onset Type 2 diabetes (Hani et al. 1999; Oliver-Krasinski et al. 2009). Another protein associated with Type 2 diabetes is High-mobility group A1 (HMGA1) which has been shown to regulate expression of the insulin receptor (*INSR*) (Foti et al. 2003). Indeed, studies comparing healthy and Type 2 diabetic patients suggested that gene variants of *HMGA1* can lead to Type 2 diabetes (Chiefari et al. 2011).

1.3.2 Exocrine Disease: Pancreatitis

1.3.2.1 Epidemiology

Acute pancreatitis (AP), a gastrointestinal pancreatic inflammatory disorder, is the most common reason for pancreas symptom hospitalization which accounts for 275,000 admissions in 2009 in the United States alone (Peery et al. 2012; Yadav & Lowenfels 2013). The yearly AP incidence in the United States is approximately 50 individuals per 100,000 people (Yadav & Lowenfels 2013) of which 30% of cases are thought to be caused by gallstone, 50% is non-gallstone related events and 20% caused by recurrent AP (Yadav & Lowenfels 2013). 80% of the AP patients present with mild conditions and recover. However, 20% of patients die of AP complications (Lund et al. 2006; Wang et al. 2009).

Although genetic factors, smoking, diet and obesity can cause AP, gallstones and alcohol are the two most common etiologic factors of AP (Yadav & Lowenfels 2013; Wang et al. 2009). Gallstone-related AP is induced when the pancreatic duct and/or bile duct are obstructed. This blockade results in duct pressure followed by the activation of cascades of pancreatic enzymes from the exocrine compartment of the pancreas leading to autodigestion of the organ (Hazem 2009; Diehl et al. 1997). In cases of alcohol-related pancreatitis, *in vivo* studies have revealed that upon alcohol consumption, cholecystokinin stimulation takes place leading to activation of zymogens in the acinar cells making the cells susceptible to pancreatitis (Gorelick 2003). Most patients with AP recover. However, some patients develop systemic inflammatory response syndrome which predisposes the patients to multiorgan failure including lung injury

(Banerjee et al. 1995; Pandol et al. 2007). Common treatment options for gallstone-related AP is to perform a cholecystectomy - removal of the gallbladder (Vitale 2007). Universal treatment options for acute pancreatitis typically involve fasting and short-term intravenous feeding and pain management by using non-steroidal anti-inflammatory drugs (Banks et al. 2010). Importantly, acute pancreatitis is mostly curable. However, multiple bouts of AP can lead to a severe form of pancreatitis commonly known as chronic pancreatitis (Yadav & Lowenfels 2013) and is also a precursor for PDAC (Pinho et al. 2014; Guerra et al. 2007). A wide range of different treatment options are under investigation to prevent the causative factor that leads to AP occurrence.

1.3.2.2 AP Pathophysiology

Pancreatitis initiation occurs when zymogens in the acinar cells are prematurely activated upon insults such as gallstones. Zymogen activation triggers the release and autoactivation of a cascade of enzymes including the proteases trypsin and elastase, causing acinar cell injury. Furthermore, the leakage of enzymes leads to autodigestion of the tissue and subsequently injury markers elevate, edema, cell necrosis and vascular damage (Bhatia et al. 2005; Stevenson & Carter 2013). However, the mechanism behind the autoactivation of zymogens has not been fully elucidated. In order to better understand the mechanism behind acute pancreatitis and ultimately develop effective treatment options, various experimental models have been utilized including hormone-induced pancreatitis (Willemer et al. 1992). Caerulein, a cholecystokinin (CCK) analogue, has been

extensively used to induce cell injury in pancreatic acinar cell culture (Saluja et al. 1999) and in acute pancreatitis in rodents (Bragado et al. 1996). Administration of supramaximal doses of caerulein leads to disturbances in calcium signaling which triggers activation of trypsinogen inducing acinar cell injury (Ward et al. 1996). The finding of calcium dependent premature zymogen activation has been critical in our understanding of acute pancreatitis. In mice, injection of caerulein into the intraperitoneal cavity leads to cathepsin-B mediated hyperstimulation of enzymes from acinar cells that leak into the interstitial space. Consequently, enzymes get activated in the interstitial space and start digesting the cells (Halangk et al. 2000). This results in inflammation, edema, increased serum-amylase levels and necrosis marking the onset of acute pancreatitis (Husain et al. 2007; Mayerle et al. 2013). This model presents various advantages including that it can lead to AP in mice, rats, dogs and hamsters; it does not require a surgical procedure; intraperitoneal injections are sufficient to induce AP; it is a simple and inexpensive procedure; experiments can be performed under controlled injections of caerulein that are easy to monitor and highly reproducible; and most importantly, this model allows us to study tissue injury post-AP induction (Su et al. 2006; Mayerle et al. 2013). However, the disadvantage of this model is that only mild AP is induced with no overt mortality as can be found in the human condition (Mayerle et al. 2013).

Pancreatitis presents with various hallmark events in patients and these events have been key in investigating the disease in experimental models. Inflammation and edema are among the first events post-injury. Early activation of trypsinogen triggers AP injury. Studies performed in *Trypsinogen-7*^{KO} mice

revealed that indeed, *Trypsinogen-7* is activated within the acinar cells post-AP insult, acting as a mediator of AP initiation. In post-AP initiation, the immune cells (neutrophils and macrophages) are recruited immediately upon acinar cell injury. As a result, pro-inflammatory markers (tumor necrosis factor-α (TNF-α), interleukin (IL)-1, IL-2, IL-6) and anti-inflammatory markers (IL-10 and IL-1 receptor) are markedly increased (Pandol et al. 2007; Bhatia 2005; Davies & Hagen 1997). Among these markers, TNF-α specifically plays a role in protease activation along with induction of cell death. This further triggers macrophage activation to progress the injury pathway (Sendler et al. 2012). Murine AP studies have also revealed that neutrophil depletion attenuates the AP response (Frossard et al. 1999). Likewise, intracellular nuclear factor-κβ (NF-κβ) signaling is commonly associated with early AP responses (Gukovsky et al. 1998) and upon early activation of NF-κβ in mouse acinar cells AP responses become more severe (Haojie Huang et al. 2013). These findings reveal that NF-κβ signaling plays a critical role in AP initiation and progression (Jr et al. 2008).

One of the characteristics of AP is cell death (necrosis and apoptosis). Apoptosis (programmed cell death) of acinar cells in AP occurs primarily by the activation of cysteine proteases called caspases. Inactive forms of caspases are activated when proteases act to cleave them (Pandol et al. 2007; Bhatia et al. 2012). Cell necrosis during AP occurs when calcium levels in the cytoplasm are elevated. The increase in calcium concentration in gallstone-related AP affects the function of mitochondria which leads to cell necrosis (Criddle et al. 2007; Kim et al. 2002). Activation of NF-κβ also contributes to acinar cell death upon AP induction

(Murtaugh & Keefe 2014). The initiation and progression of AP is illustrated in **Figure 1-4**. Various biomarkers are being utilized to diagnose acute pancreatitis in patients. These biomarkers include amylase, lipase and trypsinogen which are elevated in the early AP stages (Matull et al. 2006).

Another key hallmark of AP is alteration of acinar cell identity where acinar cells acquire ductal characteristics through a process known as acinar-ductal metaplasia (ADM) (Strobel et al. 2007; Molero et al. 2012; Prévot et al. 2012). In experimental models of AP the presence of ADM lesions are confirmed by detecting ductal markers including SOX9, K-19 and HNF6 within acinar cells (Strobel et al. 2007; Kopp et al. 2012; Prévot et al. 2012). Furthermore, NF-κβ signaling is closely associated with both initiation and maintenance of ADM (Murtaugh & Keefe 2014).

In summary, calcium-dependent activation of trypsinogen causes AP initiation followed by disease progression through the recruitment of pro- and anti-inflammatory markers, cell-death and activation of signaling pathways. Importantly, during AP acinar cells transiently acquire a ductal phenotype upon the loss of acinar markers suggesting that there is a significant change in the acinar cell transcription network that helps to orchestrate these events.

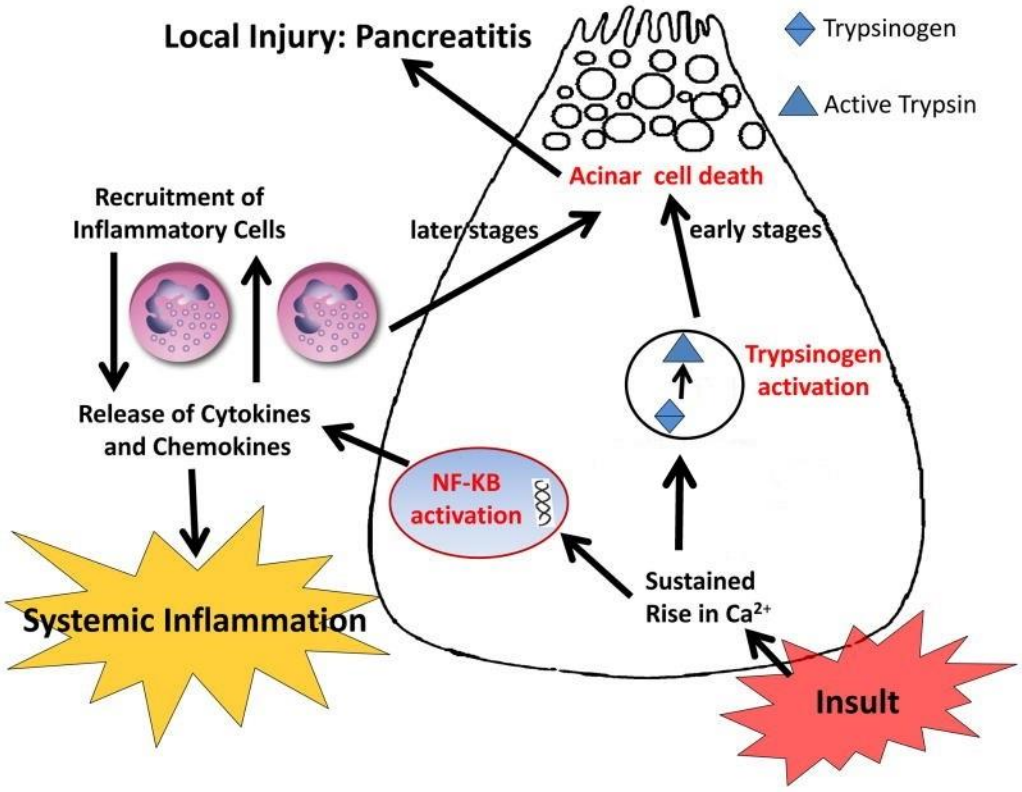

Figure 1-4. Schematic summarizing the pathogenesis of acute pancreatitis. Upon insults such as gallstones, alcohol or hormone-induced pancreatitis, activation of trypsinogen and NF-κβ occur independently in the early onset of AP. Activated trypsin leads to activation of proteases such as lipase and amylase which lead to autodigestion of the tissue. Likewise, NF-κβ activation recruits pro- and anti-inflammatory markers to progress the disease and assist in local injury. In the severe form of inflammation, systemic inflammation of organs such as lung injury occurs. Adapted from (Dawra et al. 2011).

1.3.2.3 Tissue Regeneration post-AP

Acute pancreatitis presents with acinar cell destruction and loss. However, in most cases the tissue repairs by regeneration of acinar cells (Murtaugh & Keefe 2014). The cell of origin in pancreas regeneration post-AP has been controversial. Results from different models of regeneration reveal participation of various cell types (acinar cells and ductal cells) to heal the organ. Transgenic mouse-model studies using diphtheria-toxin to ablate acinar cells and endocrine cells, but not ductal cells, revealed that pancreas regeneration occurred via ductal cell proliferation (Criscimanna et al. 2011). In contrast, lineage tracing studies in murine models, implied that only preexisting acinar cells give rise to acinar cells post-pancreatectomy (Desai et al. 2007). This finding was further confirmed by another group via Cre-loxP-based lineage tracing in a chronic injury model. Indeed, new acinar cells are derived from the acinar cells (Strobel et al. 2007). Taken together, there are multiple lines of evidence that support that acinar cells are the main contributors of pancreas regeneration post-pancreatitis.

The regeneration of the pancreas has been extensively studied via mouse models dedicated to various transcription factors. Deletion of Nr5a2, a transcription factor required for acinar cell differentiation, leads to ADM formation, increases in fibrosis and inflammation followed by tissue atrophy upon pancreatitis induction, suggesting that Nr5a2 is critical to maintain proper organ homeostasis (von Figura et al. 2014). SOX9, a duct specific transcription factor is upregulated in ADM post-acute pancreatitis and acinar cell specific

overexpression of SOX9, upon injury leads to the formation of metaplastic lesions, precursors for pancreatic ductal adenocarcinoma (PDAC) (Kopp et al. 2012). Likewise, germline deletion of MIST1, an acinar cell maturation transcription factor, delays tissue recovery post-AP (Kowalik et al. 2007). Recent studies with conditional knockout of *Ptf1a* in mice, led to acinar atrophy along with elevated inflammation and stroma accumulation upon acute pancreatitis induction (Krah et al. 2015). Taken together, these findings suggest that studying transcription factors in the context of tissue regeneration can assist in designing effective drug therapies to treat patients.

1.4 MIST1 Transcription Factor Review

MIST1 (Bhlha15) is a basic helix-loop-helix (bHLH) transcription factor, consisting of a loop in between two alpha-helices and a basic region required for DNA binding. MIST1 was first isolated by a yeast one-hybrid technique (commonly used to determine a protein's affinity to a certain DNA element) by its affinity to bind to a conserved DNA motif referred to as an E- box (-CANNTG-) (Lemercier et al. 1997). Detail characterization of the rat *Mist1* gene revealed the presence of two exons with the entire coding region situated in the second exon and a 2.8 kb 3' untranslated region (Lemercier et al. 1997; Lemercier et al. 1998; Lemercier et al. 2000). The *Mist1* gene encodes a 197 amino acid MIST1 protein. Studies utilizing various MIST1 truncations showed that the HLH domain is essential for MIST1 dimerization while addition of the basic region (bHLH) is essential for active DNA binding and gene transcription (Zhu et al. 2004; Tran et al. 2007; Lemercier

et al. 1998). Interestingly, MIST1 lacks a separate transcription activation domain (TAD) or a separate transcription repression domain (TRD) (Tran et al. 2007) suggesting that it utilizes cofactor proteins in order to regulate transcription. *In vitro* studies performed to identify protein binding partners identified Sin3-associated polypeptide 18 (SAP18), a component of the histone deacetylase complex, as a possible binding partner of MIST1. This finding suggests that a MIST1:SAP18 complex could be one mechanism by which MIST1 functions as a repressor (Jia 2008). However, because this study utilized pancreatic cancer cells to identify the binding partners of MIST1, a better model is required. An ideal mammalian system needs to be established to find the relevant binding partners to MIST1.

Molecular studies on MIST1 have demonstrated that MIST1 can both homodimerize and heterodimerize with other bHLH factors (Lemercier et al. 1998; Zhu et al. 2004). *In vitro* studies using electrophoretic mobility shift assays (EMSA) suggested that MIST1 can form homodimer (MIST1:MIST1) and heterodimer (MIST1:E12; MIST1:E47) complexes (Lemercier et al. 1998). However, *in vivo* studies performed by Tran et al., demonstrated that MIST1 preferably forms homodimers and binds to TA-E-box DNA conserved sites (Tran et al. 2007).

Mist1 is an evolutionary conserved gene across various organisms. In *Drosophila melanogaster*, its homolog is known as *DIMMED* and has 78% similarity in the bHLH domain to mammalian *Mist1* (Moore et al. 2000). DIMMED is dedicated to regulate neuroendocrine cells and to help determine their fate. Loss of function studies revealed severe reduction in neurosecretory peptides (Hewes et al. 2006; Hewes et al. 2003; Park & Taghert 2009). Likewise, the zebrafish

(*Danio rerio*) *Mist1* was first identified in 2007 with 77% similarity in the bHLH region to mouse *Mist1* (Guo et al. 2007). *Mist1* knockdown in zebrafish develop morphological embryonic defects. *In situ* hybridization studies revealed that *Mist1* morpholino injected (to induce gene knockdown) zebrafish were unable to develop a normal pancreas and the embryos also lost the hindbrain boundary (Guo et al. 2007).

MIST1 is not only evolutionarily conserved, but is also expressed in various mammalian tissues. MIST1 is expressed primarily in serous secretory cells including the acinar cells of the submandibular and lacrimal of the salivary glands (Pin et al. 2000), chief cells of the stomach (Ramsey et al. 2007; Pin et al. 2000), and lactating cells of the mammary gland (Zhao et al. 2006; Pin et al. 2000). Recent studies have also revealed MIST1 expression in antibody secreting plasma cells (Yeung et al. 2011). In the adult pancreas, MIST1 is expressed in the acinar cells of the exocrine compartment (Pin et al. 2000). This ubiquitous expression of MIST1 in secretory cells strongly suggests its role in establishing or maintaining proper secretory capabilities.

1.4.1 MIST1 in the Pancreas and Pancreatic Diseases

During pancreas development, MIST1 expression is first detected at e.13.5 in mice (Pin et al. 2000) and in the adult pancreas, MIST1 is exclusively restricted to the acinar cells of the exocrine compartment (Pin et al. 2001). Studies conducted to investigate the role of MIST1 in the pancreas involved the generation of *Mist1*^{KO} mice by replacing the *Mist1* alleles with *LacZ* gene. These mice revealed that

embryonic deletion of *Mist1* disrupts the apical-basal polarity in acinar cells which was confirmed by mislocalization of nuclei, ER, golgi apparatus and zymogens (Luo et al. 2005; Pin et al. 2001). Additionally, *Mist1*^{KO} mice also show increased nuclear dysplasia and vacuole formation (Pin et al. 2001).

Furthermore, Pin et. al. (2001) confirmed that in the absence of the *Mist1* gene, the genes dedicated to perform calcium exocytosis, including the *CCK A receptor* and *IP$_3$ Receptor Type 3* are all affected, suggesting a key role for MIST1 in maintaining proper cellular exocytosis.

Acinar cells closely depend on cell-cell communication to perform their task of synthesizing, packaging and secreting digestive enzymes. Studies performed in *Mist1*^{KO} mice also confirmed that CONNEXIN32 (a gap junction protein) was markedly reduced suggesting that indeed *Mist1* is essential for maintaining the proper communication among acinar cells (Rukstalis et al. 2003). Confirming the critical role of *Mist1* in exocytosis, *Mist1*^{KO} mice were defective in proper calcium signaling (Luo et al. 2005). Defects in calcium signaling directly affected enzyme secretion (Williams 2001). Indeed, *Mist1*^{KO} mice are deficient in secreting digestive enzymes including amylase, trypsin and lipase (Luo et al. 2005; Direnzo et al. 2012). Taken together, MIST1 plays a role of gatekeeper in maintaining acinar cell identity, cell-cell communication and exocytosis.

As a TF, MIST1 is tasked with controlling gene transcription. *Mist1*^{KO} mice show decreased transcripts level of *Connexin32* (*Cx32*), which encodes a gap junction protein involved in exocytosis and cell-cell communication (Rukstalis et al. 2003). Likewise, studies performed in chief cells of the stomach revealed that

MIST1 regulates the transcription of *Rab26* and *Rab3D*, which encode for small GTPases and are essential for granule maturation (Tian et al. 2010). Additionally, MIST1 directly regulates a gene encoding a secretory calcium ATPase (*Atp2c2*) that is required for proper calcium-mediated exocytosis in pancreatic acinar cells (Garside et al, 2010). In contrast, gene transcription of *Rnd2*, a gene in the small Rho GTPase family, is repressed by MIST1 binding (Direnzo et al. 2012). A gene array analysis helped to identify the gene targets of MIST1 where. whole genome expression revealed 949 genes that were differentially expressed between $Mist1^{WT}$ and $Mist1^{KO}$ mice (Direnzo et al. 2012). This study further validated two sets of genes (activated/repressed) that MIST1 directly regulated including the MIST1 target genes that were confirmed previously. For example, *Rab3d*, *Htra2*, *Uba5*, *Rab27a*, *Abcb6*, *Cx32*, *Atp2c2*, *Wdyhv1*, *Copz2* and *Foxp2* were directly activated by MIST1. In contrast, *Slc35d1*, *Nox4*, *Gstm4*, *Nfe2l2*, *Rnd2*, *Aldh1a1*, *Ptgr1*, *Cldn10*, *Ppap2b* and *Smarca1* genes were repressed by MIST1 (Direnzo et al. 2012). Together, this study established that MIST1 regulates a wide array of genes and that understanding these genes can be helpful in further elucidating the role of MIST1.

Mouse models have been essential tools in deciphering the roles of various transcription factors in human pancreatic diseases including pancreatitis and pancreatic cancer and MIST1 is not an exception. Studies have revealed that $Mist1^{KO}$ mice alone can form pancreatic lesions (a precursor to pancreatic cancer development), as the mice age. Immunohistology of the mice pancreata showed increased ductal markers including cytokeratin-20. The lesion formation in these

mice was directly associated with the loss of β-catenin (required for cell-cell adhesion) (Pin et al. 2001), suggesting that MIST1 is essential in preventing pancreatic lesion formation. Likewise, in a caerulein (analog of cholecystokinin) acute pancreatitis model, *Mist1*^{KO} mice were shown to develop pancreatitis with a significant delay in organ recovery (Kowalik et al. 2011). Additionally, *Mist1*^{KO} mice developed accelerated pancreatic intraepithelial neoplasia (PanIN) lesions upon oncogenic *Kras*^{G12D} activation (Shi et al. 2009). This phenomenon is associated with epidermal growth factor receptor (EGFR) and Notch signaling pathways (Shi et al. 2009). Together, these studies show that MIST1 plays a protective role in the diseases including acute pancreatitis and PDAC, suggesting its role as a tumor suppressor.

Interestingly, the defects of *Mist1*^{KO} mice can becompletely restored by using a Cre-mediated inducible *Mist1* transgenic mouse model (*Mist1*^{KO}*; LSL-Mist1*^{Myc}) (Direnzo et al. 2012). Upon *Mist1* re-expression in adult *Mist1*^{KO} mice, these mice were able to form organized apical-basal polarity. Likewise, cytoskeletal restoration occurred with membranous actin and E-cadherin expression being induced upon *Mist1* expression in pancreatic acinar cells. Additionally, the mice also re-established proper cell-cell communication and amylase secretion. Importantly, gene array analysis performed in *Mist1*^{WT}, *Mist1*^{KO} and *Mist1*^{KO}*; LSL-Mist1*^{Myc} mice revealed 37% of MIST1 target genes were re-expressed in *Mist1*^{KO}*; LSL-Mist1*^{Myc} mice as early as 36 hours (Direnzo et al. 2012). The inducible *Mist1* transgenic mouse model also showed that sustained *Mist1* expression was able to inhibit PanIN and ADM formation under Kras conditions

(Shi et al. 2013). These findings suggest that MIST1 has a role in preventing diseases.

Most of the above mentioned studies utilized germline *Mist1*^{KO} mice to characterize the role of MIST1 in the context of pancreatic diseases. It is yet to be explored if the embryonic defects in *Mist1*^{KO} mice make these mice more susceptible to diseases. One focus of this thesis was to generate a conditional *Mist1*^{KO} mouse in order to fully elucidate the role of MIST1 is diseases, including pancreatitis and pancreatic cancer.

CHAPTER 2. MATERIALS AND METHODS

2.1 Mouse Strains

Mist1$^{CreERT/+}$ and *LSL-Mist1*^{myc} (*iMist1*^{myc}) mice used in this research have been described previously (Shi et al. 2009; Direnzo et al. 2012; Habbe et al. 2008). *Mist1*$^{lox/+}$ mice were produced by generating a *Mist1* targeting vector containing *loxP* sites flanking the entire *Mist1* coding region within exon 2 (Pin et al. 1999). In addition, a small biotin-tag (de Boer et al. 2003) and MYC-tag were added to the N-terminus and C-terminus of the MIST1 open reading frame, respectively. ES cell electroporation and blastocyst injections were performed by the Purdue University Transgenic Mouse Core Facility. *Mist1* conditional knock-out (*Mist1 cKO*) mice (*Mist1*$^{CreERT/lox}$) were produced by standard crosses. Induction of Cre-ER^{T2} activity was accomplished by administration of tamoxifen (Tam) (200 µl of 20 mg/ml) via oral gavage to adult mice (6-8 wk). A typical experiment involved two injections on two consecutive days. The zero time point post-Tam was taken at seven days following the last administration. All experiments were performed with mice on a C57BL/6 background and all animal studies were conducted in compliance with NIH and the Purdue University IACUC guidelines.

2.2 Tamoxifen Preparation

Tamoxifen (SIGMA: T-5648) was freshly prepared in corn oil (SIGMA: C-8267) a day before each oral gavage administration. In order to make 20mg/mL concentration, 5 mL corn oil was placed in a scintillation vial and heated to 42°C in a water bath for 30 mins. The equilibrated (at room temperature) tamoxifen was then weighed and added to the oil. The vial was covered in aluminum foil to keep it from light and placed on a shaker incubator at 37°C incubator for six hrs or until the tamoxifen was completely dissolved. Tamoxifen was then stored at 4°C until use.

2.3 Acute Pancreatitis (AP) Induction

Caerulein (Sigma-Aldrich) preparation for injections was done by dissolving in sterile PBS. The stock solution was stored at -20°C and the dilution was prepared fresh on the day of injections. AP was induced by caerulein via intraperitoneal (i.p) injections. In brief, 6-8 wk adult mice were given eight hourly i.p. injections of caerulein for two consecutive days (50-µg/kg) body weight). Control mice received PBS, a vehicle control. Mice were sacrificed by CO_2 inhalation and pancreata samples were harvested for paraffin blocks, protein and RNA at various time points following the last caerulein injection, which was considered time 0.

The mice were also administered the thymidine analog BrdU (5-bromo-2'-deoxyuridine) (200µl of 10mg/ml) in PBS at least six hours prior to sacrifice. For all analyses, 3-7 mice per time point/genotype/experimental condition were used.

2.4 Histology and Immunohistochemistry

Mouse pancreata were immediately fixed in 10% neutral buffered formalin. Fixed tissues were processed using Shandon Citadel 1000 tissue processor and then embedded in paraffin. Sections were cut at thickness of 5µm and used for histological staining including immunohistochemistry (IHC), immunofluorescence (IF) and hematoxylin and eosin (H&E). For all histological techniques, sections were deparaffinized in Xylenes (3X) and a series of Ethanol (100% (2X), 95% (2X), 70% (1X) and 50% (1X)) followed by ddH_2O (2X) and retrieved using the 2100-Retriever (Electron Microscopy Sciences, Hatfield, PA) and antigen unmasking solution (Vector Laboratories, Burlingame, CA). For IHC, sections were incubated in 3% H_2O_2 for 5 min to block endogenous peroxidase activity followed by an hour long blocking using the M.O.M. blocking reagent (Vector Laboratories, Burlingame, CA). Tissue sections were incubated in primary antibodies for 1 hr at room temperature. Biotinylated secondary antibodies were used at 1:200 dilution for 20 min at room temperature. IHC development was performed using vector reagents and DAB (diamonibenzidine) peroxidase substrate (Vector Labs, Burlingame, CA). Immunoflurescence secondary antibodies typically used an avidin-conjugated Alexa Fluor 588 or anti-rabbit Alexa Fluor 555 antibodies (Invitrogen, Camarillo, CA). The detailed information of the primary antibodies used in this research is listed in **Table 1**.

Table 1. Antibodies used for IHC, IF and IB

Antibody	Specie	Source	Catalog	Dilution (IB)	Dilution (IHC, IF)
CLUSTERIN	goat	Santa Cruz	sc-6420	1:1000	1:200
AMYLASE	goat	Santa Cruz	sc-12821	1:1000	n/a
TRYPSINOGEN	mouse	Sigma	sab1400226	1:1000	n/a
CYTOKERATIN-19	rat	Dev. Studies Hybridoma Bank	troma3	1:1000	1:100
SOX9	rabbit	Millipore	ab5535	1:3000	1:4000
HSP90	rabbit	Santa Cruz	sc-7947	1:1000	n/a
MIST1 (c175)	rabbit	Konieczny Lab	n/a		1:500
S6	mouse	Santa Cruz	sc-74459	1:1000	n/a
VIMENTIN	rabbit	Cell Signaling	57415	1:1000	1:100
MYC	mouse	Konieczny Lab	n/a	1:500	1:500
E-CADHERIN	rabbit	Abcam	ab53033	n/a	1:50
SMA (IA4)	mouse	Santa Cruz	sc-32251	1:100	n/a
CD45	mouse	Pharminogen	550286	n/a	1:50
INSULIN	rabbit	Proteintech	15848-1-AP	n/a	1:100
CONNEXIN-32	rabbit	Abcam	ab66613	n/a	1:100
BRDU	rat	Abcam	ab6326	n/a	1:100
AMYLASE	rabbit	Abcam	ab21156	n/a	1:100

2.5 Immunoblots

Pancreata samples were lysed in ice-cold Radioimmunoprecipitation assay (RIPA) buffer (125 mM Tris pH 7.6, 750mM NaCl, 5% NP-40, 5% sodium deoxycholate, 0.5% SDS) supplemented with 50µM protease and 100uM phosphatase inhibitors (Roche) and 200µM sodium orthovanadate (an inhibitor of protein tyrosine phosphatases and ATPases). Pancreata were lysed with 5-7 pulses using Tissue Tearer (Biospec Products, Inc). Protein samples were centrifuged at 4°C at 5000 rpm for 10 mins to remove debris. Protein concentrations were measured using the BCA protein assay kit (Thermo Scientific, Waltham, MA). Thirty micrograms of protein whole cell protein extracts were resolved on 12% SDS-PAGE, and transferred onto PVDF membranes (Bio Rad, Hercules, CA). Membranes were blocked overnight at 4°C in 5% non-fat dry milk prepared in Tris-buffered saline plus 0.1% Tween 20. The membranes were incubated in primary antibodies (**Table 1**) at room temperature for 1 hour followed by three 10 minute washes. The membranes were then incubated in horseradish peroxidase (HRP) conjugated secondary antibodies at 1:5000 dilution at room temperature for 30 minutes followed by three 10 mins washes. Immunoblots were visualized on X-ray films using an enhanced chemilluninescence (ECL) kit (Thermo Scientific, Waltham, MA) or on a ChemiDoc Touch Imaging System (Bio Rad, Hercules, CA).

2.6 RNA Expression Analysis

Total cellular RNA from pancreata was isolated using the E.Z.N.A midi kit (Omega Bio-Tek, Inc, Norcross, GA). For quantitative RT-PCR analysis, reverse transcription on 1µg of RNA was performed using the iScript cDNA synthesis kit (Bio-Rad, Hercules, CA) and gene amplification was performed using FastStart Universal SYBR Green (Roche Applied Science, Indianapolis, IN) using a Roche LightCycler 96 thermocycler (Roche Diagnostics Corporation, Indianapolis, IN). PCR was performed in duplicates and all genes were normalized to RNA encoding the ribosomal protein Rplp0 as a control. The basic procedure for performing a quantitative Real Time-Polymerase Chain Reaction (qRT-PCR) is as follows. Each PCR set-up consists of SYBR Green fluorescent mix (Roche, 10µl), cDNA (2µl), forward and reverse primers (10uM each, 1µl) and ddH_2O (7µl) for a total working volume of 20µl (performed in 96-well plates). The thermal cycling parameters for 40 cycles were as follows: 95°C for 10 sec, 59°C for 10 sec and 72°C for 10 sec. Quantitative RT-PCR primers are listed in **Table 2**. GraphPad Prism 6 software (GraphPad Software, Inc, La Jolla, CA) was used for all graphs included in this study.

Table 2. RT-qPCR Primer Sets

Gene	Oligos
Rplp0	5'-agaaactgctgcctcacatcc-3', 5'-caatggtgcctctggagatt-3
Cpa1	5'-ttaaaaaggcctcagacctca-3', 5'-cttcaagtgctccaactcctc-3'
Amylase	5'-cagagacatggtgacaaggtg-3', 5'-atcgttaaagtcccaagcaga-3'
K19	5'-cctcccgagattacaaccact-3', 5'-aggcgtgttctgtctcaaact-3'
Sox9	5'-cacggaacagactcacatctc-3', 5'-cctctcgcttcagatcaactt-3'
Mist1	5'-tggtggctaaagctacgtgt-3', 5'-catagctccaggctggtttt-3'
Atp2c2	5'-ttccagactgaaaacctgagc-3', 5'-ccccttggagtggttagtaca-3'
Copz2	5'-cttagataatgacgggcgaag-3', 5'-aagcacagacatgagcatcag-3'
Rab3d	5'-agtgtgacctggaagacgaac-3', 5'-ccagggattcattcatcttgt-3'
Rnd2	5'-tgtcctcaagaagtggcaag-3', 5'-tgacagggatgagtctctgc-3'
Mist1 cKO	5'-ggctaaagctacgtgtccttg-3', 5'-tccatcttttgggagtctagg-3'
Cx32	5'-gtgccagggaggtgtgaat-3', 5'-gataagctgcagggaccatag-3'
Elastase	5'-gcaccgagcagtatgtgaac-3', 5'-gggagagttgttagccaggat-3'
Vimentin	5'-tttccaagcctgacctcact-3', 5'-tccggtactcgtttgactcc-3'
Sma	5'-tgtgctggactctggagatg-3', 5'-gcacagcttctccttgatgtc-3'
p21	5'-gaagaccaatctgcgcttggag-3', 5'-ccacagcgatatccagacattc-3'

2.7 Microscopy, Image Analysis and Statistics

All H&E, IHC and IF images were taken using an Olympus BX51 microscope and a Dual CCD DP80 camera (Olympus Life Science Solutions). Image analysis including cell counts and area quantification, were performed using ImageJ software (NIH). In order to quantify INSULIN, AMYLASE and immune cell areas, 12-15 randomly chosen 10X fields were imaged. The pixels were first converted to µm within ImageJ in order to establish the area quantification in μm^2. MYC^+ and MYC^- acinar cells were counted in ImageJ software. All calculations were performed in GraphPad Prism 6. All the statistical analyses were presented using standard error of the mean.

P values were determined using two-tailed unpaired tests and P values of less than 0.05 were considered as statistically significant.

2.8 Image Fluorescence Quantification

Overall fluorescence intensity was measured using ImageJ, a public domain program supported by the National Institutes of Health. For each staining and time point, three image fields in the fluorescent channel for each respective staining were measured for mean gray value across the field. These values were then compiled, averaged, and normalized to control values to determine relative fluorescent intensity at various time points. The normalized values and their respective statistical measures were plotted as grouped bar graphs using GraphPad Prism.

2.9 Generation of *Elastase$_{pr}$-HA-BirA* construct

The coding sequence for HA-tagged-BirA was cloned into an Elastase promoter to permit pancreatic acinar cell specific expression. Briefly, the HA-BirA plasmid was generated by amplifying the full length HA-BirA by PCR from pcDNA-HA-BirA. The ends of the insert were digested with MfeI and inserted into the EcoRI site of the *Elastase$_{pr}$-Cre-ER^{T2}* plasmid in which Cre-ER^{T2} was removed by EcoRI digest. This elastase promoter drives exocrine pancreas-specific (acinar cells) expression. It is designed to work in transgenic animals. To release the El$_{pr}$-HA-BirA region for transgenic pronuclear injections, the DNA was digested with Not1 and the 2.7Kb fragment was isolated from the 2.9 Kb plasmid band. A NotI/XmnI double digest cut the vector fragment into a 1 Kb and 1.9 Kb fragment to permit better gel separation of the 2.7 Kb fragment. The targeting construct was then sent to the Purdue Transgenic Mouse Core Facility where Judy Hallet performed electroporation of the *El$_{pr}$-HA-BirA* (2.7. Kb product) **Figure 3-7**A construct into the. pronuclei of mouse embryos. Embryos were then implanted into the pseudo pregnant female mice. From this procedure we obtained four founder lines (F0). Genomic DNA was extracted from tail clips according to the Konieczny Lab Protocol. We identified the presence of *BirA* transgene by PCR using the following primer set: 5'-ATG CGC CGT GTT GAA GAG- 3' and 5'GGA TAT TTC ACC GCC CAT CC-3'.

2.10 Cell Culture

Transient transfections were performed using HEK293 (kidney cells). HEK293 cells were cultured in high glucose Dulbecco Eagle's medium (Gibco) and 10% fetal bovine serum (FBS). Transfections were performed using Fugene6 transfection reagent. Cells were plated in 60mm dish using $5x10^5$ cells/plate. All DNA constructs used for the transfections were used at 1 µg/µl concentration. Protein harvests were done 48 hrs post transfection in RIPA buffer with protease inhibitor cocktails at 1:50 dilution.

2.11 Nuclear and Cytoplasmic Protein Extraction from Mouse Pancreata for Mass spectrometry Analysis Using NE-PER Kit

2.11.1 Tissue Preparation

In order to prepare pure nuclear extracts from mouse pancreata to perform mass spectrometry, we decided to utilize an NE-PER Nuclear and Cytoplasm Extraction Kit from ThermoFisher Scientific. First, 100 mg of mouse pancreas was diced into small pieces and were transferred into a 1.5 ml centrifuge tube. The tissue was washed with 1 mL of sterile PBS followed by centrifugation of the tissue at 800 x g for 5 minutes. The supernatant was discarded using a pipette allowing the pellet to stay dry. The tissue was resuspended in 1 mL Cytoplasmic Extraction Reagent I - CER I (with protease inhibitor cocktail, EDTA free, Roche) which helped in cell membrane disruption to release the cytoplasmic content. A Dounce homogenizer (8-10 strokes) was used to homogenize the tissue.

2.11.2 Cytoplasmic and Nuclear Protein Extraction

The sample containing 1mL of CER I buffer was vortexted vigorously for 15 seconds to fully suspend the cell pellet and was placed on ice for 10 minutes. Ice cold Cytoplasmic Extraction Reagent II - CER II buffer was added to the tube followed by vortexing for 5 seconds. The sample was placed back on ice for another minute. After vortexing for 5 seconds the sample was centrifuged at 16,000 x g for 5 minutes. This procedure separated cytoplasmic proteins in the supernatant whereas the nuclear extract formed a pellet. After separating the supernatant in a pre-chilled tube, the pellet was resuspended in ice-cold NER buffer containing protease inhibitor cocktail. The tube content was vortexed for 15 seconds and placed on ice for 40 minutes for the nuclear proteins to be extracted. In order to separate the debris and the nuclear proteins the tube was centrifuged at 16,000 x g for 10 minutes at 4°C. The final step was to store the supernatant containing soluble nuclear proteins at -80°C until further use. A summary of inhibitors and phosphatases used per milligram of tissue is as follows:

Tissue Weight	CER I	CER II	NER	Protease inhibitor cocktail	Sodium orthovanadate	Phosphatase 2	Phosphatase 3
1 mg	1 mL	88 µL	800 µL	1:50	1:200	1:100	1:100

2.12 His-tag Pull-Down

In order to perform His-tag pull-downs using Dyanbeads, I used the recommended protocol provided by Invitrogen (Cat.no.101.03D). Briefly, 50µl of the His-tag Dynabeads were transferred to a sterile eppendorf tube. The beads were resuspended gently before use. Next, the tubes with beads were placed on

a magnetic stand until the beads and buffer separated distinctly. The supernatant was disposed via aspiration. Next 1000 µg of nuclear protein (*R26*$^{HA\text{-}BirA}$ and *Mist1*$^{BT/BT}$; *R26HA*$^{\text{-}BirA}$ mouse extracts) were added to the beads. The total volume was then brought to 700 µl using Binding/Wash buffer (50 mM NA-Phosphate, pH 8.0; 300 mM NaCl; 0.02% Tween-20). Beads and the protein were mixed well in a rotator for 20 mins at 4°C.The tubes were then placed on a magnetic stand for the beads with bound His-tag MIST1 complex to be separated from the supernatant. The supernatant was discarded and the beads with protein complexes were washed four times (3 mins each) with Binding/Wash Buffer by placing them back on the magnetic stand. In order to elute the His-tagged protein complexes, 100 µl of Elution buffer (300 mM Imidazole; 50 mM Na-Phosphate, pH 8.0; 300 mM NaCl and 0.01% Tween-20) was used. The suspension was placed in a rotater for 5 mins at 4°C. The final step was to place the suspension on a magnetic stand to separate beads and supernatant.

The beads were resuspended 100µl of His-Elution Buffer (300mM Imidazole, 50mM Na-phosphate pH, 8.0, 300mM NaCl and 0.01% Tween-20).

2.13 Streptavidin-beads Pull down Assay

In order to purify biotinylated MIST1 complexes streptavidin magnetic beads (Dynabeads M-280, Invitrogen) were used. Protein extracts from *Mist1*$^{BT/BT}$; *R26*$^{HA\text{-}BirA}$ and *R26*$^{HA\text{-}BirA}$ mice were taken for performing pull-down assays. 100µl of Dynabeads -280 were aliquoted in microcentrifuge tube after a thorough

resuspension. The supernatant was discarded using magnetic separation. The beads were then washed 4X using 700 µl of Blocking buffer (10mM Tris-HCl, 150mM NaCl, 10mg/mL BSA) and resuspended in 100µl of TBS-N buffer (10mM Tris HCl, 150mM of NaCl and 0.03% of NP-40 detergent). One milligram of nuclear protein extracts were added to the beads. The volume was brought to 600 µl using TBS-N buffer. The mixture content was placed on a rocker at 4°C for 2 hrs. After every 30 mins, the tubes were rotated. The supernatant was separated from the beads using magnetic stand, and the beads with protein complexes were washed 5Xusing 500 µl of TBS-N per wash. The beads were further washed 5X with a reducing agent TMAB buffer (Tetramethylammonium borohydride) and resuspended in 150 µl of 50mM TMAB with 0.1% Rapigest detergent. The beads were heated at 95°C for 10 mins for denaturing proteins. Upon separating the supernatant, the beads were resuspended in 150 µl of 50mM Ammonium Bicarbonate and submitted to Keerthi Jayasundera at Dr. Andy Tao's laboratory at Purdue University to perform mass spectrometry.

For each round of pull-down samples were collected for silver staining and western blot to confirm the pull-down of MIST1 complexes.

2.14 Silver Staining

Silver staining was performed to visualize protein bands present in the input and pull-down samples in 12.5% SDS-polyacrylamide gels. The gels were fixed in

40% EtOH, 10% Acetic acid, 50% ddH_2O for 1.5 hrs in a shaker at room temperature. After washing the gels in ddH_2O, the gels were sensitized in a solution containing 0.02% Sodium thiosulfate for 2 min at room temperature. The gels were washed 3X in ddH_2O. The gels were then incubated in ice cold 0.1% silver nitrate solution containing 0.02% formaldehyde. The gels were further washed in ddH_2O to get rid of extra silver nitrate. Finally, the gels were developed in 3% sodium carbonate with 0.05% formaldehyde. Yellow coloration of the gel indicated the proper development of the proteins in the gels. In order to quench the developing reaction, the gels were incubated in 5% acetic acid for 5 mins. The gels were imaged using a scanner

2.15 DNA Tail Isolation

DNA tail extractions were performed using a standard lab protocol. Briefly, 1 cm tail was clipped for DNA extraction from mouse. Tails are placed in 500 µL of Lysis buffer containing 100mM Tri-HCl, pH 8.5; 10mM EDTA; 200 mM NaCl and 0.2% SDS detergent along with proteinase K (10mg/mL) and incubated at 56°C overnight for efficient digestion. The samples were then vortexted briefly and spun at 14,000 rpm for 10 minutes at room temperature. The supernatant was separated from the debris pellet and transferred to fresh tubes. In order to precipitate DNA from the supernatant, 500 µL of isopropyl alcohol was added and incubated at -20°C for 10 minutes. The samples were quickly mixed and spun at 14,000 rpm for 10 minutes at room temperature. The supernatant was discarded and the pellet

was washed with 500μL of 70% ethanol and spun at 14,000 rpm for 5 minutes. The supernatant was discarded and the pellet was completely air-dried at room temperature. The DNA was resuspended in 100 μL of TE buffer (10mM Tris-Hcl, pH 8.0; 1mM EDTA) and was dissolved at 56°C for 10 minutes. In order to perform PCR analysis, 2 μL of DNA was used. Genotyping primers used for all the projects are listed in **Table 3**.

Table 3.Genotyping Primer Sets

Genotype	Oligos
Mist1$^{CreER/+}$	5'-ggttaaagcaaattgtcaagtacgg-3'; 5'- atagtaagtatgtgcgtcagcg-3';5'-gaagcattttccaggtatgctcag-3'
LSL-Mist1^{Myc}	5'-cgggatccttggtacctatgaag-3'; 5'-cgggatcctcagaagccatagag-3'
Mist1$^{CreERT/lox}$	5'- agc tgc act ggc taa gga ag-3' ; 5'-gcc ggt tct tgg tct tca ta-3';5'-gcc ggt ttt tgg tct tca ta-3'
LSL-Kras^{G12D}	5’ - tct gaa tta gct gta tcg tca agg- 3’; 5’- gtc gag gga cct aat aac ttc gta-3’
R26-BirA	5’- gtg taa ctg tgg aca gag gag-3’; 5’- gaa ctt gat gtg tag acc agg-3’
ZsGreen1	5’- aag gga gct gca gtg gag ta- 3’; 5’- ccg aaa atc tgt ggg aag tc -3’; 5’- ccg aaa atc tgt ggg aag tc - 3’; 5’- aac cag aag tgg cac ctg ac – 3’

.

CHAPTER 3. UTILIZATION OF A NOVEL MOUSE MODEL TO STUDY THE IMPORTANCE OF MIST1-DEPENDENT TRANSCRIPTIONAL REGULATION IN PANCREATIC ACINAR CELLS

3.1 Introduction

MIST1 is a 197 amino acid basic helix-loop-helix (bHLH) transcription factor expressed in pancreatic acinar cells of the adult pancreas (Lemercier et al. 1997; Pin et al. 2001). Mice lacking the *Mist1* alleles (*Mist1*^{KO}) exhibit defects in acinar cell organization, including improper zymogen localization, impaired secretion and defective cell-cell communication, highlighting the importance of MIST1 in normal acinar cell physiology. MIST1 is also expressed in other serous secretory cells including the acinar cells of the salivary glands, chief cells of the stomach, and lactating cells of the mammary gland (Pin et al. 2001; Johnson et al. 2004; Ramsey et al. 2007; Pin et al. 2000). This ubiquitous presence in secretory cells and the common phenotype observed in *Mist1*^{KO} cells in these different organs strongly suggests a role for MIST1 in establishing or maintaining proper secretory capabilities.

Molecular studies on MIST1 have demonstrated that MIST1 can both homodimerize and heterodimerize with other bHLH factors (Lemercier et al. 1998; Zhu et al. 2004). *In vitro* studies using electrophoretic mobility shift assays (EMSA) suggested that MIST1 can form homodimer (MIST1:MIST1) and heterodimer

(MIST1:E12; MIST1:E47) complexes (Lemercier et al. 1998) and bind to a conserved DNA motif referred to as an E-box (-CANNTG-). A study using pancreatic cell lines confirmed MIST1's preference to forming a homodimer complex and its affinity towards TA-E-box DNA sequences (-CATATG-) (Tran et al. 2007).

MIST1 regulates transcription of numerous genes. The transcript levels of *Connexin32* (*Cx32*), which encodes a gap junction protein involved in exocytosis and cell-cell communication, are decreased in *Mist1*^{KO} mice (Rukstalis et al. 2003). Likewise, Tian et al. (2010) confirmed that *Rab26* and *Rab3D*, which encode for small GTPases and are essential for granule maturation are directly regulated by MIST1. Additionally, another group confirmed that MIST1 directly regulates a gene encoding a secretory calcium ATPase (*Atp2c2*) that is required for proper calcium-mediated exocytosis in pancreatic acinar cells (Garside et al, 2010). Work by other Konieczny lab members, however, has established that transcription of *Rnd2*, a gene in the small Rho GTPases family, is actually repressed by MIST1 binding (Direnzo et al. 2012). Importantly, whole genome expression analyses have revealed that 949 genes were significantly different in their expression patterns between *Mist1*^{WT} and *Mist1*^{KO} mice (Direnzo et al. 2012). The same study validated two sets of genes (activated/repressed) that MIST1 directly regulated including the MIST1 target genes that were confirmed previously. For example, in a subset of target genes we showed that MIST1 activated *Rab3d*, *Htra2*, *Uba5*, *Rab27a*, *Abcb6*, *Cx32*, *Atp2c2*, *Wdyhv1*, *Copz2* and *Foxp2* expression whereas repressed *Slc35d1*, *Nox4*, *Gstm4*, *Nfe2l2*, *Rnd2*, *Aldh1a1*, *Ptgr1*, *Cldn10*, *Ppap2b* and

Smarca1 genes (Direnzo et al. 2012). Additionally, the same study confirmed that MIST1 preferentially bound CATATG or CAGCTG E-box sites to regulate its target genes (Direnzo et al. 2012).

The dual activator/repressor role for MIST1 suggests that a variety of cofactors may be necessary to form complexes with MIST1 in order to either activate or repress the expression of specific target genes. Studies utilizing truncated forms of MIST1 revealed that the HLH domain is essential for MIST1 dimerization while addition of the basic region (bHLH) is adequate for active DNA binding and gene transcription (Zhu et al. 2004; Tran et al. 2007) (**Figure 3-1**). Interestingly, MIST1 lacks a separate transcription activation domain (TAD) or a separate transcription repression domain (TRD). Together, findings from MIST1 protein and gene target studies led us to hypothesize that MIST1 utilizes cofactor proteins as a means to activate or repress specific target genes.

Experimental approaches to identify and characterize the role of cofactors involved in MIST1 transcriptional activity have previously been conducted utilizing cell culture approaches (Jia 2008). Here, an *in vitro* biotin-streptavidin system was employed to purify MIST1 complexes from the rat exocrine pancreatic tumor cell line, AR42J. In order to identify protein partners from these complexes a tandem mass spectrometry approach was used. Jia et al. (2008) identified Sin3-associated polypeptide 18 (SAP18) as a potential binding partner of MIST1.

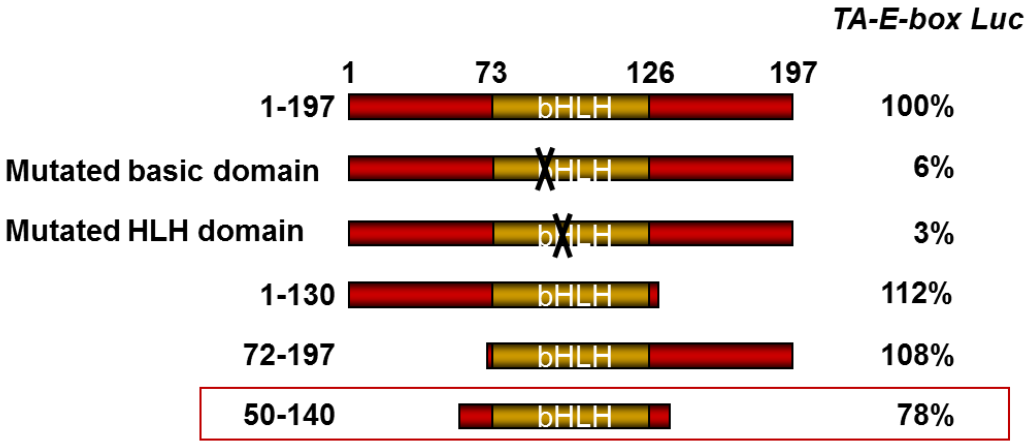

Figure 3-1. The bHLH domain is sufficient for MIST1 transcriptional activity. Selected truncations of MIST1 and their respective transcriptional activity on TA-E-Box luciferase reporter genes are displayed. Despite the severe truncation, the bHLH region (50 - 140 aa) is sufficient to drive transcription (Modified from (Tran et al. 2007)).

SAP18 is a component of the histone deacetylase complex suggesting that a MIST1:SAP18 complex could be one mechanism by which MIST1 functions as atranscriptional repressor of gene targets, including *Rnd2* and *K19* (Jia 2008). Unfortunately, although these studies were suggestive of MIST1 having unique co-factors, cell culture studies have significant limitations. For example, AR42J cells are pancreatic cancer cells and may not be representative of normal acinar cell function, including exhibiting regulated secretion. Additionally, this study involved overexpression of a MIST1 protein that was far above normal levels. These represented serious deficiencies, necessitating the need to develop an alternative approach that would allow efficient formation of MIST1-cofactor complexes within a physiologically normal environment and that could be easily purified and analyzed. One of the alternative approaches to achieve this goal was to use an efficient mouse model.

In an attempt to characterize the normal function of MIST1, we hypothesized that MIST1's transcriptional activity is dependent on cofactor interactions. This hypothesis was addressed by taking advantage of a novel BT-MIST1$^{His\text{-}Myc}$ mouse model where a modified MIST1 protein was expressed from the endogenous *Mist1* locus, permitting us to co-immunoprecipitate MIST1 protein complexes using Streptavidin-HRP conjugated magnetic beads. In order to identify potential MIST1 binding partners, Liquid Chromatography-Mass Spectrometry/Mass Spectrometry (MS/MS) was performed. Following MS/MS, candidate proteins were analyzed by bioinformatics approaches.

3.2 Results

3.2.1 Biotin-Streptavidin System to Purify MIST1 Protein Complexes

Protein immunoprecipitation is a powerful tool to study protein function and regulatory pathways. In order to purify protein complexes for studying protein-protein interactions, there are a number of affinity-based systems that can be used. These systems typically utilize antibodies raised against the protein of interest or raised against a specific peptide epitope tag that can be associated with the protein of interest (Jarvik & Telmer 1998; Rigaut et al. 1999). These techniques involve multi-step affinity purification where the protein complex can be easily washed away during the process. To overcome this issue, single-step approaches have been developed to purify biotinylated proteins via the use of the streptavidin/biotin system (de Boer et al. 2003).

Biotinylated purification consists of using Biotin (Vitamin H), a small coenzyme that is produced by plants, fungi and many bacteria (Cronan 1990). In the presence of a biotin ligase, such as BirA, the biotin molecule is covalently added to specific lysine residues in an amino acid sequence specific fashion. Individual biotin ligases exhibit different specificities. The *E. coli* biotin ligase BirA recognizes a single lysine (K) residue in the amino acid sequence MASSLRQILDSQ**K**MEWRSNAGGS. Thus, proteins containing this biotin tag (BT) can be specifically modified solely by BirA. (Streaker & Beckett 2006; Choi-Rhee et al. 2004; Wilson et al. 1992).

The affinity of biotin to avidin/streptavidin is remarkably high compared to that of any generic affinity purification system. This noncovalent interaction is the

strongest characterized protein-ligand non-covalent interaction known, with a dissociation constant (Kd) of 10^{-15} M (Anon n.d.). Due to this property, avidin-biotin interactions have been utilized to purify biotinylated proteins from cell or tissue extracts in many different systems (Driegen et al. 2005; Huang & Jacobson 2010; Cronan 1990). The biotin/streptavidin technique has multiple advantages over other affinity-purification strategies including (i) high affinity allows efficient protein purification; (ii) the avidin-biotin interaction can endure stringent washing conditions; (iii) the high affinity minimizes non-specific background proteins; and (iv) this system avoids the use of antibodies which are likely to bind to non-specific proteins (Kim et al. 2009; de Boer et al. 2003). Given these advantages, I set out to generate a biotinylated mouse model to study the binding partners of MIST1.

3.2.2 Efficient Biotinylation of BT-tagged MIST1 via Cell Transfection Studies in HEK293 Cells.

Prior to generating a biotinylated mouse model to study MIST1 co-factors, it was essential to validate the streptavidin/biotin system in cell culture. Our laboratory had successfully introduced a 23 aa BT tag (a biotin acceptor) on to the N terminus of MIST1 along with two other epitope tags: (i) 10 aa MYC tag and (ii) 6X His-tag to the C-terminus (BT-MIST1$^{Myc/HIS}$- hereafter known as MIST1$^{BT/Myc}$). The presence of two tags (BT, MYC) allows efficient purification of biotinylated proteins via a tandem purification process. Likewise, another epitope tag, HA was introduced onto the BirA ligase (HA-BirA).

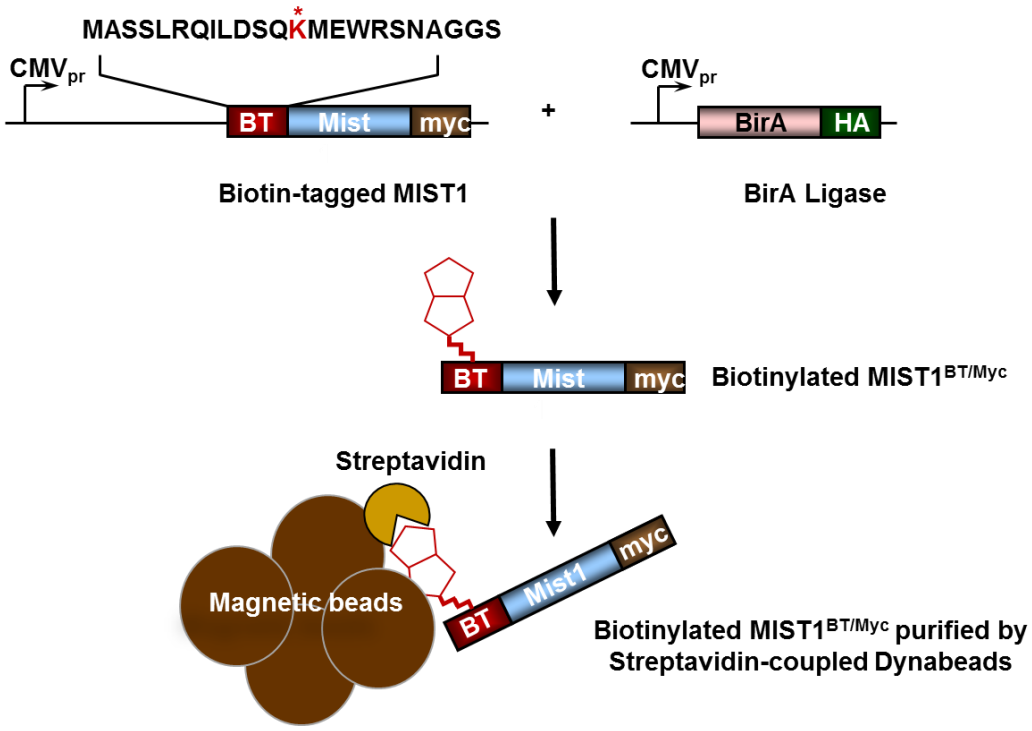

Figure 3-2. Schematic for the biotinylation of MIST1$^{BT/Myc}$ by BirA ligase. HEK293 cells were transfected with expression plasmids Mist1$^{BT/Myc}$ and HA-BirA. Both DNA constructs are driven by the CMV promoter. The 23 aa BT tag fused to the N terminus of MIST1 is shown above with the asterisk indicating the central lysine residue that is biotinylated by BirA ligase. This biotinylated complex was purified using Streptavidin-coupled magnetics beads. Adapted from (Jia 2008).

In order to perform cell culture experiments to validate the efficiency of the streptavidin/biotin system, MIST1$^{BT/Myc}$ and HA-BirA (biotin ligase) cDNA constructs were cloned into pcDNA3.1 vector plasmids that utilize a human cytomegalovirus (CMV) promoter to achieve high-level gene expression (Jia 2008). These two constructs were used to carry out transient transfections in human embryonic kidney (HEK) 293 cells.

The schematic to achieve biotinylation of BT-tagged MIST1 by BirA ligase is illustrated in **Figure 3-2**. Briefly, HEK293 cells were transfected with expression plasmids encoding different forms of *Mist1* and *BirA* and then whole cell protein extracts were harvested 48 hours post-transfection to monitor protein expression and biotinylation by immunoblots. As illustrated in **Figure 3-3**, immunoblot analysis using anti-MYC antibody revealed two patterns of bands for MIST1. The shifted bands in lane 3 and 4 represent the lower mobility biotin-tagged BT-MIST1 protein whereas the lower band in lane 2 represents the unmodified-MIST1^{Myc} protein. Another immunoblot using anti-HA antibody confirmed the expression of BirA ligase from the transfected *HA-BirA* construct. Efficient biotinylation of MIST1$^{BT/MYC}$ was confirmed using a Streptavidin-HRP conjugate. The biotinylation process did not occur when the cells were transfected with unmodified-MIST1^{Myc} only (lane 4) or co-transfected with unmodified-MIST1^{Myc} and HA-BirA (lane 2). These results also confirmed the absence of endogenous biotin ligases in the HEK293 cells to biotinylate MIST1$^{BT/Myc}$. However, biotinylation did occur when MIST1$^{BT/Myc}$ and HA-BirA were co-expressed (lane 3). In all the immunoblots cells transfected with pcDNA3 only served as a negative control.

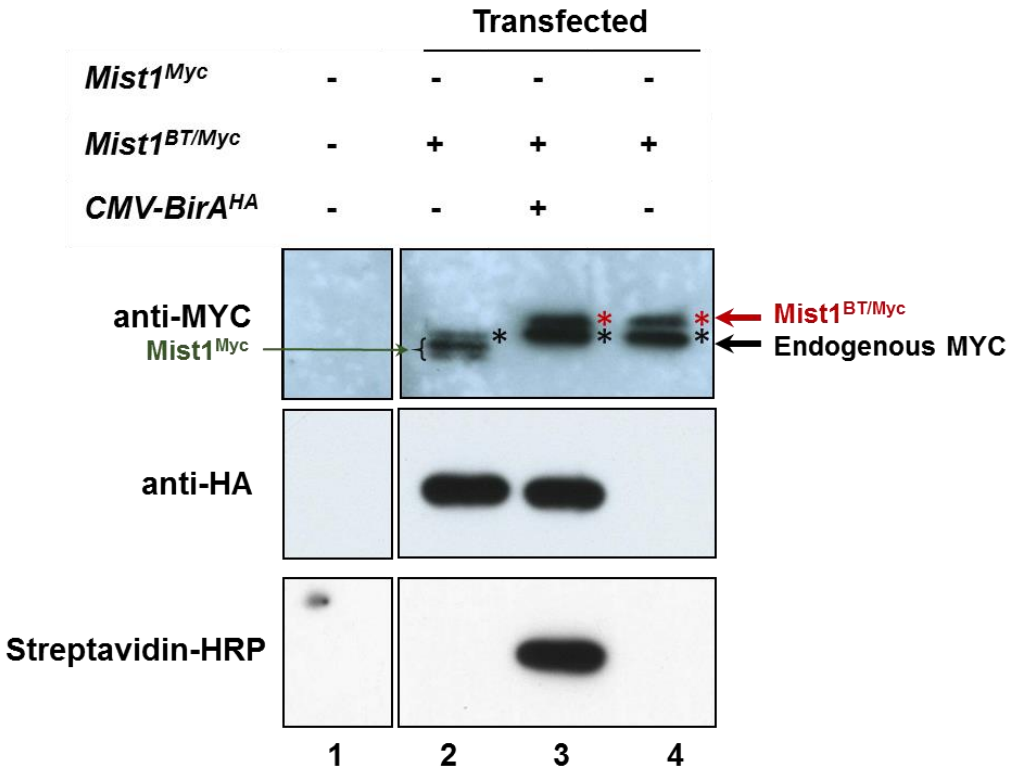

Figure 3-3. Immunoblots with anti-MYC, anti-HA and Streptavidin-HRP conjugate confirmed the expression and specific biotinylation of MIST1$^{BT/Myc}$ by HA-BirA ligase in HEK293. HEK293 cells were transfected with the pcDNA3.1 vector only as a negative control for the experiment (lane 1), co-transfected with unmodified-Mist1^{Myc} and HA-BirA constructs (lane 2), co-transfected with Mist1$^{BT/Myc}$ and HA-BirA constructs (lane 3) and Mist1$^{BT/Myc}$ alone. Anti-MYC antibody detected the expression of both tagged and untagged MIST1 (lanes 2, 3 and 4). Likewise, an anti-HA antibody confirmed the expression of BirA ligase (lanes 2 and 3). Streptavidin-HRP conjugate specifically detected only the biotinylated MIST1 (lane 3).

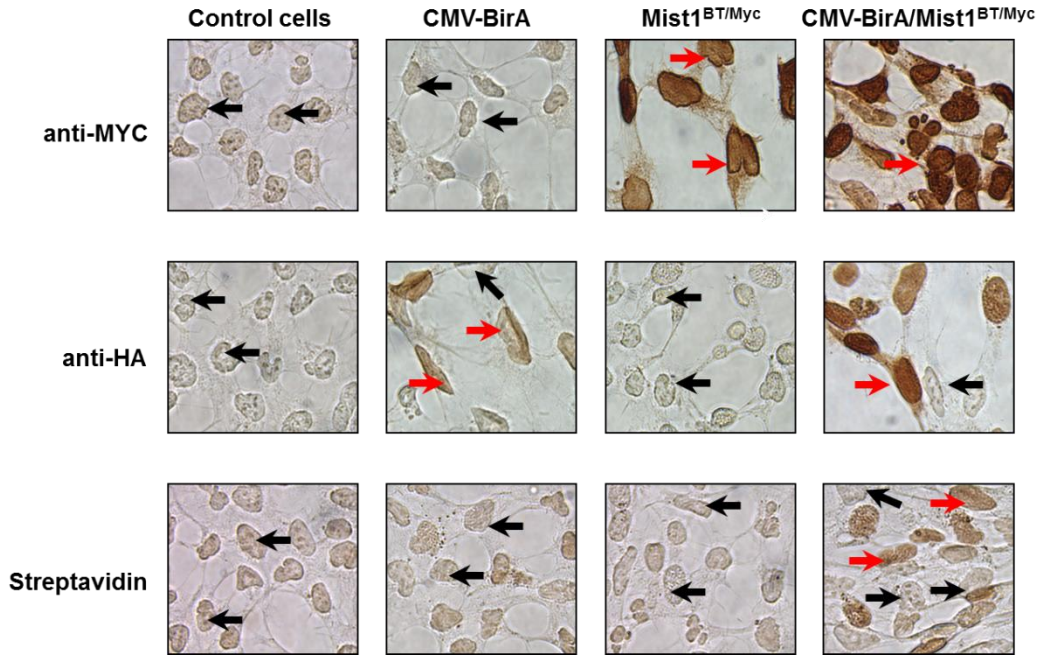

Figure 3-4. Immunohistochemistry of tranfected HEK293 cells revealed the appropriate expression of MIST1$^{BT/Myc}$, HA-BirA and biotinylation of BT-tagged MIST1 by BirA ligase. After transfection with empty vector pcDNA3.1, HA-BirA only or Mist1$^{BT/Myc}$ only and co-transfection with HA-BirA /Mist1$^{BT/Myc}$ the cells were immunostained with anti-MYC, anti-HA and streptavidin-HRP conjugate antibodies. Anti-MYC staining was positive in cells expressing MIST1$^{BT/Myc}$. Anti-HA antibody confirmed the expression of HA-tagged BirA ligase. The cells which expressed MIST1$^{BT/Myc}$ were biotinylated by BirA ligase (Streptavidin staining). Arrows indicated positive (red) and negative (black) stained cells.

The above results were further confirmed by performing cell staining immunohistochemistry on transfected HEK293 cells (**Figure 3-4**). Briefly, HEK293 cells were transfected using the same plasmids as before, and then the cells were fixed 48h post-transfection and stained using the DAB peroxide substrate method. MYC and HA antibodies confirmed the expression of MIST1 and BirA respectively. As predicted, Streptavidin-HRP conjugate detected biotinylated MIST1 only in cells co-transfected with $Mist1^{BT/MYC}$/HA-BirA plasmids. Altogether, these results confirm the synthesis of active $MIST1^{BT/MYC}$ and BirA ligase and efficient biotinylation of MIST1. Hence, we established an efficient and functional biotin-streptavidin system which allowed us to proceed to our next step.

The next goal was to test if the biotinylated $MIST1^{BT/Myc}$ complex could be purified using Streptavidin magnetic beads. Transient transfection was again carried out in HEK293 cells using the $Mist1^{BT/Myc}$ construct in the presence and absence of HA-BirA. 48 hrs post-transfection protein extracts were harvested. The quantified samples were then incubated to bind to streptavidin-coupled Dynabeads and washed to remove background/non-specific proteins. The eluted products from the beads were subjected to immunoblotting using anti-MYC antibody and Streptavidin-HRP conjugate (**Figure 3-5**). MYC immunoblotting with $Mist1^{BT/Myc}$ alone and in combination with BirA confirmed the expression of $MIST1^{BT/Myc}$ (lanes 1 and 2). Analysis of the “pulled-down” material using MYC antibody and Streptavidin-HRP showed efficient biotinylation of $MIST1^{BT/Myc}$ by BirA ligase and effective capturing of the biotinylated MIST1 complex by the beads (lane 4). As expected, $MIST1^{BT/Myc}$ alone was not biotinylated and the beads did not capture

any of the proteins (lane 3). Interestingly, the input materials detected non-specific protein bands in the Mist1$^{BT/Myc}$ alone and Mist1$^{BT/Myc}$/HA-BirA transfected cells. However, in the “pulled-down” samples the background bands were absent. This phenomenon confirms the efficiency of the Streptavidin beads in capturing true binding partners of MIST1 protein. Overall, these results confirmed that tagged MIST1 is efficiently biotinylated by BirA ligase and can be purified using the Streptavidin-coupled Dynabeads with limited non-specific biotinylation.

Once we established the efficacy of the streptavidin/biotin system *in vitro*, I sought out to translate this approach into an *in vivo* mouse model in order to purify and analyze MIST1 binding factors.

3.2.3 Generation of *Elastase$_{pr}$- HA-BirA* mice

In an attempt to generate biotin-tagged MIST1 protein exclusively in the pancreas we first decided to generate a transgenic mouse that would express the *BirA* biotin ligase only in pancreatic acinar cells. To accomplish this goal we took advantage of the rat 500 *elastase* gene’s bp promoter region that is known to drive transgene expression in pancreatic acinar cells (Zhu et al. 2004). Briefly, the coding sequence for HA-tagged-BirA (generated by PCR) was cloned into the pBS-*Elastase$_{pr}$* plasmid by standard procedures to generate *Elastase$_{pr}$-HA-BirA* (*El$_{pr}$-HA-BirA*) (**Figure 3-6**). The *El$_{pr}$-HA-BirA* plasmid was then further processed to generate a transgenic mouse.

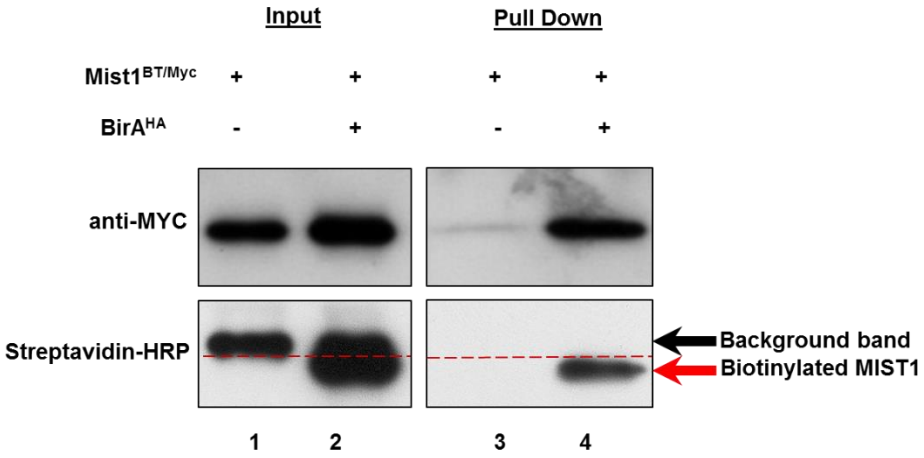

Figure 3-5. Immunoblot analysis confirms a successful pull-down of biotinylated MIST1$^{BT/Myc}$ using Streptavidin-coupled magnetic beads. Anti-MYC antibody detected the expression of MIST1$^{BT/Myc}$. A Streptavidin-HRP conjugate immunoblot confirmed that the MIST1$^{BT/Myc}$ protein can be "pulled-down" efficiently (red arrow). In the input samples Streptavidin-HRP detected background protein (black arrow,bands above the red dotted line).

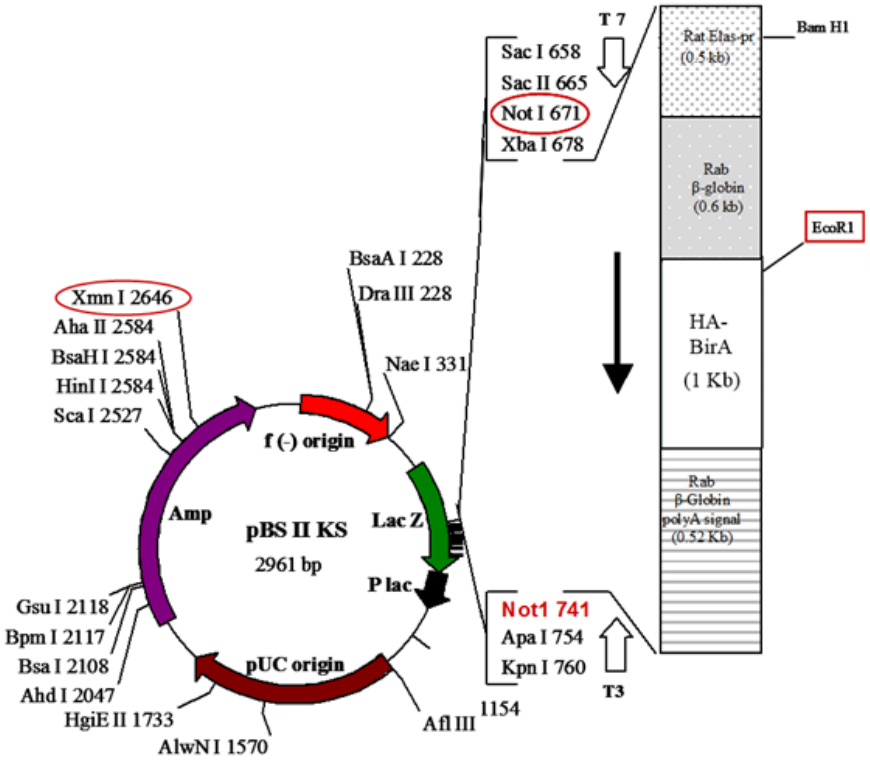

Figure 3-6. **Map of *El$_{pr}$-HA-BirA* plasmid construct generated to make a pancreatic acinar cell specific BirA ligase mouse.** The *El$_{pr}$-HA-BirA* inserted was released by Not1 digestion and this fragment was sent to the Purdue Transgenic Mouse Core Facility to generate *El$_{pr}$-HA-BirA* transgenic mice.

To generate transgenic mice expressing acinar-cell specific *BirA*, I first had to release the *El$_{pr}$-HA-BirA* region for mouse embryo pronuclear injections. The DNA was digested with Not1/Xmn1 and the 2.7 Kb fragment containing the 500 bp *Elastase* promoter, rabbit *β-globin* intron, the *HA-BirA* coding region and a 3' *β-globin* flanking region was isolated (**Figure 3-6**). The transgene construct was then sent to the Purdue Transgenic Mouse Core Facility for pronuclear injection into C57Bl/6 embryos (**Figure 3-7A**). This procedure resulted in the generation of twelve founder lines (F0). Genomic DNA was extracted from tail clips and used for genomic PCR strategies to identify which founders contained the *El$_{pr}$-HA-BirA* transgene. As shown in **Figure 3-7B**, 4 out of 12 animals (1BX, 1BY, 2BZ, 4BX) showed the expected 315 bp product, confirming incorporation of the *El$_{pr}$-HA-BirA* transgene into the mouse genome.

In order to confirm appropriate transgene expression of *El$_{pr}$-HA-BirA* in acinar cells, pancreata were harvested from lines 1BX, 1BY, 2BZ and 4BX and processed for protein and paraffin tissue blocks. Immunoblot analysis using anti-HA antibody revealed the presence of the 36 kDa HA-BirA ligase in the pancreas of the newly generated transgenic mouse lines (*El$_{pr}$-HA-BirA)* as illustrated in **Figure 3-8A**. Similarly, immunohistochemistry (IHC) performed using anti-HA antibody revealed expression of the HA-BirA ligase exclusively in acinar cells (**Figure 3-8B**). Interestingly, there was a slight mosaic expression pattern detected which has been shown to occur in other transgenic settings using the *elastase* promoter (Zhu et al. 2007). Nonetheless, expression was acinar specific. Islet and duct cells remained HA-BirA negative (**Figure 3-8**B).

In summary, we were able to generate a functional transgenic mouse line that faithfully expressed *BirA* ligase exclusively in pancreatic acinar cells. This line could therefore be used to biotinylate MIST1$^{BT/Myc}$ in pursuing our quest to identify interacting partners of MIST1.

3.2.4 Generation of *Mist1$^{BT/Myc}$* Mice

Having generated a functional *BirA* ligase transgenic (*El$_{pr}$-HA-BirA*) mouse line, we next proceeded to establish a BT-tagged MIST1 mouse model that would be required to test if BirA-mediated biotinylation would be feasible *in vivo* using transgenic mouse approaches. The goal was to generate a *Mist1$^{BT/BT}$; El$_{pr}$-HA-BirA* mouse where pancreatic MIST1 proteins and any associated co-factors could be purified by Streptavidin pull-down and analyzed by LC-MS/MS.

We independently generated a mouse line in which the BT tag was incorporated into the N-terminus of the MIST1 protein through homologous recombination strategies (Karki et al. 2015). Briefly, *Mist1$^{BT/+}$* mice were produced by generating a *Mist1* targeting vector containing *loxP* sites flanking the entire *Mist1* coding region within exon 2 (Pin et al. 1999). In addition, a small biotin-tag (de Boer et al. 2003) and MYC-tag were added to the N-terminus and C-terminus of the MIST1 open reading frame, respectively (**Figure 3-9A**). ES cell electroporation and blastocyst injections were performed by the Purdue University Transgenic Mouse Core Facility.

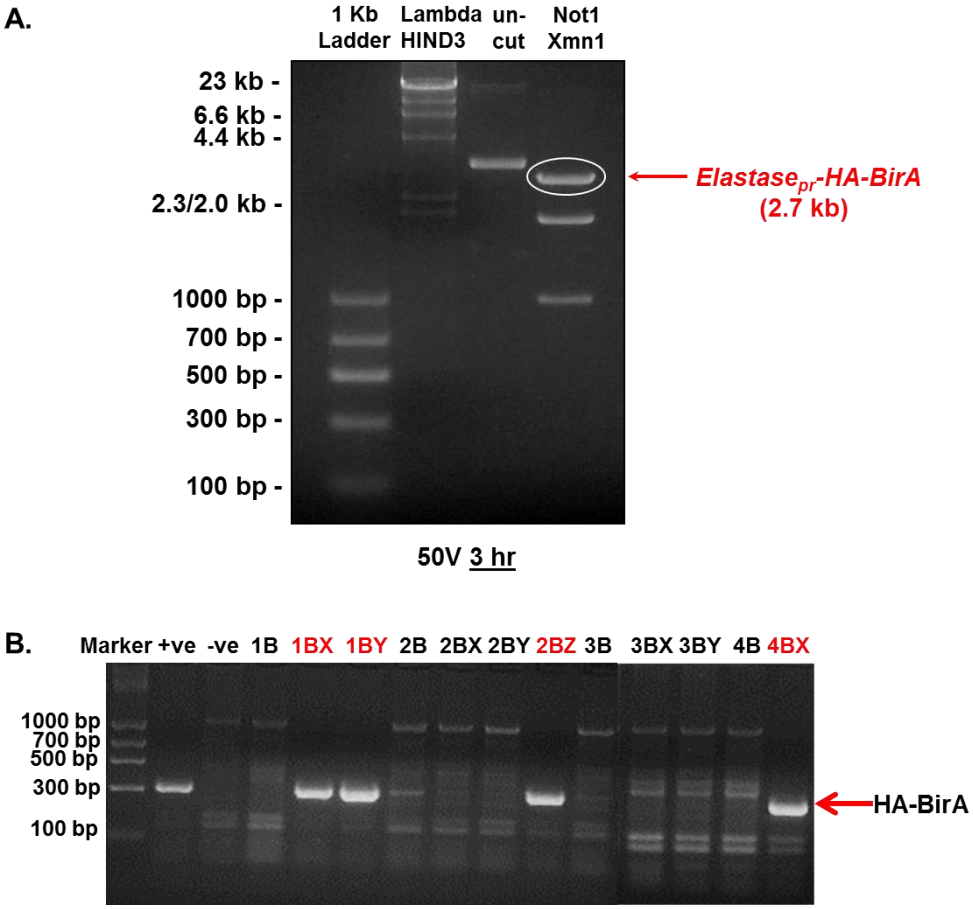

Figure 3-7. *El$_{pr}$-HA-BirA* was used to generate *El$_{pr}$-HA-BirA* transgenic mice. **(A)** Final DNA fragment of *El$_{pr}$-HA-BirA* (2.7 Kb product) generated to inject into embryo pronuclei. **(B)** PCR analysis of genomic DNA confirmed the incorporation of the *El$_{pr}$-HA-BirA* transgene in 4 of the 12 founder lines (1BX, 1BY, 2BZ, 4BX). The transgene is identified as a 315 bp product (indicated by the red arrow). WT genomic DNA was used as a negative control and the original *BirA* plasmid was used as a positive control.

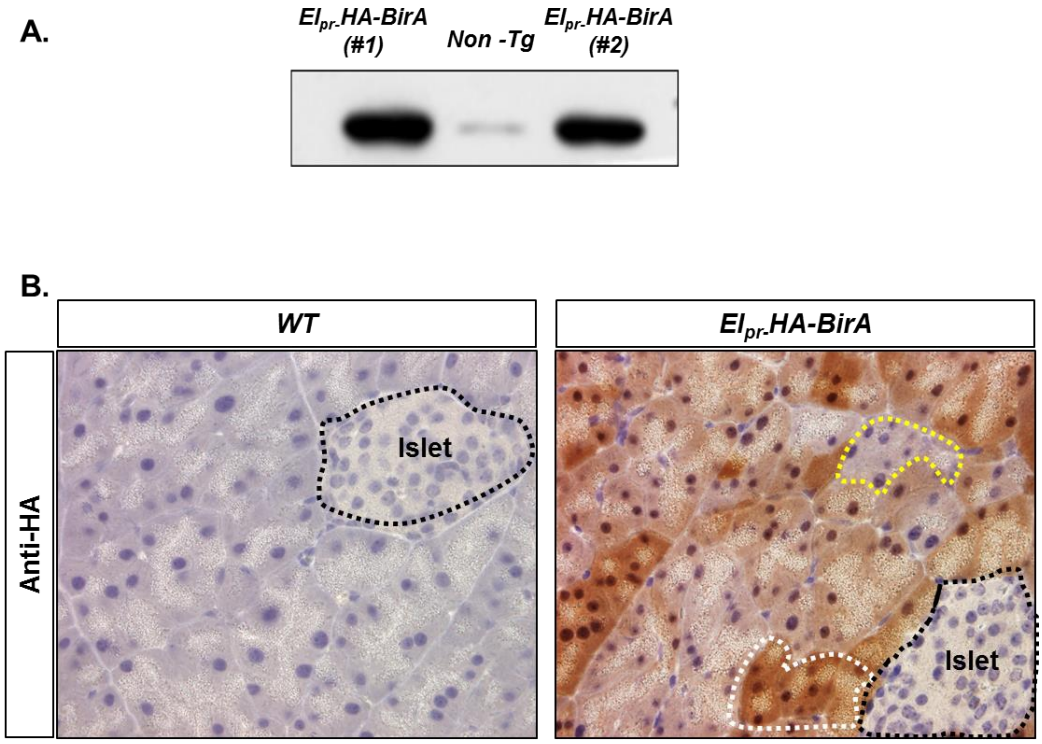

Figure 3-8. HA-tagged BirA ligase expressed in the pancreas and found in the nuclei and cytoplasm of pancreatic acinar cells harvested from *El$_{pr}$-HA-BirA* transgenic mice. (A) Immunoblot with an anti-HA antibody demonstrated the presence and expression of HA-BirA ligase in the pancreas of transgenic mice. **(B)** IHC using anti-HA antibody showed heterogeneous expression of HA-BirA ligase in both the cytoplasm and nuclei of pancreatic acinar cells. (red dotted line). Absence of BirA ligase in a subset of acinar cells (designated by yellow dotted line) confirmed the specificity of the staining. As expected, expression of HA-BirA was absent in islets (black dotted line). WT mice were used as negative control.

Subsequent screening on individual 129/SV ES cell clones identified a correctly targeted line that was used to generate chimeric mice. The chimeric mice were then crossed to C57BL/6 animals to generate germline transmission. The new *Mist1*$^{BT/+}$ animals were then backcrossed 10 generations on to a C57BL/6 background and used for subsequent studies (**Figure 3-9B).**

3.2.5 Characterization of *Mist1*$^{BT/+}$ Mice

Before generating the required mouse lines for further experiments, functionality tests had to be performed to determine if tagged MIST1 was expressed correctly in mouse tissues. In order to carry out these tests, pancreata from *Mist1*^{WT} and heterozygous *Mist1*$^{BT/+}$ mice were harvested for paraffin sections followed by IHC with anti-MYC antibody. As expected, *Mist1*^{WT} pancreata were not stained by anti-MYC antibody while *Mist1*$^{BT/+}$ pancreata exhibited strong nuclear expression of MIST1 exclusively in pancreatic acinar cells, indicating successful homologous recombination, expression, and nuclear localization of the MIST$^{BT/Myc}$ protein (**Figure 3-10**). In order to demonstrate that MIST1$^{BT/Myc}$ protein could functionally substitute for MIST1^{WT} protein in acinar cell development and function I performed studies to verify that *Mist1*$^{BT/BT}$ and *Mist1*$^{BT/+}$ mice were morphologically, phenotypically and functionally identical to *Mist1*^{WT} mice. For these studies, pancreata from *Mist1*^{WT} and *Mist1*$^{BT/BT}$ littermates were harvested for paraffin sections, proteins and RNA samples. As shown in **Figure 3-11A**,

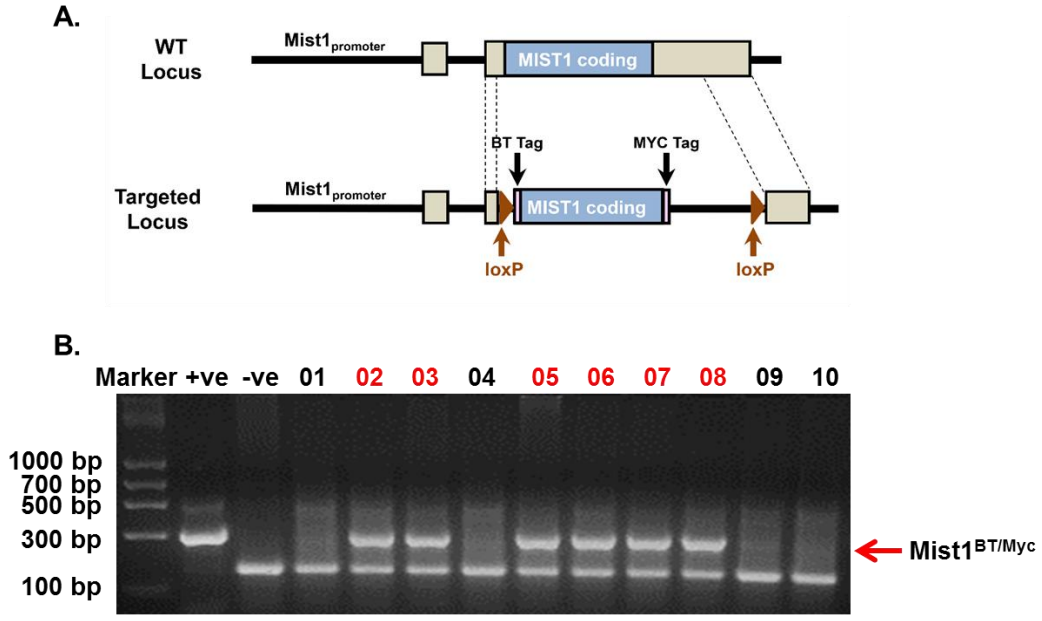

Figure 3-9. Generation of *Mist1*$^{BT/+}$ mice. (A) Schematic of how the *Mist1*$^{BT/+}$ mice were generated through homologous recombination. LoxP sites flank the entire *Mist1* coding region which is contained within exon 2. *Mist1*$^{BT/+}$ contains an N-terminal BT tag as well as a C-terminal MYC tag, allowing for tandem purification techniques. **(B)** Genotyping of F2 generations. *Mist1*$^{BT/+}$ positive offspring are identified as containing two bands (330 bp and150 bp) while the *Mist1*^{WT} shows only the expected 150 bp band. Genomic DNA from a WT mouse was used as a negative control and the targeting DNA construct was used as a positive control. Mice 02, 03, 05, 06, 07, and 08 are positive for the *Mist1*$^{BT/Myc}$ allele.

IHC using anti-MIST1 antibody detected MIST1 in *Mist1*^{WT} samples but no signal in *Mist1*^{KO} mouse pancreata. Anti-MYC staining on *Mist1*$^{BT/BT}$ mice showed acinar-specific expression of the *Mist1*$^{BT/Myc}$ gene. Importantly, *Mist1*$^{BT/BT}$ mouse pancreata also exhibited correct acinar polarity when compared to *Mist1*^{KO} acini which exhibit defective apical-basal organization (**Figure 3-11A**). Immunoblot analysis confirmed that *Mist1*$^{BT/BT}$ mice express 2-fold higher levels of MIST1$^{BT/Myc}$ when compared to *Mist1*$^{BT/+}$ mice (**Figure 3-11B**). These results confirmed that *Mist1*$^{BT/BT}$, *Mist1*$^{BT/+}$ and *Mist1*^{WT} mice were phenotypically similar.

To further verify that *Mist1*$^{BT/BT}$ mice are functionally identical to *Mist1*^{WT} mice, we examined the expression patterns of known MIST1 target genes. RT-qPCR analysis revealed that normal MIST1 target genes are expressed to appropriate levels in both *Mist1*^{WT} and *Mist1*$^{BT/BT}$ mice. As demonstrated in **Figure 3-12**, *Cx32*, *Foxp2*, *Rnd2* and *Atp2c2* gene expression was similar in *Mist1*$^{+/-}$ and *Mist1*$^{BT/BT}$ pancreata. These experiments confirmed that acinar cell morphology and transcriptional activity in *Mist1*$^{+/+}$ and *Mist1*$^{BT/BT}$ mice are identical. This allowed us to proceed to generate a mouse line consisting of both BT tagged MIST1 and the biotin ligase, BirA.

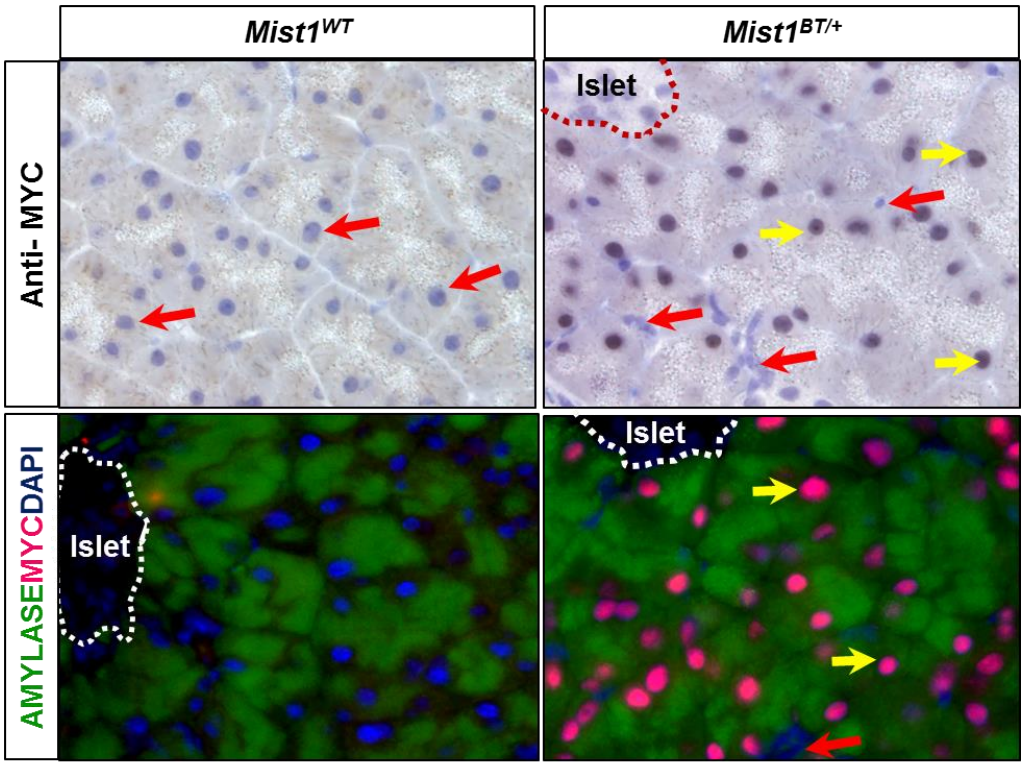

Figure 3-10. Myc-tagged MIST1 is expressed in *Mist1*$^{BT/+}$ acinar cells. IHC using anti-MYC antibody detected no signal in *Mist1*^{WT} pancreata (left- red arrows). In contrast, anti-MYC staining revealed positive nuclear staining in *Mist1*$^{BT/+}$ acinar cells (right-yellow arrows), but not in islet cells (red dashed lines) centroacinar and duct cells (red arrows). IF staining using anti-MYC and AMYLASE also confirm the expression of BT-tagged MIST1 exclusively in the nuclei of acinar cells in *Mist1*$^{BT/+}$ mice (yellow arrows) but not in *Mist1*^{WT} mice. As expected islets (white dotted lines) and duct cells (red arrow) stained negative for MYC. The cytoplasmic AMYLASE is shown by green staining. DAPI was used to mark all the nuclei.

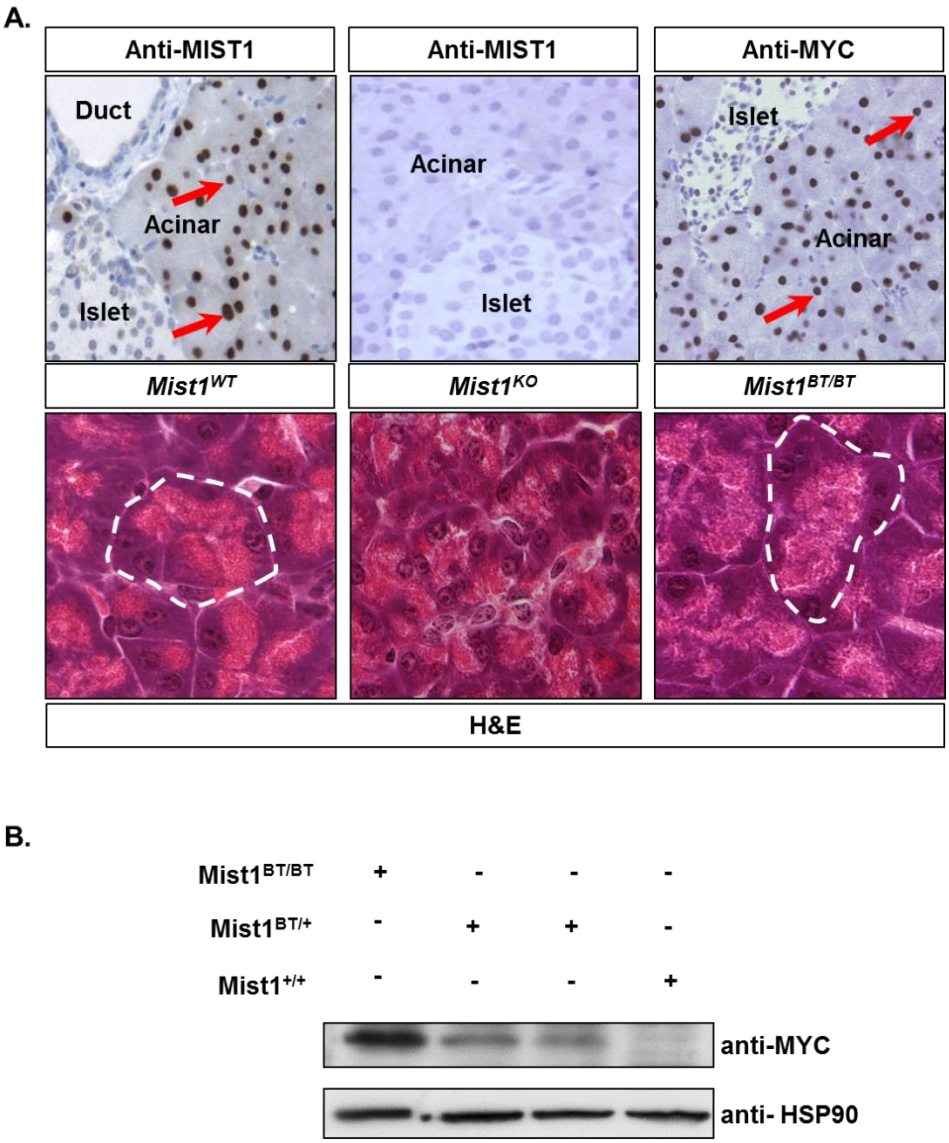

Figure 3-11. *MIST1*$^{BT/BT}$ mouse acinar cell organization is identical to *Mist1*^{WT} mice. (A) IHC using anti-MIST1 antibody detected MIST1 protein in *Mist1*^{WT} and no signal in *Mist1*^{KO} mouse pancreata. Anti-MYC staining on *Mist1*$^{BT/BT}$ mice showed the proper incorporation of the *Mist1*$^{BT/Myc}$ gene and appropriate MIST1$^{BT/Myc}$ protein localization in the nuclei of acinar cells but not in islet cells. *Mist1*$^{BT/BT}$ mice pancreata have similar acinar cell polarity as observed in *Mist1*^{WT}. Representative H&E stains revealed that *Mist1*^{WT} and *Mist1*$^{BT/BT}$ pancreata exhibit similar apical-basal polarity relative to the disrupted *Mist1*^{KO} phenotype. Dotted lines outline a single acinus. **(B)** Immunoblot analysis of protein samples revealed that there was a 2-fold increase in MIST1 protein in *Mist1*$^{BT/BT}$ mice when compared to *Mist1*$^{BT/+}$ mice. Anti-HSP90 was used as a loading control.

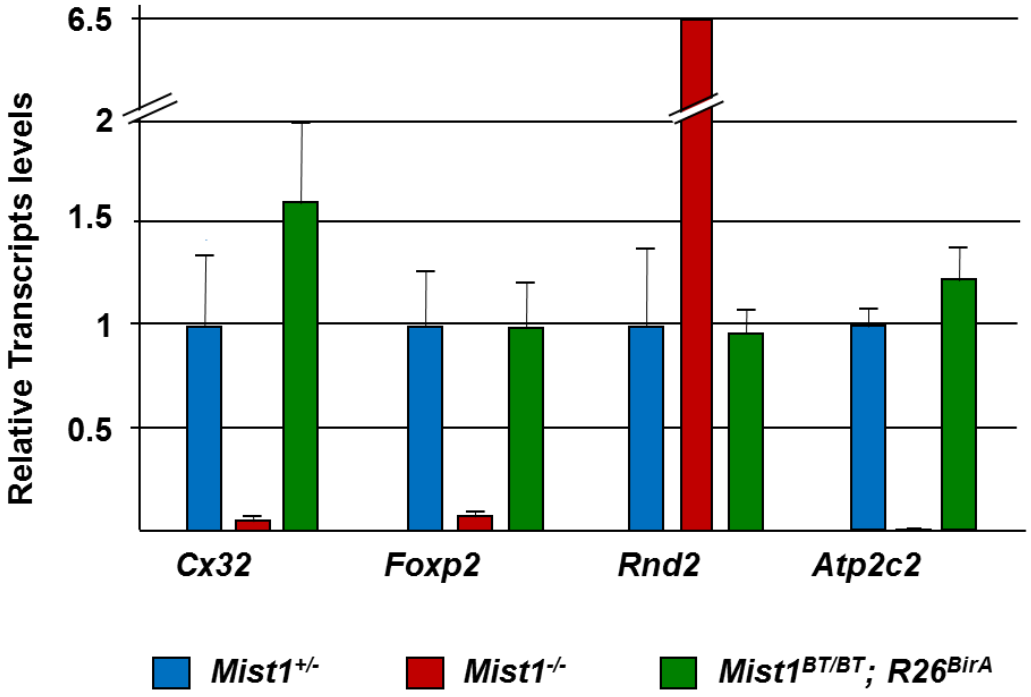

Figure 3-12. Gene expression of MIST1 target genes. Quantitative Real Time PCR revealed the gene expression patterns of MIST1 target genes where *Cx32*, *Foxp2* and *Atp2c2* were up-regulated in both *Mist1*$^{+/-}$ and *Mist1*$^{BT/BT}$ mice in a similar manner. As predicted, transcript levels of *Rnd2* decreased in both *Mist1*$^{+/-}$ and *Mist1*$^{BT/BT}$ mice.

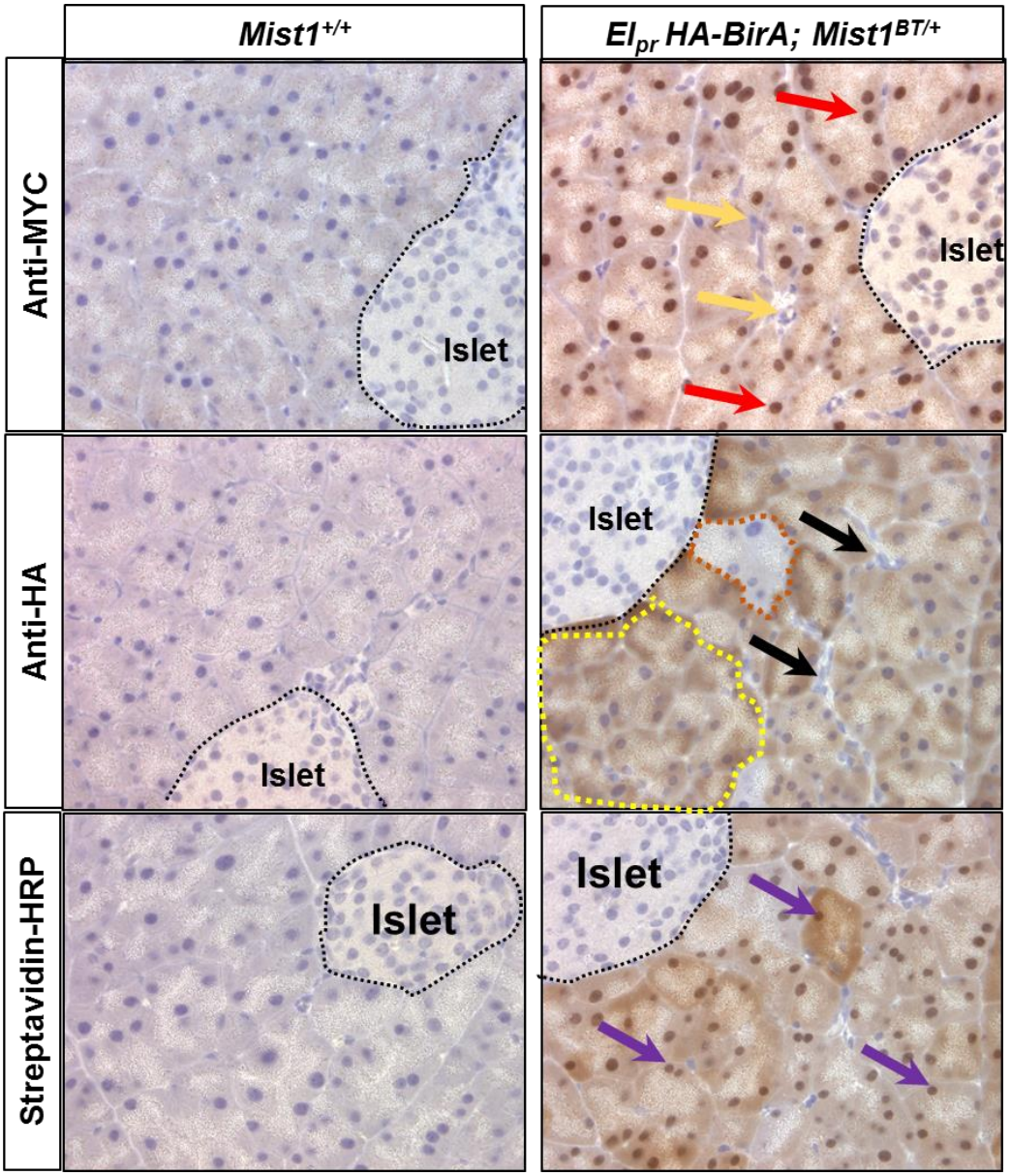

Figure 3-13. MIST1$^{BT/Myc}$ is biotinylated by BirA ligase expressed by *El$_{pr}$-HA-BirA* transgenic mice. IHC using anti-MYC antibody detected MIST1 in the nuclei of acinar cells (red arrows) but not in islets (black dotted lines) and ducts/centroacinar cells (yellow arrows). Anti-HA antibody revealed the patchy expression of BirA ligase mostly in the cytoplasm of acinar cells (yellow dotted lines). The absence of BirA is designated by black arrows and orange dotted lines. Streptavidin-HRP staining showed mostly positive nuclear staining (purple arrows) and also showed cytoplasmic staining, indicating the presence of biotinylated protein in the cytoplasmic compartment as well.

3.2.6 Generation of *Mist1$^{BT/BT}$; El$_{pr}$-HA-BirA* Mice

Once we generated two independent *Mist1$^{BT/Myc}$* and *El$_{pr}$-HA-BirA* mouse lines, we next sought to generate a mouse line containing both alleles. Hence, *Mist1$^{BT/Myc}$* mice were crossed to *Elpr-HA-BirA* mice to generate *Mist1$^{BT/+}$; El$_{pr}$ -HA-BirA* offspring. Male and female pups (*Mist1$^{BT/+}$*; *El$_{pr}$ -HA-BirA*) were then crossed to generate *Mist1$^{BT/BT}$*; *Elpr-HA-BirA* mice. The assessment of expression and biotinylation of MIST1$^{BT/Myc}$ by BirA ligase (expressed specifically in the pancreas) in *Mist1$^{BT/BT}$*; *Elpr-HA-BirA* mice was accomplished by performing immunohistochemistry and immunoblotting. IHC using anti-MYC antibody detected the expected nuclear localization of MIST1$^{BT/Myc}$ in *Mist1$^{BT/BT}$*; *Elpr-HA-BirA* mice (**Figure 3-13**). Unfortunately, anti-HA identified BirA ligase expression mostly in the cytoplasm of acinar cells and very low expression in the nuclei (**Figure 3-13**). The localization of BirA in the nuclei is essential for nuclear MIST1 biotinylation. This could be a problem in conducting further experiments to pull-down MIST1 complexes. Surprisingly, upon using Streptavidin-HRP to detect biotinylated MIST1$^{BT/Myc}$ protein, we confirmed that HA-tagged BirA successfully biotinylated the acinar-specific BT-tagged MIST1 protein (**Figure 3-13**). We next subjected the protein samples for immunoblotting. Although anti-MYC and anti-HA antibodies revealed the appropriate expression of MIST1 and BirA respectively,

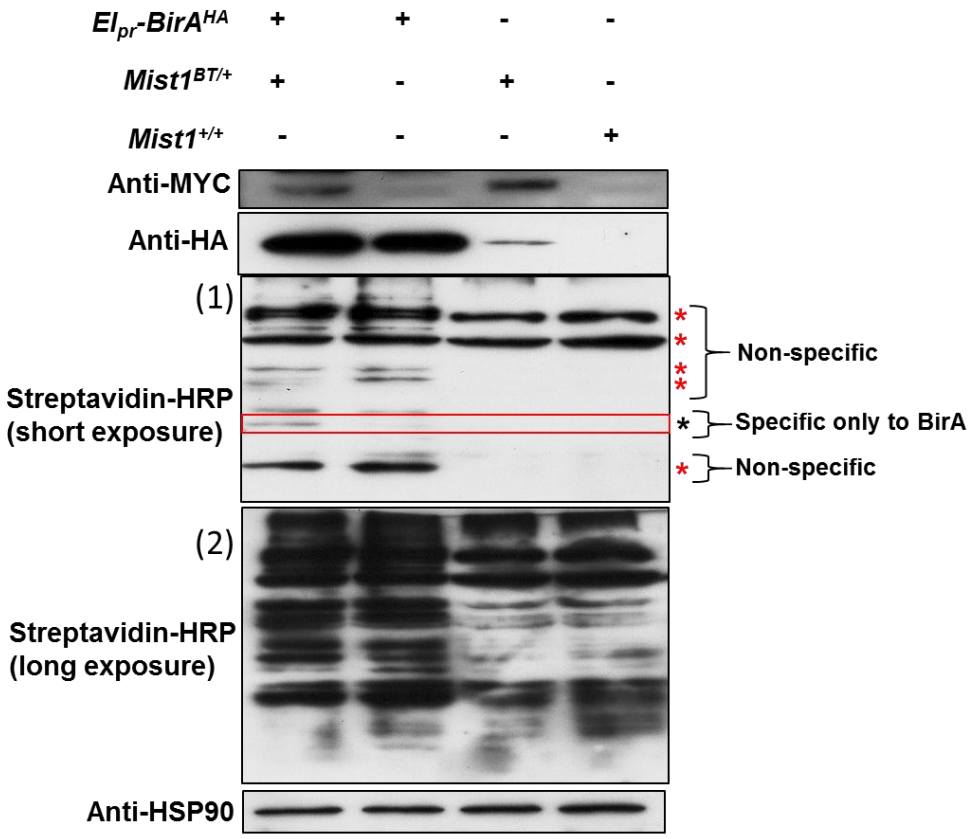

Figure 3-14. ***El$_{pr}$-HA-BirA ligase*** **failed to specifically biotinylate only the MIST1$^{BT/Myc}$ protein.** Although immunoblots using anti-MYC and anti-HA antibodies showed the presence of MIST1$^{BT/Myc}$ and HA-BirA ligase respectively, Streptavidin-HRP blots revealed the presence of numerous background proteins besides the biotinylated MIST1 protein extracted from *Mist1$^{BT/+}$;El$_{pr}$-HA-BirA* mice. Blot (1) designates a short exposure blot where the red asterisks show the non-specific proteins and black asterisk show the biotinylated MIST1 by BirA ligase as detected by Streptavidin-HRP. Blot (2) designates a long exposure of the Streptavidin-blot showing a numerous amount of background proteins in all in all genotypes.Anti-HSP90 served as a loading control.

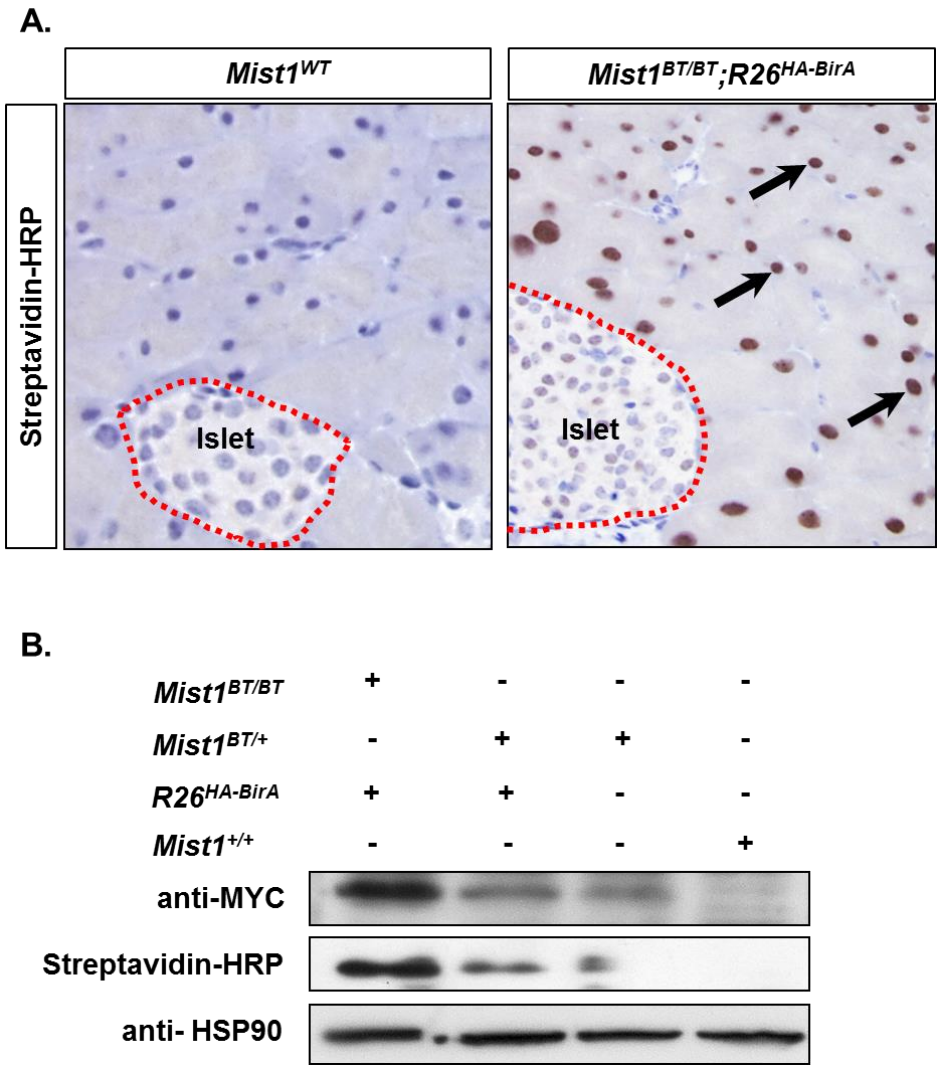

Figure 3-15. **Successful biotinylation of MIST1$^{BT/BT}$ by R26$^{HA\text{-}BirA}$. (A)** Streptavidin-HRP IHC staining showed that there was no biotinylation in *Mist1*$^{+/+}$ mice. However, *Mist1*$^{BT/BT}$*;R26*$^{HA\text{-}BirA}$ pancreata showed positive nuclear staining in acinar cells (arrows), indicating the presence of biotinylated MIST1 protein. **(B)** Immunoblot analysis of protein samples showed successful biotinylation in *Mist1*$^{BT/BT}$; *R26*$^{HA\text{-}BirA}$ and *Mist1*$^{BT/+}$; *R26*$^{HA\text{-}BirA}$ mice. The MIST1 level in *Mist1*$^{BT/BT}$ samples was comparatively higher than found in *Mist1*$^{BT/+}$ samples as detected by anti-MYC antibody. The biotinylated MIST1$^{BT/Myc}$ was detected by Streptavidin-HRP. Anti-HSP90 served as a loading control. The extra band on the third lane in the Streptavidin-HRP blot occurred because of lane spillover.

Streptavidin-HRP detected a large number of background proteins that were present in all tested genotypes (**Figure 3-14**). Therefore, although the *Mist1*$^{BT/BT}$; *El*$_{pr}$*-HA-BirA* mice showed promising results for use in pull-down experiments on biotinylated MIST1$^{BT/Myc}$, the detection of non-specific proteins by Streptavidin-HRP made us seek an alternative approach.

3.2.7 Generation of *Mist1*$^{BT/BT}$*; R26*$^{HA\text{-}BirA}$ Mice

Because *Mist1*$^{BT/BT}$; *El*$_{pr}$*-HA-BirA* mice contained numerous amount of unspecific proteins we did not proceed to perform pull-down experiments with this model. Instead, we decided to utilize an alternative *BirA* mouse, the *R26*$^{HA\text{-}BirA}$ line that was provided by Dr. Dies Meijer from Erasmus University Medical Center, Netherlands. *R26*$^{HA\text{-}BirA}$ mice contain an HA-tagged *birA* coding region incorporated into the *Gt(ROSA)26Sor* locus, allowing for constitutive gene expression of the *HA-BirA* transcript (Driegen et al. 2005). Although these mice presumably constitutively express *HA-BirA* in all tissues, it was unknown whether *BirA* was expressed in the pancreas. Thus, *R26*$^{HA\text{-}BirA}$ mice were crossed with *Mist1*$^{BT/Myc}$ mice to generate *Mist1*$^{BT/BT}$*; R26*$^{HA\text{-}BirA}$ progeny. In this fashion we could take advantage of the acinar-specific expression of the *Mist1*$^{BT/Myc}$ locus to insure acinar-restricted MIST1 biotinylation.

Analysis of BirA activity in *Mist1*$^{BT/BT}$*; R26*$^{HA\text{-}BirA}$ mice using Streptavidin-HRP IHC staining revealed strong, positive nuclear staining exclusively in pancreatic acinar cells (**Figure 3-15**A). In contrast, there was no detected biotinylation in *Mist1*$^{+/+}$ samples. Analysis of protein extracts from *Mist1*$^{+/+}$,

Mist1$^{BT/BT}$, *Mist1*$^{BT/+}$; *R26*$^{HA\text{-}BirA}$ and *Mist1*$^{BT/BT}$; *R26*$^{HA\text{-}BirA}$ mice using anti-MYC and Streptavidin-HRP showed that MIST1$^{BT/Myc}$ protein was successfully biotinylated by HA-BirA (**Figure 3-15B**). As expected, the protein level MIST1 in *Mist1*$^{BT/BT}$ mice was higher than that in *Mist1*$^{BT/+}$ mice (**Figure 3-15B)**. This also verified that homozygous BT-tagged-MIST1 could enhance the amount of MIST1 protein available for pull-down experiments. Hence, we decided to use *Mist1*$^{BT/BT}$*; R26*$^{HA\text{-}BirA}$ mice instead of *Mist1*$^{BT/+}$*; R26*$^{HA\text{-}BirA}$ mice for our MS/MS studies.

The successful biotinylation of BT-tagged MIST1 by BirA ligase in *R26*$^{HA\text{-}BirA}$ mice allowed us to proceed to immunoprecipitate MIST1 protein complexes. Studies have shown that there are very few naturally biotinylated proteins in mice (de Boer et al. 2003) and of these most are located in the cytoplasmic and mitochondrial compartments. To eliminate or minimize background binding proteins in the biotinylated MIST1 protein complexes, we focused on preparing pure nuclear extracts from mouse pancreata to perform mass spectrometry. To test the fractionation of the cytoplasmic and nuclear proteins, immunoblot analysis was performed using antibodies for the nuclear marker-SP1 and the cytoplasmic marker-GAPDH **(Figure 3-16)**. As predicted, SP1 protein was mostly detected in nuclear extracts whereas GAPDH was predominantly found in the cytoplasmic fractions. Hence, this procedure efficiently permitted enriching for nuclear proteins.

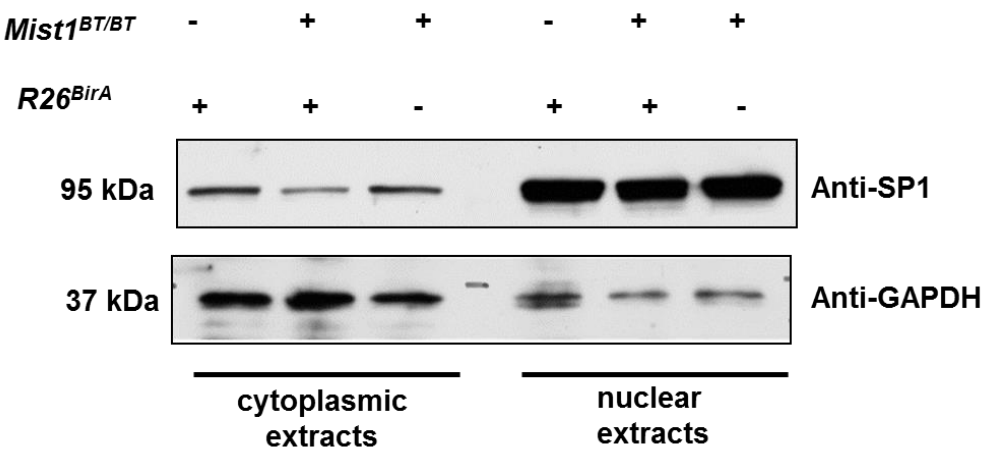

Figure 3-16. Immunoblots of cytoplasmic and nuclear extracts fractionated using the NE-PER kit. Cytoplasmic and nuclear extracts from *Mist1*$^{BT/BT}$ mice, *R26* $^{HA\text{-}BirA}$ mice and *Mist1*$^{BT/BT}$; *R26*$^{HA\text{-}BirA}$ mouse pancreata were immunoblotted using SP1 (nuclear protein marker) and GAPDH (cytoplasmic marker) antibodies. The immunoblots confirmed that the NE-PER kit successfully enriched for nuclear and cytoplasmic proteins. The same kit was used to prepare nuclear samples for mass spectrometry analysis.

3.2.8 Co-immunoprecitation of MIST1$^{BT/Myc}$ Complexes from *Mist1$^{BT/BT}$; R26$^{HA\text{-}BirA}$* mice Using Streptavidin-Dynabeads

Once we optimized the conditions to isolate pure nuclear extracts from mouse pancreata, the next step was to perform a pull-down assay to purify MIST1-interacting protein complexes. Pancreatic nuclear protein extracts were isolated from *R26$^{HA\text{-}BirA}$* and *Mist1$^{BT/BT}$; R26$^{HA\text{-}BirA}$* mice as in **Figure 3-16**. Biotinylated MIST1 from the nuclear extracts was pulled down using Streptavidin-coated magnetic beads. Immunoblot analysis showed a successful immunoprecipitation of MIST1 protein where anti-MYC antibody detected the presence of MIST1$^{BT/Myc}$. Likewise, a Streptavidin-HRP blot demonstrated that the biotinylated MIST1$^{BT/Myc}$ protein could be pulled down efficiently (**Figure 3-17A**). We also attempted an alternative pull-down using His-tag magnetic beads. This method also produced a successful pull-down of the MIST1 complexes (**Figure 3-17B**). As predicted, a Streptavidin-HRP blot confirmed the effective pull-down of biotinylated MIST1 by the His-tag magnetic beads (**Figure 3-17B**).

3.2.9 Mass Spectometry Analysis

In order to prepare samples for mass spectrometry analysis, 1000 µg of protein samples from *R26$^{HA\text{-}BirA}$* (control) and *Mist1$^{BT/BT}$; R26$^{HA\text{-}BirA}$* mouse pancreata were used. For on-bead digestion, the Streptavidin Dynabeads along with the MIST1 complexes were washed and re-suspended in 50 mM ammonium bicarbonate and 6M urea to denature and reduce proteins. Upon purification of the complex, input and pull-down aliquots were subjected to immunoblot analysis. Representative immunoblots are shown in **Figure 3-18**.

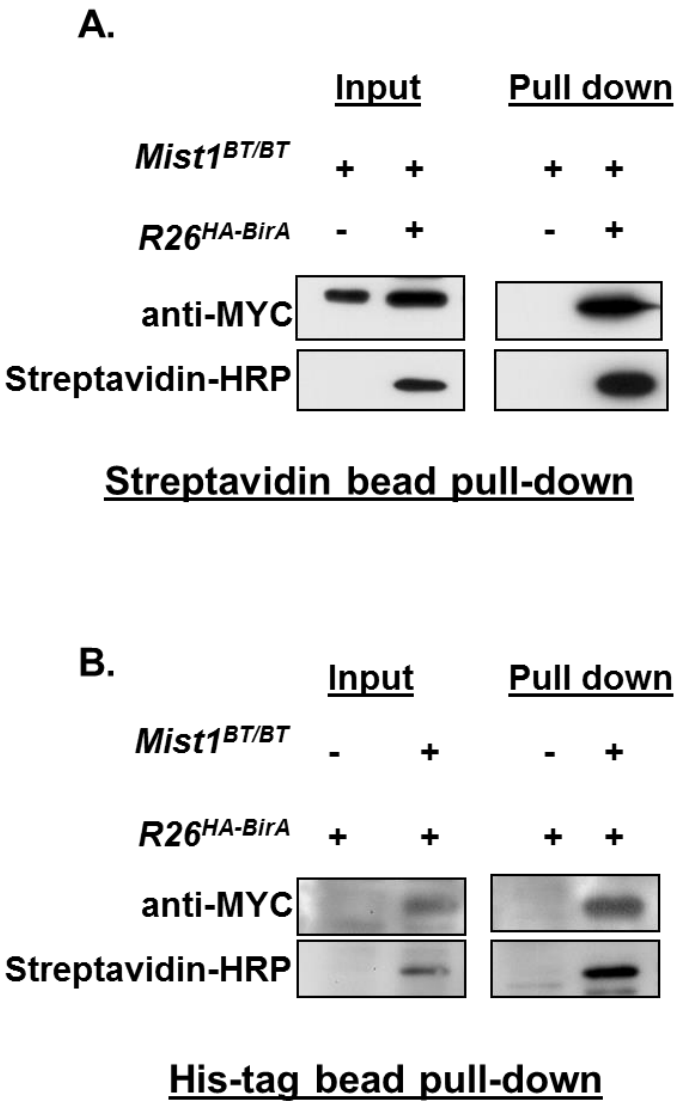

Figure 3-17. **Immunoblot analysis showing successful pull-down of MIST1 using Streptavidin coupled magnetic beads and His-tag magnetic beads. (A)** Immunoblot analysis of pull down of MIST1 using Streptavidin-coupled magnetic beads. Anti-MYC antibody revealed the presence of $MIST1^{BT/Myc}$. The Streptavidin-HRP blot demonstrates that the biotinylated BT-tagged MIST1 protein can be isolated. **(B)** Immunoblot analysis showing successful pull down of MIST1 using His-tag magnetic beads. Anti-MYC showed the presence of $MIST1^{BT/Myc}$. The Streptavidin-HRP blot showed that the biotinylated MIST1 protein was successfully isolated.

Immunoblot analysis revealed a successful pull-down of MIST1 complexes using Streptavidin-coated magnetic beads. Silver staining of SDS-PAGE was performed to determine if additional protein bands could be detected from the pull-down material. As illustrated in **Figure 3-18**, Streptavidin-HRP immunoblot confirmed a successful pull-down of the biotinylated MIST1 complex. Lane 2 detected the input material whereas lane 4 revealed the biotinylated MIST1 protein. As predicted an anti-MYC immunoblot showed the presence of $MIST1^{BT/Myc}$ in both input and pulled-down groups (lane 2 and lane 4, respectively) materials only in the *Mist1*$^{BT/BT}$*; R26*$^{HA\text{-}BirA}$ mice. Silver staining SDS-PAGE showed a similar band pattern in the input protein samples from *R26*$^{HA\text{-}BirA}$ and *Mist1*$^{BT/BT}$*; R26*$^{HA\text{-}BirA}$ mice pancreata (lane 1 and 2). The pulled-down samples from *Mist1*$^{BT/BT}$*; R26*$^{HA\text{-}BirA}$ mice pancreata showed numerous protein bands associated with biotinylated MIST1 protein (lane 4). As expected, pulled-down samples from control mice (*R26*$^{HA\text{-}BirA}$) showed fewer protein bands (lane 3) confirming the enrichment using Streptavidin-Dynabeads (**Figure 3-18**). The remaining protein samples were denatured and reduced for 30 mins at 50°C in a buffer, consisting of 50mM trimethyl ammonium bicarbonate with 0.1% RapiGest (Waters) and 5mM dithiothreitol. Additionally, the proteins were alkylated in 15mM iodoacetamide for one hour at room temperature in a dark room. This was followed by digesting the samples with proteomics grade trypsin at 1 to 100 dilution at 37°C overnight. In order to lower the pH (below pH3), 100mM HCl was added to the peptide mix. The samples were then incubated for 40 mins at 37°C. The samples were centrifuged at 16,100xg for efficient removal of RapiGest and the supernatant collected.

The sample was mixed in equal volume of 1% trifluoroacetic acid and cleaned using a Sep-Pak C18 tips (Waters) to remove buffer and small molecules. The peptides were eluted in a buffer containing 0.1% trifluoroacetic acid in 80% acetonitrile. The samples were dried completely using a SpeedVac before processing through a LC-MS/MS system to identify the proteins in the MIST1 complexes. The mass spectrometry analysis of the digested samples was performed by Keerthi Jayasundera in Dr. Andy Tao's laboratory at Purdue University.

We performed a total of 6 independent rounds of MS/MS using *R26*$^{HA\text{-}BirA}$ mouse (control) and *Mist1*$^{BT/BT}$*; R26*$^{HA\text{-}BirA}$ mouse (experimental) samples. The data collected from each run was further analyzed by Dr. Ernesto Nakayasu using MAXQuant software (Tyanova et al. 2015) dedicated to perform a quantitative proteomics of multiple datasets. This allowed us to refine/filter the dataset for further analysis. Dr. Hyung Won-Choi then processed these datasets using another computational scoring tool named Significance Analysis of INTeractome (SAINT) which generated confidence scores of bait-prey interactions in order to precisely identify true interacting protein partners (Choi et al. 2011). This tool used spectral count-based scoring for quantitative analyses of the mass spectrometry data. The principle idea of determining the true interaction between MIST1 and another protein using this system is that if a particular protein is a real binding partner of MIST1, then its concentration in the experimental pull-down material should be greater than in the control.

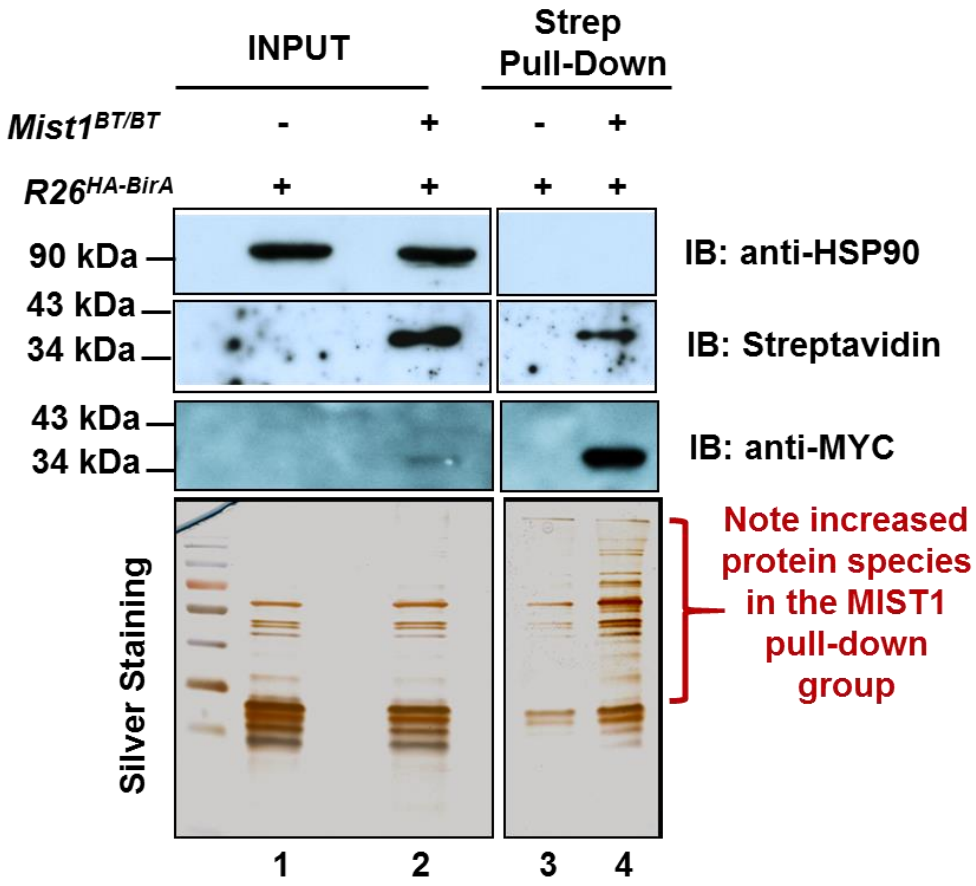

Figure 3-18. Representative immunoblots and silver staining analysis on the samples prepared for various rounds of mass spectrometry. Immunoblots performed on the input and the pull-down samples using anti-MYC antibody and Streptavidin-HRP confirmed the effective pull-down of the MIST1 complex. HSP90 immunoblot served as a control. Silver staining gel image is the visual representation of the proteins that are associated with the pull-down complexes.

Hence, the greater the spectral counts in the experimental sample signifies a real interaction. The data output is summarized in **Table 4**.

After the proteins were sorted out based on each round, I further sorted the proteins that were captured in at least 2 replicates (**Table 5**).There were a total of 23 unique proteins that were identified from the six MS/MS runs. As predicted, MIST1 (*Bhlha15*) was pulled-down in each round with a Saint score of 1 (confirming a true interaction). Studies have shown that MIST1 can homodimerize (Tran et al. 2007) and therefore the presence of MIST1 in each round validated the efficiency of the pull-downs performed for mass spectrometry. Previously, cell culture studies had identified SAP18 as a binding partner of MIST1 (Jia 2008). However, in this mouse study I was unable to detect SAP18 on the prey protein list, suggesting that tissue culture and intact pancreata utilize different transcription mechanisms.

Besides MIST1, another frequently pulled-down (3 times) prey protein was Cathepsin B, a lysosomal protease, which is often overexpressed in various cancers such as brain and lung (Rempel et al. 1994; Krepela et al. 1990). Likewise, Syndecan-1, a cell surface proteoglyacan essential for cell-cell adhesion in epithelial cells (Leppä et al. 1996; Teng et al. 2012) and involved in inflammatory responses was also identified as a putative MIST1 partner. Filamin, Tropomodulin and Fam28 were other proteins that showed up in 3 pull-downs.

Table 4. **Summary of protein-protein interactions analyzed by SAINT analysis**. The terms in each column are as follows: Bait name and round of mass spectrometry (For example MIST1 1.1 refers to round 1 (Column 1); Prey UNIPROT ID (Column 2); Prey gene symbol (Column 3); Spec: spectral count of the prey in that purification of bait (Column 4); CtrlCounts: spectral counts in the control purifications i.e *R26*$^{HA\text{-}BirA}$ samples (Column 5); SaintScore: probability of true interaction (between 0 and 1) (Column 6); FoldChange: estimated fold change between prey protein abundance in real bait purification over controls (Column 7); BFDR: Bayesian false discovery rate (usually the criterion for selection, e.g. 1%, 5%, depending on the stringency) (Column 8); Prey Protein Description: Based on MaxQuant analysis (Column 9).

Bait	Prey	PreyGene	Spec	ctrlCounts	SaintScore	FoldChange	BFDR	Prey Protein Description
MIST1.1	A0JNZ0	Nedd4	2	0|0|0|0|0|0	0.9	20	0.01	HECT (E6AP-type E3 ubiquitin-protein ligase)
MIST1.1	A1BN54	Actn1	9	0|0|0|1|0|0	1	18	0	Actin binding
MIST1.1	D3YWL1	Rab3d	2	0|0|0|0|0|0	0.9	20	0.01	Ras-related protein rab-3D
MIST1.1	D3Z637	Tpd52	2	0|0|0|0|0|0	0.9	20	0.01	Tumor-protein D52
MIST1.1	E9Q5B2	0610011F06Rik	2	0|0|0|0|0|0	0.9	20	0.01	T-complex protein 1 subunit delta
MIST1.1	G5E839	Cct4	4	0|0|0|0|0|0	1	40	0	T-complex protein 1 subunit delta
MIST1.1	P00688	Amy2	151	42|12|54|58|50|5	1	2.7	0	Pancreatic alpha-amylase
MIST1.1	P05132	Prkaca	9	0|0|0|0|0|0	1	90	0	cAMP-dependent protein kinase catalytic subunit alpha
MIST1.1	P48036	Anxa5	2	0|0|0|0|0|0	0.9	20	0.01	Annexin A5
MIST1.1	P62814	Atp6v1b2	2	0|0|0|0|0|0	0.9	20	0.01	V-type proton ATPase subunit B, brain isoform
MIST1.1	P63028	Tpt1	32	0|0|6|4|0|2	1	6.4	0	Translationally-controlled tumor protein
MIST1.1	P70562	Bhlha15	8	0|0|1|0|0|0	1	16	0	Class A basic helix-loop-helix protein 15
MIST1.1	Q059I1	Rps28	10	0|0|2|2|1|2	0.98	5	0.01	40S ribosomal protein S28
MIST1.1	Q3TBF1	Padi2	3	0|0|0|0|0|0	0.98	30	0	Protein-arginine deiminase type-2
MIST1.1	Q3TFB5	Nans	2	0|0|0|0|0|0	0.9	20	0.01	Putative uncharacterized protein
MIST1.1	Q3UD94	Psmc3	2	0|0|0|0|0|0	0.9	20	0.01	26S protease regulatory subunit 6A
MIST1.1	Q3UL02	Gspt1	2	0|0|0|0|0|0	0.9	20	0.01	Eukaryotic peptide chain release factor GTP-binding subunit ERF3B
MIST1.1	Q3UL78	Cdc42	2	0|0|0|0|0|0	0.9	20	0.01	Cell division control protein 42 homolog
MIST1.1	Q3UMP2	Hmgcl	3	0|0|0|0|0|0	0.98	30	0	Hydroxymethylglutaryl-CoA lyase, mitochondrial
MIST1.1	Q3UPH1	Prrc1	2	0|0|0|0|0|0	0.9	20	0.01	Protein PRRC1
MIST1.1	Q4V9T8	Eif1	3	0|0|0|0|0|0	0.98	30	0	Eukaryotic translation initiation factor 1A, X-chromosomal
MIST1.1	Q544B1	Aldh2	6	0|0|0|0|0|0	1	60	0	Aldehyde dehydrogenase, mitochondrial
MIST1.1	Q545F0	Mif	2	0|0|0|0|0|0	0.9	20	0.01	Macrophage migration inhibitory factor
MIST1.1	Q561N4	Ube2l3	2	0|0|0|0|0|0	0.9	20	0.01	Ubiquitin-conjugating enzyme E2 L3
MIST1.1	Q5NC81	Nme1	2	0|0|0|0|0|0	0.9	20	0.01	Nucleoside diphosphate kinase;Nucleoside diphosphate kinase A
MIST1.1	Q65ZC0	Igkc	5	0|0|0|0|0|0	1	50	0	Ig kappa chain C region;Ig kappa chain V-II region 26-10
MIST1.1	Q6LAF6	Ctsb	2	0|0|0|0|0|0	0.9	20	0.01	Cathepsin B;Cathepsin B light chain;Cathepsin B heavy chain
MIST1.1	Q7JD03	COX2	3	0|0|0|0|0|0	0.98	30	0	Cytochrome c oxidase subunit 2
MIST1.1	Q80X90	Flnb	3	0|0|0|0|0|0	0.98	30	0	Filamin-B;Filamin-C
MIST1.1	Q8BH64	Ehd2	3	0|0|0|0|0|0	0.98	30	0	EH domain-containing protein 2
MIST1.1	Q8BKE0	Psma2	2	0|0|0|0|0|0	0.9	20	0.01	Proteasome subunit alpha type;Proteasome subunit alpha type-2
MIST1.1	Q8BP47	Nars	4	0|0|0|0|0|0	1	40	0	Asparagine--tRNA ligase, cytoplasmic
MIST1.1	Q8BPD3	Prdx6	3	0|0|0|0|0|0	0.98	30	0	Peroxiredoxin-6
MIST1.1	Q8BSZ7	Ap1g1	2	0|0|0|0|0|0	0.9	20	0.01	AP-1 complex subunit gamma-1
MIST1.1	Q8BTU6	Eif4a2	2	0|0|0|0|0|0	0.9	20	0.01	Eukaryotic initiation factor 4A-II
MIST1.1	Q8BWT1	Acaa2	4	0|0|0|0|0|0	1	40	0	3-ketoacyl-CoA thiolase, mitochondrial
MIST1.1	Q8C165	Pm20d1	3	0|0|0|0|0|0	0.98	30	0	Probable carboxypeptidase PM20D1
MIST1.1	Q8CCJ3	Ufl1	3	0|0|0|0|0|0	0.98	30	0	E3 UFM1-protein ligase 1
MIST1.1	Q8R2E9	Ero1lb	21	0|0|4|6|0|3	1	4.2	0	ERO1-like protein beta
MIST1.1	Q8R3V2	Aimp2	3	0|0|0|0|0|0	0.98	30	0	Aminoacyl tRNA synthase complex-interacting multifunctional protein 2
MIST1.1	Q8VCT4	Ces1d	5	0|0|0|1|0|0	0.96	10	0.01	Carboxylesterase 1D
MIST1.1	Q8VE47	Uba5	2	0|0|0|0|0|0	0.9	20	0.01	Ubiquitin-like modifier-activating enzyme 5
MIST1.1	Q99JZ4	Sar1a	2	0|0|0|0|0|0	0.9	20	0.01	GTP-binding protein SAR1a
MIST1.1	Q9CRF4	Oxct1	2	0|0|0|0|0|0	0.9	20	0.01	Succinyl-CoA:3-ketoacid-coenzyme A transferase
MIST1.1	Q9D8V7	Sec11c	5	0|0|0|1|0|0	0.96	10	0.01	Signal peptidase complex catalytic subunit SEC11C
MIST1.1	Q9DB27	Mcts1	2	0|0|0|0|0|0	0.9	20	0.01	Malignant T-cell-amplified sequence 1
MIST1.1	Q9JJD8	Cct2	7	0|0|0|0|0|0	1	70	0	T-complex protein 1 subunit beta
MIST1.1	Q9QXB9	Drg2	3	0|0|0|0|0|0	0.98	30	0	Developmentally-regulated GTP-binding protein 2
MIST1.1	Q9QXT0	Cnpy2	2	0|0|0|0|0|0	0.9	20	0.01	Protein canopy homolog 2
MIST1.1	Q9R071	Eif6	2	0|0|0|0|0|0	0.9	20	0.01	Eukaryotic translation initiation factor 6
MIST1.1	Q9WTP6	Ak2	2	0|0|0|0|0|0	0.9	20	0.01	Adenylate kinase 2, mitochondrial
MIST1.2	E9Q5B6	Hnrnpd	2	0|0|0|0|0|0	0.9	20	0.01	Heterogeneous nuclear ribonucleoprotein D0
MIST1.2	P70562	Bhlha15	5	0|0|1|0|0|0	0.96	10	0.01	Class A basic helix-loop-helix protein 15
MIST1.2	Q3TYX1	Srebf1	2	0|0|0|0|0|0	0.9	20	0.01	Sterol regulatory element-binding protein 1
MIST1.2	Q6ZWX2	Tmsb4x	2	0|0|0|0|0|0	0.9	20	0.01	Thymosin beta-4
MIST1.2	Q7JD03	COX2	2	0|0|0|0|0|0	0.9	20	0.01	Cytochrome c oxidase subunit 2
MIST1.2	Q80WW4	Serpinb9c	2	0|0|0|0|0|0	0.9	20	0.01	Serine (or cysteine) peptidase inhibitor, clade B, member 9c
MIST1.2	Q8BL32	Hnrnpr	2	0|0|0|0|0|0	0.9	20	0.01	Heterogeneous Nuclear Ribonucleoprotein R
MIST1.2	Q9D094	Hars	2	0|0|0|0|0|0	0.9	20	0.01	Histidine--tRNA ligase, cytoplasmic
MIST1.3	A2BGI8	Ppih	2	0|0|0|0|0|0	0.9	20	0.01	Peptidyl-prolyl cis-trans isomerase
MIST1.3	P11983	Tcp1	2	0|0|0|0|0|0	0.9	20	0.01	T-complex protein 1 subunit alpha
MIST1.3	P43275	Hist1h1a	5	0|0|0|1|0|0	0.96	10	0.01	Histone H1.1
MIST1.3	P70562	Bhlha15	12	0|0|1|0|0|0	1	24	0	Class A basic helix-loop-helix protein 15
MIST1.3	Q1WWK3	Hist1h1b	2	0|0|0|0|0|0	0.9	20	0.01	Histone H1.5
MIST1.3	Q3TQS1	Larp1b	2	0|0|0|0|0|0	0.9	20	0.01	La Ribonucleoprotein Domain Family, Member 1B
MIST1.3	Q3UDX4	Dhx15	2	0|0|0|0|0|0	0.9	20	0.01	Putative pre-mRNA-splicing factor ATP-dependent RNA helicase DHX15
MIST1.3	Q3UWI9	Kif5b	2	0|0|0|0|0|0	0.9	20	0.01	Kinesin heavy chain isoform 5C;Kinesin-1 heavy chain;Kinesin heavy chain isoform 5A
MIST1.3	Q5NTY0	Dnaja1	2	0|0|0|0|0|0	0.9	20	0.01	DnaJ homolog subfamily A member 1
MIST1.3	Q6LAF6	Ctsb	2	0|0|0|0|0|0	0.9	20	0.01	Cathepsin B;Cathepsin B light chain;Cathepsin B heavy chain
MIST1.3	Q6ZPS0	Rrbp1	8	0|0|0|0|0|0	1	80	0	Ribosome Binding Protein 1
MIST1.3	Q923D4	Sf3b5	2	0|0|0|0|0|0	0.9	20	0.01	Splicing factor 3B subunit 5
MIST1.3	Q9ME04	mt-Nd4	3	0|0|0|0|0|0	0.98	30	0	NADH-ubiquinone oxidoreductase chain 4
1	2	3	4	5	6	7	8	9

Different colors in the table symbolize six different mass spectrometry rounds.

Bait	Prey	PreyGene	Spec	ctrlCounts	SaintScore	FoldChange	BFDR	Prey Protein Description
MIST1.4	A2A6U3	Sept9	4	0|0|0|0|0|0	1	40	0	Septin-type G (guanine nucleotide-binding)
MIST1.4	A2AFS1	Sars	2	0|0|0|0|0|0	0.9	20	0.01	Serine--tRNA ligase, cytoplasmic
MIST1.4	A4FUV5	Sec24a	2	0|0|0|0|0|0	0.9	20	0.01	Protein transport protein Sec24A
MIST1.4	E9Q5B6	Hnrnpd	2	0|0|0|0|0|0	0.9	20	0.01	Heterogeneous nuclear ribonucleoprotein D0
MIST1.4	E9Q6T6	Tdrd3	2	0|0|0|0|0|0	0.9	20	0.01	Tudor domain-containing protein 3
MIST1.4	G3XA10	Hnrnpu	13	0|0|3|4|0|0	0.96	3.71	0.01	Heterogeneous nuclear ribonucleoprotein U
MIST1.4	K3W4L0	Myo18a	2	0|0|0|0|0|0	0.9	20	0.01	Unconventional myosin-XVIIIa
MIST1.4	P00920	Ca2	2	0|0|0|0|0|0	0.9	20	0.01	Carbonic anhydrase 2
MIST1.4	P70562	Bhlha15	11	0|0|1|0|0|0	1	22	0	Class A basic helix-loop-helix protein 15
MIST1.4	Q1A602	Actn4	2	0|0|0|0|0|0	0.9	20	0.01	Alpha-actinin-4
MIST1.4	Q3U6K9	Psat1	2	0|0|0|0|0|0	0.9	20	0.01	Phosphoserine aminotransferase
MIST1.4	Q3UWI9	Kif5b	2	0|0|0|0|0|0	0.9	20	0.01	Kinesin heavy chain isoform 5C;Kinesin-1 heavy chain
MIST1.4	Q3UZ06	Sec22b	3	0|0|0|0|0|0	0.98	30	0	Vesicle-trafficking protein SEC22b
MIST1.4	Q545K5	Rbm3	2	0|0|0|0|0|0	0.9	20	0.01	Putative RNA-binding protein 3
MIST1.4	Q5RL79	Krtcap2	2	0|0|0|0|0|0	0.9	20	0.01	Keratinocyte-associated protein 2
MIST1.4	Q6LAF6	Ctsb	4	0|0|0|0|0|0	1	40	0	Cathepsin B;Cathepsin B light chain;Cathepsin B heavy chain
MIST1.4	Q6ZWX2	Tmsb4x	2	0|0|0|0|0|0	0.9	20	0.01	Thymosin beta-4
MIST1.4	Q8BN32	Pabpc1	5	0|0|0|1|0|0	0.96	10	0.01	Polyadenylate-binding protein 1
MIST1.4	Q8C2A3	Sept7	2	0|0|0|0|0|0	0.9	20	0.01	Septin-7
MIST1.4	Q8CB58	Ptbp1	2	0|0|0|0|0|0	0.9	20	0.01	Polypyrimidine tract-binding protein 1;Polypyrimidine tract-binding protein 3
MIST1.4	Q8R5C5	Actr1b	2	0|0|0|0|0|0	0.9	20	0.01	Beta-centractin;Alpha-centractin
MIST1.4	Q91VL2	Thrap3	5	0|0|0|0|0|0	1	50	0	Thyroid hormone receptor-associated protein 3
MIST1.4	Q91VM5	Rbmxl1	5	0|0|0|0|0|0	1	50	0	RNA binding motif protein, X-linked-like-1
MIST1.4	Q99PT1	Arhgdia	2	0|0|0|0|0|0	0.9	20	0.01	Rho GDP-dissociation inhibitor 1
MIST1.4	Q9D094	Hars	2	0|0|0|0|0|0	0.9	20	0.01	Histidine--tRNA ligase, cytoplasmic
MIST1.4	Q9D958	Spcs1	2	0|0|0|0|0|0	0.9	20	0.01	Signal peptidase complex subunit 1
MIST1.4	Q9DBR7	Ppp1r12a	4	0|0|0|0|0|0	1	40	0	Protein phosphatase 1 regulatory subunit 12A
MIST1.4	Q9JMG1	Edf1	2	0|0|0|0|0|0	0.9	20	0.01	Endothelial differentiation-related factor 1
MIST1.4	Q9QXT0	Cnpy2	2	0|0|0|0|0|0	0.9	20	0.01	Protein canopy homolog 2
MIST1.4	Q9Z1R9	Prss1	2	0|0|0|0|0|0	0.9	20	0.01	Protease, Serine, 1 (Trypsin 1)
MIST1.5	E9Q3W4	Plec	5	0|0|0|0|1|0	0.96	10	0.01	Plectin
MIST1.5	E9QNH6	Myo1b	5	0|0|0|0|1|0	0.96	10	0.01	Unconventional myosin-Ib
MIST1.5	P70562	Bhlha15	39	0|0|1|0|0|0	1	78	0	Class A basic helix-loop-helix protein 15
MIST1.5	Q1WWK3	Hist1h1b	2	0|0|0|0|0|0	0.9	20	0.01	Histone H1.5
MIST1.5	Q3TJZ6	Fam98a	2	0|0|0|0|0|0	0.9	20	0.01	Protein FAM98A
MIST1.5	Q3UKZ1	Sdc4	2	0|0|0|0|0|0	0.9	20	0.01	Syndecan;Syndecan-4
MIST1.5	Q571K0	Dlg1	2	0|0|0|0|0|0	0.9	20	0.01	Disks large homolog 1
MIST1.5	Q5SYD0	Myo1d	3	0|0|0|0|0|0	0.98	30	0	Unconventional myosin-Id
MIST1.5	Q61879	Myh10	6	0|0|0|0|0|0	1	60	0	Myosin-10
MIST1.5	Q62261	Sptbn1	6	0|0|0|1|0|0	0.99	12	0	Spectrin beta chain, non-erythrocytic 1
MIST1.5	Q9CS50	Prkar1a	2	0|0|0|0|0|0	0.9	20	0.01	cAMP-dependent protein kinase type I-alpha regulatory subunit
MIST1.5	Q9JHJ0	Tmod3	4	0|0|0|0|0|0	1	40	0	Tropomodulin-3
MIST1.5	Q9R071	Eif6	2	0|0|0|0|0|0	0.9	20	0.01	Eukaryotic translation initiation factor 6
MIST1.5	Q9WTI7	Myo1c	4	0|0|0|0|0|0	1	40	0	Unconventional myosin-Ic
MIST1.6	P70562	Bhlha15	9	0|0|1|0|0|0	1	18	0	Class A basic helix-loop-helix protein 15
MIST1.6	Q3UKZ1	Sdc4	2	0|0|0|0|0|0	0.9	20	0.01	Syndecan;Syndecan-4
MIST1.6	Q5SZA3	Hist1h1c	2	0|0|0|0|0|0	0.9	20	0.01	Histone H1.2
MIST1.6	Q60675	Lama2	2	0|0|0|0|0|0	0.9	20	0.01	Laminin subunit alpha-2
MIST1.7	A2AFS1	Sars	2	0|0|0|0|0|0	0.9	20	0.01	Serine--tRNA ligase, cytoplasmic
MIST1.7	G3UYK9	Dtnb	2	0|0|0|0|0|0	0.9	20	0.01	Dystrobrevin beta
MIST1.7	G5E839	Cct4	2	0|0|0|0|0|0	0.9	20	0.01	T-complex protein 1 subunit delta
MIST1.7	P48036	Anxa5	4	0|0|0|0|0|0	1	40	0	Annexin A5
MIST1.7	P70562	Bhlha15	9	0|0|1|0|0|0	1	18	0	Class A basic helix-loop-helix protein 15
MIST1.7	Q3TJZ6	Fam98a	5	0|0|0|0|0|0	1	50	0	Protein FAM98A
MIST1.7	Q3TML0	Pdia6	2	0|0|0|0|0|0	0.9	20	0.01	Protein disulfide-isomerase A6
MIST1.7	Q3UKZ1	Sdc4	2	0|0|0|0|0|0	0.9	20	0.01	Syndecan;Syndecan-4
MIST1.7	Q65ZC0	Igkc	2	0|0|0|0|0|0	0.9	20	0.01	Ig kappa chain C region;Ig kappa chain V-II region 26-10
MIST1.7	Q80X90	Flnb	2	0|0|0|0|0|0	0.9	20	0.01	Filamin-B;Filamin-C
MIST1.7	Q8R5C5	Actr1b	2	0|0|0|0|0|0	0.9	20	0.01	Beta-centractin;Alpha-centractin
MIST1.7	Q91VA7	Idh3b	2	0|0|0|0|0|0	0.9	20	0.01	Isocitrate Dehydrogenase 3 (NAD+) Beta
MIST1.7	Q9D6R2	Idh3a	2	0|0|0|0|0|0	0.9	20	0.01	Isocitrate Dehydrogenase 3 (NAD+) Alpha
MIST1.7	Q9JHJ0	Tmod3	2	0|0|0|0|0|0	0.9	20	0.01	Tropomodulin-3
MIST1.7	Q9WTI7	Myo1c	2	0|0|0|0|0|0	0.9	20	0.01	Unconventional myosin-Ic
MIST1.8	D3Z369	Wdr12	2	0|0|0|0|0|0	0.9	20	0.01	Ribosome biogenesis protein WDR12
MIST1.8	E9QPE7	Myh11	28	0|0|0|0|3|2	1	11.2	0	Myosin-11
MIST1.8	G5E839	Cct4	2	0|0|0|0|0|0	0.9	20	0.01	T-complex protein 1 subunit delta
MIST1.8	P70562	Bhlha15	12	0|0|1|0|0|0	1	24	0	Class A basic helix-loop-helix protein 15
MIST1.8	Q3TJZ6	Fam98a	2	0|0|0|0|0|0	0.9	20	0.01	Protein FAM98A
MIST1.8	Q5SYD0	Myo1d	4	0|0|0|0|0|0	1	40	0	Unconventional myosin-Id
MIST1.8	Q61879	Myh10	6	0|0|0|0|0|0	1	60	0	Myosin-10
MIST1.8	Q6NV50	Ctnna1	2	0|0|0|0|0|0	0.9	20	0.01	Catenin alpha-1
MIST1.8	Q6R891	Ppp1r9b	2	0|0|0|0|0|0	0.9	20	0.01	Neurabin-2
MIST1.8	Q80X73	Pelo	2	0|0|0|0|0|0	0.9	20	0.01	Protein pelota homolog
MIST1.8	Q80X90	Flnb	2	0|0|0|0|0|0	0.9	20	0.01	Filamin-B;Filamin-C
MIST1.8	Q8K419	Lgals4	2	0|0|0|0|0|0	0.9	20	0.01	Galectin-4
MIST1.8	Q8R3V2	Aimp2	2	0|0|0|0|0|0	0.9	20	0.01	Aminoacyl tRNA synthase complex-interacting multifunctional protein 2
MIST1.8	Q9JHJ0	Tmod3	2	0|0|0|0|0|0	0.9	20	0.01	Tropomodulin-3
1	2	3	4	5	6	7	8	9

Table 5. List of highest represented proteins that were identified by mass spectrometry analysis. MIST1 protein (highlighted in yellow color) was pulled-down in each round confirming its ability to homodimerize.

Protein ID	Gene ID	Protein Description	Pull-down Frequency
Q8R5C5	*Actr1b*	Beta-centractin;Alpha-centractin	2
Q8R3V2	*Aimp2*	Aminoacyl tRNA synthase complex-interacting multifunctional protein 2	2
P48036	*Anxa5*	Annexin A5	2
P70562	*Bhlha15*	Class A basic helix-loop-helix protein 15	8
G5E839	*Cct4*	T-complex protein 1 subunit delta	3
Q9QXT0	*Cnpy2*	Protein canopy homolog 2	2
Q7JD03	*COX2*	Cytochrome c oxidase subunit 2	2
Q6LAF6	*Ctsb*	Cathepsin B;Cathepsin B light chain;Cathepsin B heavy chain	3
Q9R071	*Eif6*	Eukaryotic translation initiation factor 6	2
Q3TJZ6	*Fam98a*	Family With Sequence Similarity 98, Member A	3
Q80X90	*Flnb*	Filamin-B;Filamin-C	3
Q9D094	*Hars*	Histidine--tRNA ligase, cytoplasmic	2
Q1WWK3	*Hist1h1b*	Histone H1.5	2
E9Q5B6	*Hnrnpd*	Heterogeneous nuclear ribonucleoprotein D0	2
Q65ZC0	*Igkc*	Ig kappa chain C region;Ig kappa chain V-II region 26-10	2
Q3UWI9	*Kif5b*	Kinesin heavy chain isoform 5C;Kinesin-1 heavy chain	2
Q61879	*Myh10*	Myosin-10	2
Q9WTI7	*Myo1c*	Unconventional myosin-Ic	2
Q5SYD0	*Myo1d*	Unconventional myosin-Id	2
A2AFS1	*Sars*	Serine--tRNA ligase, cytoplasmic	2
Q3UKZ1	*Sdc4*	Syndecan;Syndecan-4	3
Q9JHJ0	*Tmod3*	Tropomodulin-3	3
Q6ZWX2	*Tmsb4x*	Thymosin beta-4	2

Surprisingly, despite predicting that MIST1 binds to different transcription factors, we failed to unequivocally identify any striking transcription factor in the list of the most frequently pulled-down prey proteins. In conclusion, we were unsuccessful in finding a promising binding partner of MIST1.

3.3 Discussion

MIST1 is a bHLH transcription factor expressed in pancreatic acinar cells. Gene array and ChIP-seq analyses have identified a number of MIST1 target genes where MIST1 binding activates or represses gene expression, although the molecular mechanisms underlying these responses remain unknown (Direnzo et al. 2012). Previous studies have revealed that MIST1 does not have a TAD and only the central bHLH domain of MIST1 is required for full transcriptional activity in transgenic mice (Zhu et al. 2004).Additionally, MIST1 is thought to function as a homodimer bHLH complex, suggesting that other proteins may interact with MIST1 dimer to act as c-regulators of MIST1 transcriptional activity. Herein, I exploited a novel mouse model to identify the protein binding partners of MIST1 by LC-MS/MS via a biotinylation pull-down system to immunoprecipitate MIST1-associated complexes.

In an attempt to characterize the function of MIST1, we hypothesized that the transcriptional activity of the MIST1 homodimer complex is dependent on a co-regulator binding partner. We utilized biotin/avidin approach to purify MIST1 as it is the strongest non-covalent interaction known in nature (Green 1990).

Accordingly, we generated a mouse model consisting of an N-terminal BT tag, C-terminal 6XHis-Myc tag and two loxP sites that were introduced via homologous recombination into the MIST1 locus, generating the *Mist1*$^{BT/Myc}$ line. *Mist1*$^{BT/Myc}$ mice were crossed with a BirA ligase (*R26*$^{HA\text{-}BirA}$) mouse that biotinylated the BT-tagged MIST1 protein allowing us to immunoprecipitate the MIST1 complex using streptavidin magnetic beads to perform mass spectrometry analysis. We have shown that this model is efficient in purifying the MIST1 complex as *R26*$^{HA\text{-}BirA}$ ligase specifically biotinylated the MIST1$^{BT/Myc}$ protein. Using tandem mass spectrometry and bioinformatics software (MaxQuant and SAINT), we identified 23 unique proteins that were significantly enriched in *Mist1*$^{BT/BT}$; *R26*$^{HA\text{-}BirA}$ pancreata samples. The goal of this project was to identify transcription factors that might bind to the bHLH transcription factor MIST1. Unfortunately, no definitive nuclear binding partner of MIST1 was identified in this LC-MS/MS analysis.

Cell culture studies have shown that SAP18 and SP1 serve as potential binding partners of MIST1 (Jia 2008). However, my *in vivo* study using a mouse model did not identify either of these proteins. This suggests that under correct physiological conditions (e.g.an intact pancreas), the same interactions identified using established cell lines may not occur. There are several reasons as to why these two studies do not agree. First, the pancreas is a complex organ dedicated to conducting the immense task of food digestion and maintaining a proper balance of blood glucose levels. The high content of hydrolases produced by pancreatic acinar cells makes it the most difficult tissue in the body to isolate intact proteins and protein complexes (Börner et al. 2009). Due to this challenge, I speculate that

the protein purification that we performed was not sufficient to fractionate pure, intact nuclear protein complexes. Second, the mass spectrometry analysis of my samples revealed that the identified prey proteins of MIST1 were mostly cytoplasmic or membrane associated proteins suggesting that the sample extracts that I prepared consisted of numerous non-specific background proteins which should have been eliminated during the purification process. Improper nuclear fractionation may have occurred due to inappropriate buffer conditions. It has been shown that complex organs like the pancreas require a detergent-based sequential extraction process in order to properly fractionate extracts from various compartments of the tissue (Ramsby & Makowski 2011; Börner et al. 2009). Thus, the commercial kit we used to isolate nuclear extracts (NE-PER kit) may not have been an ideal approach to prepare nuclear extracts for mass spectrometry. Because the *Mist1*$^{BT/Myc}$ mouse also contain Myc and His tags, future studies could utilize a tandem pull-down approach to see if this would improve MIST1-interacting specificity.

An additional experimental modification that could be attempted would be to adjust the detergent components in the lysis and isolation protocols. Detergents are essential to prepare samples for mass spectrometry analysis. However, ionic detergents such as NP-40 tend to inhibit ionization and also reduce the chromatographic resolution which can interfere with the analysis process (Chen et al. 2007; Katayama et al. 2001; Zhang & Li 2004). NP-40 is one of the detergents I used to prepare my samples. Therefore, I speculate that the presence of this detergent may have contributed to a low peptide-yield. Alternative nonionic

detergents, such as *n*-dodecyl-β-D-maltoside (DDM) or 5-cyclohexyl-1-pentyl-β-D-maltoside (CYMAL-5) could be tested to see if they increase overall peptide yield (Hess 2013).

Finally, it is possible that the MIST1 dimer does not actually utilize another transcription factor as a co-factor binding partner. Certain epigenetic modifications such as DNA methylation and histone modification may simply dictate which genes MIST1 binds to under different developmental or physiological contexts. Studies performed in mouse embryonic stem cells have revealed that TFs such as NRF1 cannot bind to its target motif when DNA is methylated, suggesting that NRF1 depends on other binding factors in order to create a hypomethylated condition to bind to its target site (Karemaker & Vermeulen 2016; Domcke et al. 2015).Future studies examining the importance of epigenetic regulation of MIST1 target genes will be needed to address this issue. Of course, we also need to consider that MIST1 may have other a non- transcription factor function where it binds to a cytoplasmic protein partner. Hence, in order to elucidate the role of MIST1 in other cellular processes, future studies could follow the cytoplasmic prey proteins identified in this current study (i.e.,Cathepsin-B and Syndecan-1) to determine if these interactions are biologically relevant to pancreatic acinar cells.

CHAPTER 4. SILENCING MIST1 GENE EXPRESSION IS ESSENTIAL FOR RECOVERY FROM ACUTE PANCREATITIS

4.1 Introduction

The majority of the exocrine pancreas consists of acinar cells which are tasked with synthesizing, modifying, packaging and secreting vast quantities of pro-digestive enzymes (zymogens) into the duodenum to maintain metabolic homeostasis for the organism (Stanger & Hebrok 2013; Puri & Hebrok 2010; MacDonald et al. 2010; Gittes 2009). The ability of acinar cells to produce high levels of appropriately packaged proteins requires the coordination of pathways responsible for the accumulation and assembly of critical components of the secretory apparatus, the establishment of proper apical-basal polarity and cell-cell communication and the proper management of mis-folded proteins through the Unfolded Protein Response (UPR) (MacDonald et al. 2010; Pin et al. 2015; Chevet et al. 2015; Glimcher 2010; Schröder & Randal J Kaufman 2005; Schröder & Randal J. Kaufman 2005). Because of the high levels of potentially dangerous hydrolases synthesized by the exocrine pancreas, the organ is prone to a number of disease states including pancreatitis and pancreatic cancer.

Pancreatitis is a disease that targets pancreatic acinar cells, leading to organ inflammation, fibrosis and overall tissue disruption (Pasca di Magliano et al. 2013). It is commonly associated with gallstones and excessive alcohol consumption which leads to cell damage through intracellular activation of zymogens (Grady et al. 1998). Importantly, pancreatitis is also a known risk factor for pancreatic ductal adenocarcinoma (PDAC) (Lowenfels et al. 1993; Malka et al. 2002; Pinho et al. 2014) and a number of mouse genetic studies have shown that episodes of acute pancreatitis (AP) can serve as a driving force for $KRAS^{G12D}$-induced PDAC (Carrière et al. 2009; Carrière et al. 2011; Collins et al. 2014; Guerra et al. 2011; Guerra et al. 2007; Molero et al. 2012; Pinho et al. 2011; Siveke et al. 2008; Kopp et al. 2012). Indeed, a hallmark of AP is alteration of acinar cell identity where acinar cells acquire ductal characteristics through a process known as acinar-ductal metaplasia (ADM) (Molero et al. 2012; Pinho et al. 2011; Prévot et al. 2012; Prévot et al. 2013). ADM is thought to represent a precursor state that can progress to PDAC under conditions of oncogenic and tumor suppressor mutations (Carrière et al. 2011; Collins et al. 2014; Shi et al. 2009; Zhu et al. 2007; H Huang et al. 2013; Collins et al. 2012; Ardito et al. 2012). Despite a wealth of information concerning the broad phenotype associated with pancreatitis, little is understood regarding the transcriptional regulatory networks that are susceptible to AP episodes and how these networks allow acinar cells and the exocrine organ to recover.

Key transcription factors that establish and maintain a healthy acinar cell state include PTF1a, MIST1 (also known as *Bhlha15*), GATA6, and Nr5a2 (MacDonald et al. 2010; Mills & Taghert 2012; Hale et al. 2014; Direnzo et al. 2012;

Holmstrom et al. 2011; Masui et al. 2010; Xuan et al. 2012; Martinelli et al. 2015; Flandez et al. 2013). PTF1a and MIST1 are basic helix-loop-helix (bHLH) factors that have been shown to exhibit tumor suppressor properties where acinar cells lacking each factor are highly susceptible to $KRAS^{G12D}$-induced transformation (Shi et al. 2009; Shi et al. 2013; Krah et al. 2015). Both factors play important roles in acinar differentiation events. PTF1a is essential for *Mist1* gene expression and expression of most zymogen encoding genes including *elastase*, *carboxypeptidase* and *amylase* (Hale et al. 2014; Beres et al. 2006; Masui et al. 2007; Rodolosse et al. 2004).

Although not essential for embryonic acinar development, MIST1 plays an essential role in the maturation of acinar cells by regulating genes critical for apical-basal cell polarity, the assembly and clustering of secretory granules, proper Ca^{2+} signaling, the expansion of the endoplasmic reticulum (ER), UPR pathway homeostasis, cell cycle progression and regulated exocytosis (Direnzo et al. 2012; Garside et al. 2010; Hess et al. 2011; Jia et al. 2008; Luo et al. 2005; Pin et al. 2001; Rukstalis et al. 2003; Zhu et al. 2004). What sets MIST1 apart from PTF1a is that it exhibits a broad tissue specificity, being present in most serous secretory cells in the body, including salivary acinar, stomach zymogenic, mammary alveolar and immunoglobulin secreting B cells (Aure et al. 2015; Huh et al. 2010; Pin et al. 2000; Bredemeyer et al. 2009; Capoccia et al. 2011; Tian et al. 2010; Zhao et al. 2006; Habbe et al. 2008). In all cases, MIST1 is responsible for the overall upregulation of the protein synthesis, processing and secretory machinery, often

acting as a scaling factor to insure highly efficient regulated secretion for each cell type (Mills & Taghert 2012; Hess et al. 2011; Huh et al. 2010).

The importance of MIST1 to maintaining a healthy cellular state for secretory cells is also evident in a number of different cancers. Both stomach cancer and PDAC tumors have been shown to initiate from *Mist1*-expressing secretory cells (Shi et al. 2009; Zhu et al. 2007; Habbe et al. 2008; Lennerz et al. 2010; Nam et al. 2010). However, early in the transformation process, stomach zymogenic cells and pancreatic acinar cells that are undergoing metaplasia silence *Mist1* gene expression, suggesting that inhibiting MIST1 activity is a critical step in allowing cells to enter into a proliferative phase (Shi et al. 2009; Shi et al. 2013; Jia et al. 2008; Lennerz et al. 2010; Nam et al. 2010; Nozaki et al. 2008). Furthermore, sustained *Mist1* expression in $Kras^{G12D}$-expressing acinar cells inhibits ADM and PDAC development, again highlighting the concept that MIST1 exhibits tumor suppressor properties (Shi et al. 2009; Zhu et al. 2007).

Because pancreatitis is a known risk factor for PDAC, and MIST1 is critical to PDAC development, we set out to examine if *Mist1* gene expression is silenced under AP conditions and to test if sustained MIST1 activity would alleviate AP damage responses. Our studies demonstrate that during AP damage in both mouse and human, *Mist1* gene transcription and protein accumulation are dramatically reduced. In mice subjected to caerulein-induced AP, *Mist1* silencing is a transient event. As cells recover from AP damage, the *Mist1* locus is transcriptionally re-activated and MIST1 protein levels are restored. Despite this re-expression, analysis of conditional *Mist1* knock-out (*Mist1 cKO*) mice revealed

that *Mist1*-deficient pancreata responded similarly to AP treatment as control animals, with an initial damage phase that was rapidly followed by recovery. We next examined if sustained *Mist1* expression (*iMist1*) in genetically engineered mice could alleviate AP-induced damage. Surprisingly, in *iMist1* animals, AP produced a dramatic phenotype of significant tissue damage followed by cell death in cells that expressed *iMist1*. Despite the extreme damaged response in *iMist1* mouse pancreata, the pancreas partially recovered by regenerating healthy acini from the small minority of acinar cells that failed to activate the *iMist1* transgene. We conclude that silencing *Mist1* expression is a critical event for acinar cells to survive an AP episode where down regulating MIST1 activity may allow cells to suppress their secretory function and permit a window of cell proliferation. However, to fully re-establish a functional acinar cell capable of efficient exocytosis, the *Mist1* gene must be reactivated to scale up the appropriate intracellular machinery that generates secretory vesicles, expands the ER and establishes cell communication via gap junction signaling. The importance of MIST1 to these events suggests that devising strategies to modulate transcriptional networks could ease clinical symptoms in patients diagnosed with pancreatitis and pancreatic cancer.

4.2 Results

4.2.1 *Mist1* Gene Expression is Silenced during $Kras^{G12D}$-induced PanIN and PDAC Formation

The MIST1 transcription factor (also known as BHLHA15) regulates key genes that are required for acinus polarity, cell-cell junctions and the processing of zymogen granules (Mills & Taghert 2012; Direnzo et al. 2012; Garside et al. 2010; Tian et al. 2010). Loss of MIST1 function leads to deficiencies in acinar cell integrity, cell polarity, ER expansion and regulated exocytosis (Direnzo et al. 2012; Pin et al. 2001; Zhu et al. 2004; Luo et al. 2005; Rukstalis et al. 2003). Similar defects in polarity and acinar cell properties are also hallmarks of $Kras^{G12D}$-driven transformation events where acinar cells exhibit acinar-ductal metaplasia (ADM) that progresses to pancreatic intraepithelial neoplasia (PanIN) and pancreatic ductal adenocarcinoma (PDAC) (Shi et al. 2009; Shi et al. 2013; Habbe et al. 2008). PanINs and PDAC tumors, each derived from acinar cells, lose acinar characteristics and no longer express MIST1 protein (**Figure 4-1A**) (Puri & Hebrok 2010; Shi et al. 2009; Zhu et al. 2007; Shi et al. 2013; Morris et al. 2010). The importance of cell integrity to PDAC disease is also supported by studies showing that damage to $Kras^{G12D}$-expressing acinar cells via an episode of acute pancreatitis (AP) accelerates PanIN formation (Carrière et al. 2009; Guerra et al. 2007; Guerra et al. 2011; Pinho et al. 2011).

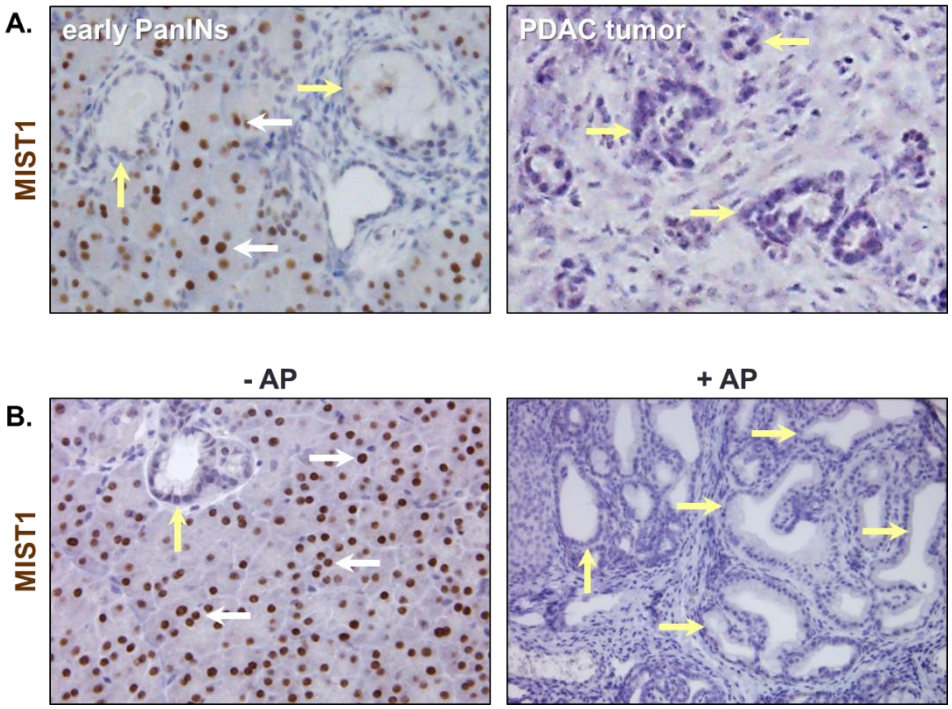

Figure 4-1. *Mist1* gene expression is silenced during Kras^{G12D}-induced PanIN and PDAC formation. (A) *Elastase$_{pr}$-CreERT, Kras$^{LSL-G12D/+}$, Trp53$^{LSL-R172H/+}$* mice were treated with Tam to activate the *Kras$^{LSL-G12D}$* and *Trp53$^{LSL-R172H/+}$* alleles and then stained with anti-MIST1. At early time points, nuclear MIST1 staining is detected in normal acinar cells (white arrows) whereas PanINs and late stage PDAC tumors are MIST1 negative (yellow arrows). **(B)** In the absence of AP, *Mist1$^{CreERT/+}$, Kras$^{LSL-G12D/+}$* mice develop sporadic MIST1 negative PanIN lesions (yellow arrow) while non-transformed acinar cells remain MIST1 positive (white arrows). However, a brief episode of AP quickly transforms the majority of *Mist1$^{CreERT/+}$, Kras$^{LSL-G12D/+}$* acinar cells to MIST1 negative PanINs (yellow arrows).

Mist1$^{CreERT/+}$, *Kras*$^{LSL-\ G12D/+}$ mice treated with tamoxifen (to activate *Kras*^{G12D} expression) and caerulein (to induce AP) exhibit extensive PanIN development when compared to the no AP control group (**Figure 4-1B**). In all cases, acinar-derived PanIN/PDAC epithelial cells remain MIST1 negative.

4.2.2 *Mist1* Gene Expression is Transiently Silenced upon Acute Pancreatitis Damage

4.2.2.1 Characterization of *Mist1*$^{CreERT/+}$ Mice Following Acute Pancreatitis

To evaluate the importance of MIST1 during acinar metaplasia, we characterized *Mist1* expression during the damage and subsequent recovery phases of AP, a known driver of PDAC tumor development (Carrière et al. 2009; Guerra et al. 2011; Guerra et al. 2007; Pinho et al. 2011). For these studies, *Mist1*$^{CreERT/+}$ mice were used as controls as all subsequent mouse lines contained the *Mist1*^{CreERT} knock-in allele (Shi et al. 2009; Habbe et al. 2008). Standard caerulein treatment (**Figure 4-2A**) of 8 week *Mist1*$^{CreERT/+}$ mice led to significant and rapid damage to the exocrine acinar cells. As early as 6h post-AP, acinar lumens were distended and zymogen granules were rapidly lost (**Figure 4-2B).** Morphometric analysis of *Mist1*$^{CreERT/+}$ mouse pancreata also confirmed increased tissue damage and edema during AP injury (**Figure 4-11A**). By 1d post-AP, significant increases in edema and inflammatory cell infiltrates were observed, accompanied by extensive formation of Keratin19 (K19)+/Amylase (AMY)+ ADM lesions. Expression of CLUSTERIN, a known marker of acinar cell damage (Greer et al. 2013; von Figura et al. 2014), also was greatly elevated at 6h post-AP (**Figure**

4-2B,C and **Figure 4-3A**). Transcript and protein levels of acinar cell markers, including *Amylase* (*Amy*), *Trypsinogen* (*Tryp*) and *Carboxypeptidase* (*Cpa*), were significantly reduced over the 6h-2d post-AP period (**Figure 4-2C** and **Figure 4-3A,B**). In contrast, ductal markers (K19, SOX9) were greatly elevated, confirming the formation of extensive ADM (**Figure 4-2B,C** and **Figure 4-3A**,**B**). Identical ADM responses were obtained with caerulein-treated wild-type mice (data not shown). Despite significant development of ADM lesions upon AP induction, AP metaplasia was transient as lesions resolved 4d-10d post-AP. In all cases, *Clusterin*, *K19* and *Sox9* transcript and protein levels returned to their low control states while acinar markers (*Amylase*, *Trypsinogen*, *Carboxypeptidase*) re-established high expression thresholds as illustrated in **Figure 4-2B,C** and **Figure 4-3A,B**.

4.2.2.2 The *Mist1* Gene is Transcriptionally Silenced during Acute Pancreatitis

The major phenotype associated with caerulein-induced AP is loss of acinar cell integrity (Siveke et al. 2008; Jensen et al. 2005; Kowalik et al. 2007; Lerch & Gorelick 2013). Because the transcription factor MIST1 is critical for maintaining acinar cell polarity and function, we examined if MIST1 protein accumulation was altered in AP mice. As shown in **Figure 4-5B,C**, high levels of MIST1 protein were detected in all control acinar cells, whereas duct and islet cells remained MIST1

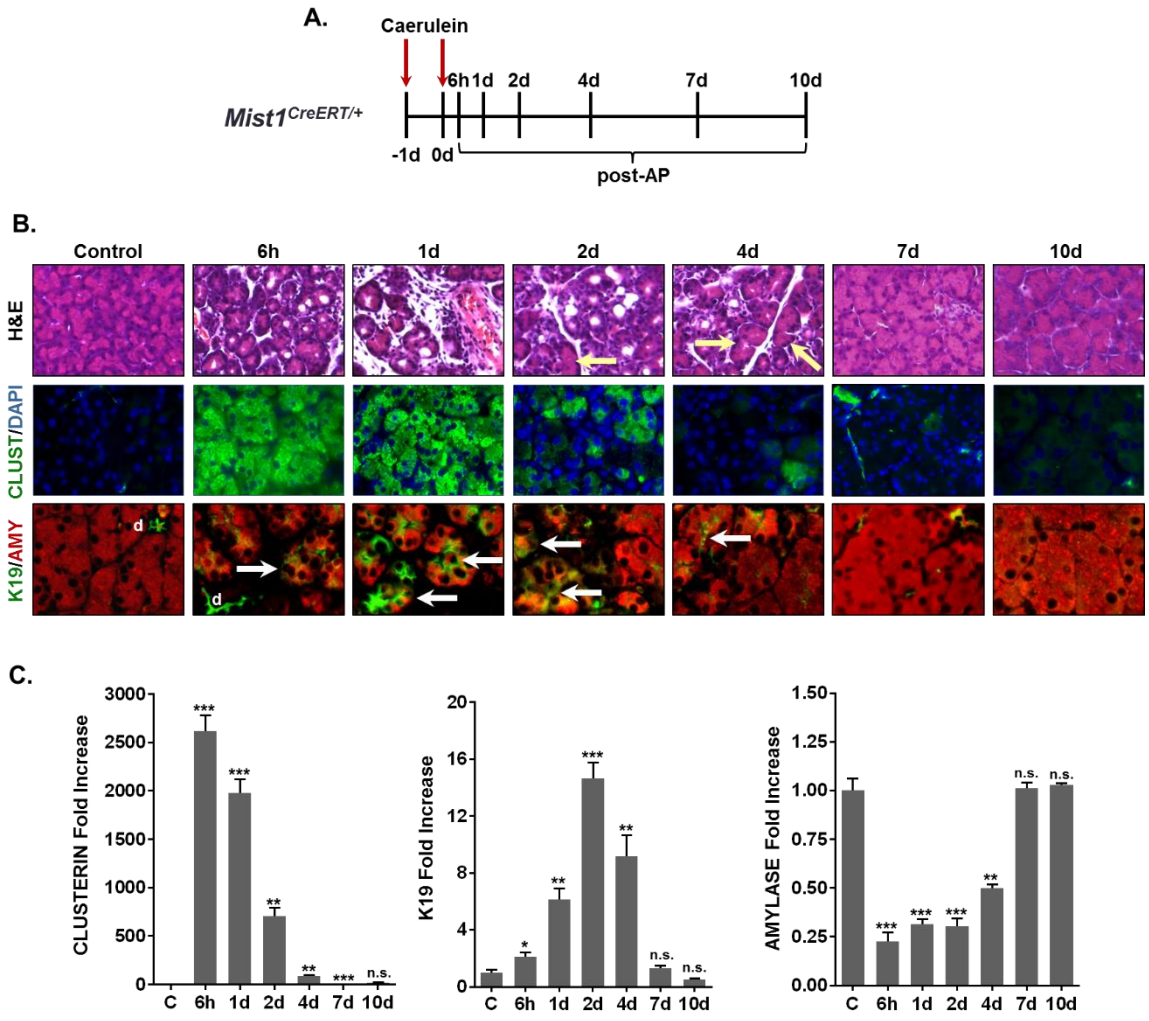

Figure 4-2. Characterization of *Mist1*$^{CreERT/+}$ mice following acute pancreatitis. **(A)** Time course diagram of caerulein-induced acute pancreatitis. **(B)** H&E and IF analyses of *Mist1*$^{CreERT/+}$ pancreas samples in the absence of AP treatment (control) or post-AP for the indicated times. At early times acinar cells exhibit elevated levels of CLUSTERIN expression and Amylase+/K19+ ADM lesions. However, by 10d post-AP the majority of the tissue fully recovers. Arrows in the H&E section point out recovered acini whereas arrows in the K19/AMY panels indicate ADM lesions. (d, duct) **(C)** Relative CLUSTERIN, K19 and AMYLASE protein levels in IF sections from *Mist1*$^{CreERT/+}$ pancreata at the indicated times and normalized to control values. *p≤0.05;**p≤0.01; ***p≤0.001; n.s.-not significant

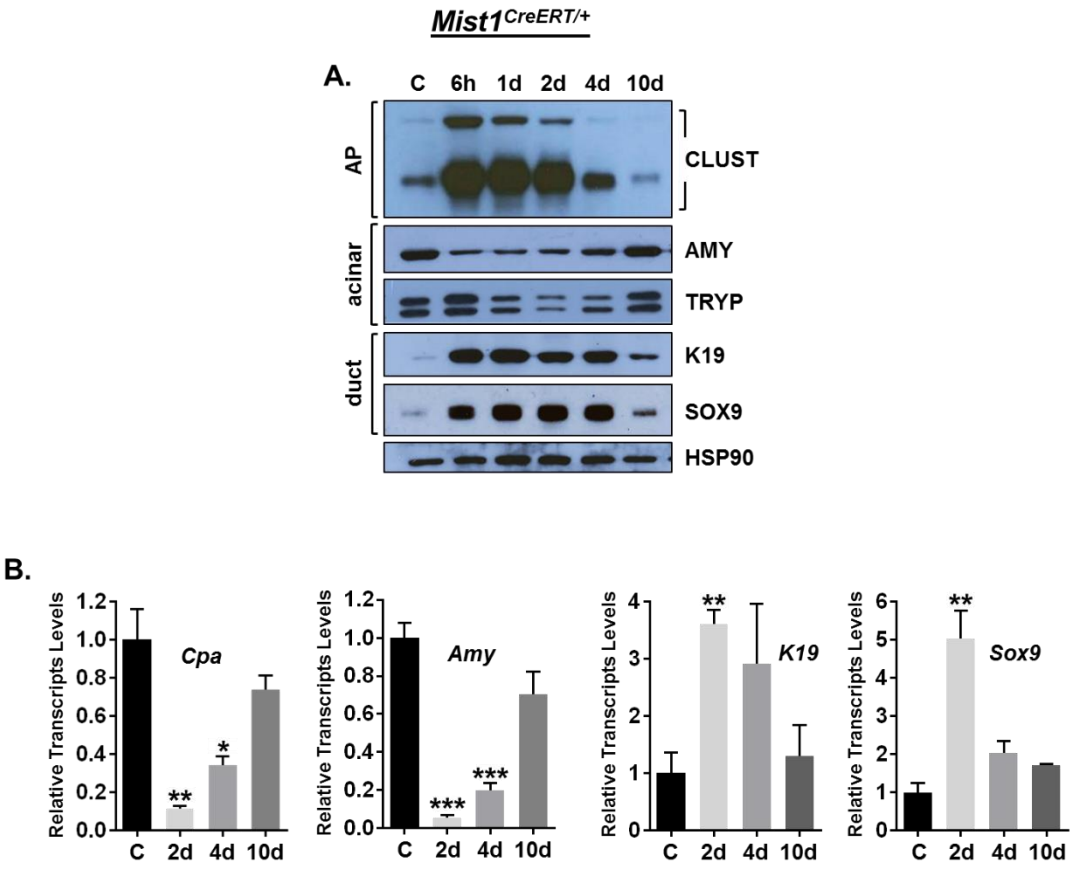

Figure 4-3. Acinar and ductal markers in *Mist1*$^{CreERT/+}$ mice following acute pancreatitis (A) Immunoblot analysis of *Mist1*$^{CreERT/+}$ pancreata post-AP. CLUSTERIN levels were increased during AP damage. AMYLASE and TRYPSINOGEN levels (acinar markers) decreased during AP and returned to their high control states upon recovery. In contrast ductal markers K19 and SOX9 became greatly elevated during AP, confirming the formation of extensive ADM. **(B)** RT-qPCR analysis of gene transcripts confirmed the initial ADM phenotype followed by recovery at 10d post-AP. *p ≤ 0.05; **p ≤ 0.01; ***p ≤ 0.001.

negative (**Figure 4-4**). However, in AP mice, *Mist1* transcripts and protein were rapidly lost in damaged acinar cells (**Figure 4-5B**-**D**). The absence of MIST1 was observed 6h-2d post-AP during the period corresponding to the major time frame for ADM lesion induction. Identical loss of MIST1 protein was also observed in patients exhibiting pancreatitis- associated ADM (**Figure 4-5A)**. Nonetheless, as mouse acinar cells recovered (4d-10d post-AP), *Mist1* transcript and protein levels greatly increased, achieving levels that were comparable to those observed in control acinar cells. The transient change in *Mist1* transcripts and protein during the AP response was also reflected in the expression profiles of known MIST1 target genes (Direnzo et al. 2012; Garside et al. 2010; Tian et al. 2010). Transcripts from MIST1-induced genes *Atp2c2*, *Copz2* and *Rab3d* were reduced during the 6h-2d post-AP period while transcripts from MIST1-repressed genes (*e.g.*, *Rnd2*) were up-regulated (**Figure 4-6**). Thus, transient silencing of *Mist1* influences a number of key events associated with acinar cell integrity. These results suggest that the process of silencing and then re-expressing *Mist1* may be critical in allowing the exocrine pancreas to properly recover from an acute pancreatitis episode.

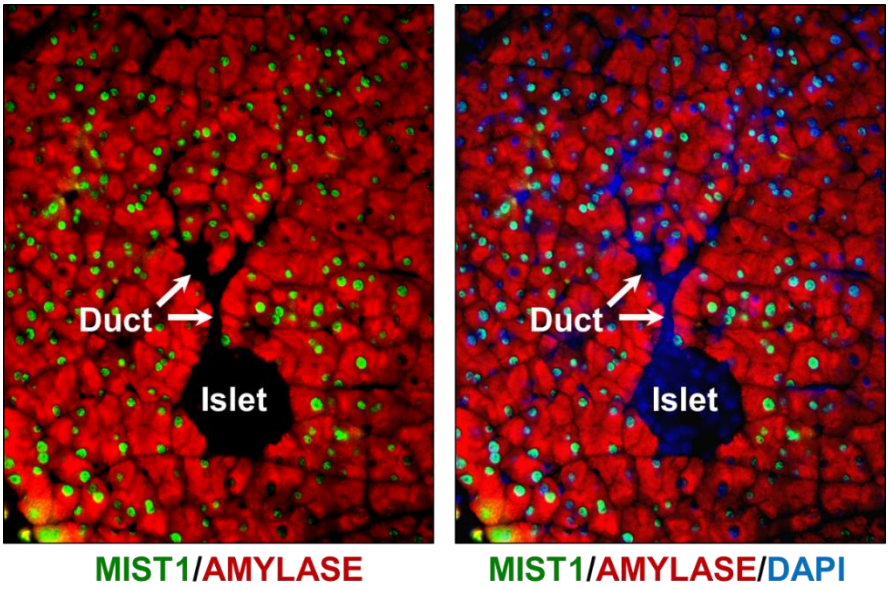

Figure 4-4. IF images of *Mist1*$^{CreERT/+}$ pancreata revealing nuclear MIST1 protein exclusively in acinar cells. Nuclei are stained with DAPI and green nuclear staining signifying MIST1 localization in the nuclei. Islets and ducts remain MIST1 negative.

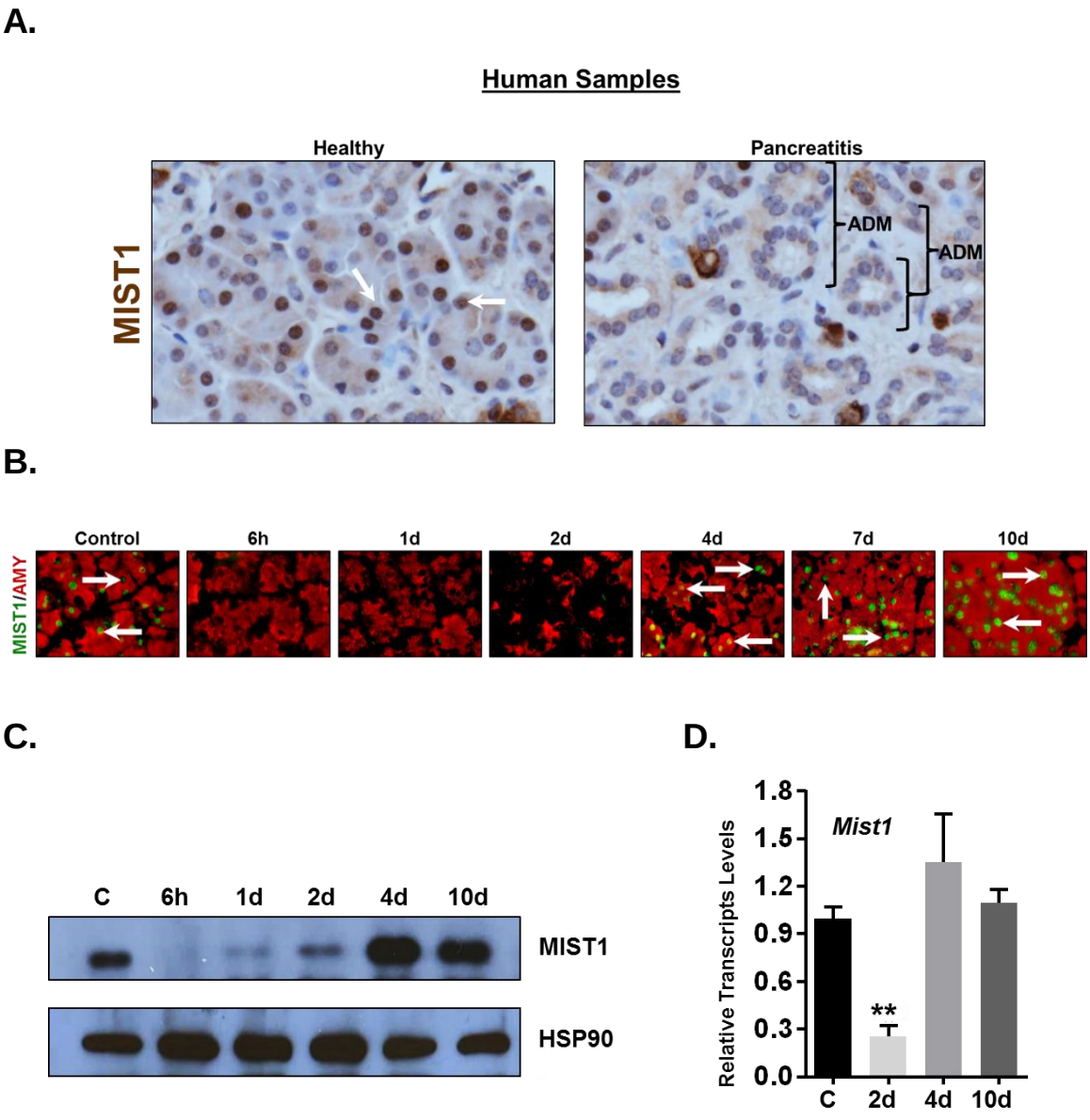

Figure 4-5. The *Mist1* gene is transcriptionally silenced during acute pancreatitis. (A) MIST1 IHC staining (arrows) of healthy and pancreatitis patient samples. Human acinar cells undergoing ADM are MIST1 negative. **(B)** Analysis of MIST1 (arrows) in *Mist1*$^{CreERT/+}$ pancreata. Damaged acinar cells exhibit greatly reduced MIST1 levels that recover by 10d post-AP. **(C)** MIST1 immunoblot analysis of *Mist1*$^{CreERT/+}$ pancreata over the indicated post-AP time points. **(D)** RT-qPCR analysis of *Mist1* gene expression during AP damage and recovery.

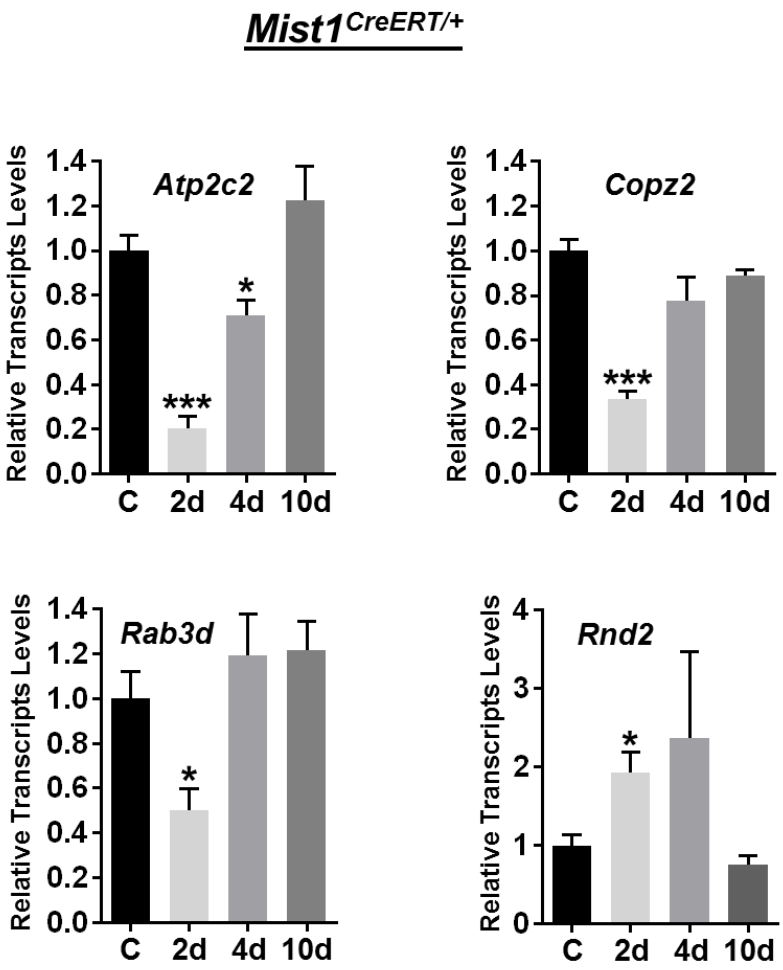

Figure 4-6. MIST1 gene targets during acute pancreatitis. RT-qPCR of MIST1 gene targets, *Atp2c2*, *Copz2*, *Rab3d* and *Rnd2* during AP. *p ≤ 0.05; **p ≤ 0.01; ***p ≤ 0.001.

4.2.3 Generation and Characterization of *Mist1*$^{lox/lox}$ Mice

4.2.3.1 Establishing the *Mist1*$^{CreERT/lox}$ Model System

Previous studies reported that *Mist1* null animals exhibited a pronounced AP phenotype, suggesting that the absence of MIST1 sensitizes acinar cells to an AP episode (Kowalik et al. 2007; Johnson et al. 2014; Mehmood et al. 2014). However, because these studies could only use germline *Mist1* nulls, it was not possible to establish if the enhanced AP phenotype was due to embryonic loss of MIST1 protein or was the result of inducing AP in already damaged adult pancreata. Thus, to directly test if MIST1 protein is required for acute pancreatitis recovery, we generated and characterized a conditional *Mist1*$^{lox/lox}$ mouse line (**Figure 4-7**). *Mist1*$^{CreERT/+}$ mice were crossed to *Mist1*$^{lox/+}$ animals to generate *Mist1*$^{CreERT/lox}$ offspring where one *Mist1* allele expressed CreER^{T2} while the other *Mist1* allele, engineered with an N-terminal BT-tag and a C-terminal MYC-tag, was flanked by LoxP sites (**Figure 4-7**). Treatment of 8 wk *Mist1*$^{CreERT/lox}$ mice with tamoxifen (Tam) led to efficient recombination and rapid loss of MIST1 protein in 99.6% acinar cells as early as 24h post-Tam (**Figure 4-8A-C**). Deletion of *Mist1* also led to significant changes in the expression patterns of MIST1 target genes. As predicted, expression of *Atp2c2* and *Cx32* decreased while *Rnd2* gene transcripts (which are normally repressed by MIST1 protein) increased following Tam treatment (**Figure 4-9A**). Similarly, MIST1-regulated CX32 gap junctions (Direnzo et al. 2012; Rukstalis et al. 2003) were rapidly lost upon Tam treatment of *Mist1*$^{CreERT/lox}$ mice (**Figure 4-9B**).

4.2.3.2 *Mist1*$^{CreERT/lox}$ mice exhibit similar AP recovery as *Mist1*$^{CreERT/+}$ animals

To determine if AP-induction in *Mist1*$^{CreERT/lox}$ animals produced a recovery delay when compared to *Mist1*$^{CreERT/+}$ mice, *Mist1*$^{CreERT/lox}$ animals were treated with Tam (to delete the *Mist1* coding region) (*Mist1 cKO*) and then induced with caerulein to generate an AP response (**Figure 4-10A**). As expected, control and AP-treated *Mist1 cKO* mice failed to express MIST1 protein (**Figure 4-13A**). Caerulein injections in *Mist1 cKO* animals elicited strong edema, inflammatory cell infiltrates and extensive ADM lesions as early as 6h post-AP (**Figure 4-10B** and **Figure 4-12**). ADM was accompanied by significant increases in *Clusterin*, *K19* and *Sox9* transcript and protein levels with a concomitant decrease in *Amylase*, *Elastase* and *Carboxypeptidase* levels (**Figure 4-10B-C; Figure 4-12** and **Figure 4-13A-B**). As with *Mist1*$^{CreERT/+}$ mice, the ADM phenotype was transient and the *Mist1 cKO* pancreas returned to a relatively normal status by 10d post-AP, although *Mist1 cKO* acini remained defective in acinar cell polarity and organization due to the absence of MIST1 protein. Surprisingly, with the exception of sustained elevated SOX9 protein levels at 10d post-AP, there was little difference between the AP responses for *Mist1*$^{CreERT/+}$ (**Figure 4-2**; **Figure 4-11** and **Figure 4-3**) and *Mist1 cKO* animals (**Figure 4-12**; **Figure 4-10** and **Figure 4-13**).

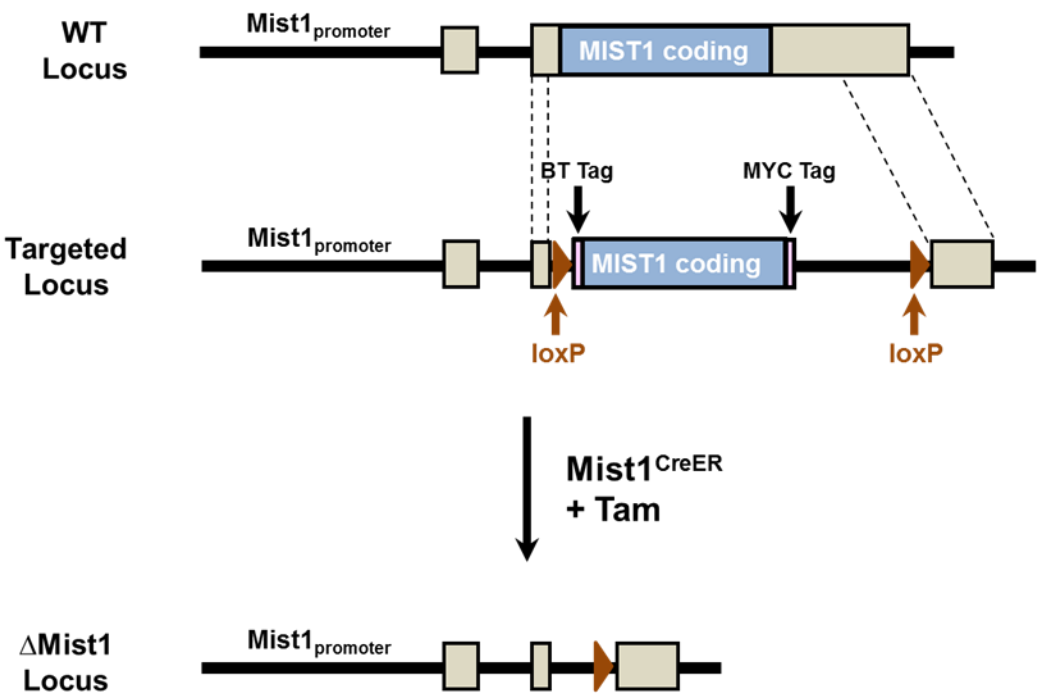

Figure 4-7. **Schematic of how the *Mist1*$^{lox/+}$ mice were generated through homologous recombination.** LoxP sites flank the entire *Mist1* coding region which is contained within exon 2.

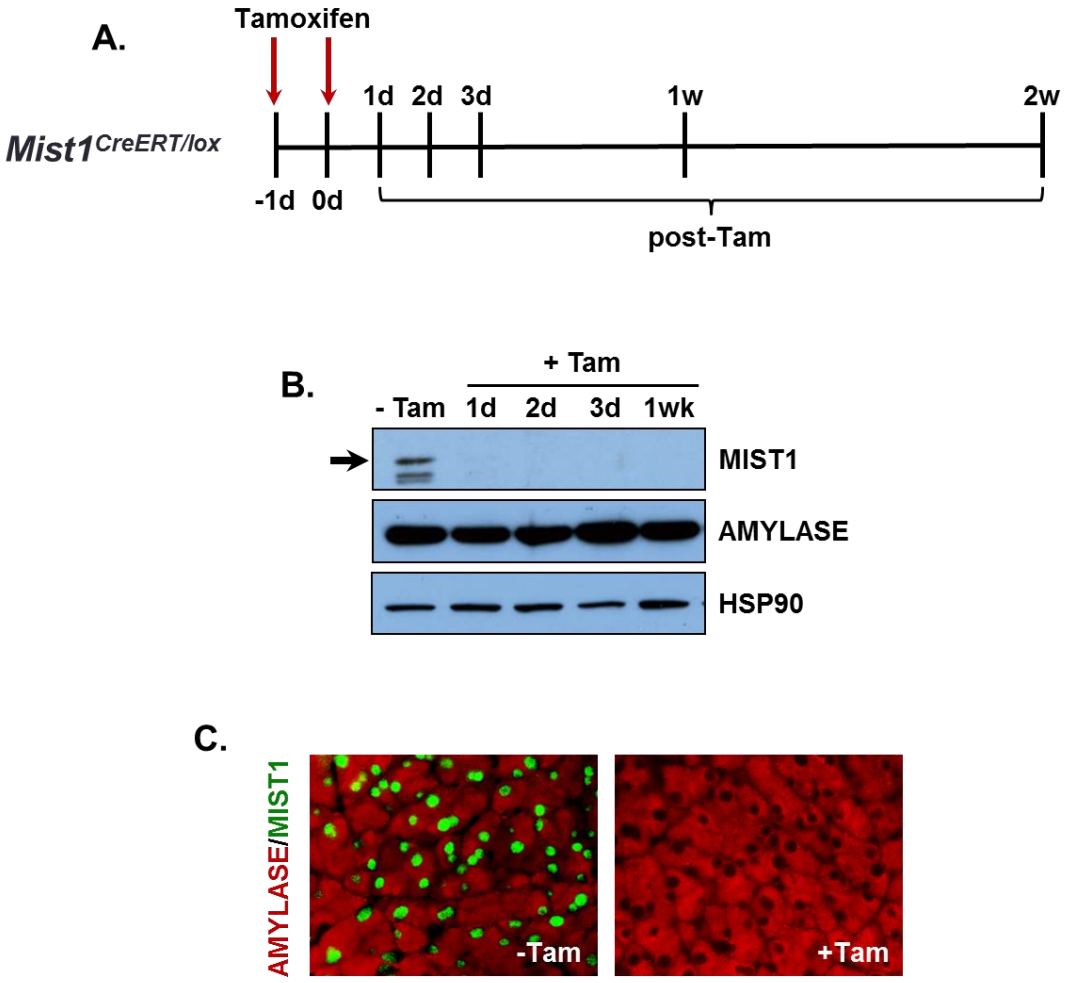

Figure 4-8. Functional analysis of *Mist1*$^{CreERT/lox}$ model system. (A) Schematic of Tam treatment and time course analysis for *Mist1*$^{CreERT/lox}$ mice. **(B)** Immunoblot demonstrating the absence of MIST1 protein in pancreata from Tam-treated *Mist1*$^{CreER/lox}$ mice. **(C)** IF staining with anti-MIST1 confirming that the vast majority of acinar cells are MIST1 negative following Tam treatment.

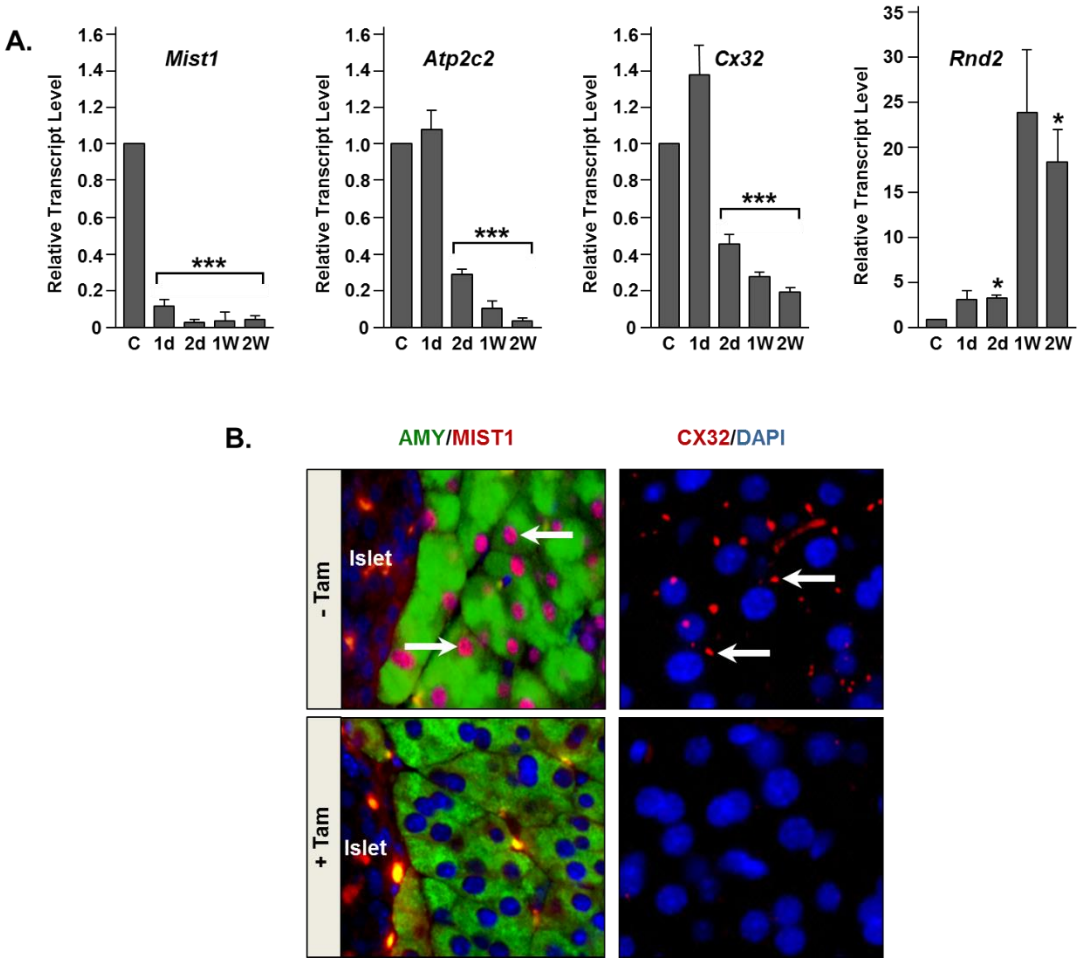

Figure 4-9. Establishing the *Mist1*$^{CreERT/lox}$ model system. (A). RT-qPCR analysis of MIST1 gene targets revealing loss of MIST1 regulation post-Tam. **(B)** CX32 gap junctions are readily detected in pancreata from -Tam treated *Mist1*$^{CreERT/lox}$ mice but are completely absent in +Tam samples. *p ≤ 0.05; ***p ≤ 0.001.

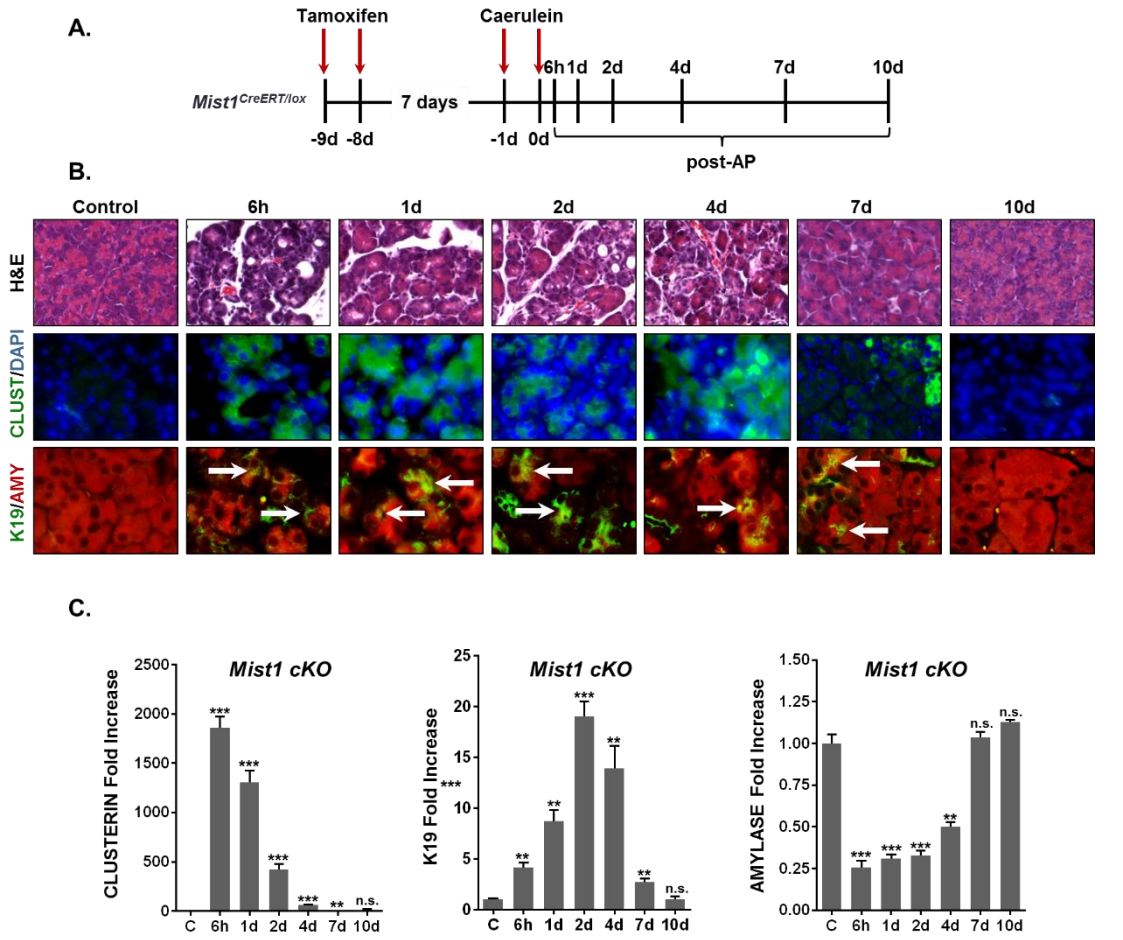

Figure 4-10. ***Characterization of Mist1$^{CreERT/lox}$ mice following acute pancreatitis.*** **(A)** Time course diagram of caerulein-induced acute pancreatitis in *Mist1$^{CreERT/lox}$* mice (*Mist1 cKO*). **(B)** H&E and IF analyses of *Mist1 cKO* pancreas samples in the absence of AP treatment (control) or post-AP for the indicated times. Arrows indicate AMY+/K19+ ADM lesions. **(C)** Relative CLUSTERIN, K19 and AMYLASE protein levels in IF sections from *Mist1 cKO* pancreata at the indicated times and normalized to control values. *p≤0.05;**p≤0.01; ***p≤0.001; n.s.-not significant

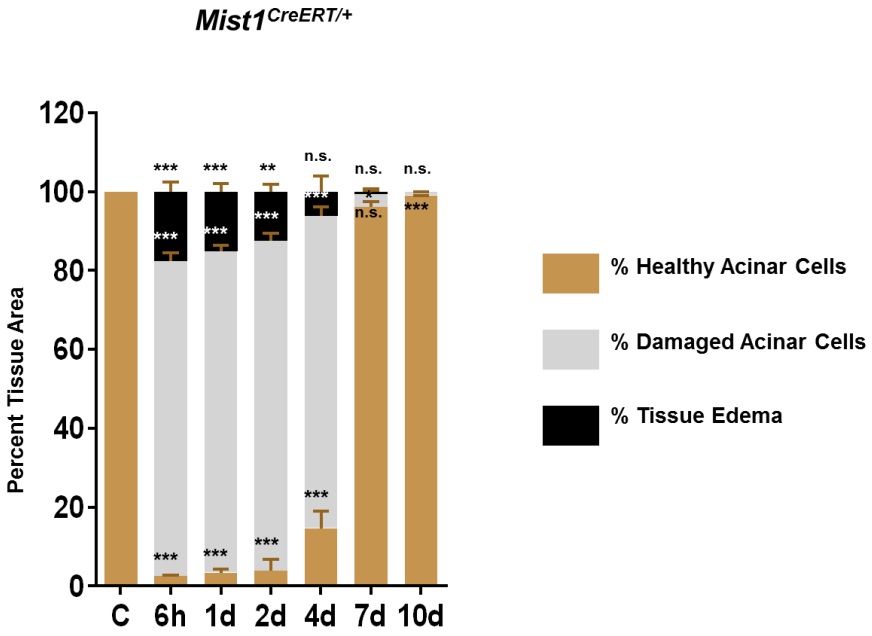

Figure 4-11.Quantification of AP damage in *Mist1*$^{CreERT/+}$ animals. H&E images were used to perform morphometric analysis of *Mist1*$^{CreERT/+}$ pancreata over the indicated times (C-Control, 6h, 1d, 2d, 4d, 7d and 10d). *p≤0.05;**p≤0.01; ***p≤0.001; n.s.-not significant

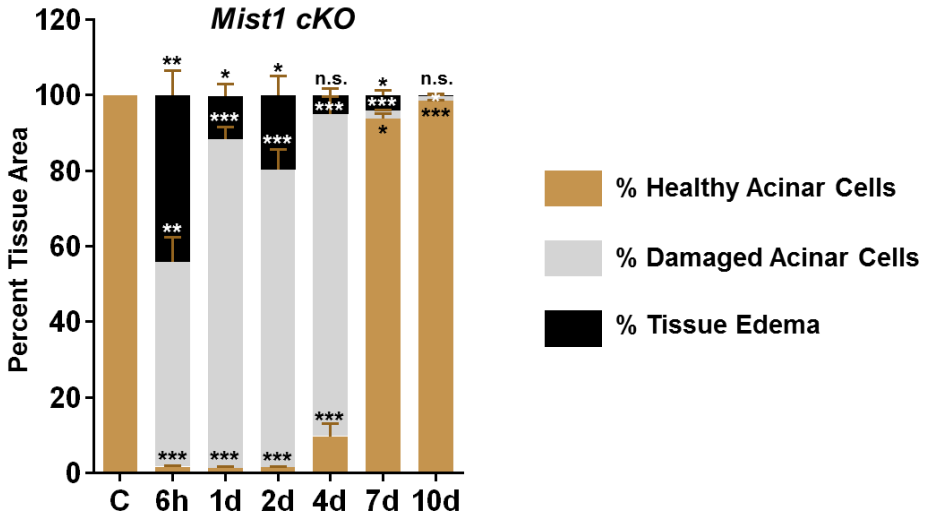

Figure 4-12. Quantification of AP damage in *Mist1*$^{CreERT/lox}$ (*Mist1 cKO*) animals. (A) Morphometric analysis of *Mist1 cKO* pancreata over the indicated times. *p≤0.05;**p≤0.01; ***p≤0.001; n.s.-not significant

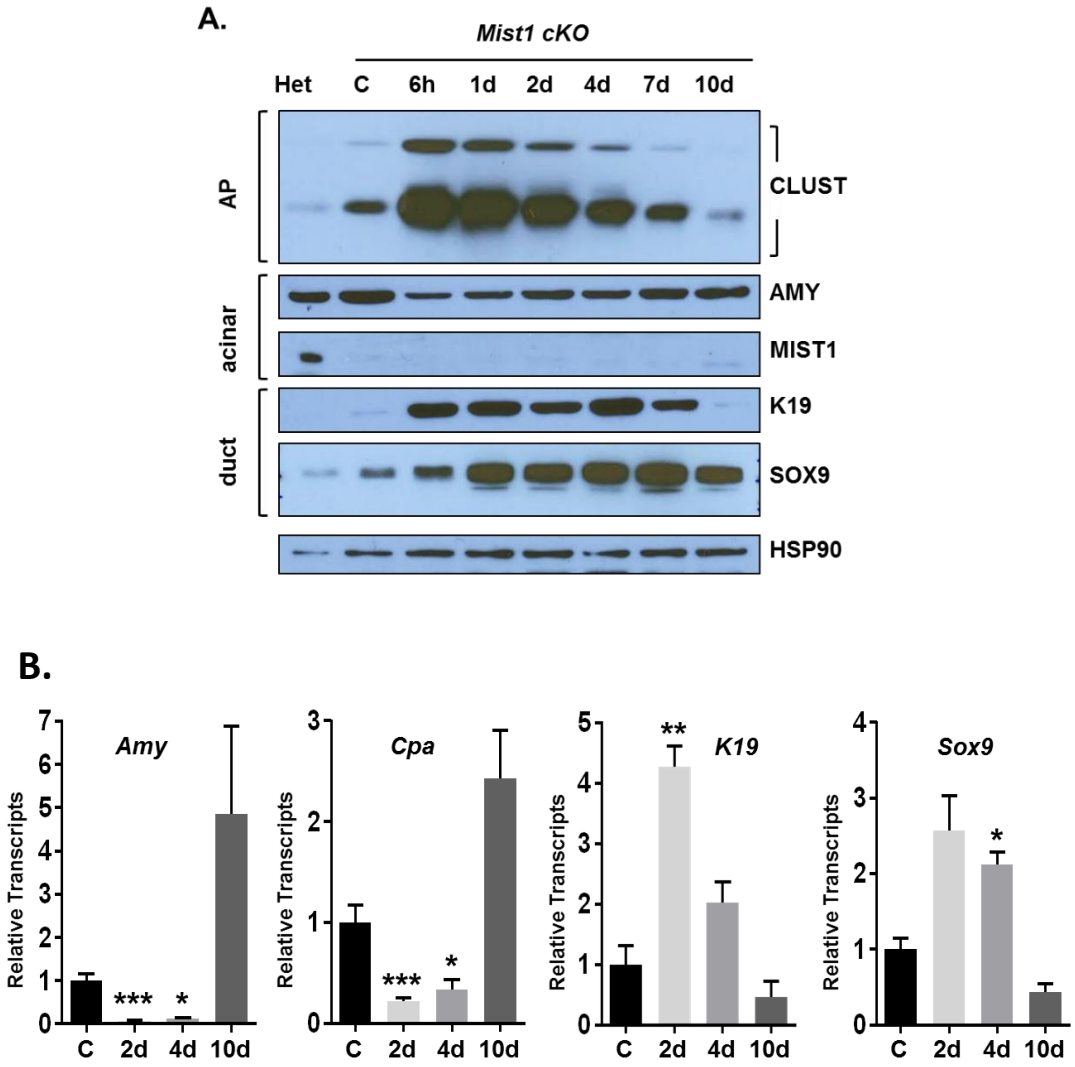

Figure 4-13. Characterization of *Mist1*$^{CreERT/lox}$ (*Mist1 cKO*) mice following acute pancreatitis. (A) Immunoblot analysis of protein expression from *Mist1 cKO* samples post-AP. Het is a control *Mist1*$^{CreERT/+}$ sample. HSP90 was used as a loading control. **(B)** RT-qPCR analysis of acinar and duct gene products during an AP time course study. *p ≤ 0.05; **p ≤ 0.01; ***p ≤ 0.001.

The ability of *Mist1 cKO* pancreata to recover from an acute pancreatitis episode with the same kinetics as *Mist1*$^{CreERT/+}$ mice was surprising given previous reports showing that *Mist1* null pancreata exhibited an enhanced AP response (Kowalik et al. 2007; Johnson et al. 2014; Mehmood et al. 2014). The main difference between the two models is that with germline *Mist1*$^{-/-}$ mice, the pancreas is significantly disorganized and defective by 8 wk of age (Pin et al. 2001). In contrast, *Mist1*$^{CreERT/lox}$ mice allow us to delete the *Mist1* allele in adult animals and induce AP prior to the development of overt pancreas damage caused by the absence of MIST1. Thus, to establish if short versus long-term loss of MIST1 activity differentially influences AP responses, *Mist1*$^{CreERT/lox}$ animals were given Tam and then treated with caerulein at 1 week post-Tam or 8 week post-Tam. As shown in **Figure 4-14A-B**, even in the absence of AP, *Mist1 cKO* pancreata at 8 week post-Tam exhibited early signs of ADM, with large increases in SOX9 and K19 protein levels (compare -AP 1 week versus 8 week). The increase in ductal gene expression reflected the ADM damage response that was observed in adult *Mist1*$^{CreERT/CreERT}$ (*Mist1* null) animals where the *Mist1* locus was absent in the germline. Interestingly, AP episodes in 1 week versus 8 week post-*Mist1* deletion did not reveal a significant difference in how the pancreas responded to this acute damage (**Figure 4-14A-B**). In all cases, 1 week and 8 week post-tam treated mice still managed to recover from the bulk of AP-induced damage by 10d post-AP (data not shown).

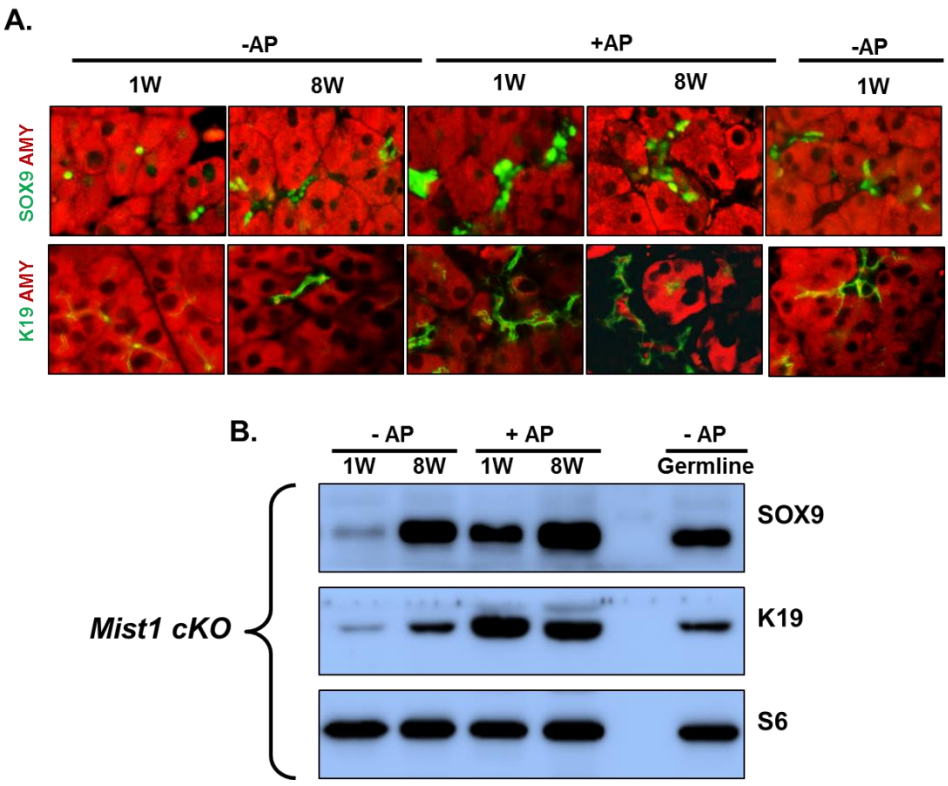

Figure 4-14. The absence MIST1 protein in adult acinar cells has little impact in allowing cells to recover from acute pancreatitis. Comparison of 1 week and 8 week post-*Mist1* deletion in the *Mist1 cKO* model. *Mist1*$^{CreERT/lox}$ mice were treated with Tam and then analyzed for protein expression **(A)** IF images and **(B)** immunoblots at the indicated times for -AP and +AP groups. S6 was used as a loading control. *Mist1*$^{CreERT/CreERT}$ (germline *Mist1* null) mice were used as a reference control

Taken together, we conclude that the absence of MIST1 protein in adult acinar cells has little impact in allowing cells to recover from acute pancreatitis.

4.2.4 Preventing *Mist1* gene silencing alters the acinar AP response

4.2.4.1 *Mist1*$^{CreERT/+}$/*LSL-Mist1*^{myc} mice (*iMist1*) exhibit acinar-specific *Mist1*^{myc} expression upon *CreER*^{T2} activity

Our studies have shown that *Mist1* expression is transiently silenced during the peak of AP damage and that *Mist1* re-expression is not required for the pancreas to recover from an AP episode. Nonetheless, given the importance of MIST1 to normal acinar cell polarity and secretory function (Direnzo et al. 2012; Jia et al. 2008; Luo et al. 2005; Pin et al. 2001; Rukstalis et al. 2003; Johnson et al. 2014; Johnson et al. 2004), we investigated if sustained MIST1 protein expression could be used to limit the initial AP damage response. Previous studies have shown that formation of ADM and PanIN lesions is significantly attenuated when *Mist1* expression is maintained in the presence of oncogenic KRAS^{G12D} (Shi et al. 2009; Shi et al. 2013). Therefore, we hypothesized that a similar lessening of AP damage might be achieved by maintaining MIST1 transcriptional activity. For these studies, we utilized a Cre-inducible *LSL-Mist1*^{myc} (*iMist1*^{myc}) transgenic mouse model (**Figure 4-15**) (Direnzo et al. 2012) and generated *Mist1*$^{CreERT/+}$/*iMist1*^{myc} offspring. Administering Tam to *Mist1*$^{CreERT/+}$/*iMist1*^{myc} mice induced *iMist1*^{myc} transgene expression in 94.7% pancreatic acinar cells (**Figure 4-16A-C**).

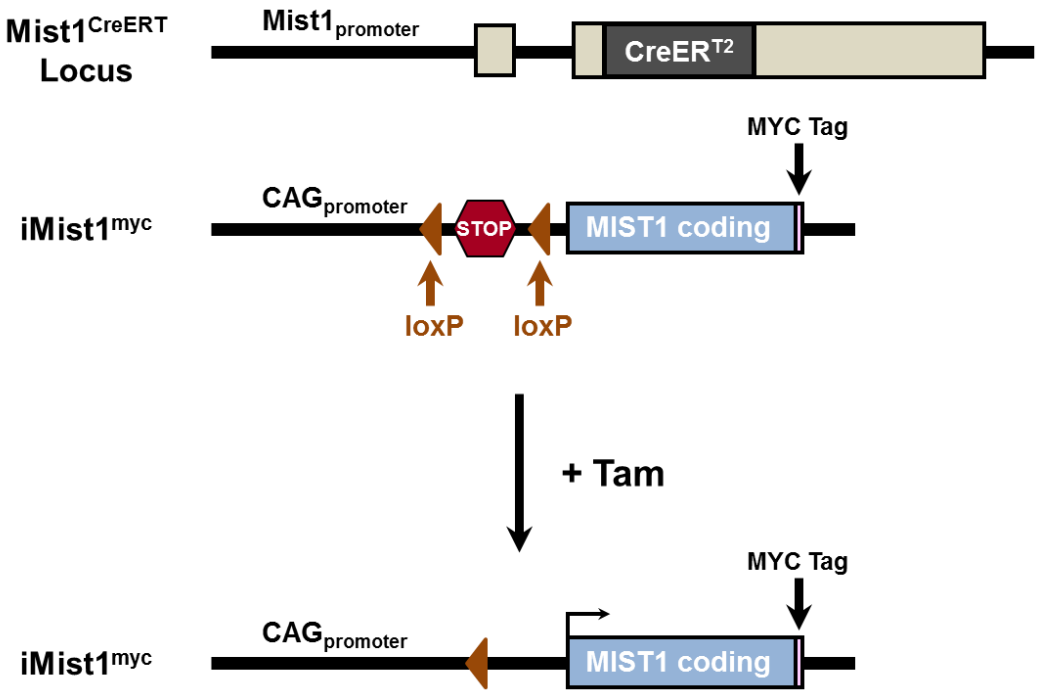

Figure 4-15. **Schematic of the *LSL-Mist1^{myc}* transgene in *iMist1^{myc}* mice.** *Mist1$^{CreERT/+}$/iMist1^{myc}* mice express the *iMist1^{myc}* transgene exclusively in acinar cells upon Tam induction ((Direnzo et al. 2012)

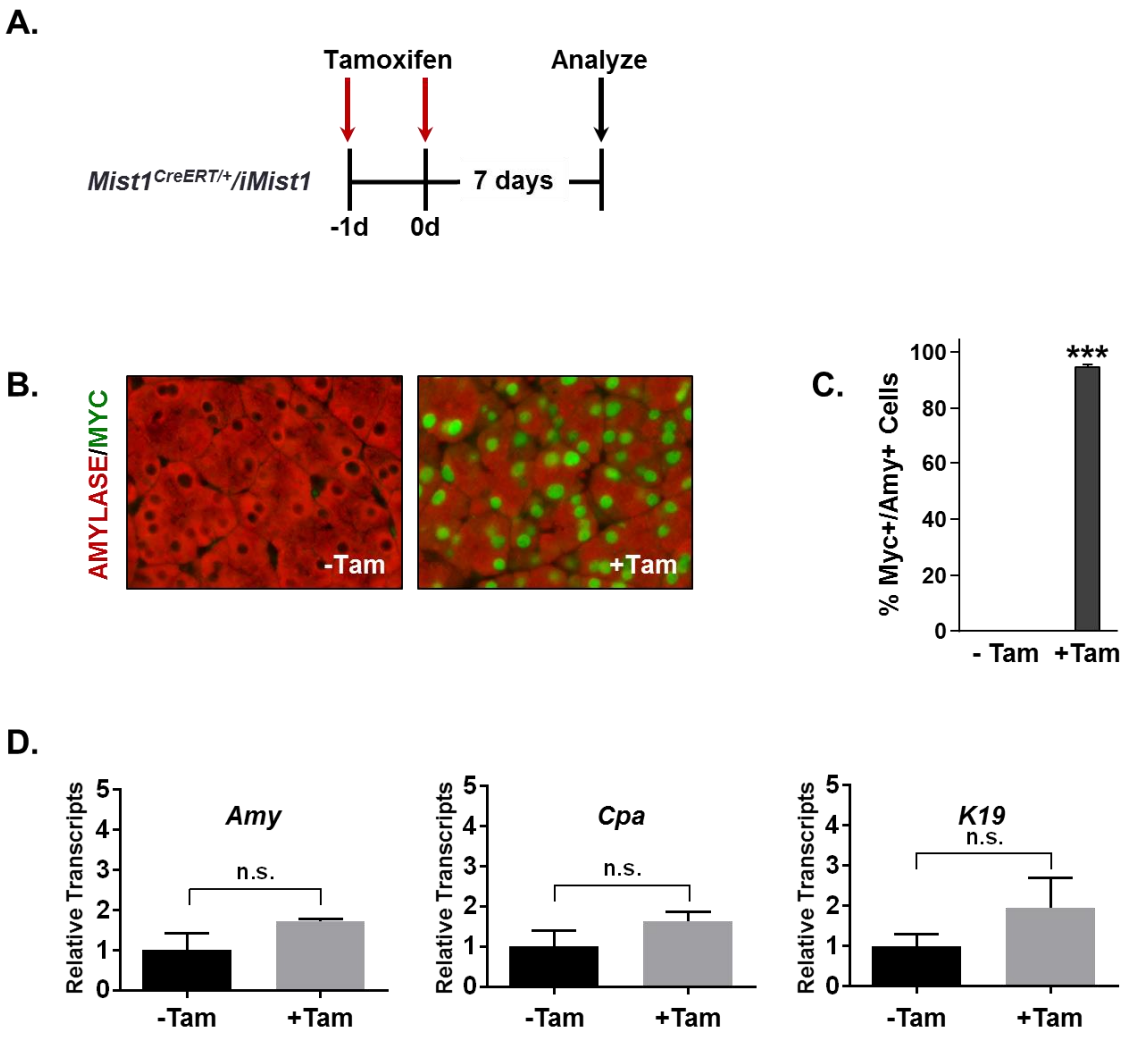

Figure 4-16. *Mist1*$^{CreERT/+}$*/LSL-Mist1*^{myc} mice *(iMist1)* exhibit acinar-specific *Mist1*^{myc} expression upon *CreER*^{T2} activity. (A) Diagram outlining the time course of the study. **(B)** Tam treatment of *iMist1* mice leads to rapid accumulation of nuclear MIST1^{myc} protein exclusively in pancreatic acinar cells. **(C)** Quantification of MIST1^{myc}+ acinar cells following Tam induction. **(D)** RT-qPCR analysis reveals no deleterious effects on general pancreas properties from *Mist1*^{myc} induction. See (Direnzo et al. 2012) for a full characterization of the *iMist1* model. ***p ≤ 0.001. n.s. - not significant.

Despite elevated levels of MIST1, *Mist1*$^{CreERT/+}$*/iMist1*^{myc} mice exhibited a completely normal pancreas phenotype with no significant changes in the expression of acinar and ductal genes (**Figure 4-16D)**, data not shown) (Direnzo et al. 2012).

4.2.4.2 *Mist1*^{myc} pancreata exhibit extensive stromal infiltrates following AP induction and *Mist1*^{myc} acinar cells fail to recover from AP

We next induced *iMist1*^{myc} expression by treating *Mist1*$^{CreERT/+}$*/iMist1*^{myc} mice with Tam, followed by PBS (control) or caerulein to initiate an AP phenotype (**Figure 4-17A**). Surprisingly, instead of attenuating the AP response, *Mist1*$^{CreERT/+}$*/iMist1*^{myc} mice exhibited enhanced damage as early as 6h post-AP where extensive disruption of the exocrine pancreas occurred (**Figure 4-17B** and **Figure 4-24**). By 2d-4d post-AP, the majority of acini structures were grossly altered with disorganized and distended lumens, a severe absence of eosinophilic zymogens, sustained elevated CLUSTERIN levels, and a large accumulation of infiltrating cells that included CD45+ immune cell populations (**Figure 4-17B-C**; **Figure 4-24** and **Figure 4-18A-B**). During this period, the epithelial tissue mass was largely replaced by VIMENTIN+ and alpha-SMOOTH MUSCLE ACTIN (SMA)+ stromal cells (**Figure 4-18A-D**). The tissue also exhibited an increased islet density as the normal tissue mass that occupied space between available islets decreased, leaving the majority of the pancreas consisting of ductal, stromal and islet cells. (**Figure 4-18A** and **Figure 4-21A-B**). Protein immunoblots and RT-qPCR analyses revealed a typical AP damage profile with activation of *Clusterin*

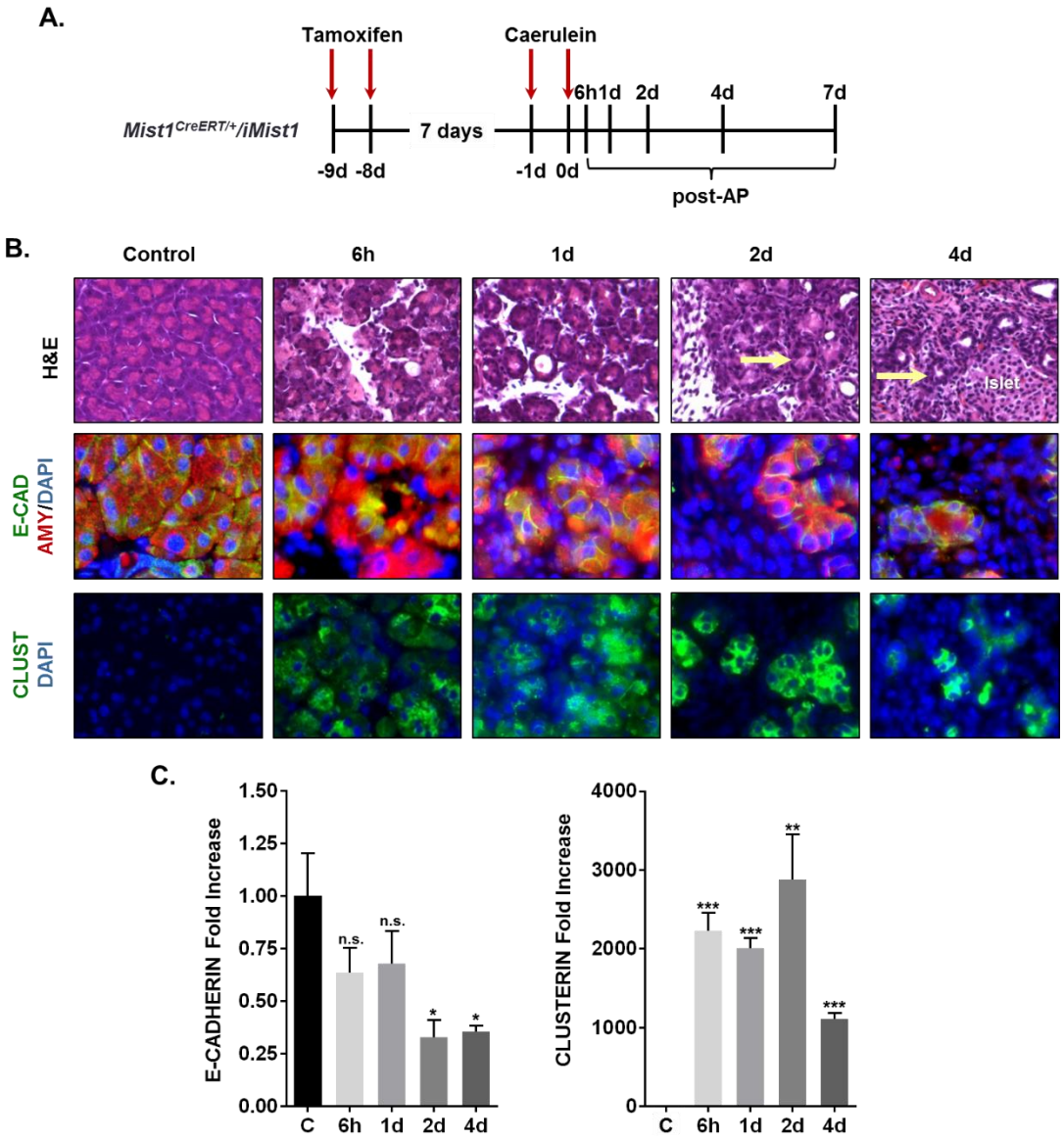

Figure 4-17. ***Mist1^{myc}*** **acinar cells exhibit extensive stromal infiltrates following AP induction. (A)** Time course of *iMist1^{myc}* induction and AP treatment. **(B)** H&E and IF analysis of *iMist1^{myc}* pancreata post-AP. Arrows indicate remnants of acini structures. IF images of E-CADHERIN and CLUSTERIN revealed the loss of acinar cells during AP in *iMist1* mice. **(C)** Relative E-CADHERIN and CLUSTERIN protein levels in IF sections from *iMist1* pancreata at the indicated times and normalized to control values. *p ≤ 0.05; **p ≤ 0.01; ***p ≤ 0.001.

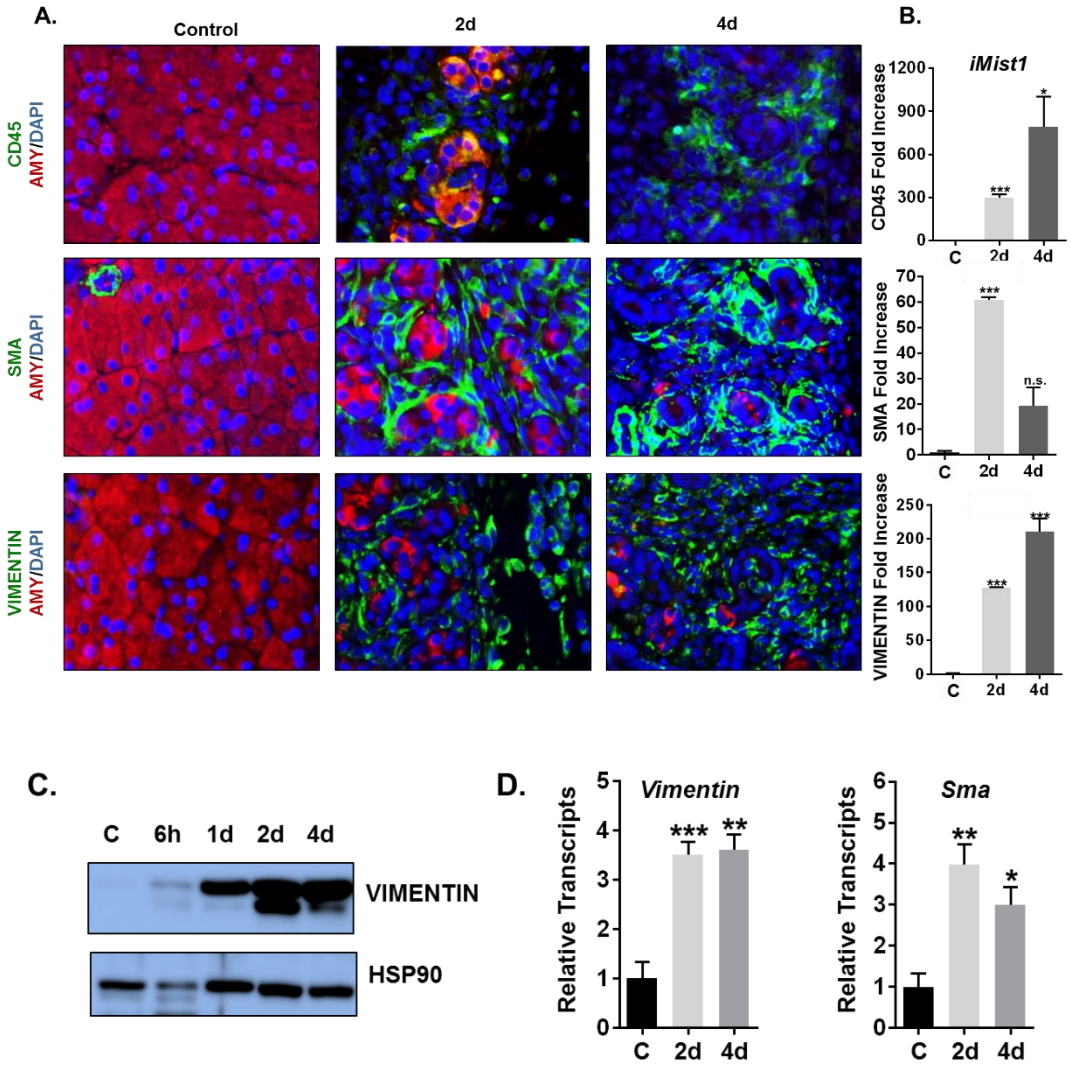

Figure 4-18. *Mist1*^{myc} pancreata exhibit extensive stromal infiltrates following AP induction. (A) *iMist1* pancreata develop large increases in CD45+ immune infiltrates as well as VIMENTIN and SMOOTH MUSCLE ACTIN (SMA) expressing stromal cells. **(B)** Relative CD45, SMA and VIMENTIN protein levels in IF sections from *iMist1* pancreata at the indicated times and normalized to control values. **(C)** Immunoblot and **(D)** RT-qPCR analysis of *Vimentin* and *Sma* levels in *iMist1* samples post-AP. *p ≤ 0.05; **p ≤ 0.01; ***p ≤ 0.001. n.s-not significant.

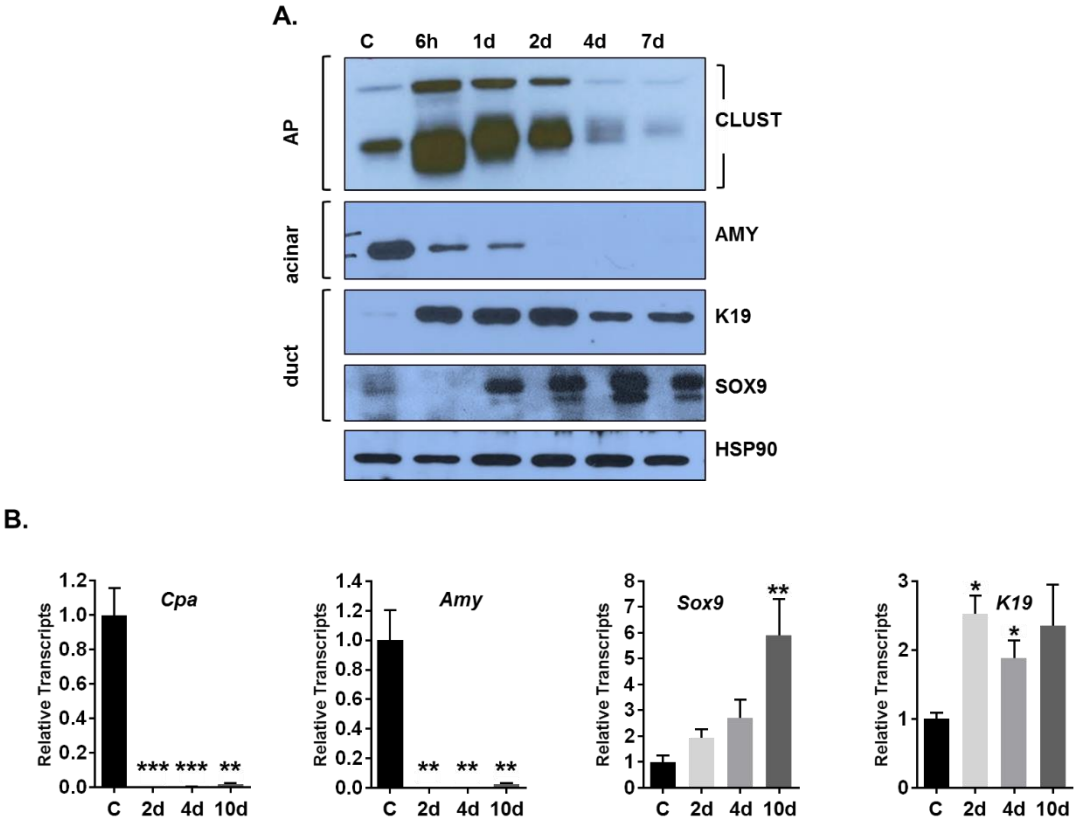

Figure 4-19. ***Mist1*^{myc} acinar cells fail to recover from AP. (A)** Immunoblots revealing sustained expression of duct markers in *iMist1* samples. **(B)** RT-qPCR analysis of ADM markers showing that *iMist1* pancreata do not recover by 10d. *p ≤ 0.05; **p ≤ 0.01; ***p ≤ 0.001.

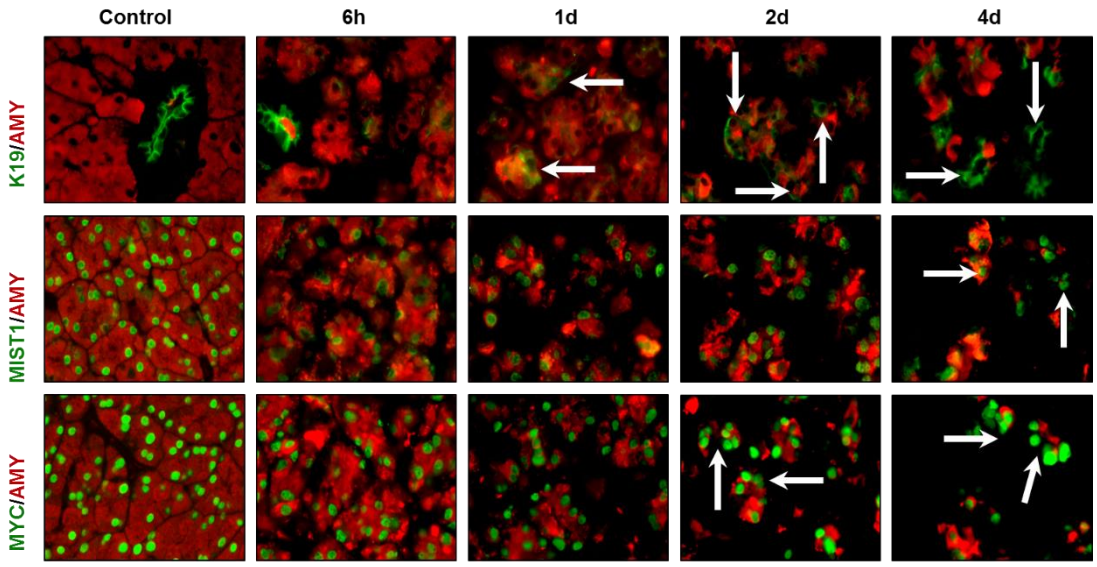

Figure 4-20. *Mist1*^{myc} acinar cells fail to recover from AP. IF analysis showing the substantial loss of amylase expressing acinar cells and the persistence of K19+/AMY+ ADM lesions (arrows). Note that 4d post-AP acini structures are small with very low levels of AMYLASE.

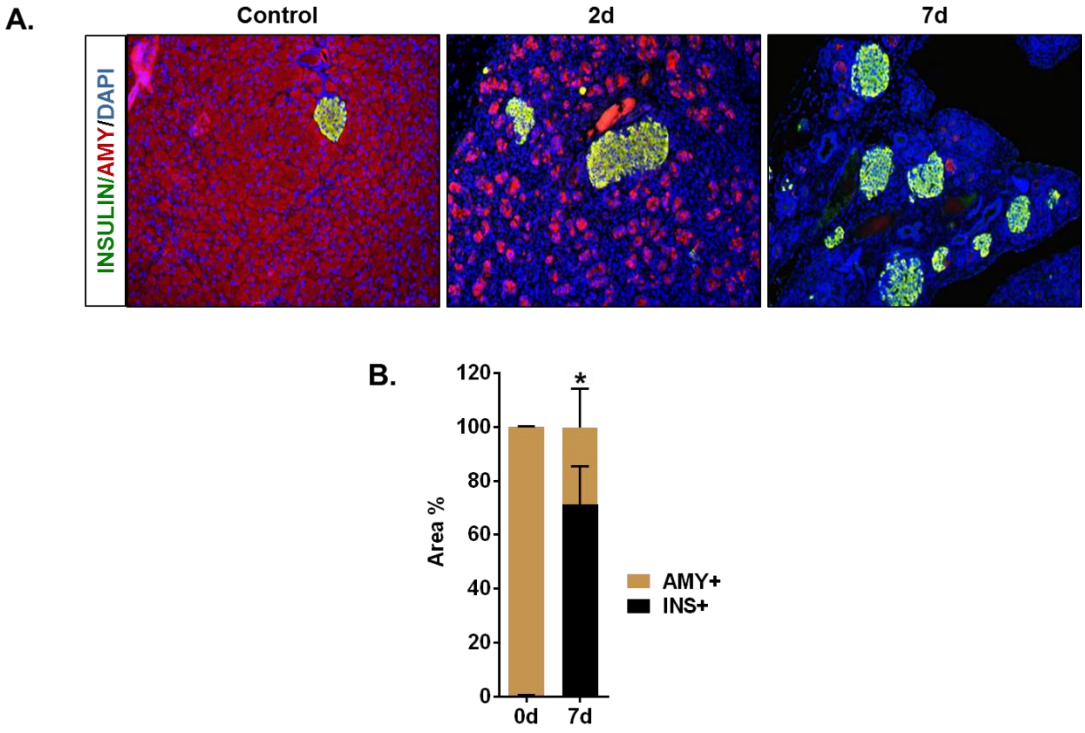

Figure 4-21. Increase in islet tissue density post-acute pancreatitis in *Mist1*^{myc} mouse pancreata. (A) IF images and quantitative analysis of AMYLASE and INSULIN positive areas at 2d-7d post-AP. As a consequence of losing acinar cell mass, islet tissue density increases substantially.

expression, decreased expression of acinar gene products and increased expression of duct gene products over the 6h-2d post-AP period (**Figure 4-19A-B** and **Figure 4-20**). However, by 7d-10d post-AP, despite reduced CLUSTERIN levels, ADM markers did not recover. Acinar genes (*Amy*, *Cpa*) remained suppressed while duct genes (*K19*, *Sox9*) continued to be expressed (**Figure 4-19A-B** and **Figure 4-20**). Further analysis of these animals revealed a greatly decreased AMY+ acinar cell mass. At 2d and 4d post-AP, the vast majority of AMY+ acini co-expressed K19 in ADM structures (**Figure 4-20**). Similarly, MIST1+ acinar cells were greatly decreased while stromal cells became more prominent within the exocrine tissue (**Figure 4-18A-B**; **Figure 4-21A-B** and **Figure 4-20**).

4.2.4.3 *iMist1*^{myc} acinar cells undergo apoptosis but the *iMist1*^{myc} pancreata recover from AP damage through regeneration of a minority *iMist1*^{myc}-negative acinar cell population

The inability of *iMist1*^{myc} mice to recover from AP damage by 7d prompted us to examine animals at extended times. During 7d-10d post-AP, *iMist1*^{myc} pancreata were grossly reduced in size (**Figure 4-23A**) with no evidence of normal acini structures. Instead, the tissue was composed of loose connective tissue containing VIMENTIN+ fibroblasts, CD45+ immune cells and areas of edema (**Figure 4-23A**). Within the remaining pancreas tissue, we observed small pockets of epithelial ADM structures that exhibited elevated levels of CLUSTERIN and retained co-expression of AMY and K19 (**Figure 4-22A,B**; **Figure 4-23A** and **Figure 4-25**). However, the number of AMY+ acinar cells greatly decreased over

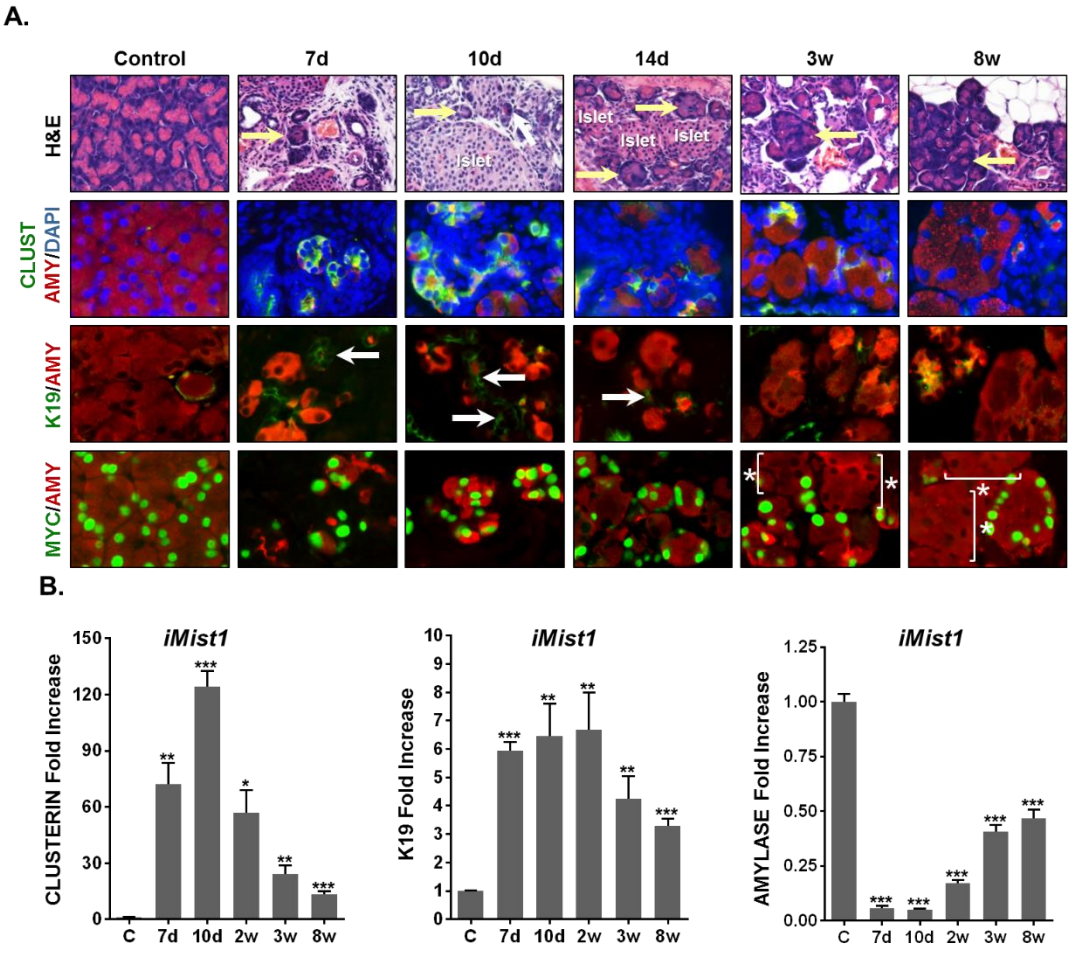

Figure 4-22. ***iMist1^{myc}* pancreata recover from AP damage through regeneration of a minority *iMist1^{myc}*-negative acinar cell population. (A)** H&E and IF analysis of *iMist1^{myc}* pancreata over the indicated post-AP time course. Arrows in the H&E images indicate acini structures that recover over the 8 week post-AP period. Arrows in the K19/AMY stained group show ADM lesions that slowly resolve by 3-8 weeks post-AP. The majority of healthy acini present at 3w-8w post-AP are MIST1^{myc} negative (brackets and asterisks). **(B)** Relative CLUSTERIN, K19 and AMYLASE protein levels in IF sections from *iMist1* pancreata at the indicated times and normalized to control values. *p ≤ 0.05; **p ≤ 0.01; ***p ≤ 0.001; n.s. - not significant.

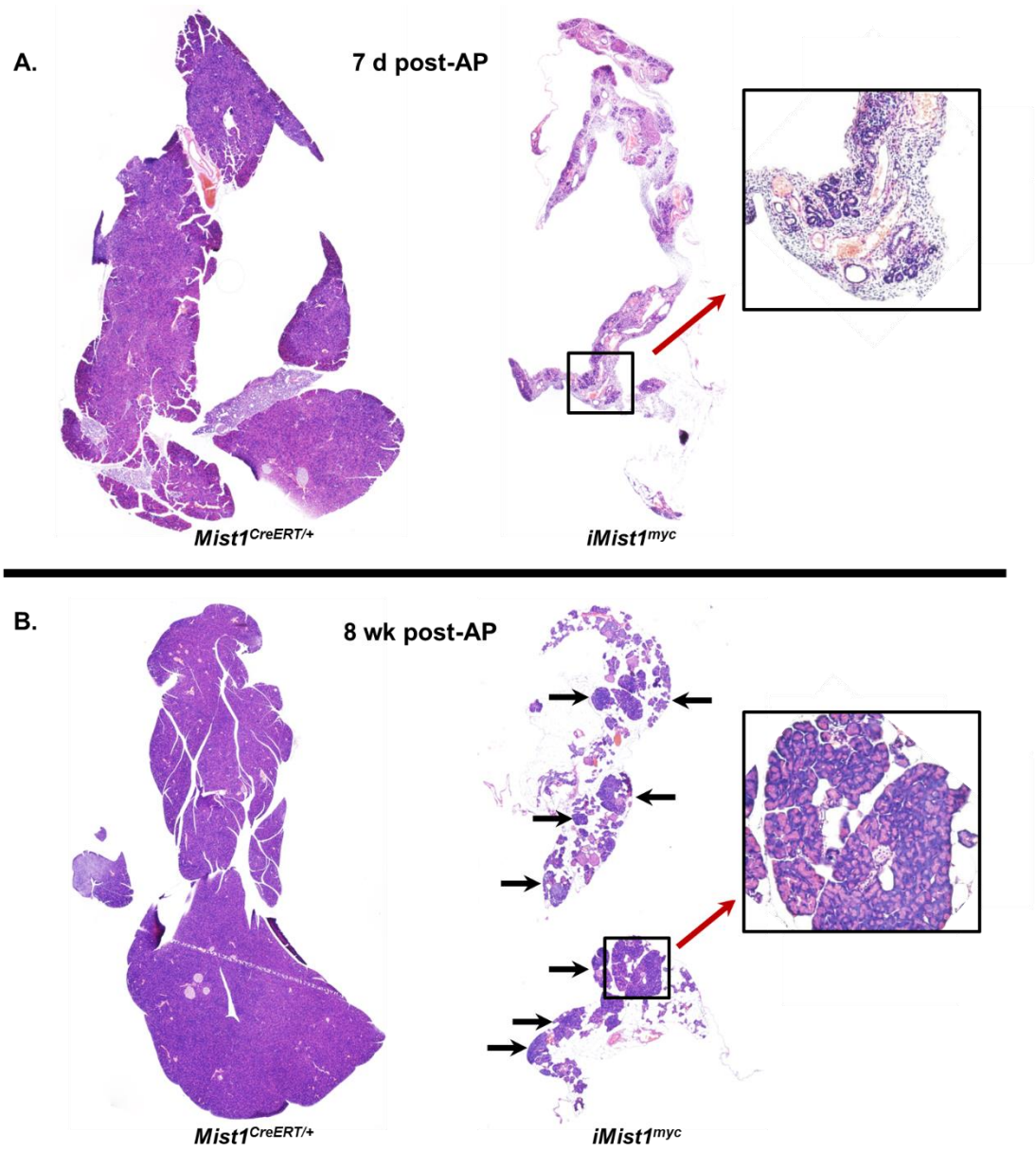

Figure 4-23. H&E images of whole sections from post-AP *iMist1^{myc}* pancreata. **(A)** *Mist1$^{CreERT/+}$* (left) and *iMist1^{myc}* (right) pancreata 7d post-AP. *iMist1^{myc}* pancreata contain very few Amylase+ acini structures at this time point. Inset shows a higher magnification of the boxed area. **(B)** *Mist1$^{CreERT/+}$* (left) and *iMist1^{myc}* (right) pancreata 8w post-AP. At this time, *iMist1^{myc}* pancreata show substantial regeneration of healthy acini (arrows). Inset shows a higher magnification of the boxed area.

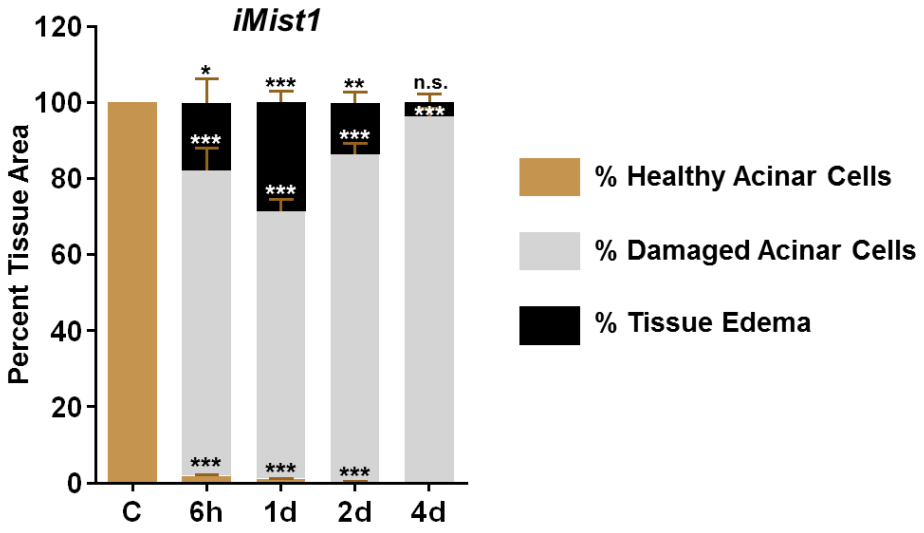

Figure 4-24. **Quantification of AP damage in *iMist1* animals 6h-4d post-AP.** Morphometric analysis of *iMist1* pancreata over the indicated times. *p≤0.05;**p≤0.01; ***p≤0.001; n.s.-not significant.

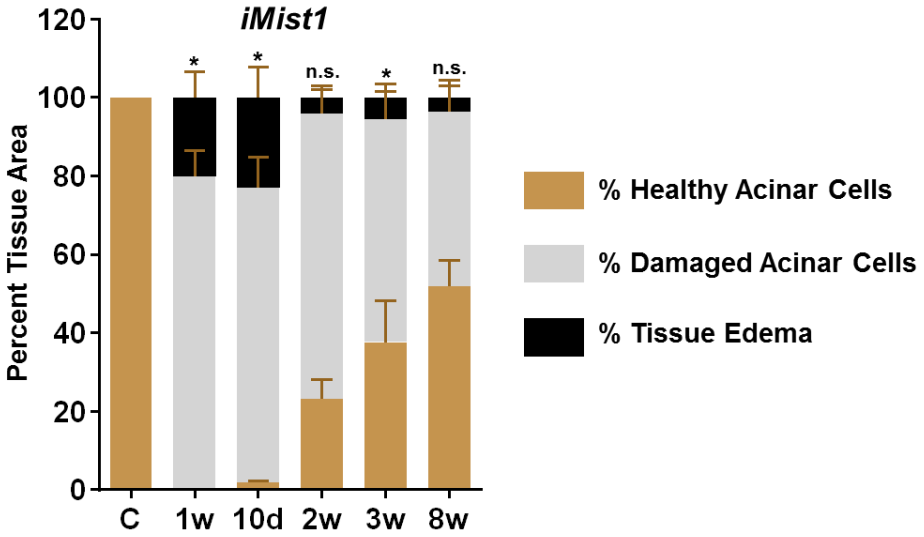

Figure 4-25. Quantification of AP damage in iMist1 animals 7d-8w post-AP. Morphometric analysis of *iMist1* pancreata over the indicated extended times.*p ≤ 0.05; **p ≤ 0.01; ***p ≤ 0.001; n.s. - not significant.

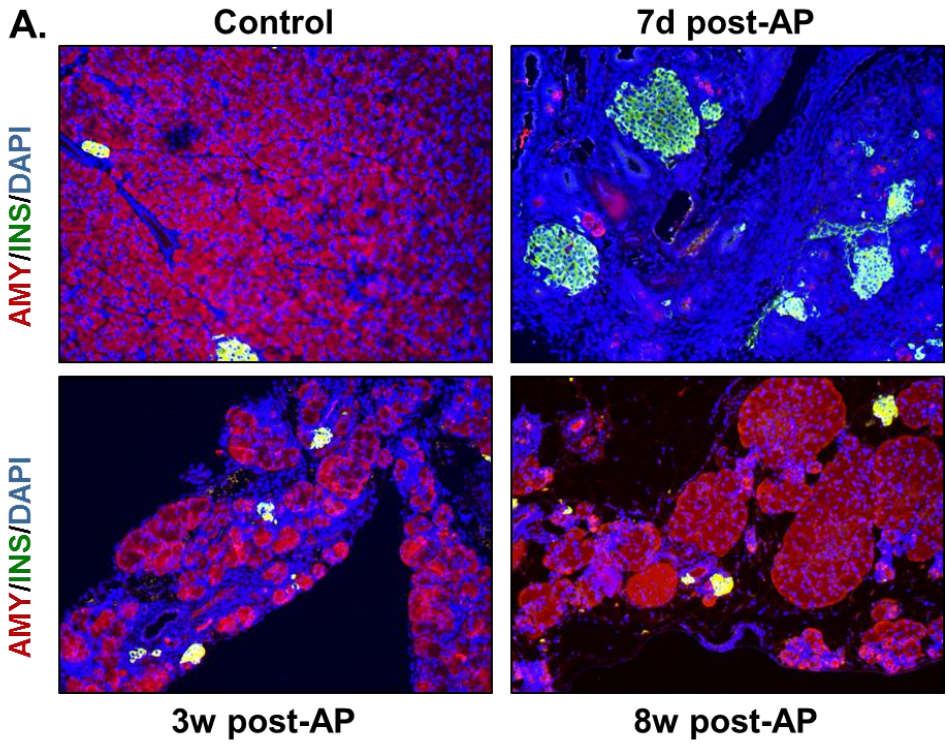

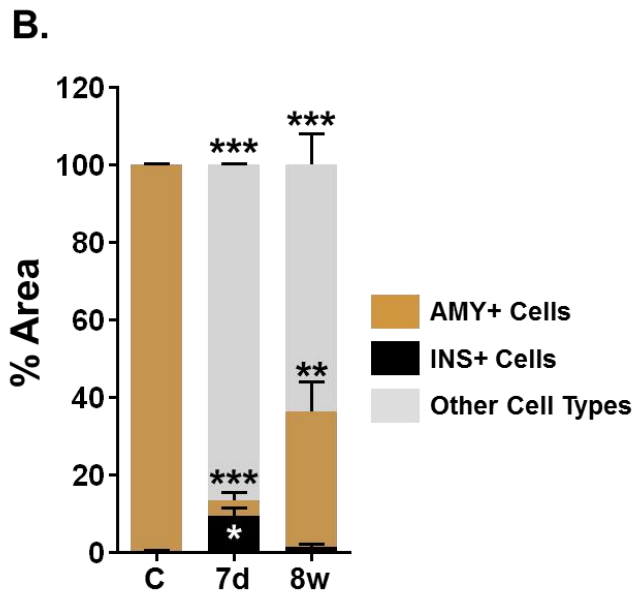

Figure 4-26. *iMist1*^{myc} pancreata recover from AP damage through regeneration of a minority *iMist1*^{myc}-negative acinar cell population. (A) IF analysis of tissue disruption and the dramatic loss of acinar cells in 7d post-AP *iMist1*^{myc} pancreata followed by regeneration of Amylase+ acinar cells from 3w-8w post-AP time points. **(B)** Quantitative analysis of cell types associated with *iMist1*^{myc} pancreata in control and 7d and 8w post-AP. **p ≤ 0.01; ***p ≤ 0.001.

A.

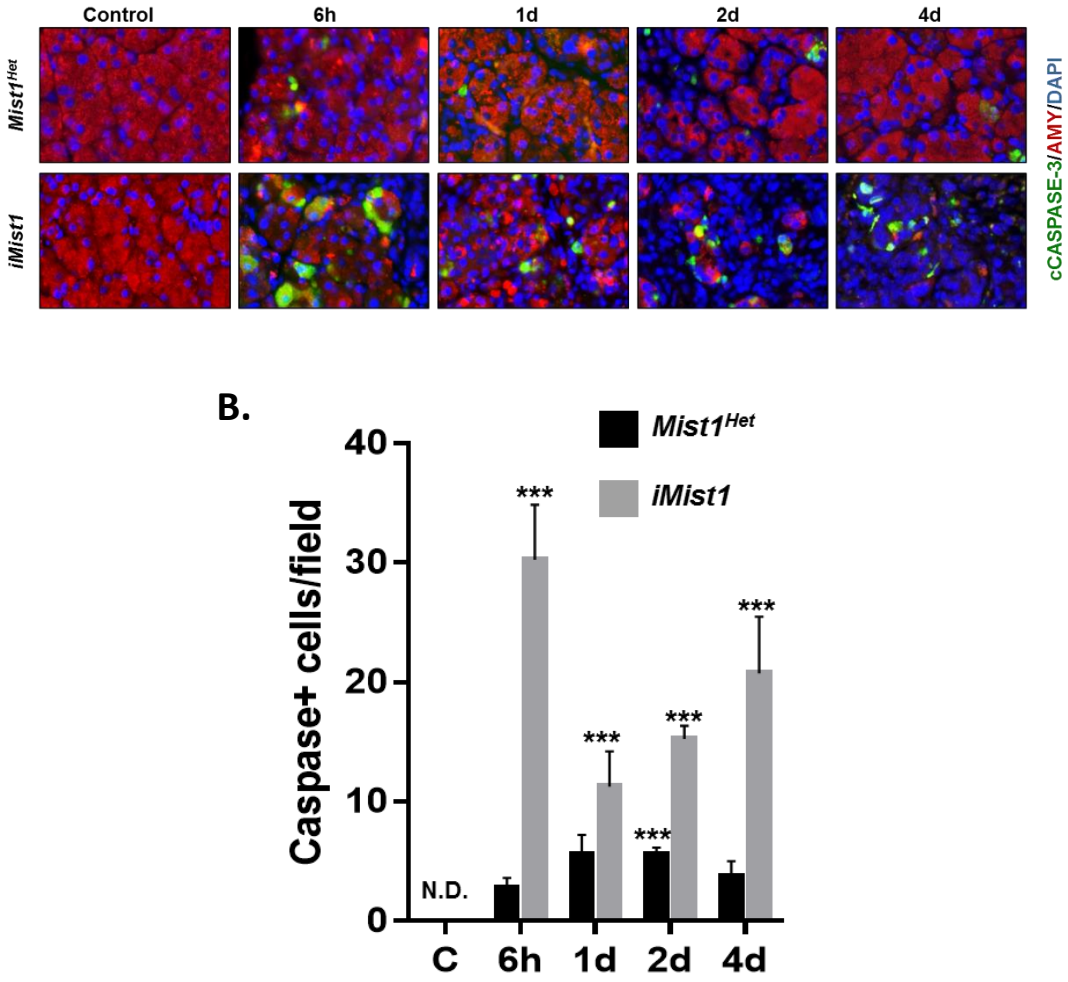

Figure 4-27. *iMist1^{myc}* acinar cells undergo apoptosis followed by regeneration of *iMIST1^{myc}*-negative cells upon AP induction. (A) Acinar cells in *iMist1^{myc}* pancreata undergo extensive apoptosis as detected by cleaved CASPASE 3 staining in AMY+ cells. **(B)** Quantification of Caspase+ cells per field using IF images. ***p ≤ 0.001.n.d. - non-detectable

this time period with only small groupings of acinar cells remaining at 7d post-AP (**Figure 4-26A,B**). During this time frame there was a significant increase in cleaved CASPASE3+/AMY+ epithelial cells, suggesting that cell death was primarily responsible for the vivid loss of acini structures (**Figure 4-27A,B**). Over the ensuing 3-8 weeks post-AP *iMist1*^{myc} pancreata underwent a significant recovery as healthy acinar tissue began to appear in the disrupted organs (**Figure 4-23B**). Areas of ADM were replaced with relatively normal acini that were AMY+ and CLUSTERIN negative (**Figure 4-22A** and **Figure 4-26A,B**). Interestingly, lineage-tracing revealed that the majority of the recovered acini were MIST1^{myc} negative. This was particularly evident in the later (3-8 wk post-AP) times. Quantification of these tissues showed that approximately 75% of AMY+ acinar cells did not express the iMIST1^{myc} protein (**Figure 4-28A,B**). The increase in AMY+/MYC- acinar cells was exclusively due to an increase in cell proliferation of the MYC- population. At 3w post-AP there was an 18.7-fold increase in BrdU-labelled cells when compared to control pancreas samples. Importantly, of the regenerating cell population >90% BrdU+ cells were MYC- (**Figure 4-29A,B**). At 8w post-AP pancreata also accumulated small amounts of adipose tissue that typically associated with the periphery of the organ (**Figure 4-22A**). Taken together, these results show that sustained MIST1 protein is detrimental to AP recovery and that the *iMist1*^{myc} pancreas recovers from an AP episode by relying on the small percentage of acinar cells that failed to initially activate *iMist1*^{myc} expression, allowing this population to re-enter a proliferative state and repopulate the organ.

We conclude that sustained *Mist1* expression does not alleviate the initial AP damage and instead is detrimental to maintaining a healthy acinar cell state under AP conditions.

4.3 Discussion

MIST1 is a bHLH transcription factor expressed exclusively in exocrine secretory cells, including pancreatic acinar, salivary acinar and stomach zymogenic cells (Pin et al. 2001; Aure et al. 2015; Pin et al. 2000; Johnson et al. 2004; Ramsey et al. 2007). A number of studies have shown that MIST1 is critical to establishing intracellular apical-basal polarity, appropriate secretory vesicle formation, expansion of the ER and the ability of cells to exhibit proper regulated exocytosis of pro-digestive enzymes (Direnzo et al. 2012; Jia et al. 2008; Luo et al. 2005; Pin et al. 2001; Tian et al. 2010; Johnson et al. 2004). Additionally, MIST1 is necessary for maintaining appropriate protein synthesis and processing rates when cells are under ER stress (Hess et al. 2011; Huh et al. 2010). In all cases, defects in MIST1 activity greatly impact the secretory function of these organs.

The importance of the MIST1 transcriptional network also has been defined in pancreatic and stomach cancer. In both systems, silencing of *Mist1* gene expression is an early event associated with metaplasia of stomach zymogenic and pancreatic acinar cells (Shi et al. 2009; Zhao et al. 2006; Habbe et al. 2008; Lennerz et al. 2010; Nam et al. 2010).

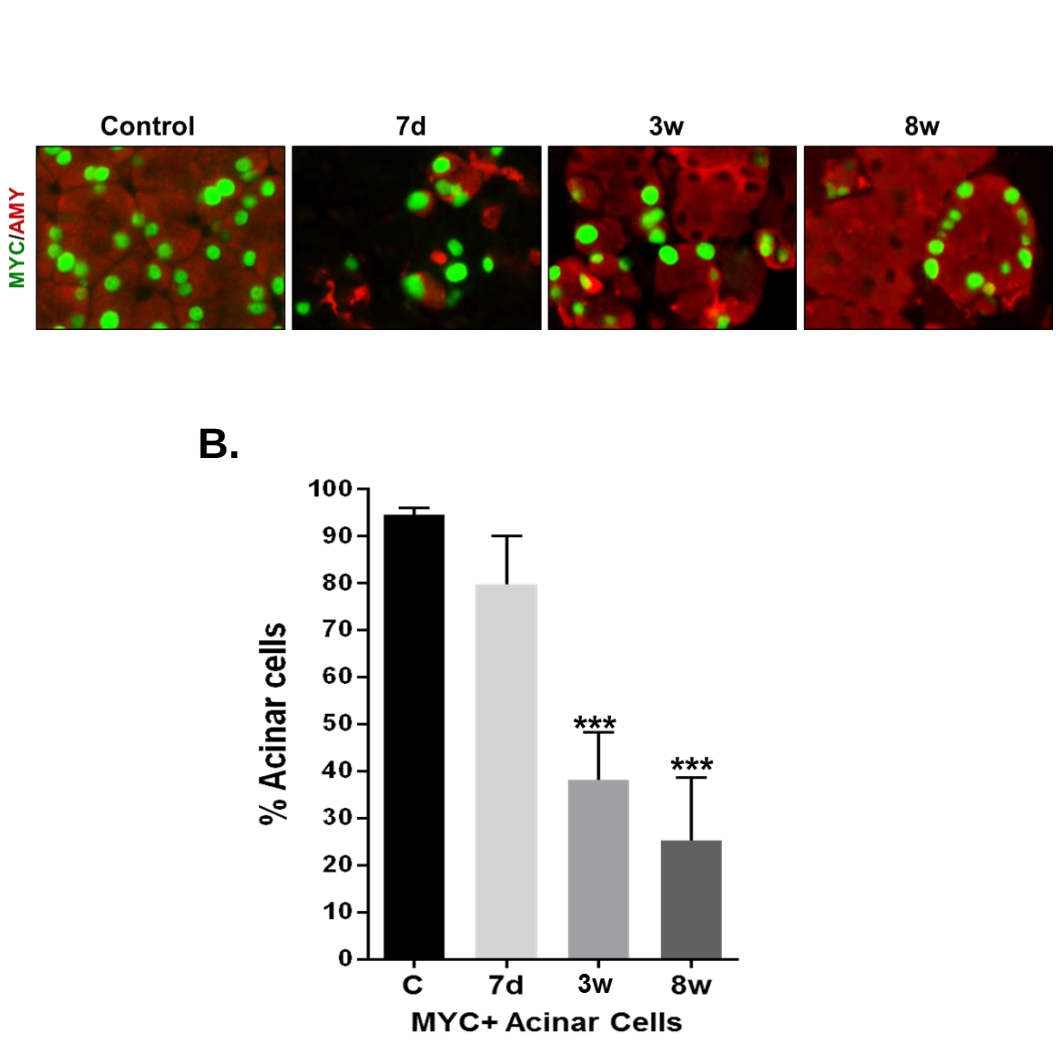

Figure 4-28. *iMist1^{myc}* acinar cells exhibit apoptosis followed by regeneration of *iMIST1^{myc}*-negative cells upon AP induction. (A) Representative IF images for anti-MYC staining used to perform lineage tracing. **(B)** Over time the number of MIST1^{myc}+ cells is greatly decreased as the *iMist1^{myc}* pancreas recovers post-AP. ***p ≤ 0.001

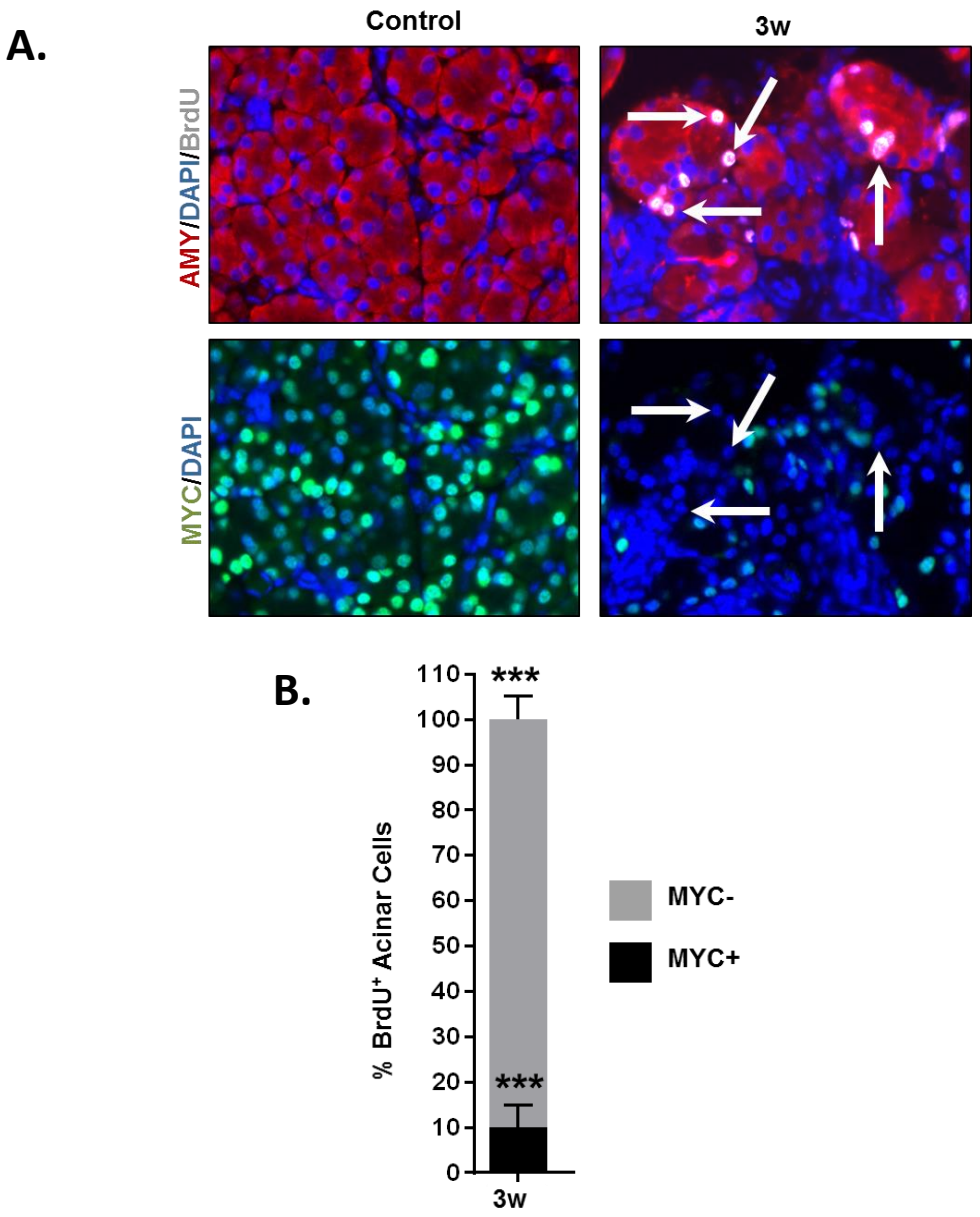

Figure 4-29. *iMist1*^{myc} acinar cells exhibit apoptosis followed by regeneration of *iMIST1*^{myc}-negative cells upon AP induction. (A) BrdU pulse labeling revealed that regeneration of *iMist1*^{myc} pancreata following AP is due to proliferation of rare acinar cells that did not activate expression of *iMist1*^{myc} during the initial Tam treatment. Arrows indicate AMY+/BrdU+/MYC- cells. **(B)** Quantification of proliferating MYC+ and MYC- acinar cells. ***p ≤ 0.001.

Indeed, *Mist1* silencing is one of the first events associated with *Kras*-induced pancreatic ductal adenocarcinoma (PDAC) with MIST1 negative acinar cells exhibiting early activation of EGFR signaling and downstream MAPK pathways (Zhu et al. 2007; Shi et al. 2009). Similarly, *Mist1*-deficient acinar cells are highly sensitized to *Kras* transformation, suggesting that MIST1 plays a tumor suppressive role in the adult pancreas (Shi et al. 2009; Shi et al. 2013). In support of this hypothesis, sustained *Mist1* expression in the presence of oncogenic $KRAS^{G12D}$ dramatically prevents PanIN/PDAC development (Shi et al. 2013). A similar phenotype has been shown for the bHLH transcription factor PTF1a where deletion of *Ptf1a* also sensitizes cells to PDAC formation (Krah et al. 2015). Thus, bHLH factors are essential for maintaining quiescent, healthy acinar cells. Indeed, altering the bHLH transcriptional network can force human PDAC tumor cells to redifferentiate into functional acinar cells (Kim et al. 2015)

Lineage tracing strategies have confirmed that mouse and human PDAC can develop from adult acinar cells upon $Kras^{G12D}$ and other oncogenic or tumor suppressor gene mutations (Habbe et al. 2008; De La O et al. 2008; Houbracken et al. 2011). However, despite the presence of a $KRAS^{G12D}$ driver, most acinar cells remain refractile to transformation unless secondary stressors are placed upon the cells (H Huang et al. 2013; di Magliano & Logsdon 2013). Although loss of *Mist1* can be a secondary driver to PDAC development, there is little evidence that homozygous deletion of *Mist1* alleles occurs in PDAC patients. Instead, other pathways that result in decreased *Mist1* expression could be responsible for enhancing PDAC development. For this reason, we investigated how pancreatitis,

a known risk factor for PDAC (Lowenfels et al. 1993; Malka et al. 2002; Pinho et al. 2014), influences *Mist1* gene expression and activity and ultimately the development of ADM lesions, the precursors to PanIN/PDAC progression. Our studies revealed that the *Mist1* locus is transiently silenced during the initial damage stage of AP. The *Mist1* gene continues to be repressed as acinar cells enter an early recovery phase during which a significant increase in cell proliferation aids the organ in regenerating. However, as this recovery continues, *Mist1* transcripts and protein return to normal levels, allowing the restored acinar tissue to resume normal secretory activity. This is in contrast to instances where AP damage is combined with $KRAS^{G12D}$. In this setting, ADM and PanIN lesions never recover *Mist1* expression, suggesting that KRAS signaling events permanently inhibit the *Mist1* gene in a cancer setting.

Despite re-expression of *Mist1* following an AP episode, MIST1 is not necessary for acinar cells to recover from AP damage. *Mist1 cKO* acini recovered with similar kinetics as observed for $Mist1^{+/+}$ and $Mist1^{+/-}$ acinar cells, although *Mist1 cKO* cells continued to exhibit the secretory defects ascribed to *Mist1* deficient cells. The similar response of $Mist1^{+/-}$ and *Mist1 cKO* pancreata to AP was surprising given that previous studies have shown that $Mist1^{-/-}$ ($Mist1^{KO}$) mice display an increased sensitivity to AP with amplified damage responses and a delay in regeneration (Kowalik et al. 2007). Related studies have shown that $Mist1^{KO}$ pancreata are highly prone to ethanol-induced pancreas damage (Alahari et al. 2011), suggesting that the absence of MIST1 sensitizes acinar cells to general stress/insult events. The apparent disparity between these reports and our

current results is likely due to differences in the *Mist1* model systems. In the case of *Mist1*^{KO} mice, the developing and adult pancreas always lacks MIST1 protein, leading to a significantly damaged acinar cell state in post-weaned animals (Direnzo et al. 2012; Pin et al. 2001). Indeed, the enhanced stress and cell damage associated with *Mist1*^{KO} pancreata highly sensitizes the organ to KRAS^{G12D}-induced transformation events (Shi et al. 2009; Shi et al. 2012). In contrast, *Mist1 cKO* animals allow for the conditional deletion of the *Mist1* loci in adult animals so that episodes of AP occur in *Mist1* null, but otherwise healthy cells. This new model allows for the direct examination of the role of MIST1 in AP recovery in the absence of the long-term stress and injury conditions associated with germ-line *Mist1*^{KO} mice. Thus, we show that deleting *Mist1* just prior to induced AP has little effect on pancreas recovery, suggesting that the increased sensitivity of *Mist1*^{KO} pancreata to AP was likely due to the prior damaged status of the *Mist1*^{KO} organ. In support of this hypothesis, *Mist1 cKO* mice expressed increased ADM markers over time that approached levels observed in *Mist1*^{KO} animals. Interestingly, Mehmood *et al.* (2014) recently showed that germ-line *Mist1*^{KO} pancreata are enriched for H3K4Me3 active epigenetic marks on select genes that function within pancreatitis and PDAC pathways.

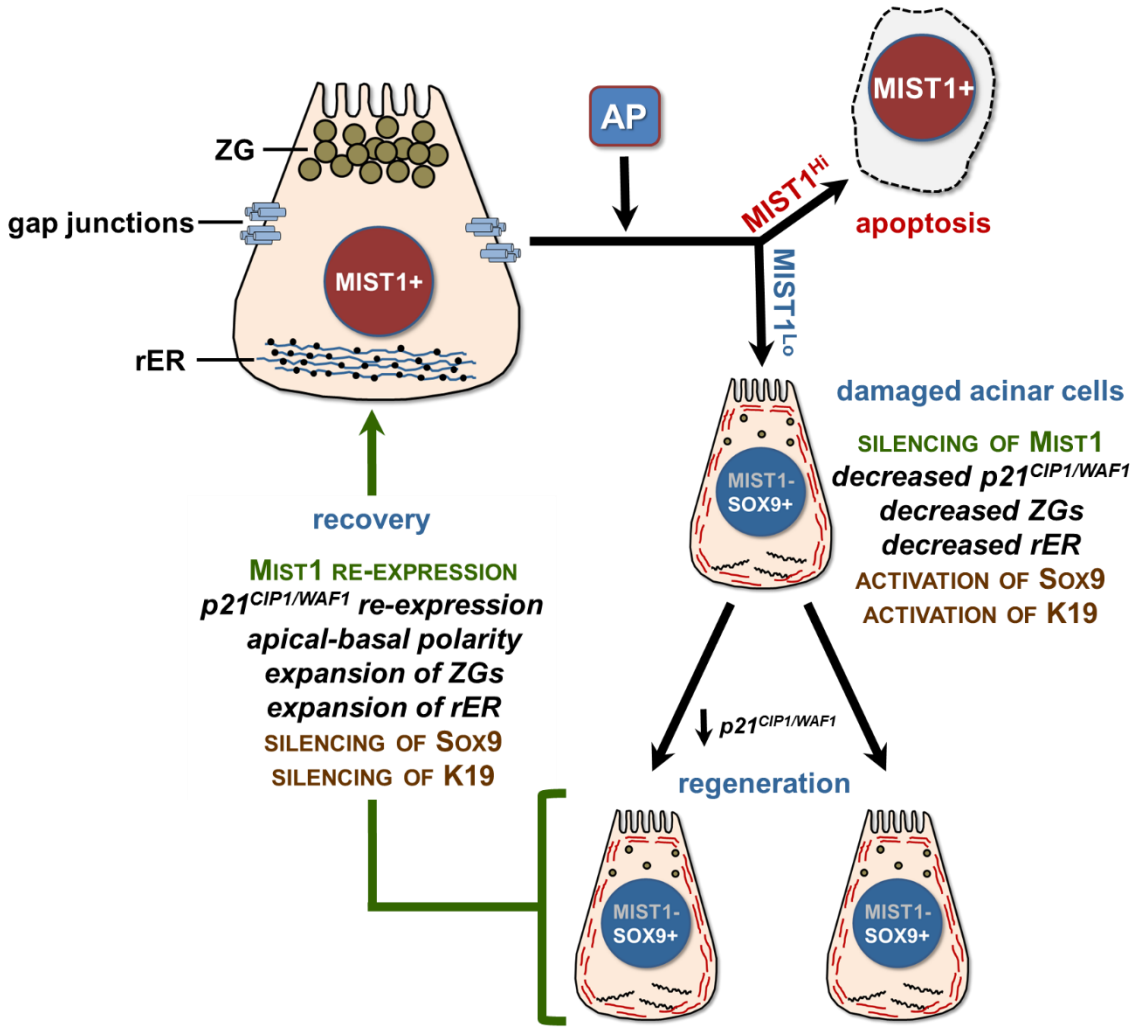

Figure 4-30. Model of *Mist1* silencing and re-expression following AP recovery. For acinar cells to recover from AP damage the *Mist1* gene is required to be transiently silenced. This allows two main events. First, it allows cells to reduce exocytosis function. Second, $p21^{CIP1/WAF1}$ (controlled by MIST1) is down-regulated allowing the cells to enter a proliferative regeneration phase (Jia et al. 2008). Sustained $iMist1^{myc}$ expression during episodes of AP leads to cell death via apoptosis. ZG - zymogen granules; rER - rough endoplasmic reticulum.

Several of these genes are differentially expressed in *Mist1*^{KO} animals in response to AP damage (Mehmood et al. 2014), demonstrating that the chronic damage and stress associated with germ-line MIST1 deficiency results in key epigenetic changes that prime cells to increased sensitivity to AP and PDAC tumor formation.

Thus, we now show that the absence of MIST1 *per se* is not sufficient to produce the increased sensitivity to disease states. Rather, it is the general damage and stress conditions associated with germ-line *Mist1*^{KO} acinar cells that lead to increased AP responses and PDAC development. Given that MIST1 is critical for maintaining a healthy acinar cell state and *Mist1* gene expression is transiently silenced during AP episodes, we investigated if sustained MIST1 activity could attenuate the initial damage response. In contrast to what had been shown for PanIN/PDAC development in *Mist1*^{KO}*/Kras*^{G12D} pancreata (Shi et al. 2009; Shi et al. 2013), sustained MIST1 activity was actually detrimental to AP recovery. Acinar cells that were prevented from down-regulating *Mist1* gene expression in the early stages of AP underwent Caspase-3 dependent apoptosis, leaving the organ grossly reduced in size with large numbers of infiltrating immune and stromal cells occupying vast areas of the pancreas. Over the initial weeks post-AP, the number of Amylase expressing acinar cells declined dramatically and most of the remaining cells were assembled into small acini that lacked large accumulations of zymogen granules. Sustained *iMist1* expression also kept the majority of cells in a quiescent state, most likely due to MIST1 controlling high *p21*$^{Cip1/Waf1}$ levels (Jia et al. 2008). MIST1 controls acinar cell growth through p21$^{CIP1/WAF1}$(Jia et al. 2008) therefore the cells need to down-regulate *Mist1*, which

allows $p21^{CIP1/WAF1}$ to be down-regulated, allowing cells to regenerate. When MIST1 levels return to normal then acinar cells become quiescent. Despite these widespread deficiencies, *iMist1* organs did slowly recover functional acini over time with lineage-tracing confirming that the majority of acinar cells at 8 weeks post-AP were descendants of the small percentage of cells that failed to activate expression of the *LSL-Mist1*^{myc} transgene during the initial tamoxifen induction. These normal (MYC-) acinar cells that silenced *Mist1* expression during AP were able to reactive the endogenous *Mist1* gene and recover from damage. Indeed, these cells regenerated and repopulated much of the damaged pancreas in this model system. We propose that silencing *Mist1* expression is a critical event that permits acinar cells to survive an AP episode (**Figure 4-30**). Down-regulating MIST1 activity may allow cells to suppress secretory functions and *p21*$^{Cip1/Waf1}$ levels and permit a window of cell proliferation. Once established, the *Mist1* gene is then reactivated so that cells have the appropriate intracellular machinery to assemble their secretory vesicles, expand the ER, communicate via CX32-containing gap junctions, and resume efficient exocytosis functions. Thus, AP damage and recovery phases involve key transcriptional networks that control the terminal differentiation and maturation status of these specialized secretory cells.

Future studies will be geared towards understanding the regulatory mechanisms that control *Mist1* expression in both AP and PDAC disease states with a long-term goal of devising strategies to modulate transcriptional networks that could alleviate clinical symptoms in patients diagnosed with pancreatitis and pancreatic cancer.

CHAPTER 5. CONDITIONAL KNOCKOUT OF THE ACINAR CELL-SPECIFIC TRANSCRIPTION FACTOR MIST1 SIGNIFICANTLY ATTENUATES K-RAS INDUCED PANCREATIC INTRAEPITHELIAL NEOPLASIA DEVELOPMENT

5.1 Introduction

Pancreatic ductal adenocarcinoma (PDAC) is one of the most devastating cancers, often being diagnosed at late stages. PDAC is the fourth leading cause of death from cancer and estimates suggest it will be the second leading cause of death by 2030 (Yadav & Lowenfels 2013; Ryan et al. 2014). Studies have speculated that it takes about twenty years for a pancreatic tumor to initiate and develop into its metastatic form (Yachida et al. 2010). Because of this long latent period, PDAC is minimally diagnosed in patients younger than forty years. Indeed, the average diagnosis age for PDAC is 71 years (Jemal et al. 2011).

Pancreatic intraepithelial neoplasia (PanIN) formation (the precursor lesions to PDAC) is one of the critical events that takes place prior to PDAC development (Hingorani et al. 2003; Collins et al. 2012). Interestingly, 90% of all PanINs contain activating KRAS mutations (Kanda et al. 2012), establishing KRAS as a critical driver of pancreatic adenocarcinoma. Nonetheless, in order for PanINs to develop to PDAC additional mutations must occur to allow the disease to progress.

For instance, the tumor suppressor genes *CDKNA2A*, *p53* and *SMAD4* are mutationally inactivated in more than 50%, 60-70% and 50%, respectively, of PDAC tumors (Ryan et al. 2014; Bardeesy, Cheng, et al. 2006; Bardeesy, Aguirre, et al. 2006). In order to better understand PDAC development and design more effective therapeutic approaches, scientists have focused their research efforts in understanding the cell of origin of the disease and dissecting the molecular pathways that are instrumental in early lesion formation. (Pin et al. 2015; Ryan et al. 2014)

It is well established that the exocrine compartment of the pancreas contributes to most PDACs (Furukawa et al. 2006). Hence, one of the much debated topics in the field has been in delineating which exocrine cell types (duct vs. acinar cells) give rise to PDAC. Because of the ductal phenotype associated with PDAC, pancreatic duct cells were thought to be the only cell types contributing to PDAC formation. However, studies using genetically engineered mouse models have demonstrated that upon *Kras* activation acinar cells give rise to both PanINs and PDAC (Kopp & Sander 2014; Kopp et al. 2012; Ji et al. 2009; Habbe et al. 2008; Shi et al. 2009; Shi et al. 2013). Surprisingly, although $Kras^{G12D}$ was expressed in all acinar cells in these mouse genetic models, only a small population of the cells initially de-differentiate to PanIN lesions, suggesting that the majority of acinar cells, despite expressing oncogenic Kras, are refractile to transformation (Bailey et al. 2014). Additionally, Kras expression in mice leads to very slow progression of PDAC where. it can take up to two years for mice to develop PDAC (Hingorani et al. 2003; Ji et al. 2009). Given this information, Ji et

al. (2009) hypothesized that PDAC progression is directly dependent on the levels of Ras activity (2009) and verified that transformed lesions contained high Kras levels. Using cell culture and mouse models these investigators also showed that elevated Ras activity in acinar cells led to spontaneous development of PanIN lesions and PDAC tumors when compared to cells that maintained only endogenous Ras activity. Another finding from this study showed that high Kras activity also led to inflammatory responses that mimicked those that develop upon pancreatitis. Thus, it was speculated that an additional insult, such as pancreatitis, might be essential for PDAC formation (Ji et al. 2009; Guerra et al. 2007).

Acinar reprogramming is one of the key events during PDAC initiation and development. In this context, fully differentiated acinar cells dedifferentiate to acinar-ductal metaplasia upon Kras oncogene activation. Furthermore, when insults such as inflammation occur along with accumulation of other mutations, Kras activity becomes enhanced, driving PanINs to progress to PDAC (Murtaugh 2014). This constant change in cell identity suggests that key transcription factor networks known to be essential for acinar cell identity and differentiation may play a vital role in PanIN and PDAC formation. Indeed, in Kras activated cell reprogramming, the acinar cell-specific transcription factors MIST1 and PTF1a are downregulated (Shi et al. 2013; Krah et al. 2015). In contrast, ductal restricted transcription factors, including SOX9 and HNF6, are upregulated in the earliest stages of reprogramming (Kopp et al. 2012). These results suggest that manipulating the transcription factor landscape could have significance consequences in Kras-driven PDAC development.

MIST1 is a transcription factor which is exclusively expressed in pancreatic acinar cells and is essential for acinar cell differentiation (Pin et al. 2000; Pin et al. 2001). Studies from our laboratory have shown that sustained *Mist1* expression, in the presence of oncogenic KRAS, dramatically prevents PanIN/PDAC development in mice (Shi et al. 2013). In contrast embryonic knockout of *Mist1* mice leads to greatly accelerated PanIN formation (Shi et al. 2009; Shi et al. 2013). Together, these studies suggest that MIST1 plays a tumor suppressive role in the pancreas. In support that acinar transcription networks are key to preventing Kras transformation, Krah et al. (2015) recently showed that conditional knockout of *Ptf1a* similarly accelerates PanIN formation upon *KRAS* activation, leading to aggressive PDAC formation.

Previous studies done with *Mist1* germline knock-out ($Mist1^{KO}$) mice have shown that lack of MIST1 disrupts pancreatic acinar cell organization and polarity (Pin et al, 2001). Hence, $Mist1^{KO}$ mice are predisposed to develop pancreatic phenotypes and pancreatic diseases. To this day the role of MIST1 in PDAC formation has not been fully defined. As discussed earlier, $Mist1^{KO}$ acinar cells are highly sensitized to Kras transformation (Shi et al. 2009). However, one of the caveats of using germline $Mist1^{KO}$ mice in studying PanIN formation is that it is impossible to determine if the cancer phenotype and sensitivity towards Kras transformation is due to the loss of MIST1 protein specifically or if it is a result of an alternative mechanism such as the loss of acinar cell polarity observed in $Mist1^{KO}$ mice prior to Kras activation. Thus, to overcome this shortcoming, we set out to study the role/importance of MIST1 by using a mouse line containing a

conditional allele of *Mist1* (*Mist1*^{cKO}) where we could delete the *Mist1* gene in adult mice. As described by Karki et al. (2015), we generated and characterized a conditional *Mist1*$^{lox/lox}$ mouse line (**Figure 4-7**) and that could be crossed with other genetically engineered mouse models including *Mist1*$^{CreER/+}$ and *LSL-Kras*$^{G12D/+}$. *LSL-Kras*$^{G12D/+}$ mice contain a single point mutation in the *Kras* gene, Glycine (G) replaced with Aspartic acid (D). Upon Cre recombinase activity, the Lox-Stop-Lox (LSL) cassette is deleted, allowing the expression of the mutant Kras oncogene (Jackson et al. 2001). This breeding scheme generated *Mist1*$^{CreER/lox}$; *LSL-Kras*$^{G12D/+}$ (*Mist1*^{cKO}/*Kras*^{G12D}) mice. Tamoxifen administration in adult animals leads to deletion of the remaining *Mist1* allele and simultaneous expression of *Kras*^{G12D}. Additionally, in an effort to determine the role of pancreatitis in pancreatic cancer development, we studied *Mist1*$^{CreER/+}$*; LSL-Kras* (*Mist1*^{Het}/*Kras*^{G12D}), *Mist1*$^{CreER/CreER}$*; LSL-Kras* (*Mist1*^{KO}/*Kras*^{G12D}) and *Mist1*^{cKO}/*Kras*^{G12D} mice. Our studies revealed that upon simultaneous *Mist1* deletion and *Kras* expression PanIN formation greatly decreased when compared to *Mist1*^{Het}/*Kras*^{G12D} and *Mist1*^{KO}/*Kras*^{G12D} animals. Upon acute pancreatitis induction, PanIN formation in *Mist1*^{cKO}/*Kras*^{G12D} mice was accelerated only 3 weeks post-AP.

5.2 Results

5.2.1 Generation of *Mist1*^{cKO}/*Kras*^{G12D} mice

Our lab has previously shown that *Mist1*^{Het}/*Kras*^{G12D} mice upon Kras expression develop PanIN lesions within two months. Importantly, the *Mist1* allele becomes silenced in the PanIN lesions. However, *Mist1*^{KO}/*Kras*^{G12D} mice revealed that germline knockout of *Mist1* makes the pancreas greatly more susceptible to developing advanced grades of PanIN lesions upon Kras expression. Indeed, there was a 3-fold increase in PanIN formation when *Mist1* was absent (Shi et al, 2009, Shi et al., 2012). Despite these results, it remained unclear if germline *Mist1*^{KO} mice are naturally prone to developing diseases due to the absence of the *Mist1* gene from the beginning of life. Thus, to better understand the role of *Mist1* we asked if conditional deletion of *Mist1* would produce similar effects in PanIN formation upon Kras expression. To test this hypothesis, *Mist1*$^{CreER/+}$ (*Mist1*^{Het}) were crossed with *LSL-Kras*$^{G12D/+}$ and *Mist1*$^{lox/+}$ to generate *Mist1*$^{CreER/+}$*; LSL-Kras*$^{G12D/+}$ (*Mist1*^{Het}/*Kras*^{G12D}), *Mist1*$^{CreER/lox}$*; LSL-Kras*$^{G12D/+}$ (*Mist1*^{cKO}/*Kras*^{G12D}) and *Mist1*$^{CreER/CreER}$*; LSL-Kras*$^{G12D/+}$ (*Mist1*^{KO}/*Kras*^{G12D}) mice. *Mist1*^{Het}/*Kras*^{G12D} and *Mist1*^{KO}/*Kras*^{G12D} mice were used as controls for the experiments. Upon tamoxifen treatment, the LSL cassette will be removed and *Kras*^{G12D} expression will take place in all groups of mice. However, in *Mist1*^{cKO}/*Kras*^{G12D} mice *Mist1* deletion take place simultaneously in the acinar cells of the pancreas in adult as illustrated in **Figure 5-1**.

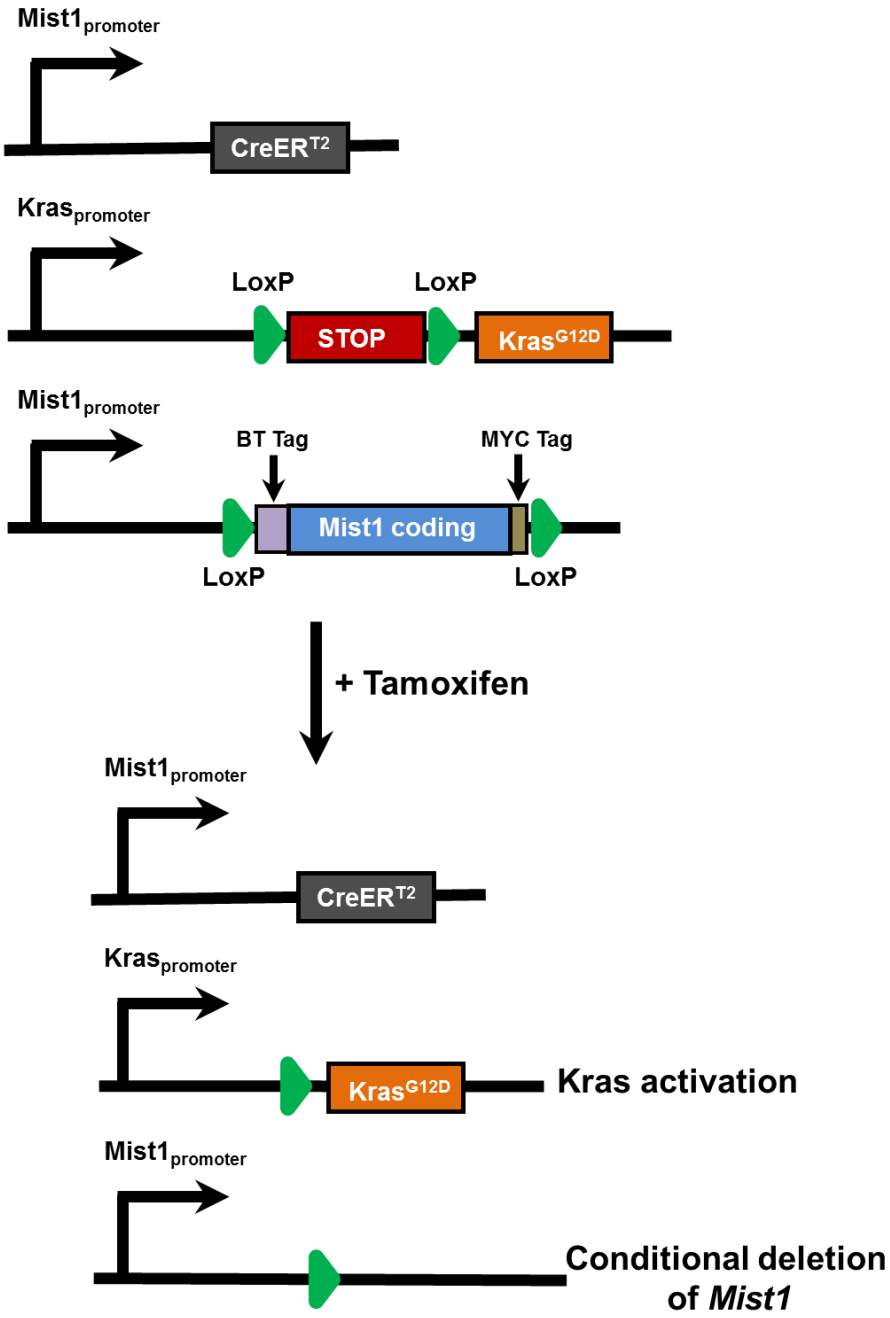

Figure 5-1. Schematic of the *Mist1*^{CreER}, *LSL-Kras*^{G12D} and *Mist1*$^{CreER/lox}$ alleles. This system utilizes tamoxifen-inducible Cre-recombination to delete *Mist1* and activate *Kras*^{G12D} expression specifically in the acinar cells of mice.

5.2.2 PanIN formation in *Mist1*^{cKO}/*Kras*^{G12D} mice is markedly decreased upon *Kras* expression

In order to monitor PanIN formation in *Mist1*^{cKO}/*Kras*^{G12D} mice, six week old animals were treated with Tamoxifen. *Mist1*^{Het}/*Kras*^{G12D} and *Mist1*^{KO}/*Kras*^{G12D} mice were used as the controls for the experiment. Mice were sacrificed 2.5 months post treatment. Our lab previously showed that upon *Kras*^{G12D} expression, PanIN formation is 5X higher in *Mist1*^{KO}/*Kras*^{G12D} mice when compared to their *Mist1*^{Het}/*Kras*^{G12D} littermates. Surprisingly, when we examined *Mist1*^{cKO}/*Kras*^{G12D} mice we observed a markedly reduced PanIN formation when compared to both *Mist1*^{KO}/*Kras*^{G12D} animals (**Figure 5-2**). It was also interesting that *Mist1*^{cKO}/*Kras*^{G12D} mice had comparable or even less PanIN formation to that of *Mist1*^{Het}/*Kras*^{G12D} mice. These results suggested that conditional deletion of *Mist1* prevents *Kras*^{G12D}-driven PanIN initiation through an unknown mechanism. One possible explanation was that perhaps the *Mist1* allele was not efficiently deleted in *Mist1*^{KO}/*Kras*^{G12D} animals. As illustrated in **Figure 5-3**, the *Mist1* allele was deleted from nearly all acinar cells and, as reported previously (Shi et al. 2009), all PanINs failed to express any MIST1.

Taken together, these data suggest that the conditional deletion of *Mist1* from six-week old mice somehow deters PanIN initiation, possibly by inactivating *Kras*^{G12D} activity through some unknown mechanism. Germline *Mist1*^{KO} mice lose acinar cell polarity and have deficiency in enzyme secretion (Direnzo et al. 2012).

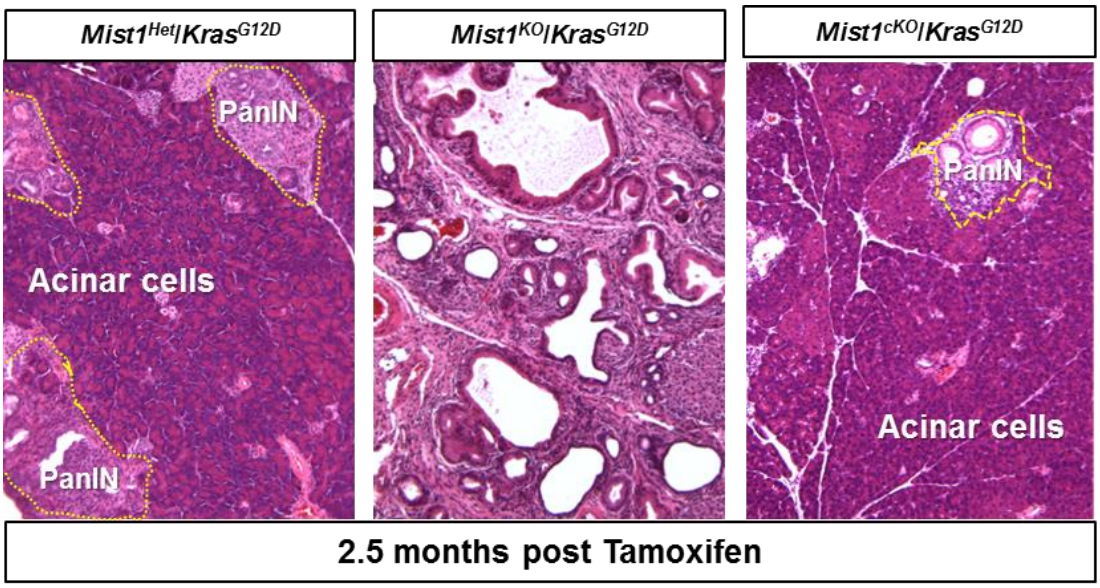

Figure 5-2. ***Mist1^{cKO}/Kras^{G12D}* mice develop markedly reduced PanIN lesions compared to that of *Mist1^{Het}/Kras^{G12D}* and *Mist1^{KO}/Kras^{G12D}* counterparts 2.5 months post-*Kras^{G12D}* expression.** Our lab previously showed that upon *Kras^{G12D}* expression, PanIN formation is 5X higher in *Mist1^{KO}/Kras^{G12D}* mice than *Mist1^{Het}/Kras^{G12D}* littermates. As illustrated above, conditional deletion of *Mist1* and *Kras^{G12D}* expression markedly reduced PanIN formation.

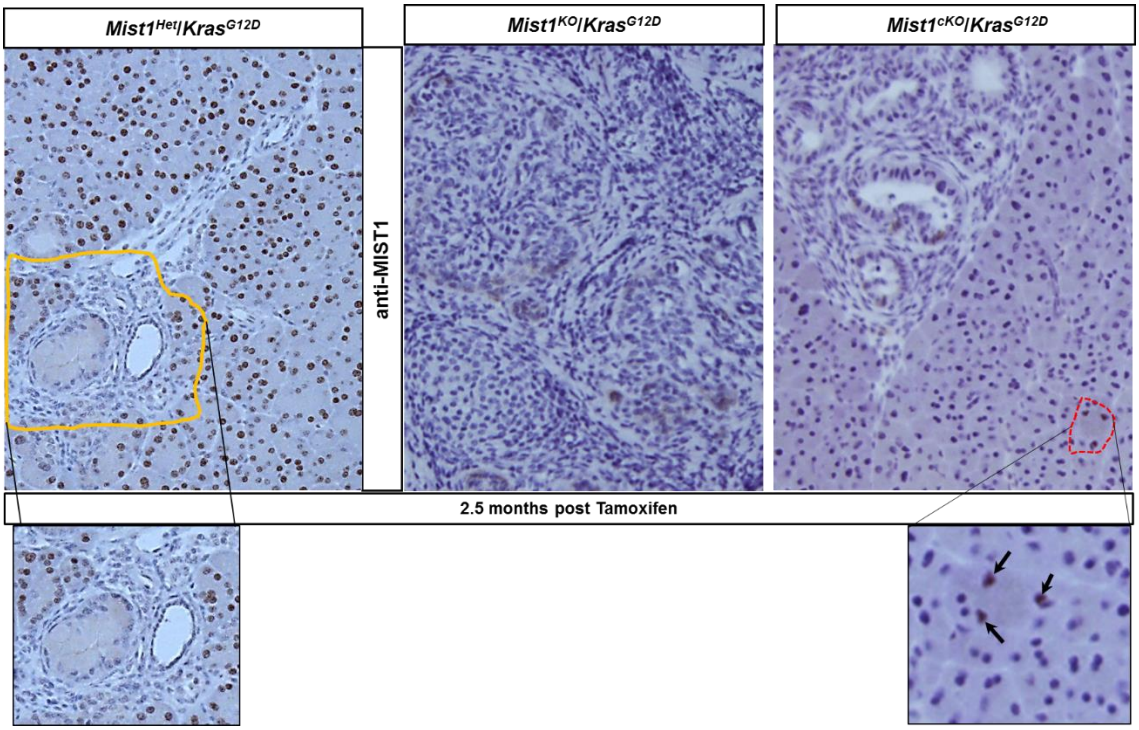

Figure 5-3. Efficient deletion of *Mist1* in *Mist1*^{cKO}*/Kras*^{G12D} mice post-tamoxifen administration. Anti-MIST1 IHC revealed that the majority of the acinar cells were MIST1 negative, indicating that efficient deletion of the *Mist1* allele occurred through Cre recombination. Red dotted area indicates a few rare unrecombined acinar cells which are MIST1 positive (indicated by arrows). Healthy acinar cells in *Mist1*^{Het}*/Kras*^{G12D} mice are MIST1 positive and PanIN lesions are MIST1 negative (yellow outline and inset).

Thus we might speculate that germline *Mist1*^{KO} mice are predisposed to insults due to the lack of *Mist1* since the beginning of their life and hence exhibit accelerated PanIN formation upon expression of mutated *Kras*^{G12D} oncogene.

5.2.3 Decreased acinar-ductal-metaplasia and rare PanIN initiation persisted in *Mist1*^{cKO}/*Kras*^{G12D} mice 7d post-inflammation

Studies done in genetically engineered mouse models have hinted that inflammation could be a possible mediator in PDAC progression (Carrière et al. 2011; Ji et al. 2009). Ji et al (2009), used a transgenic mouse model to ascertain the effects of elevated Ras activity. Their mouse consisted of K-Ras^{G12V} driven by a human CMV and chicken-β-actin promoter (CAG) along with a transcription stop loxP-GFP-STOP-loxP construct. This mouse was further crossed with acinar cell-specific Elastase-CreERT mice. Upon tamoxifen administration, these mice developed a phenotype similar to that of chronic pancreatitis, consisting of increased fibrosis, loss of acinar cells, formation of acinar-ductal metaplasia and immune cell infiltrates (Ji et al. 2009). The phenotype remarkably mimicked human chronic pancreatitis. Additionally, these animals developed PDAC. This finding elucidated that insults such as inflammation could accelerate PDAC formation and lead to high Kras activity. Another study used a second strain of mice with loxP-STOP-loxP-Kras^{G12D} and was crossed with a Pdx1-CreERT (targeted towards pancreatic progenitor population) to directly investigate that pancreatitis could accelerate the PDAC development. These mice were developed PDAC within 2.5 months post-*Kras*^{G12D} expression and acute pancreatitis induction (Carrière et al.

2009). This finding corroborated the speculation of pancreatitis being a contributor to PDAC progression.

Thus, to determine whether PanIN lesion formation and progression could be accelerated by acute pancreatitis upon simultaneous deletion of *Mist1* and $Kras^{G12D}$ oncogene expression in $Mist1^{cKO}/Kras^{G12D}$ mice, all three groups of, $Mist1^{Het}/Kras^{G12D}$, $Mist1^{cKO}/Kras^{G12D}$ and $Mist1^{KO}/Kras^{G12D}$ mice were subjected to two-dosages of tamoxifen treatment. One week post-tamoxifen, these mice were administered eight hourly injections for two consecutive days of cholecystokinin (CCK) analog caerulein which binds to the CCK receptor to induce acute pancreatitis (AP) (protocol similar to experiments in Chapter 3). Mouse pancreata were harvested 7 and 21 days post-AP induction for protein, RNA and paraffin sections for further analyses (**Figure 5-4A)**. Hematoxylin and eosin (H&E) analyses revealed that overall, $Mist1^{cKO}/Kras^{G12D}$ mice contained dramatically increased healthy acinar cells and reduced inflammation in comparison to their $Mist1^{Het}/Kras^{G12D}$ and $Mist1^{KO}/Kras^{G12D}$ control counterparts (**Figure 5-4B)**.Closer analyses of pancreata showed that significantly delayed ADM formation and infrequent occurrence of PanIN initiation in $Mist1^{cKO}/Kras^{G12D}$ mice **(Figure 5-4C)**. These findings suggest that in the initial stages of pancreatitis (7d) $Mist1^{cKO}/Kras^{G12D}$ mice fail to initiate ADMs (precursors for PanIN formation). As a result, there in delayed PanIN formation in these mice.

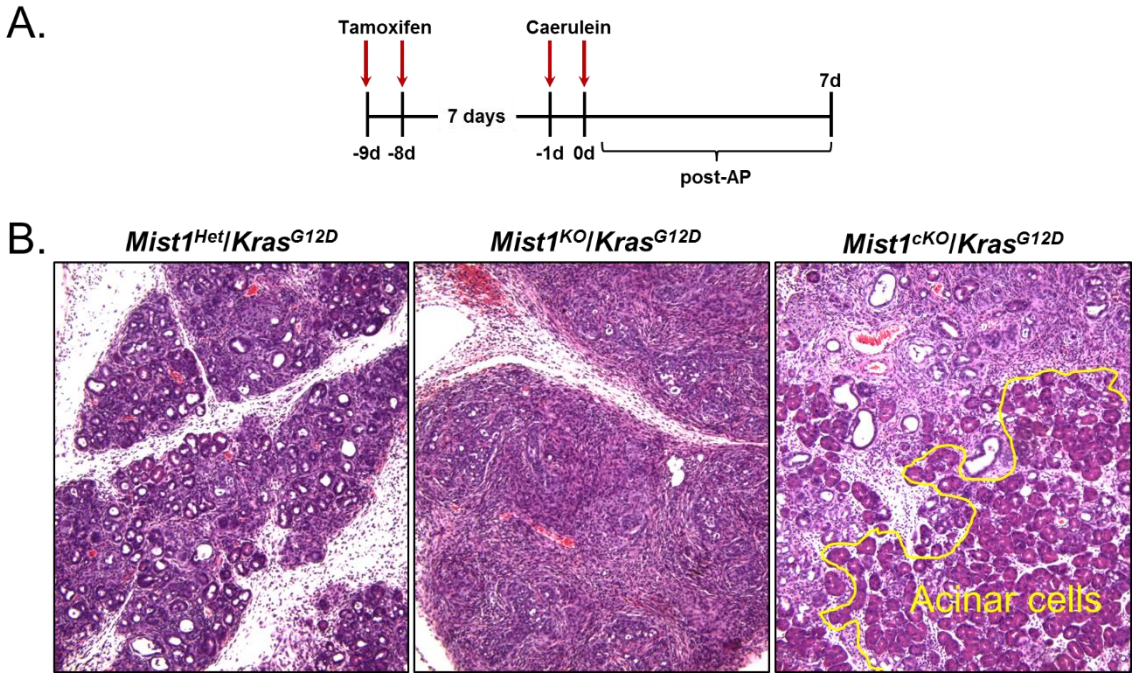

Figure 5-4. Decreased ADM and PanIN formation in *Mist1^{cKO}/ Kras^{G12D}* mice 7d post-AP. (A) Schematic of Tam treatment and AP induction in *Mist1^{Het}/ Kras^{G12D}, Mist1^{KO}/Kras^{G12D}* and *Mist1^{cKO}/Kras^{G12D}* mice. Pancreatic samples were harvested 7 days post-AP. **(B)** Gross phenotype of the mice pancreata post *Kras^{G12D}* expression and AP induction. *Mist1^{cKO}/Kras^{G12D}* mice contain increased acinar cells and low inflammation in comparison to their control *Mist1^{Het}/ Kras^{G12D}* counterparts.

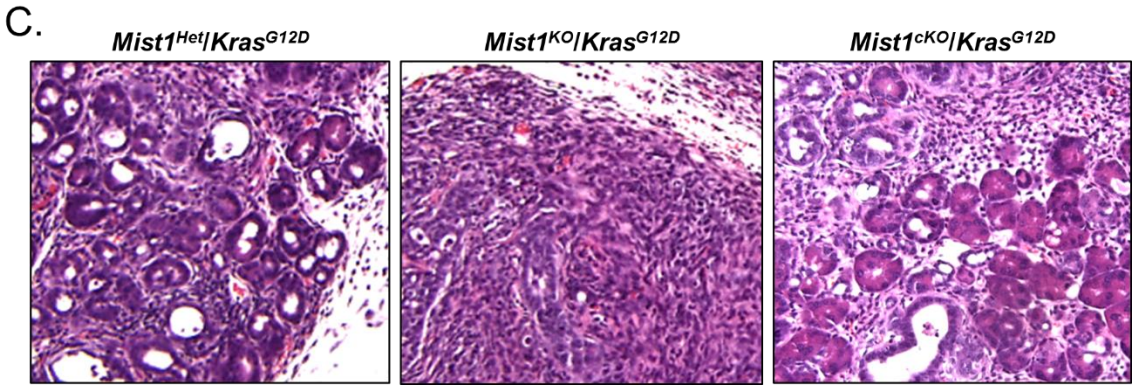

Figure 5-4. Decreased ADM and PanIN formation in *Mist1*^{cKO}*/ Kras*^{G12D} mice. (C) *Mist1*^{Het}*/Kras*^{G12D} and *Mist1*^{KO}*/Kras*^{G12D} mice present increased cellular infiltrates, ADMs and early PanINs. Acinar-ductal-metaplasia (ADM), early PanINs and inflammation are reduced in *Mist*^{cKO}*/Kras*^{G12D} mice upon *Kras*^{G12D} expression and pancreatitis induction.

The low inflammation occurrence in *Mist1*^{cKO}/*Kras*^{G12D} mice also suggest that endogenous KRAS^{G12D} activity is insufficient or inhibited to initiate the cellular reprogramming required for PanIN progression.

We next examined the acinar and ductal characteristics of the *Mist1*^{cKO}/ *Kras*^{G12D} mice by evaluating whole cell protein extracts using immunoblot analysis. Absence of MIST1 protein confirmed efficient deletion of *Mist1* post-tamoxifen administration (**Figure 5-5**, lanes 3 and III). Established acinar marker, AMYLASE was elevated in *Mist1*^{cKO}/ *Kras*^{G12D} mice confirming the presence of healthy acinar cells post-*Kras*^{G12D} expression and AP induction (lanes 3 and III). ADM and ductal markers, SOX9 and K19 levels were decreased in comparison to *Mist1*^{Het}/ *Kras*^{G12D} and *Mist1*^{KO}/ *Kras*^{G12D} mouse samples as illustrated in **Figure 5-5**.These data further confirm that ADM and PanIN formation is still inhibited in *Mist1*^{cKO}/ *Kras*^{G12D} mice at early stage (7d) post AP induction.

In order to further confirm reduced ADM and PanIN formation in *Mist1*^{cKO}/*Kras*^{G12D} mice 7d post-AP insult, we set out to perform RT-qPCR analyses on RNA samples from these animals. As demonstrated by the immunoblots, RT-qPCR also confirmed the presence of significantly increased acinar cells (*Amylase)* in *Mist1*^{cKO}/*Kras*^{G12D} mice in comparison to control *Mist1*^{Het}/*Kras*^{G12D} and *Mist1*^{KO}/*Kras*^{G12D} mice.

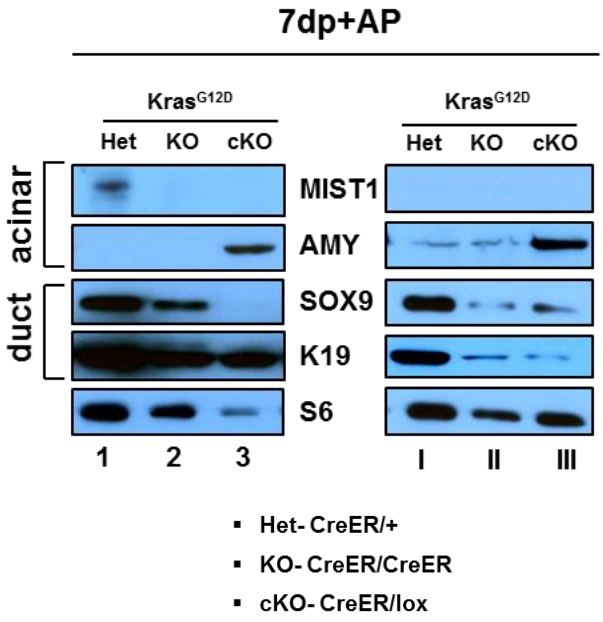

Figure 5-5. *Mist1*^{cKO}/*Kras*^{G12D} mice show increased acinar marker (AMYLASE) and decreased ADM and ductal markers (SOX9 and K19) in comparison to their control counterparts 7d-post AP. Anti-MIST1 IHC confirmed efficient deletion of *Mist1* in *Mist1*^{cKO}/*Kras*^{G12D} mice (lanes 3 and III). Established acinar marker, AMYLASE was elevated in *Mist1*^{cKO}/*Kras*^{G12D} mice confirming the presence of healthy acinar cells post *Kras*^{G12D} expression and AP induction (lanes 3 and III). Both ADM marker SOX9 and ductal marker K19 levels were decreased in comparison to both *Mist1*^{Het}/*Kras*^{G12D} and *Mist1*^{KO}/*Kras*^{G12D} mouse samples. S6 was used as a loading control. Note: Immunoblots represent two sets of mice (Immunoblot experiment performed by Rebecca Steele).

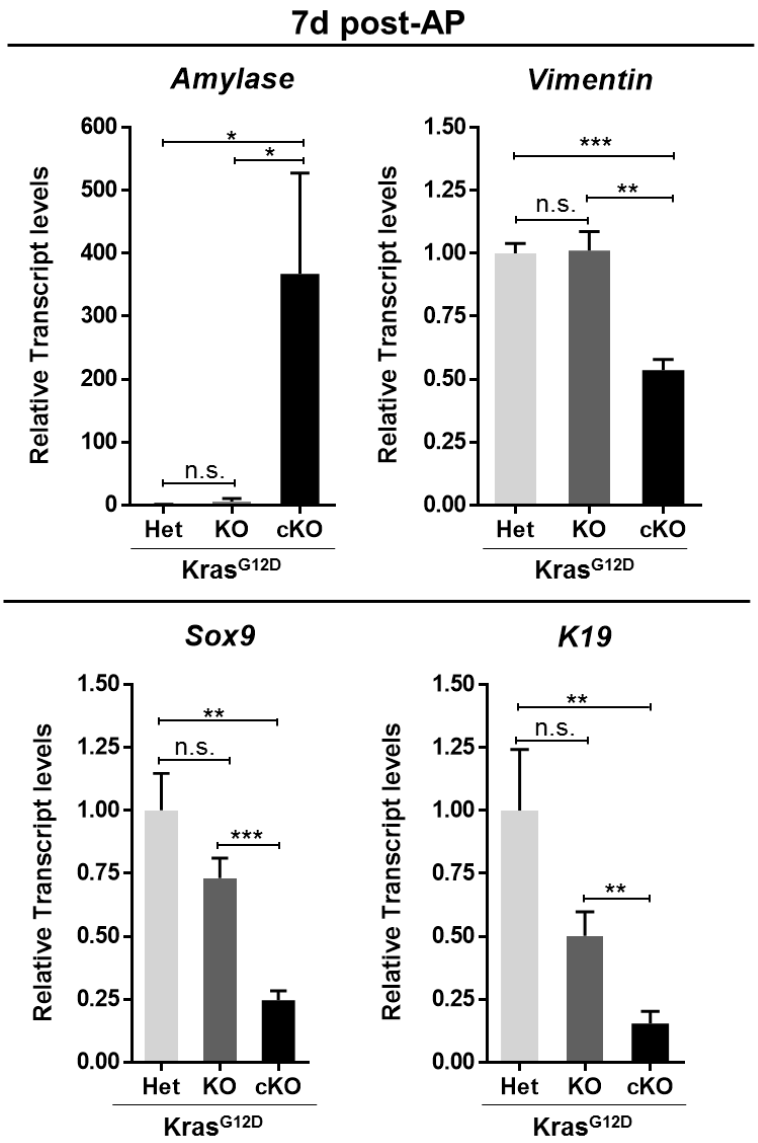

Figure 5-6. Gene expression analysis confirms the presence of increased acinar cells which fail to initiate PanINs and decreased inflammation in *Mist1^{cKO}/Kras^{G12D}* mice 7d post-AP. RT-qPCR analysis of the known acinar gene, *Amylase* showed elevated transcript levels and decreased ADM marker, SOX9 in *Mist1^{cKO}/Kras^{G12D} mice* in comparison to *Mist1^{Het}/Kras^{G12D}* and *Mist1^{KO}/Kras^{G12D}* littermates confirming the presence of healthy acinar cells that failed to form ADM and PanINs 7d post-AP insult. Furthermore, the stromal marker *Vimentin* was decreased compared to the control mice suggesting that *Mist1^{cKO}/Kras^{G12D}* animals exhibit significantly lower inflammation when compared to *Mist1^{Het}/Kras^{G12D}* and *Mist1^{KO}/Kras^{G12D}* animals (RT-qPCR performed by Rebecca Steele).

Significantly decreased *Sox9* and *K19* transcript levels confirmed that acinar cells in *Mist1*^{cKO}/*Kras*^{G12D} mice did not undergo ADM events (a precursor for PanIN initiation), confirming the overall decrease in PanIN formation. Furthermore, stromal markers such as *Vimentin*, showed significantly reduced transcript levels in *Mist1*^{cKO}/*Kras*^{G12D} mice than control littermates **(Figure 5-6)**. Taken together, these results demonstrate that ADM and PanIN formation were significantly delayed in *Mist1*^{cKO}/*Kras*^{G12D} mice, even upon *Kras*^{G12D} expression and AP insult. However, the dramatic phenotype in *Mist1*^{KO}/*Kras*^{G12D} mice as early as 1 week post-AP confirmed that embryonic knockout of *Mist1* leads to rapid PanIN formation.

5.2.4 Surprisingly PanIN formation is accelerated in *Mist1*^{cKO}/*Kras*^{G12D} mice by 3 weeks post-AP

We showed that *Mist1*^{cKO}/*Kras*^{G12D} mice failed to initiate ADM and PanIN formation upon *Kras*^{G12D} expression and 7d post-AP in comparison to *Mist1*^{Het}/*Kras*^{G12D} and *Mist1*^{KO}/*Kras*^{G12D} littermates. This was a surprising result because we expected that AP insult would accelerate overall ADM and PanIN formation in *Mist1*^{cKO}/*Kras*^{G12D} mice. Other investigators had previously demonstrated that high grade PanIN formation and ADM occurred only around 1 month following the AP insult (Carrière et al. 2009). Thus we speculated that *Mist1*^{cKO}/*Kras*^{G12D} mice might be able to accelerate PanIN formation after longer time post-AP.

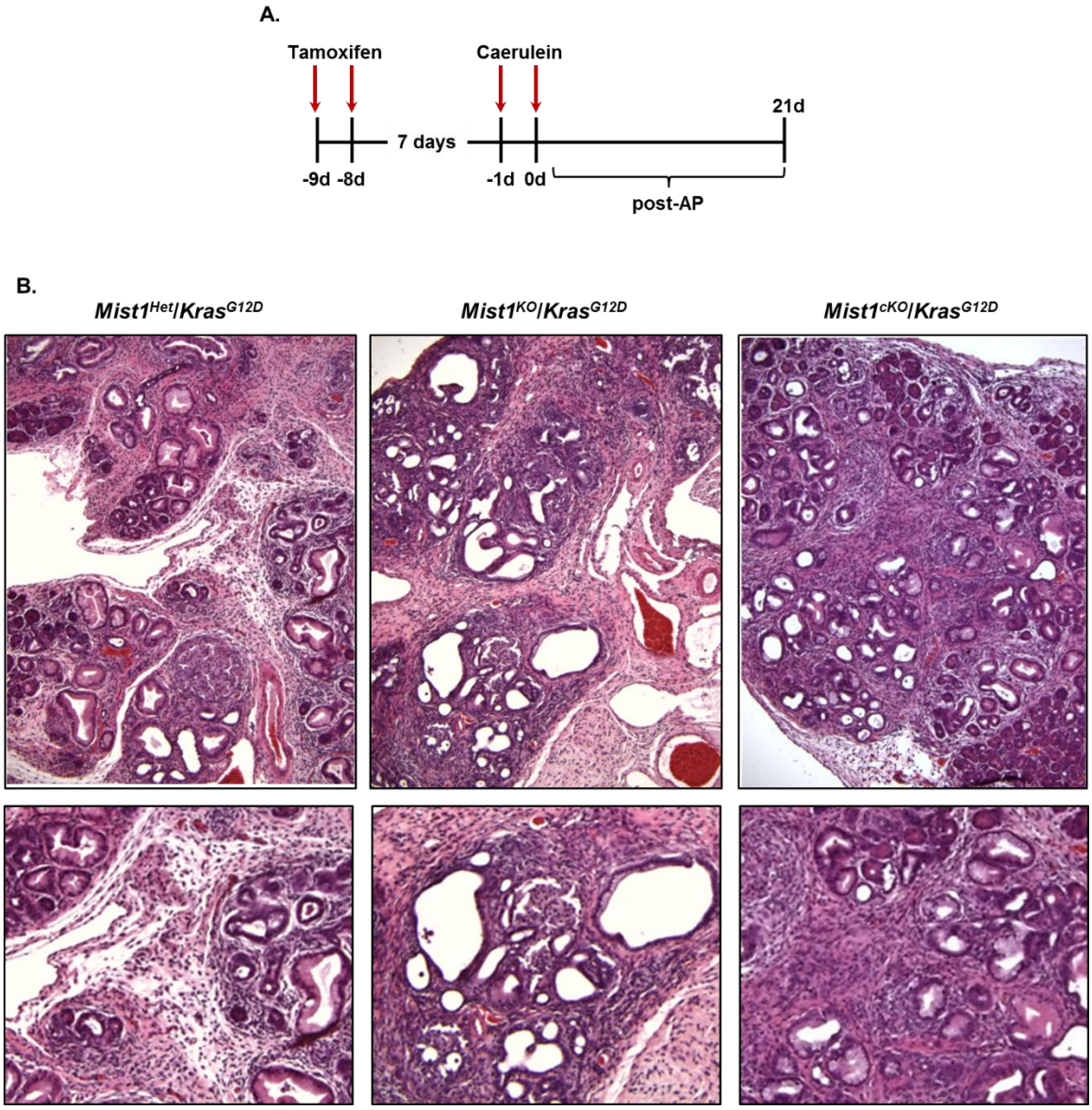

Figure 5-7. Accelerated PanIN progression 3 weeks post-AP in *Mist1^{cKO}/Kras^{G12D}* mice. (A) Schematic of Tam treatment and AP induction in *Mist1^{Het}/ Kras^{G12D}*, *Mist1^{KO}/Kras^{G12D}* and *Mist1^{cKO}/Kras^{G12D}* mice. Pancreatic samples were harvested 21 days post-AP. **(B)** Gross phenotype of the mice pancreata post-*Kras^{G12D}* expression and AP induction. ADM and PanIN formation in *Mist1^{cKO}/Kras^{G12D}* mice were markedly elevated 3 weeks post inflammation. Although some pockets of acinar cells were seen, the overall PanIN population was increased compared to 7d post-AP in *Mist1^{cKO}/Kras^{G12D}* mice.

In order to determine whether PanIN progression was elevated in 3w post AP treated *Mist1*^{cKO}/*Kras*^{G12D} mice, paraffin sections, protein and RNA samples were utilized to perform immunostaining, immunoblots and RT-qPCR, respectively **(Figure 5-7A)**. H&E analysis of the mice pancreata revealed decreased acinar cell clusters, increased PanIN formation along with elevated inflammation in *Mist1*^{cKO}/*Kras*^{G12D} mice as illustrated in **Figure 5-7B.** The phenotype of all three groups of mice were comparable. However, there were a few mice in *Mist1*^{cKO}/*Kras*^{G12D} group that failed to form ADMs and PanINs as verified by the presence of increased acinar cell pockets **(Figure 5-8)**. These results suggest that PanIN formation accelerates in *Mist1*^{cKO}/*Kras*^{G12D} mice post- *Kras*^{G12D} expression and 3wks after AP induction in comparison to 1 wk post-AP mice. I speculate that *Kras*^{G12D} expression was elevated during the 3 week window and this led *Mist1*^{cKO}/*Kras*^{G12D} mice to form comparable PanIN formation across all three genotypes (*Mist1*^{Het}/*Kras*^{G12D}, *Mist1*^{KO}/*Kras*^{G12D} and *Mist1*^{cKO}/*Kras*^{G12D}).

In order to verify the increased presence of PanIN lesions in *Mist1*^{cKO}/ *Kras*^{G12D} *pancreata*, IHC was performed using a ductal and PanIN marker. K19 expression was prevalent in PanINs and ADMs in all groups of mice **(Figure 5-9)**. Marked increase in K19 expression in *Mist1*^{cKO}; *LSL-Kras*^{G12D} mice confirmed the elevated PanIN formation over the three week period

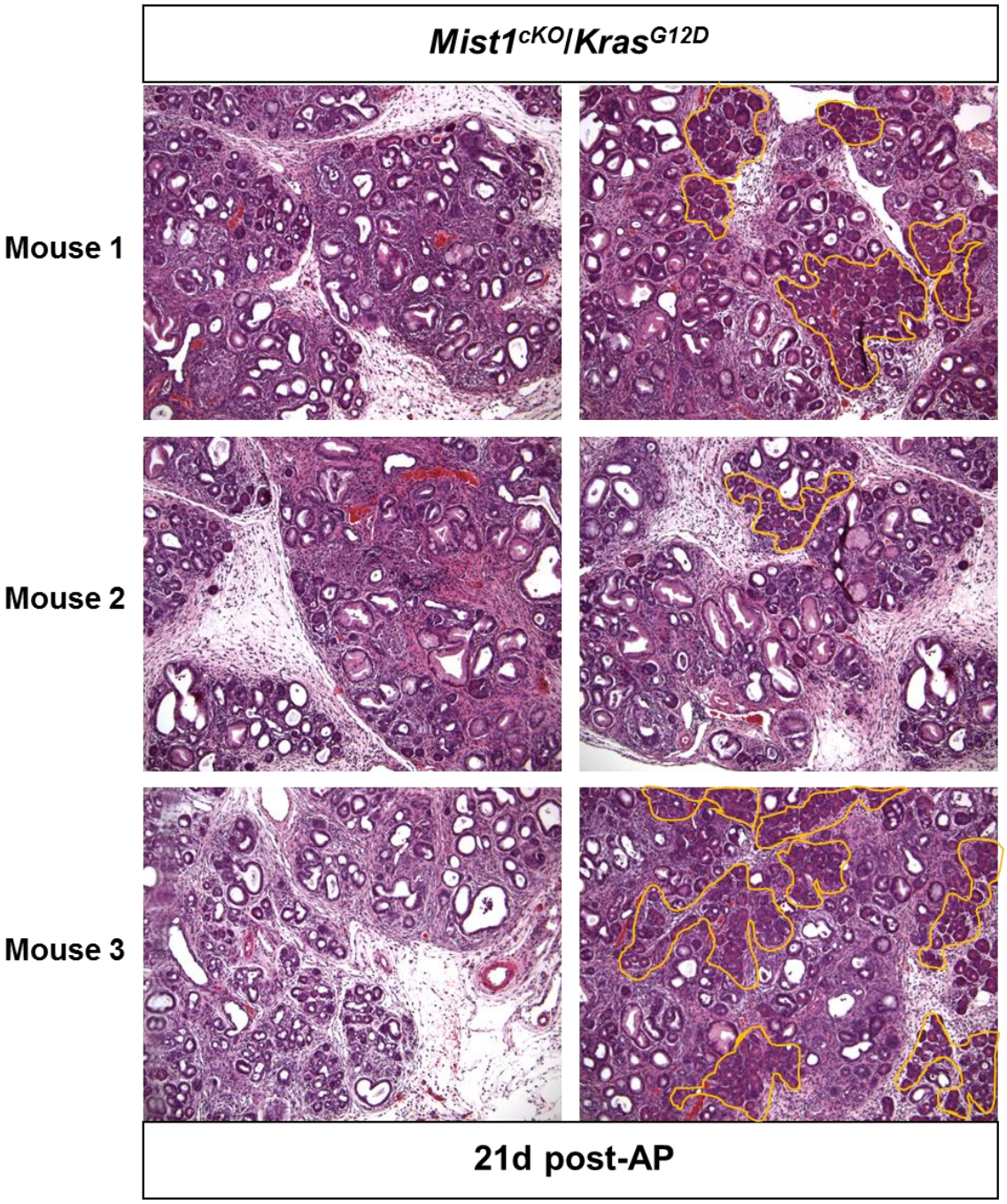

Figure 5-8. Variation in PanIN formation in *Mist1*^{cKO}/*Kras*^{G12D} mice 21d post-AP. H&E images reveal that there is mouse to mouse variation in PanIN formation in *Mist1*^{cKO}/*Kras*^{G12D} mice. Some mice present increased pancreatic acinar cells than the others (acinar cells outlined in yellow).

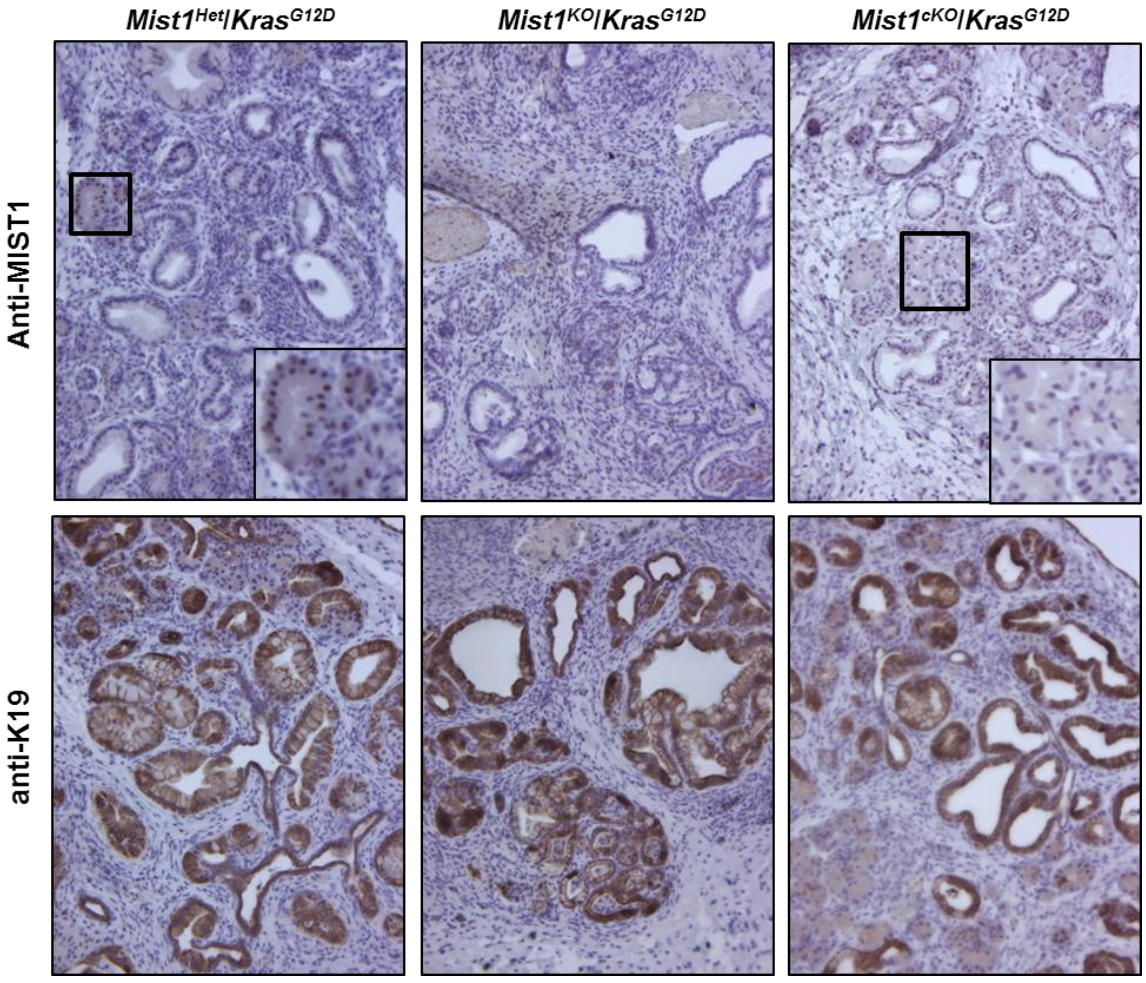

Figure 5-9. Marked increase in PanIN formation in *Mist1^{cKO}/Kras^{G12D}* mice assessed by ductal and PanIN marker K19. Anti-MIST1 antibody IHC staining showed a few positive acinar cell populations in *Mist1^{Het}/Kras^{G12D}* mice. No MIST1 positive cells were present in *Mist1^{cKO}/Kras^{G12D}* mice (insets show MIST1 positive and MIST1 negative acinar cell populations in *Mist1^{Het}/Kras^{G12D}* and *Mist1^{cKO}/Kras^{G12D}* mice, respectively (upper panel). K19 staining marks PanINs in all groups of mice (lower panel).

In order to further determine elevated PanIN formation, immunoblot experiments were performed. Anti-AMYLASE immunoblot confirmed decreased amylase expression and decreased pancreatic acinar cells in all groups of mice. SOX9 and K19 protein levels were comparable in all groups indicating a similar presence of ADMs and PanINs **(Figure 5-10).** Next, RT-qPCR analyses were conducted to determine the gene expression of acinar, ADM, PanIN and stromal markers in *Mist1*^{cKO}/*Kras*^{G12D} mice. Comparable *Amylase* expression was observed in *Mist1*^{Het}/*Kras*^{G12D} and *Mist1*^{cKO} /*Kras*^{G12D} mice. *Sox9* and *K19* gene expression were comparable in all three groups of mice suggesting the elevated ADM and PanIN formation in *Mist1*^{cKO}/*Kras*^{G12D} mice. The stromal marker *Vimentin* also revealed the presence of a significant fibroblast cell population (**Figure 5-11**). Taken together, these findings confirmed that PanIN formation in *Mist1*^{cKO}/*Kras*^{G12D} mice were elevated after 3 weeks post-AP compared to 1 week post-AP. This also suggests that *Kras*^{G12D} expression was elevated in *Mist1*^{cKO} /*Kras*^{G12D} mice 3 week post-AP. However, further experiments are needed to assess the *Kras*^{G12D} levels. It was surprising to get remarkably similar results in both *Mist1*^{Het} /*Kras*^{G12D} and *Mist1*^{cKO}/*Kras*^{G12D} mice although *Mist1*^{Het} /*Kras*^{G12D} mice formed increased PanIN formation in 7d post-AP animals. This indicates that conditional knockout of *Mist1* in adult mice are sensitive to PanIN formation over a longer period of time post- AP and *Kras*^{G12D} *expression.*

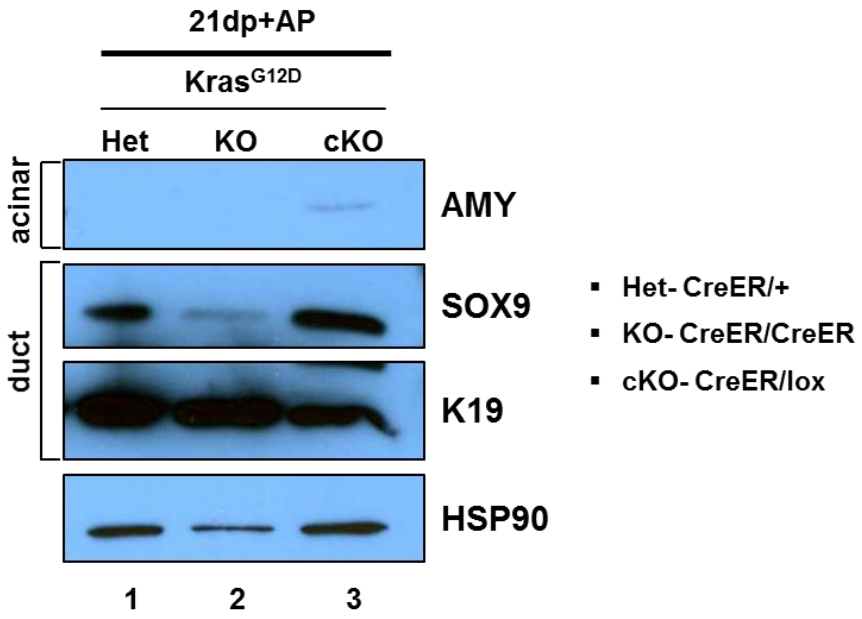

Figure 5-10. Increased PanIN formation in *Mist1^{cKO}/Kras^{G12D}* mice 21d post AP. *Mist1^{cKO}/Kras^{G12D} mice* contain slightly higher levels of acinar cells than *Mist1^{Het}/Kras^{G12D}* and *Mist1^{KO}/Kras^{G12D}* mice as shown by anti-AMYLASE. K19 level was slightly lower in *Mist1^{cKO}*; *LSL-Kras^{G12D}* when compared to the control littermates. HSP90 was used as a loading control. Note SOX9 expression in *Mist1^{KO}/Kras^{G12D}* mice (lane 2) is lower than the other two mouse groups. This might be due to lower concentration of protein loaded (confirmed by loading control). (Immunoblot experiment performed by Rebecca Steele).

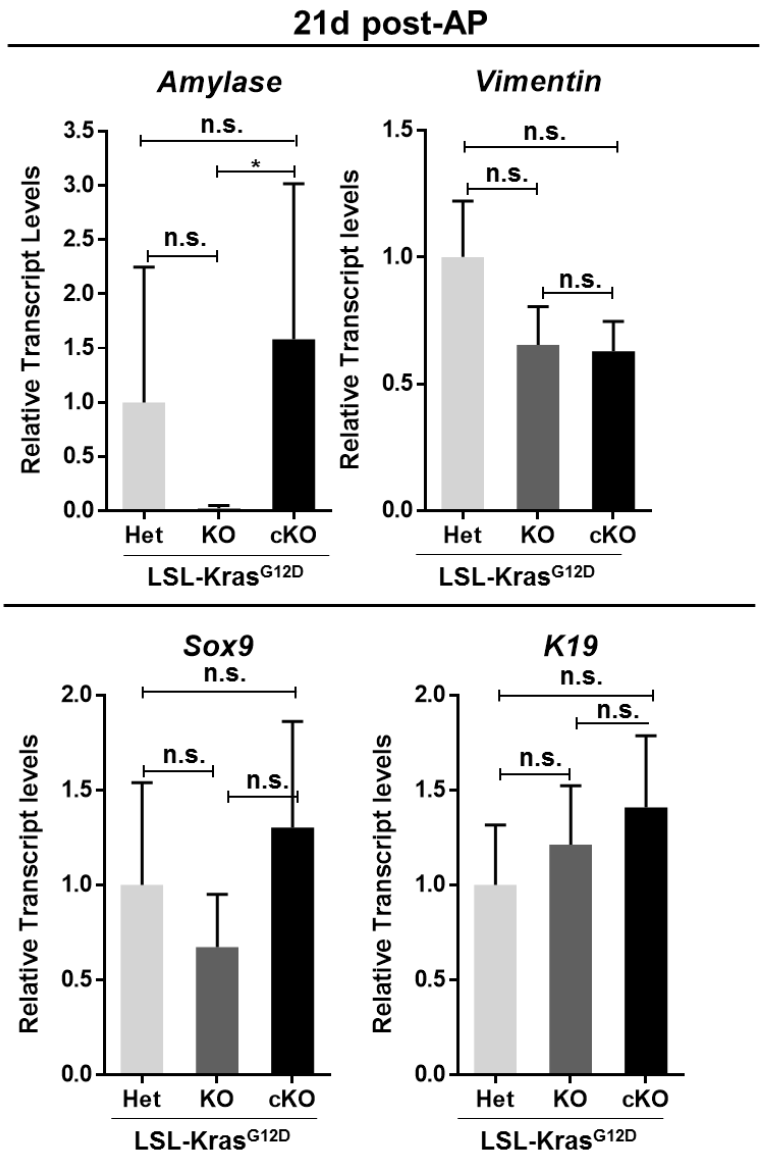

Figure 5-11. **Gene expression analysis confirmed accelerated PanIN formation in *Mist1^{cKO}/Kras^{G12D}* mice 21d post-AP.** RT-qPCR showing comparable levels of *Amylase* in *Mist1^{cKO}/Kras^{G12D}* and *Mist1^{Het}/Kras^{G12D}* mice. *Sox9* and *K19* gene expression in all sets of mice were similar indicating the development of ADM and PanIN. Occurrence of similar levels of stromal cells was confirmed by *Vimentin*. RT-qPCR performed by Rebecca Steele.

Table 6. Summary of PanIN formation in *Mist1^{Het}/Kras^{G12D}*, *Mist1^{KO}/Kras^{G12D}* and *Mist1^{cKO}/Kras^{G12D}* mice post-*Kras^{G12D}* expression only and post-*Kras^{G12D}* expression followed by an acute pancreatitis insult. (+) denotes the frequency of PanIN lesions post insults)

Genotype	+Tamoxifen (2.5 months)	7d post-AP	21d post-AP
Mist1^{Het}/Kras^{G12D}	++	+++++	+++++
Mist1^{KO}/Kras^{G12D}	++++++	+++++++	++++++
Mist1^{cKO}/Kras^{G12D}	+	++	+++++

5.3 Discussion

Genetically engineered mouse models have been instrumental in studying human pancreatic diseases such as pancreatitis and pancreatic cancer. These mouse models have played an immense role in elucidating molecular mechanisms including identifying the cell-of-origin in order to better understand diseases and hence develop better therapeutic options. Because of the ductal phenotype of PDAC, pancreatic duct cells were thought to be the ultimate cell types contributing to PDAC formation. However, studies using genetically engineered mouse models have established that upon *Kras*^{G12D} expression acinar cells give rise to both PanINs and PDAC (Kopp & Sander 2014; Kopp et al. 2012; Ji et al. 2009; Habbe et al. 2008; Shi et al. 2009; Shi et al. 2013). This finding instigated researchers to investigate acinar cell specific transcription factors. One such factor is MIST1(Pin et al. 2000). MIST1 is essential for maintaining well-differentiated acinar cells. Embryonic *Mist1*^{KO} are susceptible to diseases including pancreatitis and PDAC (Kowalik et al. 2007; Shi et al. 2009) suggesting that MIST1 can play a tumor suppressive role.

In order to better understand the role of MIST1 in PanIN development, we utilized a novel mouse model which allows us to conditionally delete *Mist1* in the adult acinar cells (Karki et al. 2015). Here, we demonstrate that conditional loss of *Mist1* upon *Kras*^{G12D} activation delayed ADM and PanIN formation. Additionally, upon AP insult, acinar cells initially are refractile to Kras transformation. However, as early as 3 weeks post-AP induction the PanIN formation are rapidly accelerated in *Mist1*^{cKO}/*Kras*^{G12D} mice.

Mist1^{cKO}/*Kras*^{G12D} mice were generated to study the role of MIST1. These mice allowed simultaneous deletion of *Mist1* and *Kras*^{G12D} expression in adult pancreata. Our analyses revealed that these mice developed very low numbers of PanIN lesions two months post-*Kras*^{G12D} expression in comparison to embryonic *Mist1*^{KO} mice. These findings led us to confirm that embryonic loss of *Mist1* makes acinar cells more susceptible to oncogenic transformation as they develop increased PanIN lesions upon *Kras*^{G12D} expression. Indeed, previous findings have confirmed that embryonic *Mist1*^{KO} mice lose proper apical-basal polarity revealed by improper zymogen localization (Pin et al. 2001). Likewise, acinar cells in these mice fail to secrete digestive enzymes including amylase (Direnzo et al. 2012). Most importantly, *Mist1*^{KO} mice fail to establish proper communication with the neighboring cells which is confirmed by loss of CONNEXIN32 (a gap junction protein)(Rukstalis et al. 2003; Johnson et al. 2004). This result, for the first time verified that the defects in germline *Mist1*^{KO} mice could contribute to accelerated PanIN formation. The conditional deletion of *Mist1*, through some unknown mechanism, inhibits the spontaneous PanIN formation driven by *Kras*^{G12D} expression in contrast to *Mist1*^{KO}/*Kras*^{G12D} mice. Future studies should be directed towards measuring the activity of oncogenic KRAS^{G12D} in both *Mist1*^{KO} and *Mist1*^{cKO} mice. This experiment will be key in finding whether embryonic *Mist1*^{KO} mice begin with elevated *Kras*^{G12D} expression in comparison to *Mist1*^{cKO} mice (Ji et al. 2009). RNA-seq analysis performed on *Ptf1a* conditional knockout mice revealed that loss of *Ptf1a* alone activates genes dedicated to Ras and inflammatory pathways (Krah et al. 2015). It would be of utmost importance to

perform similar gene expression profiling of both *Mist1*^{KO} and *Mist1*^{cKO} mice to fully characterize the transcription signature during PanIN formation.

One of the findings from when *Kras*^{G12D} was expressed in *Mist1*^{Het}/*Kras*^{G12D}, *Mist1*^{KO}/*Kras*^{G12D} and *Mist1*^{cKO}/*Kras*^{G12D} mice was that PanIN formation in *Mist1*^{cKO}/*Kras*^{G12D} was rarer than the *Mist1*^{Het}/*Kras*^{G12D} littermates.

The development of minimal PanINs in *Mist1*^{cKO}/*Kras*^{G12D} mice is very surprising and peculiar. This phenomenon seen in *Mist1*^{KO}/*Kras*^{G12D} mice has to be further investigated.

Studies in mice have shown that PanIN progression and PDAC development can be accelerated by insults including pancreatitis (Guerra et al. 2007; Carrière et al. 2011; Carrière et al. 2009). In order to further elucidate the role of *Mist1* PanIN formation, we decided to add acute pancreatitis as an insult post-*Kras*^{G12D} expression. Samples taken as early as 7d post-AP revealed that PanIN formation in *Mist1*^{cKO}/*Kras*^{G12D} mice was dramatically lower in comparison to *Mist1*^{Het}/*Kras*^{G12D} and *Mist1*^{KO}/*Kras*^{G12D} animals, revealing the presence of a high number of acinar cell pockets, decreased markers of ADM and PanINs such as SOX9 presence of low immune infiltrates and stromal cell population. This phenotype is quite intriguing as both *Kras*^{G12D} expression and an AP induction (two insults) could not accelerate the PanIN formation in *Mist1*^{cKO}/*Kras*^{G12D} mice. These results further motivate us to investigate how conditional deletion of *Mist1* protects the tissue from insults such as KRAS activity and acute pancreatitis allowing delay in *PanIN* initiation. Studies have shown that advanced PanIN formation takes place as early as one month post pancreatitis induction (Carrière et al. 2009). Next we

wanted to investigate whether *Mist1*^{cKO}/*Kras*^{G12D} mice eventually accelerate PanIN formation. Consistent with this finding, indeed *Mist1*^{cKO}/*Kras*^{G12D} mice exhibited increased PanIN formation upon *Kras*^{G12D} expression and 3 week post-AP. The frequency of PanINs were comparable to *Mist1*^{Het}/*Kras*^{G12D} and *Mist1*^{KO}/*Kras*^{G12D} mice which was confirmed by paraffin staining, gene expression and immunoblot analyses. The PanIN formation is accelerated over time in *Mist1*^{cKO}/*Kras*^{G12D} mice suggesting that these mice take time to progress lesions. We show that AP pancreatitis can accelerate the PanIN formation as early as 3 wk post-AP. However, close examination of individual *Mist1*^{cKO}/*Kras*^{G12D} mouse revealed the some mice consists of increased acinar clusters and low PanIN lesions. In order to rule the technical errors, further analyses including AMYLASE, SOX9, MIST1 and K19 staining should be performed.

The summary of the PanIN progression is shown in **Table 6**. Overall, the delay in PanIN formation in *Mist1*^{cKO} mouse is an intriguing finding. However, to unravel the mechanism behind this phenomenon would be quintessential to establish the role of MIST1 in PanIN formation.

CHAPTER 6. SUMMARY AND FUTURE DIRECTIONS

The exocrine pancreas consists of acinar cells that are responsible for the synthesis, storage and secretion of various digestive enzymes such as amylase, elastase and carboxypeptidase into duct lumens (Slack 1995). Duct cells aid in transporting the secreted proteins to the duodenum. The pyramid shaped acinar cells prevail in a spherical structure called an acinus. The basal portion of an acinar cell consists of nuclei and rough ER (Motta et al. 1997). The apically located precursor enzymes (zymogens) produced by acinar cells remain inactive until secreted into the digestive tract via a strictly regulated exocytosis pathway (McNiven & Marlowe 1999).

Transcription factors play an essential role in maintaining the function and identity of pancreatic acinar cells including the bHLH factors PTF1a (Krapp et al. 1996) and MIST1 (Lemercier et al. 1997). PTF1a plays an important role in differentiation of pancreatic precursors into acinar cells (Kawaguchi et al. 2002; Krapp et al. 1998) while MIST1 is expressed in acinar cells of the adult pancreas and is required to maintain acinar cell organization (Pin et al. 2001). *Mist1* null (*Mist1*^{KO}) mice show disrupted acinar cell organization (Pin et al. 2001). Additionally, impaired secretion and cell-cell communication is observed in *Mist1*^{KO} mice (Rukstalis et al. 2003), highlighting the importance of MIST1 in normal acinar

cell physiology. The importance of MIST1 to regulating the secretory machinery is also suggested by its global expression pattern. Besides being expressed in pancreatic acinar cells, MIST1 is expressed in other serous secretory cells including the acinar cells of the salivary glands, chief cells of the stomach, and lactating cells of the mammary glands (Pin et al. 2001). This ubiquitous presence in secretory cells and the phenotype observed in *Mist1*^{KO} cells strongly suggest a role for Mist1 in establishing and maintaining proper secretory capabilities.

The MIST1 protein is a 197 amino acid long transcription factor that has a conserved central bHLH domain that facilitates DNA binding and dimerization (Lemercier et al. 1997; Lemercier et al. 1998). Studies utilizing truncated forms of MIST1 revealed that the HLH domain is essential for MIST1 dimerization while the basic domain is essential for DNA binding (Tran et al. 2007). Interestingly, MIST1 lacks a classic transcriptional activation domain (TAD) or transcriptional repression domain (TRD), suggesting that it utilizes cofactor proteins in order to regulate transcription. Indeed, a truncated version of Mist1 (50 aa – 140 aa) containing the central bHLH region is sufficient to generate a near complete transcriptional response (Tran et al. 2007). Thus, I hypothesized that co-factors are required to allow MIST1 to activate or repress specific target genes. One focus of this thesis was to utilize a novel mouse model to identify the binding protein partners of MIST1 by LC-MS/MS via a biotinylation pull-down system to immunoprecipitate MIST1-associated complexes. An N-terminal BT tag, C-terminal 6XHis-Myc tag and two loxP sites were introduced via homologous recombination into the *Mist1* locus, generating the *Mist1*$^{BT/Myc}$ line. *R26*$^{HA\text{-}BirA}$ mice, expressing a BT-specific biotin

ligase, were crossed to *Mist1*$^{BT/Myc}$ mice to generate *Mist1*$^{BT/BT}$*; R26*$^{HA\text{-}BirA}$ mice. Biotinylated protein complexes from mice pancreata were purified using streptavidin conjugated magnetic beads. To identify potential MIST1 binding partners, the samples were run via mass spectrometry. Unfortunately, we were unable to identify clear binding partners (a transcription factor) of MIST1 utilizing this strategy. However, future studies could analyze the mass spectrometry data list to potentially identify if any of the other proteins (non-transcription factors) could possibly serve as a putative binding partner depending on the cell context.

Another focus of this thesis was to elucidate the role of MIST1 in both AP and PDAC conditions. Interestingly, *Mist1*^{WT} mice subjected to acute pancreatitis develop damaged acinar cells that transiently silence the *Mist1* gene, but as the organ undergoes recovery, *Mist1* gene expression resumes. Similar studies on *Mist1*^{KO} mice have shown that in the absence of MIST1 protein, organ recovery is significantly impaired, suggesting that the MIST1 transcription network plays a key role in restoring normal homeostasis. In order to study the importance of MIST1 activity to pancreatitis recovery, I asked whether *Mist1* silencing is a consequence of pancreatitis damage or is actually a necessary event for organ recovery. To examine this question, I used an inducible transgenic mouse line which allows *Mist1* gene expression to be continuously on, even under pancreatitis conditions. The results reveal that sustained expression of *Mist1* in damaged acinar cells hinders the normal recovery process when compared to *Mist1*^{WT} mice. My findings also suggest that apoptosis plays a role in deterring the recovery process in pancreata that fail to silence *Mist1* expression. Lineage tracing experiments

revealed that endogenous acinar cells are involved in the pancreatitis recovery process.

Future directions for the project are to perform studies on how pancreatitis damage accelerates PDAC disease. Additionally, it would be very interesting to generate an *iMist1-ENGRAILED* model in order to determine if activated MIST1 targets are responsible for the severe cell death in *iMist1* mice. In this instance, we would use a MIST1-ENgrailed repressor fusion protein and generate a new iMIST1^{EN} mouse (Wang et al. 2004). The *Drosophila* homeodomain protein Engrailed, consists of a repression domain within amino acids 2-299 (Han & Manley 1993). The Engrailed domain will be fused with MIST1 protein with an epitope tag such as Myc. The *Mist1$^{EN\text{-}Myc}$* cDNA will then be placed into the pCAG-CAT vector containing a lox-stop-lox (LSL) cassette. Introduction of the LSL-Mist1$^{EN\text{-}Myc}$ transgene into mouse pronuclei will generate an *iMist1$^{EN\text{-}Myc}$* transgenic line. Crossing *iMist1$^{EN\text{-}Myc}$* mice to *Mist1^{CreER}* mice will generate *Mist1$^{CreERT/+}$*/*Mist1$^{EN\text{-}Myc}$* animals. Upon tamoxifen administration, this approach allows MIST1$^{EN\text{-}Myc}$ to behave as a full-time repressor. Thus, we would be able to elucidate if turning off MIST1 target genes would give different results than that of AP iMIST1 studies. Upon turning off the MIST1 targets, if the acinar cells do not undergo severe cell death, this would suggest that indeed MIST1 induced targets are contributing to the devastating phenotype in our *iMist1* AP studies. In contrast, if the cells still undergo dramatic apoptosis post-AP in *Mist1$^{CreER/+}$*/*Mist1$^{EN\text{-}Myc}$* mice, then this would indicate that presumably the genes normally repressed by MIST1,

including *Rnd2*, are responsible for causing the severe pancreas injury in the *iMist1* AP studies.

Previous studies using *Mist1*^{KO} mice revealed that upon AP insults, these mice are susceptible to severe AP phenotypes along with delay in organ recovery (Kowalik et al. 2007). Likewise, upon *Kras*^{G12D} oncogene transformation, PanIN lesion development is markedly accelerated in *Mist1*^{KO} mice (Shi et al. 2009). However, germline *Mist1*^{KO} mice show defects in cell-polarity, cell-cell communication and enzyme secretion (Johnson et al. 2004; Direnzo et al. 2012; Pin et al. 2001) since the beginning of life. Hence, we predict that these prior defects in *Mist1*^{KO} mice might be the cause of sensitivity towards diseases and not due necessarily to the absence of MIST1 protein *per se*. To overcome this sensitivity, a conditional *Mist1* knock-out mouse model was developed. The conditional knockout (*Mist1*^{cKO}) mouse was crossed with *LSL-Kras*^{G12D} mice to generate *Mist1*^{cKO}/*Kras*^{G12D} mice. Interestingly, *Mist1*^{cKO}/*Kras*^{G12D} mice develop significantly decreased PanIN lesions than *Mist1*^{KO}/*Kras*^{G12D} mice confirming that indeed the defects in pancreata of *Mist1*^{KO} mice is what makes them susceptible to insults. Furthermore, in an effort to determine the role of pancreatitis in pancreatic cancer development, we studied *Mist1*^{Het}/*Kras*^{G12D} and *Mist1*^{KO}/*Kras*^{G12D} and *Mist1*^{cKO}/*Kras*^{G12D} mice. Preliminary studies revealed that upon simultaneous *Mist1* deletion and *Kras*^{G12D} activation, alongside the induction of pancreatitis, PanIN formation decreased compared to *Mist1*^{Het}/*Kras*^{G12D} animals during the initial stages of PanIN formation. However, as early as 3 weeks post-AP induction PanIN lesions are markedly accelerated in *Mist1*^{cKO}/*Kras*^{G12D} mice.

Further experiments have to be performed to delineate the mechanism(s) behind the delayed PanIN formation in *Mist1*^{cKO}/*Kras*^{G12D} mice. Performing RNA-Seq analysis to identify differential gene expression pattern in *Mist1*^{KO} and *Mist1*^{cKO} mice would be a critical experiment to determine the role of MIST1 protein. Other key questions to be answered are: Is there a specific signaling pathway that is involved in inhibiting PanIN formation? Are there other key transcription factors besides MIST1 that could be controlling the PanIN lesion formation? Is MIST1 required for both PanIN initiation and progression?

The study of TFs is of utmost importance for understanding the origin and mechanism of pancreas related diseases. The importance of MIST1 to pancreatitis and pancreatic cancer suggests that modulating key pancreas transcription networks could ease clinical symptoms in patients diagnosed with pancreatitis and pancreatic cancer.

LIST OF REFERENCES

REFERENCES

Afelik, S., Chen, Y. & Pieler, T., 2006. Combined ectopic expression of Pdx1 and Ptf1a/p48 results in the stable conversion of posterior endoderm into endocrine and exocrine pancreatic tissue. *Genes & development*, 20(11), pp.1441–6. Available at: http://www.pubmedcentral.nih.gov/articlerender.fcgi?artid=1475757&tool=pmcentrez&rendertype=abstract [Accessed February 11, 2016].

Ahlgren, U., Jonsson, J. & Edlund, H., 1996. The morphogenesis of the pancreatic mesenchyme is uncoupled from that of the pancreatic epithelium in IPF1/PDX1-deficient mice. *Development (Cambridge, England)*, 122(5), pp.1409–16. Available at: http://www.ncbi.nlm.nih.gov/pubmed/8625829 [Accessed January 22, 2016].

Ahmed, A.M., 2002. History of diabetes mellitus. *Saudi medical journal*, 23(4), pp.373–8. Available at: http://www.ncbi.nlm.nih.gov/pubmed/11953758 [Accessed March 17, 2016].

Akiyama, H. et al., 2005. Osteo-chondroprogenitor cells are derived from Sox9 expressing precursors. *Proceedings of the National Academy of Sciences of the United States of America*, 102(41), pp.14665–70. Available at: http://www.pnas.org/content/102/41/14665.long [Accessed March 20, 2016].

Alahari, S. et al., 2011. The absence of MIST1 leads to increased ethanol sensitivity and decreased activity of the unfolded protein response in mouse pancreatic acinar cells. *PloS one*, 6(12), p.e28863. Available at: http://journals.plos.org/plosone/article?id=10.1371/journal.pone.0028863 [Accessed February 17, 2016].

Anon, Avidin-Biotin Chemistry: A Handbook: M. Dean Savage: 9780935940114: Amazon.com: Books. Available at: http://www.amazon.com/Avidin-Biotin-Chemistry-Handbook-Dean-Savage/dp/0935940111 [Accessed January 13, 2016].

Ardito, C.M. et al., 2012. EGF receptor is required for KRAS-induced pancreatic tumorigenesis. *Cancer cell*, 22(3), pp.304–17. Available at: http://www.ncbi.nlm.nih.gov/pubmed/22975374 [Accessed February 28, 2

Aure, M.H., Konieczny, S.F. & Ovitt, C.E., 2015. Salivary gland homeostasis is maintained through acinar cell self-duplication. *Developmental cell*, 33(2), pp.231–7. Available at: http://www.cell.com/article/S1534580715001318/fulltext [Accessed February 1, 2016].

Bailey, J.M., DelGiorno, K.E. & Crawford, H.C., 2014. The secret origins and surprising fates of pancreas tumors. *Carcinogenesis*.

Banerjee, A.K. et al., 1995. Respiratory failure in acute pancreatitis. *Postgraduate medical journal*, 71(836), pp.327–30. Available at: http://www.pubmedcentral.nih.gov/articlerender.fcgi?artid=2398144&tool=pmcentrez&rendertype=abstract [Accessed April 3, 2016].

Banks, P.A., Conwell, D.L. & Toskes, P.P., 2010. The management of acute and chronic pancreatitis. *Gastroenterology & hepatology*, 6(2 Suppl 3), pp.1–16. Available at: http://www.pubmedcentral.nih.gov/articlerender.fcgi?artid=2886461&tool=pmcentrez&rendertype=abstract [Accessed February 12, 2016].

Bardeesy, N., Aguirre, A.J., et al., 2006. Both p16(Ink4a) and the p19(Arf)-p53 pathway constrain progression of pancreatic adenocarcinoma in the mouse. *Proceedings of the National Academy of Sciences of the United States of America*, 103(15), pp.5947–52. Available at: http://www.pubmedcentral.nih.gov/articlerender.fcgi?artid=1458678&tool=pmcentrez&rendertype=abstract [Accessed March 24, 2016].

Bardeesy, N., Cheng, K.-H., et al., 2006. Smad4 is dispensable for normal pancreas development yet critical in progression and tumor biology of pancreas cancer. *Genes & development*, 20(22), pp.3130–46. Available at: http://www.pubmedcentral.nih.gov/articlerender.fcgi?artid=1635148&tool=pmcentrez&rendertype=abstract [Accessed March 24, 2016].

Bardeesy, N. & DePinho, R.A., 2002. Pancreatic cancer biology and genetics. *Nature reviews. Cancer*, 2(12), pp.897–909. Available at: http://www.ncbi.nlm.nih.gov/pubmed/12459728 [Accessed February 9, 2016].

van Belle, T.L., Coppieters, K.T. & von Herrath, M.G., 2011. Type 1 diabetes: etiology, immunology, and therapeutic strategies. *Physiological reviews*, 91(1), pp.79–118. Available at: http://www.ncbi.nlm.nih.gov/pubmed/21248163 [Accessed September 25, 2015].

Van Belle, T.L., Taylor, P. & von Herrath, M.G., 2009. Mouse Models for Type 1 Diabetes. *Drug discovery today. Disease models*, 6(2), pp.41–45. Available at: http://www.pubmedcentral.nih.gov/articlerender.fcgi?artid=2855847&tool=pmcentrez&rendertype=abstract [Accessed February 21, 2016].

Beres, T.M. et al., 2006. PTF1 is an organ-specific and Notch-independent basic helix-loop-helix complex containing the mammalian Suppressor of Hairless (RBP-J) or its paralogue, RBP-L. *Molecular and cellular biology*, 26(1), pp.117–30. Available at: http://www.pubmedcentral.nih.gov/articlerender.fcgi?artid=1317634&tool=pmcentrez&rendertype=abstract [Accessed February 17, 2016].

Bhatia, M. et al., 2012. Apoptosis versus necrosis in acute pancreatitis Apoptosis versus necrosis in acute pancreatitis.

Bhatia, M., 2005. Inflammatory response on the pancreatic acinar cell injury. *Scandinavian journal of surgery : SJS : official organ for the Finnish Surgical Society and the Scandinavian Surgical Society*, 94(2), pp.97–102. Available at: http://www.ncbi.nlm.nih.gov/pubmed/16111089 [Accessed April 3, 2016].

Bhatia, M. et al., 2005. Pathophysiology of acute pancreatitis. *Pancreatology : official journal of the International Association of Pancreatology (IAP) ... [et al.]*, 5(2-3), pp.132–44. Available at: http://www.sciencedirect.com/science/article/pii/S142439030580050X [Accessed April 2, 2016].

Bockman, D.E. et al., 2003. Origin and Development of the Precursor Lesions in Experimental Pancreatic Cancer in Rats. *Laboratory Investigation*, 83(6), pp.853–859. Available at: http://dx.doi.org/10.1097/01.LAB.0000074918.31303.5A [Accessed March 17, 2016].

de Boer, E. et al., 2003. Efficient biotinylation and single-step purification of tagged transcription factors in mammalian cells and transgenic mice. *Proceedings of the National Academy of Sciences of the United States of America*, 100(13), pp.7480–5. Available at: http://www.pubmedcentral.nih.gov/articlerender.fcgi?artid=164612&tool=pmcentrez&rendertype=abstract [Accessed January 20, 2016].

Börner, A. et al., 2009. Subcellular protein extraction from human pancreatic cancer tissues. *BioTechniques*, 46(4), pp.297–304. Available at: http://www.ncbi.nlm.nih.gov/pubmed/19450236 [Accessed February 16, 2016].

Bragado, M.J. et al., 1996. Impairment of intracellular calcium homoeostasis in the exocrine pancreas after caerulein-induced acute pancreatitis in the rat. *Clinical science (London, England : 1979)*, 91(3), pp.365–9. Available at: http://www.ncbi.nlm.nih.gov/pubmed/8869421 [Accessed April 3, 2016].

Bredemeyer, A.J. et al., 2009. The gastric epithelial progenitor cell niche and differentiation of the zymogenic (chief) cell lineage. *Developmental biology*, 325(1), pp.211–24. Available at: http://www.pubmedcentral.nih.gov/articlerender.fcgi?artid=2634829&tool=pmcentrez&rendertype=abstract [Accessed January 18, 2016].

Butler, A.E. et al., 2003. Beta-cell deficit and increased beta-cell apoptosis in humans with type 2 diabetes. *Diabetes*, 52(1), pp.102–10. Available at: http://www.ncbi.nlm.nih.gov/pubmed/12502499 [Accessed March 23, 2016].

Capoccia, B.J. et al., 2011. Transcription factor MIST1 in terminal differentiation of mouse and human plasma cells. *Physiological genomics*, 43(3), pp.174–86. Available at: http://www.pubmedcentral.nih.gov/articlerender.fcgi?artid=3055710&tool=pmcentrez&rendertype=abstract [Accessed June 23, 2011].

Carrière, C. et al., 2011. Acute pancreatitis accelerates initiation and progression to pancreatic cancer in mice expressing oncogenic Kras in the Nestin cell lineage. *PLoS ONE*.

Carrière, C. et al., 2009. Acute pancreatitis markedly accelerates pancreatic cancer progression in mice expressing oncogenic Kras. *Biochemical and Biophysical Research Communications*.

Chen, E.I. et al., 2007. Optimization of mass spectrometry-compatible surfactants for shotgun proteomics. *Journal of proteome research*, 6(7), pp.2529–38. Available at: http://www.pubmedcentral.nih.gov/articlerender.fcgi?artid=2570269&tool=pmcentrez&rendertype=abstract [Accessed February 16, 2016].

Chevet, E., Hetz, C. & Samali, A., 2015. Endoplasmic reticulum stress-activated cell reprogramming in oncogenesis. *Cancer discovery*, 5(6), pp.586–97. Available at: http://www.ncbi.nlm.nih.gov/pubmed/25977222 [Accessed February 17, 2016].

Chiefari, E. et al., 2011. Functional variants of the HMGA1 gene and type 2 diabetes mellitus. *JAMA*, 305(9), pp.903–12. Available at: http://jama.jamanetwork.com/article.aspx?articleid=645914#ref-joc15012-19 [Accessed February 24, 2016].

Choi, H. et al., 2011. SAINT: probabilistic scoring of affinity purification-mass spectrometry data. *Nature methods*, 8(1), pp.70–3. Available at: http://www.pubmedcentral.nih.gov/articlerender.fcgi?artid=3064265&tool=pmcentrez&rendertype=abstract [Accessed November 29, 2015].

Choi-Rhee, E., Schulman, H. & Cronan, J.E., 2004. Promiscuous protein biotinylation by Escherichia coli biotin protein ligase. *Protein science : a publication of the Protein Society*, 13(11), pp.3043–50. Available at: http://www.pubmedcentral.nih.gov/articlerender.fcgi?artid=2286582&tool=pmcentrez&rendertype=abstract [Accessed December 1, 2015].

Collins, M.A. et al., 2014. MAPK signaling is required for dedifferentiation of acinar cells and development of pancreatic intraepithelial neoplasia in mice. *Gastroenterology*.

Collins, M.A. et al., 2012. Oncogenic Kras is required for both the initiation and maintenance of pancreatic cancer in mice. *The Journal of clinical investigation*, 122(2), pp.639–53. Available at: http://www.jci.org/articles/view/59227 [Accessed January 13, 2016].

Criddle, D.N. et al., 2007. Calcium signalling and pancreatic cell death: apoptosis or necrosis? *Cell death and differentiation*, 14(7), pp.1285–94. Available at: http://dx.doi.org/10.1038/sj.cdd.4402150 [Accessed April 3, 2016].

Criscimanna, A. et al., 2011. Duct cells contribute to regeneration of endocrine and acinar cells following pancreatic damage in adult mice. *Gastroenterology*.

Cronan, J.E., 1990. Biotination of proteins in vivo. A post-translational modification to label, purify, and study proteins. *The Journal of biological chemistry*, 265(18), pp.10327–33. Available at: http://www.ncbi.nlm.nih.gov/pubmed/2113052 [Accessed December 15, 2015].

Davies, M.G. & Hagen, P.O., 1997. Systemic inflammatory response syndrome. *The British journal of surgery*, 84(7), pp.920–35. Available at: http://www.ncbi.nlm.nih.gov/pubmed/9240130 [Accessed April 3, 2016].

Dawra, R. et al., 2011. Intra-acinar trypsinogen activation mediates early stages of pancreatic injury but not inflammation in mice with acute pancreatitis. *Gastroenterology*, 141(6), pp.2210–2217.e2. Available at: http://www.pubmedcentral.nih.gov/articlerender.fcgi?artid=3587766&tool=pmcentrez&rendertype=abstract [Accessed April 3, 2016].

Desai, B.M. et al., 2007. Preexisting pancreatic acinar cells contribute to acinar cell, but not islet beta cell, regeneration. *The Journal of clinical investigation*, 117(4), pp.971–7. Available at: http://www.pubmedcentral.nih.gov/articlerender.fcgi?artid=1838936&tool=pmcentrez&rendertype=abstract [Accessed April 4, 2016].

Diehl, A.K. et al., 1997. Gallstone size and risk of pancreatitis. *Archives of internal medicine*, 157(15), pp.1674–8. Available at: http://www.ncbi.nlm.nih.gov/pubmed/9250228 [Accessed April 2, 2016].

Direnzo, D. et al., 2012. Induced Mist1 expression promotes remodeling of mouse pancreatic acinar cells. *Gastroenterology*, 143(2), pp.469–80. Available at: http://www.gastrojournal.org/article/S0016508512005616/fulltext [Accessed January 12, 2016].

Domcke, S. et al., 2015. Competition between DNA methylation and transcription factors determines binding of NRF1. *Nature*, 528(7583), pp.575–579. Available at: http://dx.doi.org/10.1038/nature16462 [Accessed December 16, 2015].

Driegen, S. et al., 2005. A generic tool for biotinylation of tagged proteins in transgenic mice. *Transgenic Research*, 14(4), pp.477–482. Available at: http://link.springer.com/10.1007/s11248-005-7220-2 [Accessed January 13, 2016].

Dutta, S. et al., 1998. Regulatory factor linked to late-onset diabetes? *Nature*, 392(6676), p.560. Available at: http://www.ncbi.nlm.nih.gov/pubmed/9560151 [Accessed March 23, 2016].

Fallon, M.B. et al., 1995. Effect of cerulein hyperstimulation on the paracellular barrier of rat exocrine pancreas. *Gastroenterology*, 108(6), pp.1863–1872. Available at: http://www.gastrojournal.org/article/0016508595901515/fulltext [Accessed March 16, 2016].

von Figura, G. et al., 2014. Nr5a2 maintains acinar cell differentiation and constrains oncogenic Kras-mediated pancreatic neoplastic initiation. *Gut*, 63(4), pp.656–64. Available at: http://www.pubmedcentral.nih.gov/articlerender.fcgi?artid=3883808&tool=pmcentrez&rendertype=abstract [Accessed February 17, 2016].

Flandez, M. et al., 2013. Nr5a2 heterozygosity sensitises to, and cooperates with, inflammation in KRasG12V-driven pancreatic tumourigenesis. *Gut*, pp.1–9. Available at: http://www.ncbi.nlm.nih.gov/pubmed/23598351 [Accessed April 24, 2013].

Foti, D. et al., 2003. A nucleoprotein complex containing Sp1, C/EBP beta, and HMGI-Y controls human insulin receptor gene transcription. *Molecular and cellular biology*, 23(8), pp.2720–32. Available at: http://www.pubmedcentral.nih.gov/articlerender.fcgi?artid=152545&tool=pmcentrez&rendertype=abstract [Accessed March 23, 2016].

Frossard, J.-L. et al., 1999. The role of intercellular adhesion molecule 1 and neutrophils in acute pancreatitis and pancreatitis-associated lung injury. *Gastroenterology*, 116(3), pp.694–701. Available at: http://www.gastrojournal.org/article/S0016508599701927/fulltext [Accessed April 3, 2016].

Furukawa, T., Sunamura, M. & Horii, A., 2006. Molecular mechanisms of pancreatic carcinogenesis. *Cancer science*, 97(1), pp.1–7. Available at: http://www.ncbi.nlm.nih.gov/pubmed/16367914 [Accessed March 24, 2016].

Gannon, M. et al., 2008. pdx-1 function is specifically required in embryonic beta cells to generate appropriate numbers of endocrine cell types and maintain glucose homeostasis. *Developmental biology*, 314(2), pp.406–17. Available at: http://www.pubmedcentral.nih.gov/articlerender.fcgi?artid=2269701&tool=pmcentrez&rendertype=abstract [Accessed March 18, 2016].

Gannon, M., Gamer, L.W. & Wright, C. V, 2001. Regulatory regions driving developmental and tissue-specific expression of the essential pancreatic gene pdx1. *Developmental biology*, 238(1), pp.185–201. Available at: http://www.ncbi.nlm.nih.gov/pubmed/11784003 [Accessed March 18, 2016].

Garside, V.C. et al., 2010. MIST1 regulates the pancreatic acinar cell expression of Atp2c2, the gene encoding secretory pathway calcium ATPase 2. *Experimental cell research*, 316(17), pp.2859–70. Available at: http://www.pubmedcentral.nih.gov/articlerender.fcgi?artid=3342848&tool=pmcentrez&rendertype=abstract [Accessed January 20, 2016].

Gittes, G.K., 2009. Developmental biology of the pancreas: a comprehensive review. *Developmental biology*, 326(1), pp.4–35. Available at: http://www.sciencedirect.com/science/article/pii/S0012160608012785 [Accessed December 28, 2015].

Glimcher, L.H., 2010. XBP1: the last two decades. *Annals of the rheumatic diseases*, 69 Suppl 1, pp.i67–71. Available at: http://www.ncbi.nlm.nih.gov/pubmed/19995749 [Accessed February 17, 2016].

Gorelick, F.S., 2003. Alcohol and zymogen activation in the pancreatic acinar cell. *Pancreas*, 27(4), pp.305–310.

Grady, T. et al., 1998. Zymogen proteolysis within the pancreatic acinar cell is associated with cellular injury. *American Journal of Physiology*, 275(5 Pt 1), pp.G1010–G1017. Available at: http://www.ncbi.nlm.nih.gov/pubmed/9815031.

Green, M., 1990. [5] Avidin and streptavidin. *Methods in Enzymology*, 184, pp.51–67. Available at: http://linkinghub.elsevier.com/retrieve/pii/007668799084259J.

Greer, R.L. et al., 2013. Numb regulates acinar cell dedifferentiation and survival during pancreatic damage and acinar-to-ductal metaplasia. *Gastroenterology*.

Gu, G., Dubauskaite, J. & Melton, D.A., 2002. Direct evidence for the pancreatic lineage: NGN3+ cells are islet progenitors and are distinct from duct progenitors. *Development (Cambridge, England)*, 129(10), pp.2447–57. Available at: http://www.ncbi.nlm.nih.gov/pubmed/11973276 [Accessed March 18, 2016].

Guerra, C. et al., 2011. Article Pancreatitis-Induced Inflammation Contributes to Pancreatic Cancer by Inhibiting Oncogene-Induced Senescence. *Cancer Cell*, pp.728–739.

Guerra, C. et al., 2007. Chronic pancreatitis is essential for induction of pancreatic ductal adenocarcinoma by K-Ras oncogenes in adult mice. *Cancer cell*, 11(3), pp.291–302. Available at: http://www.ncbi.nlm.nih.gov/pubmed/17349585 [Accessed February 27, 2013].

Gukovsky, I. et al., 1998. Early NF-kappaB activation is associated with hormone-induced pancreatitis. *The American journal of physiology*, 275(6 Pt 1), pp.G1402–14. Available at: http://www.ncbi.nlm.nih.gov/pubmed/9843778 [Accessed April 3, 2016].

Guo, X. et al., 2007. Cloning, expression, and functional characterization of zebrafish Mist1. *Biochemical and biophysical research communications*, 359(1), pp.20–6. Available at: http://www.ncbi.nlm.nih.gov/pubmed/17531198 [Accessed March 24, 2016].

Guz, Y. et al., 1995. Expression of murine STF-1, a putative insulin gene transcription factor, in beta cells of pancreas, duodenal epithelium and pancreatic exocrine and endocrine progenitors during ontogeny. *Development (Cambridge, England)*, 121(1), pp.11–8. Available at: http://www.ncbi.nlm.nih.gov/pubmed/7867492 [Accessed March 18, 2016].

Habbe, N. et al., 2008. Spontaneous induction of murine pancreatic intraepithelial neoplasia (mPanIN) by acinar cell targeting of oncogenic Kras in adult mice. *Proceedings of the National Academy of Sciences*, 105(48), pp.18913–18918. Available at: http://www.pubmedcentral.nih.gov/articlerender.fcgi?artid=2596215&tool=pmcentrez&rendertype=abstract [Accessed October 7, 2015].

Halangk, W. et al., 2000. Role of cathepsin B in intracellular trypsinogen activation and the onset of acute pancreatitis. *The Journal of clinical investigation*, 106(6), pp.773–81. Available at: http://www.pubmedcentral.nih.gov/articlerender.fcgi?artid=381392&tool=pmcentrez&rendertype=abstract [Accessed April 3, 2016].

Hale, M.A. et al., 2014. The nuclear hormone receptor family member NR5A2 controls aspects of multipotent progenitor cell formation and acinar differentiation during pancreatic organogenesis. *Development (Cambridge, England)*, 141(16), pp.3123–33. Available at: http://www.pubmedcentral.nih.gov/articlerender.fcgi?artid=4197540&tool=pmcentrez&rendertype=abstract [Accessed February 17, 2016].

Han, K. & Manley, J.L., 1993. Functional domains of the Drosophila Engrailed protein. *The EMBO journal*, 12(7), pp.2723–33. Available at: http://www.pubmedcentral.nih.gov/articlerender.fcgi?artid=413523&tool=pmcentrez&rendertype=abstract [Accessed April 22, 2016].

Hani, E.H. et al., 1999. Defective mutations in the insulin promoter factor-1 (IPF-1) gene in late-onset type 2 diabetes mellitus. *The Journal of clinical investigation*, 104(9), pp.R41–8. Available at: http://www.pubmedcentral.nih.gov/articlerender.fcgi?artid=409821&tool=pmcentrez&rendertype=abstract [Accessed March 23, 2016].

Haumaitre, C. et al., 2005. Lack of TCF2/vHNF1 in mice leads to pancreas agenesis. *Proceedings of the National Academy of Sciences of the United States of America*, 102(5), pp.1490–5. Available at: http://www.pubmedcentral.nih.gov/articlerender.fcgi?artid=547822&tool=pmcentrez&rendertype=abstract [Accessed March 20, 2016].

Hayashi, K. et al., 1999. Regional differences in the cellular proliferation activity of the regenerating rat pancreas after partial pancreatectomy. *Archives of histology and cytology*, 62(4), pp.337–46. Available at: http://www.ncbi.nlm.nih.gov/pubmed/10596944 [Accessed March 18, 2016].

Hazem, Z.M., 2009. Acute biliary pancreatitis: diagnosis and treatment. *Saudi journal of gastroenterology : official journal of the Saudi Gastroenterology Association*, 15(3), pp.147–55. Available at: http://www.pubmedcentral.nih.gov/articlerender.fcgi?artid=2841412&tool=pmcentrez&rendertype=abstract [Accessed February 26, 2016].

Hess et al., 2011. Extensive pancreas regeneration following acinar-specific disruption of Xbp1 in mice. *Gastroenterology*, 141(4), pp.1463–72. Available at: http://www.pubmedcentral.nih.gov/articlerender.fcgi?artid=3186847&tool=pmcentrez&rendertype=abstract [Accessed February 17, 2016].

Hess, S., 2013. Sample Preparation Guide for Mass Spectrometry–Based Proteomics. *Spectroscopy*. Available at: http://authors.library.caltech.edu/41345/ [Accessed February 18, 2016].

Hewes, R.S. et al., 2006. Regulation of secretory protein expression in mature cells by DIMM, a basic helix-loop-helix neuroendocrine differentiation factor. *The Journal of neuroscience : the official journal of the Society for Neuroscience*, 26(30), pp.7860–9. Available at: http://www.ncbi.nlm.nih.gov/pubmed/16870731 [Accessed February 20, 2016].

Hewes, R.S. et al., 2003. The bHLH protein Dimmed controls neuroendocrine cell differentiation in Drosophila. *Development (Cambridge, England)*, 130(9), pp.1771–81. Available at: http://www.ncbi.nlm.nih.gov/pubmed/12642483 [Accessed March 24, 2016].

Hingorani, S.R. et al., 2003. Preinvasive and invasive ductal pancreatic cancer and its early detection in the mouse. *Cancer cell*, 4(6), pp.437–50. Available at: http://www.ncbi.nlm.nih.gov/pubmed/14706336.

Hirschhorn, J.N., 2003. Genetic epidemiology of type 1 diabetes. *Pediatric diabetes*, 4(2), pp.87–100. Available at: http://www.ncbi.nlm.nih.gov/pubmed/14655265 [Accessed March 22, 2016].

Holmstrom, S.R. et al., 2011. LRH-1 and PTF1-L coregulate an exocrine pancreas-specific transcriptional network for digestive function. *Genes & development*, 25(16), pp.1674–9. Available at: http://www.pubmedcentral.nih.gov/articlerender.fcgi?artid=3165932&tool=pmcentrez&rendertype=abstract [Accessed February 17, 2016].

Houbracken, I. et al., 2011. Lineage Tracing Evidence for Transdifferentiation of Acinar to Duct Cells and Plasticity of Human Pancreas. *Gastroenterology*. Available at: http://www.ncbi.nlm.nih.gov/pubmed/21703267 [Accessed July 21, 2011].

Huang, C. & Jacobson, K., 2010. Detection of protein-protein interactions using nonimmune IgG and BirA-mediated biotinylation. *BioTechniques*, 49(6), pp.881–6. Available at: http://www.pubmedcentral.nih.gov/articlerender.fcgi?artid=4441393&tool=pmcentrez&rendertype=abstract [Accessed January 13, 2016].

Huang, H. et al., 2013. Activation of nuclear factor-κB in acinar cells increases the severity of pancreatitis in mice. *Gastroenterology*, 144(1), pp.202–10. Available at: http://www.pubmedcentral.nih.gov/articlerender.fcgi?artid=3769090&tool=pmcentrez&rendertype=abstract [Accessed April 3, 2016].

Huang, H. et al., 2013. Oncogenic K-Ras requires activation for enhanced activity. *Oncogene*, (November 2012), pp.1–4. Available at: http://www.ncbi.nlm.nih.gov/pubmed/23334325 [Accessed March 25, 2013].

Huh, W.J. et al., 2010. XBP1 controls maturation of gastric zymogenic cells by induction of MIST1 and expansion of the rough endoplasmic reticulum. *Gastroenterology*, 139(6), pp.2038–49. Available at: http://www.pubmedcentral.nih.gov/articlerender.fcgi?artid=2997137&tool=pmcentrez&rendertype=abstract [Accessed February 17, 2016].

Husain, S.Z. et al., 2007. Caerulein-induced intracellular pancreatic zymogen activation is dependent on calcineurin. *American journal of physiology. Gastrointestinal and liver physiology*, 292(6), pp.G1594–9. Available at: http://www.ncbi.nlm.nih.gov/pubmed/17332472 [Accessed April 3, 2016].

Jackson, E.L. et al., 2001. Analysis of lung tumor initiation and progression using conditional expression of oncogenic K-ras. *Genes & development*, 15(24), pp.3243–8. Available at: http://www.pubmedcentral.nih.gov/articlerender.fcgi?artid=312845&tool=pmcentrez&rendertype=abstract [Accessed January 19, 2016].

Jacquemin, P., Lemaigre, F.P. & Rousseau, G.G., 2003. The Onecut transcription factor HNF-6 (OC-1) is required for timely specification of the pancreas and acts upstream of Pdx-1 in the specification cascade. *Developmental biology*, 258(1), pp.105–16. Available at: http://www.ncbi.nlm.nih.gov/pubmed/12781686 [Accessed March 20, 2016].

Jarvik, J.W. & Telmer, C.A., 1998. Epitope tagging. *Annual review of genetics*, 32, pp.601–18. Available at: http://www.ncbi.nlm.nih.gov/pubmed/9928493 [Accessed January 13, 2016].

Jemal, A. et al., 2011. Global cancer statistics. *CA: a cancer journal for clinicians*, 61(2), pp.69–90. Available at: http://www.ncbi.nlm.nih.gov/pubmed/21296855 [Accessed July 12, 2014].

Jensen, J.N. et al., 2005. Recapitulation of elements of embryonic development in adult mouse pancreatic regeneration. *Gastroenterology*.

Ji, B. et al., 2009. Ras activity levels control the development of pancreatic diseases. *Gastroenterology*, 137(3), pp.1072–82, 1082.e1–6. Available at: http://www.pubmedcentral.nih.gov/articlerender.fcgi?artid=2789008&tool=pmcentrez&rendertype=abstract.

Jia, D., 2008. Deciphering the bHLH transcription factor Mist1: Dual roles in pancreas development. *Theses and Dissertations Available from ProQuest*, pp.1 – 188. Available at: http://docs.lib.purdue.edu/dissertations/AAI3418662 [Accessed January 12, 2016].

Jia, D., Sun, Y. & Konieczny, S.F., 2008. Mist1 regulates pancreatic acinar cell proliferation through p21 CIP1/WAF1. *Gastroenterology*, 135(5), pp.1687–97. Available at: http://www.pubmedcentral.nih.gov/articlerender.fcgi?artid=2853247&tool=pmcentrez&rendertype=abstract [Accessed February 17, 2016].

Johnson et al., 2004. Mist1 is necessary for the establishment of granule organization in serous exocrine cells of the gastrointestinal tract. *Mechanisms of development*, 121(3), pp.261–72. Available at: http://www.ncbi.nlm.nih.gov/pubmed/15003629 [Accessed January 20, 2016].

Johnson, C.L. et al., 2014. Silencing of the Fibroblast Growth Factor 21 gene is an underlying cause of acinar cell 3 injury in mice lacking MIST1. *Am J Physiol Endocrinol Metab*.

Jr, Z.R. et al., 2008. The role of NF-kB activation in the pathogenesis of acute pancreatitis. , pp.259–267.

Kanda, M. et al., 2012. Presence of Somatic Mutations in Most Early-Stage Pancreatic Intraepithelial Neoplasia. *Gastroenterology*, 142(4), pp.730–733.e9. Available at: http://www.pubmedcentral.nih.gov/articlerender.fcgi?artid=3321090&tool=pmcentrez&rendertype=abstract [Accessed January 10, 2016].

Karemaker, I.D. & Vermeulen, M., 2016. In need of good neighbours : transcription factors require local DNA hypomethylation for target binding. *EMBO Journal*, 35(4), pp.1–2.

Karki, A. et al., 2015. Silencing Mist1 Gene Expression Is Essential for Recovery from Acute Pancreatitis. *PloS one*, 10(12), p.e0145724. Available at: http://journals.plos.org/plosone/article?id=10.1371/journal.pone.0145724#references [Accessed January 12, 2016].

Katayama, H., Nagasu, T. & Oda, Y., 2001. Improvement of in-gel digestion protocol for peptide mass fingerprinting by matrix-assisted laser desorption/ionization time-of-flight mass spectrometry. *Rapid communications in mass spectrometry : RCM*, 15(16), pp.1416–21. Available at: http://www.ncbi.nlm.nih.gov/pubmed/11507753 [Accessed February 16, 2016].

Kawaguchi, Y. et al., 2002. The role of the transcriptional regulator Ptf1a in converting intestinal to pancreatic progenitors. *Nature genetics*, 32(1), pp.128–34. Available at: http://www.ncbi.nlm.nih.gov/pubmed/12185368 [Accessed January 22, 2016].

Kern, H.F., 1993. Fine Structure of the Human Exocrine Pancreas. *The Pancreas: Biology, OPathobiology and Disease*, pp.9–19.

Kim et al., 2015. The basic helix-loop-helix transcription factor E47 reprograms human pancreatic cancer cells to a quiescent acinar state with reduced tumorigenic potential. *Pancreas*, 44(5), pp.718–27. Available at: http://www.pubmedcentral.nih.gov/articlerender.fcgi?artid=4464938&tool=pmcentrez&rendertype=abstract [Accessed February 17, 2016].

Kim, J. et al., 2009. Use of in vivo biotinylation to study protein-protein and protein-DNA interactions in mouse embryonic stem cells. *Nature protocols*, 4(4), pp.506–17. Available at: http://dx.doi.org/10.1038/nprot.2009.23 [Accessed January 13, 2016].

Kim, J.Y. et al., 2002. Transporter-mediated bile acid uptake causes Ca2+-dependent cell death in rat pancreatic acinar cells. *Gastroenterology*, 122(7), pp.1941–53. Available at: http://www.ncbi.nlm.nih.gov/pubmed/12055600 [Accessed April 3, 2016].

Kopp, J.L. et al., 2012. Identification of Sox9-dependent acinar-to-ductal reprogramming as the principal mechanism for initiation of pancreatic ductal adenocarcinoma. *Cancer cell*, 22(6), pp.737–50. Available at: http://www.pubmedcentral.nih.gov/articlerender.fcgi?artid=3568632&tool=pmcentrez&rendertype=abstract [Accessed January 19, 2016].

Kopp, J.L. et al., 2011. Sox9+ ductal cells are multipotent progenitors throughout development but do not produce new endocrine cells in the normal or injured adult pancreas. *Development (Cambridge, England)*, 138(4), pp.653–65. Available at: http://www.pubmedcentral.nih.gov/articlerender.fcgi?artid=3026412&tool=pmcentrez&rendertype=abstract [Accessed March 20, 2016].

Kopp, J.L. & Sander, M., 2014. New insights into the cell lineage of pancreatic ductal adenocarcinoma: evidence for tumor stem cells in premalignant lesions? *Gastroenterology*, 146(1), pp.24–6. Available at: http://www.ncbi.nlm.nih.gov/pubmed/24275238.

Kowalik, A.S. et al., 2011. Mice lacking the transcription factor Mist1 exhibit an altered stress response and increased sensitivity to caerulein-induced pancreatitis. *American Journal Of Physiology*, (December 2006).

Kowalik, A.S. et al., 2007. Mice lacking the transcription factor Mist1 exhibit an altered stress response and increased sensitivity to caerulein-induced pancreatitis. *American journal of physiology Gastrointestinal and liver physiology*, 292(4), pp.G1123–G1132. Available at: http://www.ncbi.nlm.nih.gov/pubmed/17170023.

Krah, N. et al., 2015. The acinar differentiation determinant PTF1A inhibits initiation of pancreatic ductal adenocarcinoma. *eLife*, 4, p.e07125. Available at: http://elifesciences.org/content/4/e07125v2 [Accessed February 17, 2016].

Krapp, A. et al., 1998. The bHLH protein PTF1-p48 is essential for the formation of the exocrine and the correct spatial organization of the endocrine pancreas. *Genes & development*, 12(23), pp.3752–63. Available at: http://www.pubmedcentral.nih.gov/articlerender.fcgi?artid=317250&tool=pmcentrez&rendertype=abstract [Accessed January 22, 2016].

Krapp, A. et al., 1996. The p48 DNA-binding subunit of transcription factor PTF1 is a new exocrine pancreas-specific basic helix-loop-helix protein. *The EMBO journal*, 15(16), pp.4317–29. Available at: http://www.pubmedcentral.nih.gov/articlerender.fcgi?artid=452157&tool=pmcentrez&rendertype=abstract [Accessed February 11, 2016].

Krepela, E. et al., 1990. Increased cathepsin B activity in human lung tumors. *Neoplasma*, 37(1), pp.61–70. Available at: http://www.ncbi.nlm.nih.gov/pubmed/2320181 [Accessed February 12, 2016].

De La O, J.-P. et al., 2008. Notch and Kras reprogram pancreatic acinar cells to ductal intraepithelial neoplasia. *Proceedings of the National Academy of Sciences of the United States of America*, 105(48), pp.18907–12. Available at: http://www.pubmedcentral.nih.gov/articlerender.fcgi?artid=2585942&tool=pmcentrez&rendertype=abstract [Accessed February 17, 2016].

Lemercier, C. et al., 1997. Mist1: a novel basic helix-loop-helix transcription factor exhibits a developmentally regulated expression pattern. *Developmental Biology*, 182(1), pp.101–113. Available at: http://www.ncbi.nlm.nih.gov/pubmed/9073453.

Lemercier, C. et al., 1998. The basic helix-loop-helix transcription factor Mist1 functions as a transcriptional repressor of myoD. *The EMBO journal*, 17(5), pp.1412–22. Available at: http://emboj.embopress.org/content/17/5/1412.abstract [Accessed January 12, 2016].

Lemercier, C. et al., 2000. The rat Mist1 gene: structure and promoter characterization. *Gene*, 242(1-2), pp.209–218. Available at: http://www.sciencedirect.com/science/article/pii/S0378111999005235 [Accessed March 24, 2016].

Lennerz, J.K.M. et al., 2010. The transcription factor MIST1 is a novel human gastric chief cell marker whose expression is lost in metaplasia, dysplasia, and carcinoma. *The American journal of pathology*, 177(3), pp.1514–33. Available at: http://www.pubmedcentral.nih.gov/articlerender.fcgi?artid=2928982&tool=pmcentrez&rendertype=abstract [Accessed February 17, 2016].

Leppä, S. et al., 1996. Syndecan-1 expression in mammary epithelial tumor cells is E-cadherin-dependent. *Journal of cell science*, 109 (Pt 6, pp.1393–403. Available at: http://www.ncbi.nlm.nih.gov/pubmed/8799827 [Accessed February 12, 2016].

Lerch, M.M. & Gorelick, F.S., 2013. Models of acute and chronic pancreatitis. *Gastroenterology*, 144(6), pp.1180–93. Available at: http://www.gastrojournal.org/article/S0016508513001984/fulltext [Accessed November 29, 2015].

Lin, Y. & Sun, Z., 2010. Current views on type 2 diabetes. *Journal of Endocrinology*, 204(1), pp.1–11.

Lioubinski, O. et al., 2003. Expression of Sox transcription factors in the developing mouse pancreas. *Developmental dynamics : an official publication of the American Association of Anatomists*, 227(3), pp.402–8. Available at: http://www.ncbi.nlm.nih.gov/pubmed/12815626 [Accessed March 20, 2016].

Lowenfels, A.B. et al., 1993. Pancreatitis and the risk of pancreatic cancer. International Pancreatitis Study Group. *The New England journal of medicine*, 328(20), pp.1433–7. Available at: http://www.ncbi.nlm.nih.gov/pubmed/8479461 [Accessed February 17, 2016].

Lund, H. et al., 2006. Long-term recurrence and death rates after acute pancreatitis. *Scandinavian journal of gastroenterology*, 41(2), pp.234–8. Available at: http://www.ncbi.nlm.nih.gov/pubmed/16484129 [Accessed April 2, 2016].

Luo, X. et al., 2005. Aberrant localization of intracellular organelles, Ca2+ signaling, and exocytosis in Mist1 null mice. *The Journal of biological chemistry*, 280(13), pp.12668–75. Available at: http://www.ncbi.nlm.nih.gov/pubmed/15665001 [Accessed February 17, 2016].

MacDonald, R.J., Swift, G.H. & Real, F.X., 2010. *Transcriptional control of acinar development and homeostasis.*, Elsevier Inc. Available at: http://www.ncbi.nlm.nih.gov/pubmed/21074728 [Accessed April 24, 2013].

MacFarlane, W.M. et al., 1994. Glucose modulates the binding activity of the beta-cell transcription factor IUF1 in a phosphorylation-dependent manner. *The Biochemical journal*, 303 (Pt 2, pp.625–31. Available at: http://www.pubmedcentral.nih.gov/articlerender.fcgi?artid=1137373&tool=pmcentrez&rendertype=abstract [Accessed February 11, 2016].

di Magliano, M.P. & Logsdon, C.D., 2013. Roles for KRAS in pancreatic tumor development and progression. *Gastroenterology*, 144(6), pp.1220–9. Available at: http://www.pubmedcentral.nih.gov/articlerender.fcgi?artid=3902845&tool=pmcentrez&rendertype=abstract [Accessed February 17, 2016].

Malka, D. et al., 2002. Risk of pancreatic adenocarcinoma in chronic pancreatitis. *Gut*, 51(6), pp.849–52. Available at: http://www.pubmedcentral.nih.gov/articlerender.fcgi?artid=1773474&tool=pmcentrez&rendertype=abstract [Accessed February 17, 2016].

Martinelli, P. et al., 2015. The acinar regulator Gata6 suppresses KrasG12V-driven pancreatic tumorigenesis in mice. *Gut*, pp.1–11. Available at: http://www.ncbi.nlm.nih.gov/pubmed/25596178.

Masui, T. et al., 2007. Early pancreatic development requires the vertebrate Suppressor of Hairless (RBPJ) in the PTF1 bHLH complex. *Genes & development*, 21(20), pp.2629–43. Available at: http://www.pubmedcentral.nih.gov/articlerender.fcgi?artid=2000326&tool=pmcentrez&rendertype=abstract [Accessed February 17, 2016].

Masui, T. et al., 2010. Replacement of Rbpj with Rbpjl in the PTF1 complex controls the final maturation of pancreatic acinar cells. *Gastroenterology*, 139(1), pp.270–80. Available at: http://www.pubmedcentral.nih.gov/articlerender.fcgi?artid=2902682&tool=pmcentrez&rendertype=abstract [Accessed February 17, 2016].

Matull, W.R., Pereira, S.P. & O'Donohue, J.W., 2006. Biochemical markers of acute pancreatitis. *Journal of clinical pathology*, 59(4), pp.340–4. Available at: http://www.pubmedcentral.nih.gov/articlerender.fcgi?artid=1860356&tool=pmcentrez&rendertype=abstract [Accessed April 3, 2016].

Mayerle, J., Sendler, M. & Lerch, M., 2013. Secretagogue (Caerulein) induced pancreatitis in rodents. *The Pancreapedia*, pp.1–9.

McNiven, M.A. & Marlowe, K.J., 1999. Contributions of molecular motor enzymes to vesicle-based protein transport in gastrointestinal epithelial cells. *Gastroenterology*, 116(2), pp.438–451. Available at: http://www.sciencedirect.com/science/article/pii/S0016508599701423 [Accessed February 9, 2016].

Means, A.L. & Leach, S.D., 2001. Lineage commitment and cellular differentiation in exocrine pancreas. *Pancreatology : official journal of the International Association of Pancreatology (IAP) ... [et al.]*, 1(6), pp.587–96. Available at: http://www.ncbi.nlm.nih.gov/pubmed/12120241 [Accessed March 18, 2016].

Mehmood, R. et al., 2014. Epigenetic reprogramming in Mist1-/- mice predicts the molecular response to cerulein-induced pancreatitis. *PLoS ONE*.

Mills, J.C. & Taghert, P.H., 2012. Scaling factors: transcription factors regulating subcellular domains. *BioEssays : news and reviews in molecular, cellular and developmental biology*, 34(1), pp.10–6. Available at: http://www.pubmedcentral.nih.gov/articlerender.fcgi?artid=3692000&tool=pmcentrez&rendertype=abstract [Accessed February 17, 2016].

Molero, X. et al., 2012. Gene expression dynamics after murine pancreatitis unveils novel roles for Hnf1α in acinar cell homeostasis. *Gut*, 61(8), pp.1187–96. Available at: http://www.ncbi.nlm.nih.gov/pubmed/21948943 [Accessed April 24, 2013].

Moore, A., Bonner-Weir, S. & Weissleder, R., 2001. Noninvasive In Vivo Measurement of -Cell Mass in Mouse Model of Diabetes. *Diabetes*, 50(10), pp.2231–2236. Available at: http://diabetes.diabetesjournals.org/content/50/10/2231.full [Accessed March 22, 2016].

Moore, A.W. et al., 2000. A genomewide survey of basic helix-loop-helix factors in Drosophila. *Proceedings of the National Academy of Sciences of the United States of America*, 97(19), pp.10436–41. Available at: http://www.pnas.org/content/97/19/10436 [Accessed March 24, 2016].

Morris, J.P., Wang, S.C. & Hebrok, M., 2010. KRAS, Hedgehog, Wnt and the twisted developmental biology of pancreatic ductal adenocarcinoma. *Nature reviews. Cancer*, 10(10), pp.683–95. Available at: http://www.pubmedcentral.nih.gov/articlerender.fcgi?artid=4085546&tool=pmcentrez&rendertype=abstract [Accessed December 23, 2015].

Motta, P.M. et al., 1997. Histology of the exocrine pancreas. *Microscopy Research and Technique*, 37(5-6), pp.384–398. Available at: http://www.ncbi.nlm.nih.gov/pubmed/9220418.

Murtaugh, L.C., 2014. Pathogenesis of pancreatic cancer: lessons from animal models. *Toxicologic pathology*, 42(1), pp.217–28. Available at: http://www.ncbi.nlm.nih.gov/pubmed/24178582.

Murtaugh, L.C. & Keefe, M.D., 2014. Regeneration and Repair of the Exocrine Pancreas. *Annual review of physiology*, (October), pp.1–21. Available at: http://www.ncbi.nlm.nih.gov/pubmed/25386992.

Murtaugh, L.C. & Melton, D.A., 2003. Genes, signals, and lineages in pancreas development. *Annual review of cell and developmental biology*, 19, pp.71–89. Available at: http://www.annualreviews.org/doi/pdf/10.1146/annurev.cellbio.19.111301.144752 [Accessed March 15, 2016].

Nam, K.T. et al., 2010. Mature chief cells are cryptic progenitors for metaplasia in the stomach. *Gastroenterology*, 139(6), pp.2028–2037.e9. Available at: http://www.pubmedcentral.nih.gov/articlerender.fcgi?artid=2997152&tool=pmcentrez&rendertype=abstract [Accessed February 17, 2016].

Nozaki, K. et al., 2008. A molecular signature of gastric metaplasia arising in response to acute parietal cell loss. *Gastroenterology*, 134(2), pp.511–22. Available at: http://www.pubmedcentral.nih.gov/articlerender.fcgi?artid=2857727&tool=pmcentrez&rendertype=abstract [Accessed February 17, 2016].

Oliver-Krasinski, J.M. et al., 2009. The diabetes gene Pdx1 regulates the transcriptional network of pancreatic endocrine progenitor cells in mice. *The Journal of clinical investigation*, 119(7), pp.1888–98. Available at: https://www.jci.org/articles/view/37028#B30 [Accessed March 23, 2016].

Pandol, S.J. et al., 2007. Acute pancreatitis: bench to the bedside. *Gastroenterology*, 132(3), pp.1127–51. Available at: http://www.gastrojournal.org/article/S0016508507003095/fulltext [Accessed April 3, 2016].

Pandol, S.J., 2010. Anatomy. Available at: http://www.ncbi.nlm.nih.gov/books/NBK54134/ [Accessed March 16, 2016].

Pandol, S.J., Gorelick, F.S. & Lugea, A., 2011. Environmental and genetic stressors and the unfolded protein response in exocrine pancreatic function - a hypothesis. *Frontiers in physiology*, 2, p.8. Available at: http://journal.frontiersin.org/article/10.3389/fphys.2011.00008/abstract [Accessed March 21, 2016].

Park, D. & Taghert, P.H., 2009. Peptidergic neurosecretory cells in insects: organization and control by the bHLH protein DIMMED. *General and comparative endocrinology*, 162(1), pp.2–7. Available at: http://www.sciencedirect.com/science/article/pii/S0016648008004541 [Accessed March 24, 2016].

Pasca di Magliano, M. et al., 2013. Advances in acute and chronic pancreatitis: from development to inflammation and repair. *Gastroenterology*, 144(1), pp.e1–4. Available at: http://www.pubmedcentral.nih.gov/articlerender.fcgi?artid=4096699&tool=pmcentrez&rendertype=abstract [Accessed February 17, 2016].

Peery, A.F. et al., 2012. Burden of gastrointestinal disease in the United States: 2012 update. *Gastroenterology*, 143(5), pp.1179–87.e1–3. Available at: http://www.pubmedcentral.nih.gov/articlerender.fcgi?artid=3480553&tool=pmcentrez&rendertype=abstract [Accessed December 4, 2015].

Pictet, R.L. et al., 1972. An ultrastructural analysis of the developing embryonic pancreas. *Developmental Biology*, 29(4), pp.436–467. Available at: http://www.sciencedirect.com/science/article/pii/0012160672900838 [Accessed February 10, 2016].

Pierreux, C.E. et al., 2006. The transcription factor hepatocyte nuclear factor-6 controls the development of pancreatic ducts in the mouse. *Gastroenterology*, 130(2), pp.532–41. Available at: http://www.ncbi.nlm.nih.gov/pubmed/16472605 [Accessed March 20, 2016].

Pin et al., 2001. The bHLH transcription factor Mist1 is required to maintain exocrine pancreas cell organization and acinar cell identity. *The Journal of cell biology*, 155(4), pp.519–530. Available at: http://www.mendeley.com/catalog/bhlh-transcription-factor-mist1-required-maintain-exocrine-pancreas-cell-organization-acinar-cell-id/ [Accessed February 16, 2016].

Pin, Bonvissuto, A.C. & Konieczny, S.F., 2000. Mist1 expression is a common link among serous exocrine cells exhibiting regulated exocytosis. *The Anatomical record*, 259(2), pp.157–67. Available at: http://www.mendeley.com/research/mist1-expression-common-link-among-serous-exocrine-cells-exhibiting-regulated-exocytosis/ [Accessed February 16, 2016].

Pin, C.L., Lemercier, C. & Konieczny, S.F., 1999. Cloning of the murine Mist1 gene and assignment to mouse chromosome band 5G2-5G3. *Cytogenetics and cell genetics*, 86(3-4), pp.219–22. Available at: http://www.ncbi.nlm.nih.gov/pubmed/10575209 [Accessed January 26, 2016].

Pin, C.L., Ryan, J.F. & Mehmood, R., 2015. Acinar cell reprogramming: a clinically important target in pancreatic disease. *Epigenomics*, 7(2), pp.267–81. Available at: http://www.ncbi.nlm.nih.gov/pubmed/25942535 [Accessed February 17, 2016].

Pinho, A. V et al., 2011. Adult pancreatic acinar cells dedifferentiate to an embryonic progenitor phenotype with concomitant activation of a senescence programme that is present in chronic pancreatitis. *Gut*, 60(7), pp.958–66. Available at: http://www.ncbi.nlm.nih.gov/pubmed/21193456 [Accessed June 29, 2011].

Pinho, A. V., Chantrill, L. & Rooman, I., 2014. Chronic pancreatitis: A path to pancreatic cancer. *Cancer Letters*.

Poll, A. V et al., 2006. A vHNF1/TCF2-HNF6 cascade regulates the transcription factor network that controls generation of pancreatic precursor cells. *Diabetes*, 55(1), pp.61–9. Available at: http://www.ncbi.nlm.nih.gov/pubmed/16380477 [Accessed March 20, 2016].

Pour, P.M., 1994. Pancreatic centroacinar cells. The regulator of both exocrine and endocrine function. *International journal of pancreatology : official journal of the International Association of Pancreatology*, 15(1), pp.51–64. Available at: http://www.ncbi.nlm.nih.gov/pubmed/8195642 [Accessed March 18, 2016].

Prévot, P.P. et al., 2013. Let-7b and miR-495 stimulate differentiation and prevent metaplasia of pancreatic acinar cells by repressing HNF6. *Gastroenterology*.

Prévot, P.-P. et al., 2012. Role of the ductal transcription factors HNF6 and Sox9 in pancreatic acinar-to-ductal metaplasia. *Gut*, 61(12), pp.1723–32. Available at: http://www.ncbi.nlm.nih.gov/pubmed/22271799 [Accessed April 20, 2013].

Puri, S. & Hebrok, M., 2010. Cellular plasticity within the pancreas--lessons learned from development. *Developmental cell*, 18(3), pp.342–56. Available at: http://www.pubmedcentral.nih.gov/articlerender.fcgi?artid=4085547&tool=pmcentrez&rendertype=abstract [Accessed February 17, 2016].

Ramsby, M. & Makowski, G., 2011. Differential detergent fractionation of eukaryotic cells. *Cold Spring Harbor protocols*, 2011(3), p.prot5592. Available at: http://cshprotocols.cshlp.org/content/2011/3/prot5592.abstract [Accessed February 16, 2016].

Ramsey, V.G. et al., 2007. The maturation of mucus-secreting gastric epithelial progenitors into digestive-enzyme secreting zymogenic cells requires Mist1. *Development (Cambridge, England)*, 134(1), pp.211–22. Available at: http://www.ncbi.nlm.nih.gov/pubmed/17164426 [Accessed January 20, 2016].

Rausa, F. et al., 1997. The cut-homeodomain transcriptional activator HNF-6 is coexpressed with its target gene HNF-3 beta in the developing murine liver and pancreas. *Developmental biology*, 192(2), pp.228–46. Available at: http://www.ncbi.nlm.nih.gov/pubmed/9441664 [Accessed March 20, 2016].

Reichert, M. & Rustgi, A.K., 2011. Pancreatic ductal cells in development, regeneration, and neoplasia. *Journal of Clinical Investigation*, 121(12), pp.4572–8. Available at: http://www.pubmedcentral.nih.gov/articlerender.fcgi?artid=3225990&tool=pmcentrez&rendertype=abstract.

Rempel, S.A. et al., 1994. Cathepsin B expression and localization in glioma progression and invasion. *Cancer research*, 54(23), pp.6027–31. Available at: http://www.ncbi.nlm.nih.gov/pubmed/7954439 [Accessed February 12, 2016].

Rigaut, G. et al., 1999. A generic protein purification method for protein complex characterization and proteome exploration. *Nature biotechnology*, 17(10), pp.1030–2. Available at: http://www.ncbi.nlm.nih.gov/pubmed/10504710 [Accessed August 13, 2015].

Rodolosse, A. et al., 2004. PTF1alpha/p48 transcription factor couples proliferation and differentiation in the exocrine pancreas [corrected]. *Gastroenterology*, 127(3), pp.937–49. Available at: http://www.ncbi.nlm.nih.gov/pubmed/15362048 [Accessed February 17, 2016].

Rooman, I. & Real, F.X., 2012. Pancreatic ductal adenocarcinoma and acinar cells: a matter of differentiation and development? *Gut*, 61(3), pp.449–58. Available at: http://www.ncbi.nlm.nih.gov/pubmed/21730103 [Accessed March 17, 2016].

Rose, S.D. et al., 2001. The role of PTF1-P48 in pancreatic acinar gene expression. *The Journal of biological chemistry*, 276(47), pp.44018–26. Available at: http://www.jbc.org/content/276/47/44018.abstract [Accessed March 18, 2016].

Rovira, M. et al., 2010. Isolation and characterization of centroacinar/terminal ductal progenitor cells in adult mouse pancreas. *Proceedings of the National Academy of Sciences of the United States of America*, 107(1), pp.75–80. Available at: http://www.pubmedcentral.nih.gov/articlerender.fcgi?artid=2806716&tool=pmcentrez&rendertype=abstract [Accessed March 18, 2016].

Rukstalis, J.M. et al., 2003. Exocrine specific expression of Connexin32 is dependent on the basic helix-loop-helix transcription factor Mist1. *Journal of Cell Science*, 116(Pt 16), pp.3315–3325. Available at: http://www.ncbi.nlm.nih.gov/pubmed/12829745.

Ryan, D., Hong, T. & Bardeesy, N., 2014. Pancreatic adenocarcinoma. *New England Journal of Medicine*, 371(11), pp.1039–49.

Saluja, A.K. et al., 1999. Secretagogue-induced digestive enzyme activation and cell injury in rat pancreatic acini. *Am J Physiol Gastrointest Liver Physiol*, 276(4), pp.G835–842. Available at: http://ajpgi.physiology.org/content/276/4/G835.long [Accessed April 3, 2016].

Schröder, M. & Kaufman, R.J., 2005. ER stress and the unfolded protein response. *Mutation research*, 569(1-2), pp.29–63. Available at: http://www.ncbi.nlm.nih.gov/pubmed/15603751 [Accessed November 18, 2015].

Schröder, M. & Kaufman, R.J., 2005. THE MAMMALIAN UNFOLDED PROTEIN RESPONSE. *Annual Review of Biochemistry*, 74(1), pp.739–789. Available at: http://www.ncbi.nlm.nih.gov/pubmed/15952902 [Accessed January 8, 2016].

Sendler, M. et al., 2012. Tumour necrosis factor secretion induces protease activation and acinar cell necrosis in acute experimental pancreatitis in mice. *Gut*.

Seymour, P.A. et al., 2007. SOX9 is required for maintenance of the pancreatic progenitor cell pool. *Proceedings of the National Academy of Sciences of the United States of America*, 104(6), pp.1865–70. Available at: http://www.pubmedcentral.nih.gov/articlerender.fcgi?artid=1794281&tool=pmcentrez&rendertype=abstract [Accessed March 18, 2016].

Seymour, P.A., 2014. Sox9: a master regulator of the pancreatic program. *The review of diabetic studies : RDS*, 11(1), pp.51–83. Available at: http://www.pubmedcentral.nih.gov/articlerender.fcgi?artid=4295800&tool=pmcentrez&rendertype=abstract [Accessed March 20, 2016].

Shi, G. et al., 2009. Loss of the Acinar-Restricted Transcription Factor Mist1 Accelerates Kras-Induced Pancreatic Intraepithelial Neoplasia. *Gastroenterology*, 136(4), pp.1368–1378. Available at: http://www.gastrojournal.org/article/S0016508509000043/fulltext [Accessed January 12, 2016].

Shi, G. et al., 2012. Maintenance of acinar cell organization is critical to preventing Kras-induced acinar-ductal metaplasia. *Oncogene*, (September 2011), pp.1–9. Available at: http://www.ncbi.nlm.nih.gov/pubmed/22665051.

Shi, G. et al., 2013. Maintenance of acinar cell organization is critical to preventing Kras-induced acinar-ductal metaplasia. *Oncogene*, 32(15), pp.1950–8. Available at: http://www.pubmedcentral.nih.gov/articlerender.fcgi?artid=3435479&tool=pmcentrez&rendertype=abstract [Accessed February 17, 2016].

Siveke, J.T. et al., 2008. Notch Signaling Is Required for Exocrine Regeneration After Acute Pancreatitis. *Gastroenterology*.

Slack, J.M., 1995. Developmental biology of the pancreas. *Development (Cambridge, England)*, 121(6), pp.1569–80. Available at: http://www.ncbi.nlm.nih.gov/pubmed/7600975.

Solar, M. et al., 2009. Pancreatic exocrine duct cells give rise to insulin-producing beta cells during embryogenesis but not after birth. *Developmental cell*, 17(6), pp.849–60. Available at: http://www.cell.com/article/S1534580709004778/fulltext [Accessed March 20, 2016].

Stanger, B.Z. & Hebrok, M., 2013. Control of cell identity in pancreas development and regeneration. *Gastroenterology*.

Stefan, Y. et al., 1982. Quantitation of endocrine cell content in the pancreas of nondiabetic and diabetic humans. *Diabetes*, 31(8 Pt 1), pp.694–700. Available at: http://www.ncbi.nlm.nih.gov/pubmed/6131002 [Accessed February 9, 2016].

Stevenson, K. & Carter, C.R., 2013. Acute pancreatitis. *Surgery (Oxford)*, 31(6), pp.295–303. Available at: http://www.sciencedirect.com/science/article/pii/S0263931913000835 [Accessed April 2, 2016].

Steward, M.C., Ishiguro, H. & Case, R.M., 2005. Mechanisms of bicarbonate secretion in the pancreatic duct. *Annual review of physiology*, 67, pp.377–409. Available at: http://www.ncbi.nlm.nih.gov/pubmed/15709963 [Accessed March 16, 2016].

Streaker, E.D. & Beckett, D., 2006. Nonenzymatic biotinylation of a biotin carboxyl carrier protein: unusual reactivity of the physiological target lysine. *Protein science : a publication of the Protein Society*, 15(8), pp.1928–35. Available at: http://www.pubmedcentral.nih.gov/articlerender.fcgi?artid=2242587&tool=pmcentrez&rendertype=abstract [Accessed December 1, 2015].

Strobel, O. et al., 2007. In vivo lineage tracing defines the role of acinar-to-ductal transdifferentiation in inflammatory ductal metaplasia. *Gastroenterology*, 133(6), pp.1999–2009. Available at: http://www.pubmedcentral.nih.gov/articlerender.fcgi?artid=2254582&tool=pmcentrez&rendertype=abstract.

Su, K.H., Cuthbertson, C. & Christophi, C., 2006. Review of experimental animal models of acute pancreatitis. *HPB : the official journal of the International Hepato Pancreato Biliary Association*.

Teng, Y.H.-F., Aquino, R.S. & Park, P.W., 2012. Molecular functions of syndecan-1 in disease. *Matrix biology : journal of the International Society for Matrix Biology*, 31(1), pp.3–16. Available at: http://www.pubmedcentral.nih.gov/articlerender.fcgi?artid=3568394&tool=pmcentrez&rendertype=abstract [Accessed February 12, 2016].

Tian, X. et al., 2010. RAB26 and RAB3D are direct transcriptional targets of MIST1 that regulate exocrine granule maturation. *Molecular and cellular biology*, 30(5), pp.1269–84. Available at: http://www.pubmedcentral.nih.gov/articlerender.fcgi?artid=2820885&tool=pmcentrez&rendertype=abstract [Accessed January 12, 2016].

Tran, T. et al., 2007. The bHLH domain of Mistl is sufficient to activate gene transcription. *Gene expression*, 13(4-5), pp.241–53. Available at: http://www.ncbi.nlm.nih.gov/pubmed/17605298.

Türkvatan, A. et al., 2013. Congenital variants and anomalies of the pancreas and pancreatic duct: imaging by magnetic resonance cholangiopancreaticography and multidetector computed tomography. *Korean journal of radiology*, 14(6), pp.905–13. Available at: http://www.pubmedcentral.nih.gov/articlerender.fcgi?artid=3835637&tool=pmcentrez&rendertype=abstract [Accessed March 20, 2016].

Tyanova, S. et al., 2015. Visualization of LC-MS/MS proteomics data in MaxQuant. *Proteomics*, 15(8), pp.1453–6. Available at: http://www.ncbi.nlm.nih.gov/pubmed/25644178 [Accessed October 12, 2015].

Vitale, G.C., 2007. Early management of acute gallstone pancreatitis. *Annals of surgery*, 245(1), pp.18–9. Available at: http://www.pubmedcentral.nih.gov/articlerender.fcgi?artid=1867941&tool=pmcentrez&rendertype=abstract [Accessed April 2, 2016].

Wang, G.-J. et al., 2009. Acute pancreatitis: etiology and common pathogenesis. *World journal of gastroenterology*, 15(12), pp.1427–30. Available at: http://www.pubmedcentral.nih.gov/articlerender.fcgi?artid=2665136&tool=pmcentrez&rendertype=abstract [Accessed March 11, 2016].

Wang, N. et al., 2004. Expression of an engrailed-LMO4 fusion protein in mammary epithelial cells inhibits mammary gland development in mice. *Oncogene*, 23, pp.1507–1513.

Ward, J. et al., 1996. Progressive disruption of acinar cell calcium signaling is an early feature of cerulein-induced pancreatitis in mice. *Gastroenterology*, 111(2), pp.481–491. Available at: http://www.sciencedirect.com/science/article/pii/S0016508596003691 [Accessed April 3, 2016].

Willemer, S., Elsässer, H.P. & Adler, G., 1992. Hormone-induced pancreatitis. *European surgical research. Europäische chirurgische Forschung. Recherches chirurgicales européennes*, 24 Suppl 1, pp.29–39. Available at: http://www.ncbi.nlm.nih.gov/pubmed/1601022 [Accessed April 4, 2016].

Williams, J.A., 2001. Intracellular signaling mechanisms activated by cholecystokinin-regulating synthesis and secretion of digestive enzymes in pancreatic acinar cells. *Annual review of physiology*, 63, pp.77–97. Available at: http://www.ncbi.nlm.nih.gov/pubmed/11181949 [Accessed March 16, 2016].

Wilson, K.P. et al., 1992. Escherichia coli biotin holoenzyme synthetase/bio repressor crystal structure delineates the biotin- and DNA-binding domains. *Proceedings of the National Academy of Sciences of the United States of America*, 89(19), pp.9257–61. Available at: http://www.pubmedcentral.nih.gov/articlerender.fcgi?artid=50105&tool=pmcentrez&rendertype=abstract [Accessed January 13, 2016].

Wilson, M.E., Scheel, D. & German, M.S., 2003. Gene expression cascades in pancreatic development. *Mechanisms of Development*, 120(1), pp.65–80. Available at: http://www.sciencedirect.com/science/article/pii/S0925477302003337 [Accessed January 19, 2016].

Xuan, S. et al., 2012. Pancreas-specific deletion of mouse Gata4 and Gata6 causes pancreatic agenesis. , 122(10).

Yachida, S. et al., 2010. Distant metastasis occurs late during the genetic evolution of pancreatic cancer. *Nature*, 467(7319), pp.1114–7. Available at: http://www.ncbi.nlm.nih.gov/pubmed/20981102 [Accessed June 13, 2011].

Yadav, D. & Lowenfels, A.B., 2013. The Epidemiology of Pancreatitis and Pancreatic Cancer. *Gastroenterology*, 144(6), pp.1252–1261. Available at: http://linkinghub.elsevier.com/retrieve/pii/S0016508513001686.

Yeung, C.C.S., Mills, J. & Frater, J., 2011. An evaluation of MIST 1 as an indicator of plasmacytic differentiation. *ASCO Meeting Abstracts*, 29(15_suppl), p.8084. Available at: http://hwmaint.meeting.ascopubs.org/cgi/content/abstract/29/15_suppl/8084 [Accessed April 1, 2016].

Yule, D.I., Stuenkel, E. & Williams, J.A., 1996. Intercellular calcium waves in rat pancreatic acini: mechanism of transmission. *The American journal of physiology*, 271(4 Pt 1), pp.C1285–94. Available at: http://www.ncbi.nlm.nih.gov/pubmed/8897836 [Accessed March 16, 2016].

Zhang, N. & Li, L., 2004. Effects of common surfactants on protein digestion and matrix-assisted laser desorption/ionization mass spectrometric analysis of the digested peptides using two-layer sample preparation. *Rapid communications in mass spectrometry : RCM*, 18(8), pp.889–96. Available at: http://www.ncbi.nlm.nih.gov/pubmed/15095358 [Accessed February 16, 2016].

Zhao, Y. et al., 2006. Identification of a basic helix-loop-helix transcription factor expressed in mammary gland alveolar cells and required for maintenance of the differentiated state. *Molecular endocrinology (Baltimore, Md.)*, 20(9), pp.2187–98. Available at: http://www.ncbi.nlm.nih.gov/pubmed/16645041 [Accessed February 17, 2016].

Zhu, L. et al., 2007. Acinar cells contribute to the molecular heterogeneity of pancreatic intraepithelial neoplasia. *The American journal of pathology*, 171(1), pp.263–73. Available at: http://www.pubmedcentral.nih.gov/articlerender.fcgi?artid=1941579&tool=pmcentrez&rendertype=abstract [Accessed April 17, 2013].

Zhu, L. et al., 2004. Inhibition of Mist1 homodimer formation induces pancreatic acinar-to-ductal metaplasia. *Molecular and cellular biology*, 24(7), pp.2673–81. Available at: http://www.pubmedcentral.nih.gov/articlerender.fcgi?artid=371125&tool=pmcentrez&rendertype=abstract [Accessed January 12, 2016].

Centers for Disease Control and Prevention. *National Diabetes Statistics Report: Estimates of Diabetes and Its Burden in the United States, 2014*. Atlanta, GA: US Department of Health and Human Services; 2014.

VITA

VITA

Anju is from Nepal. She came to the United States to pursue her Bachelor's degree in 2005. She graduated from Salem College, North Carolina in 2009 with a Biology degree. Anju then was enrolled in the Department of Biological Sciences at Purdue University for a PhD degree and joined Dr. Stephen Konieczny's laboratory in 2010. Her research focused on studying the inflammation of the pancreas and its recovery using mouse models. Anju earned her PhD degree in May, 2016. She has accepted a postdoctoral position at Boston Children's Hospital to pursue a career in translational liver cancer research in Dr. Khashayar Vakili's laboratory in the Department of Surgery.

LIST OF PUBLICATIONS

PUBLICATIONS

Anju Karki, Sean E. Humphrey, Rebecca E. Steele, D.A. Hess, Elizabeth. J. Taparowsky, Stephen F. Konieczny. Silencing *Mist1* gene expression is essential for recovery from acute pancreatitis (2015). *PLOS ONE. 2015; 10(12): e0145724.*

Jie Li, **Anju Karki**, Kurt Hodges, Nihal Ahmad, Amina Zoubeidi, Klaus Strebhardt, Timothy Ratliff, Stephen F. Konieczny, Xiaoqi Liu. Co-targeting Polo-like kinase 1 (Plk1) and the Wnt/β-catenin signaling pathway in castration-resistant prostate cancer (2015). *Molecular and Cellular Biology*, *35*(24), 4185–98.

Pengpeng Bi, Feng Yue, **Anju Karki,** Chao Wang, Sarah E. Wirbisky, Abigail Durkes, Ourania M. Andrisani, Jennifer L. Freeman, Stephen F. Konieczny, Shihuan Kuang. Transformation of mature adipocytes into malignant liposarcoma by Notch activation in lipodystrophic mice (2016). *Submitted.*

Jie Li , Ruixin Wang , Patrick G. Schweickert , **Anju Karki** , Yi Yang , Yifan Kong , Nihal Ahmad , Stephen F. Konieczny, Xiaoqi Liu. Plk1 Inhibition Enhances the Efficacy of Gemcitabine in Human Pancreatic Cancer (2016). *Cell Cycle*. DOI: 10.1080/15384101.2016.1148838.

Jie Li, **Anju Karki,** Stephen F. Konieczny, Xiaoqi Liu. “The role of Polo-like kinase 1 (Plk1) in pancreatic cancer” *manuscript in preparation.*